



**FACULDADE DE ENGENHARIA  
UNIVERSIDADE DO PORTO**

# **Probabilistic Seismic Assessment of Bridges**

**Ricardo Nuno Carvalho Monteiro**

*A thesis submitted to the University of Porto in accordance with the requirements of the degree of Doctor of Philosophy in Civil Engineering, in the Faculty of Engineering*

Porto, 2011





***“We build too many walls and not enough bridges”***

Sir Isaac Newton (1643 – 1727)



# Acknowledgments

Seismic assessment of bridge structural systems is an extremely interesting field of research in which I had the opportunity to work since the last year of my Civil Engineering degree, back in 2004. Such early discovery and all the work carried out within this challenging step of my professional career became definitely more attractive and motivating due to the contribution of a number of people to whom I would like to express my most sincere gratefulness.

To Professor Raimundo Delgado, my advisor, I would like to thank for his crucial role in this work, not only academically, with his wisdom and intelligence, but personally as well, for his permanent encouragement and motivation, making everything definitely become easier. To him I believe to owe a fair amount of my scientific knowledge and interest in structural and seismic analysis.

To Professor Aníbal Costa, my co-advisor, I would like to thank for his experienced guidance and practicability, as well as his ability to introduce me to the seismic analysis topic from the beginning of my research years.

To Professor Rui Pinho and Doctors Chiara Casarotti and Helen Crowley, I'm thankful for their help and guidance throughout the enriching training periods I spent, in 2007 and 2008, at the EUCENTRE, Pavia. I would like to specially thank Professor Rui Pinho, who became a friend, for his faith in me and my work, for his incentive and leadership skills, which definitely inspired me.

To Professors António Arêde, Nelson Vila Pouca, Miguel Castro, Rui Calçada, Ana Maria Sarmiento, Paula Milheiro, Maria do Carmo Coimbra and Isabel Silva, I wish to thank for their interest in my work, for their helpful scientific contribution and supporting words.

To my PhD colleagues, friends and academic partners ever since undergraduate times, Mário, Cristina and Nuno, I would like to thank for their companionship, help in a non

measurable number of aspects at all levels, daily friendship and support. A particular mention goes to Mário for his brotherhood.

To the other colleagues and friends at FEUP or at the EUCENTRE, Sara, Sérgio, Fernando, João, Ricardo, Pedro, Patrício, Carlos, Maria Serena, Romain, Claudia and Tuba, amongst others, I'm grateful for their team spirit, help provided with no hesitation and thoughtfulness towards me and my work.

To Luís Sousa, Rui Ribeiro and Ângelo Carvalho, former MSc students I had the pleasure to work with, I wish to thank for the contribution with provided data and other elements from their individual studies.

To the Structural Department and Laboratory staff, especially Marta for her esteem, I would like to thank for their availability and support in all the logistical tasks.

To my dear friends Lisa, Maria Inês, Pedro, Rita, Andreia, Nuno and Luís Pedro I specially thank for their patience and affection, for providing me with numerous wonderful moments and for helping me to go through the toughest ones.

Finally, but firstly in my heart, I would like to deeply thank my family, who always took care of me, embracing me in every moment, allowing me, so many times, to focus on nothing else but my work, spending less time with them than I would wish to. To my parents, António and Maria Rosa, I'm thankful for their endless love and unconditional support, whichever my choices are. To my sisters, Eugénia and Susana, I'm grateful for their friendship and altruism, showed by their constant dedication to my well-being and happiness.

This research work would not have been possible without the financial support of FCT (Portuguese Foundation for Science and Technology) in the form of the PhD grant SFRH/BD/22959/2005.

# Abstract

The main goal of this thesis is to outline the entire process of assessing the seismic safety of single existing reinforced concrete bridges, within a probabilistic context. Given that several possible methodologies are currently available for seismic assessment with the inclusion of nonlinear structural behaviour, this work intends to contribute with a global overview on the essential aspects surrounding any safety assessment procedure, with particular focus on bridge structures. A specific methodology using statistical characterization of the assessment problem, conducting to the failure probability computation was employed and optimized.

Firstly, a characterization process of the seismic action has been carried out, with the purpose of portraying this sort of loading, which is well known for its complexity and variability, coming from the occurrence of highly unpredictable natural seismic hazards. Furthermore, the optimum way for seismic loading to be set up is looked for, in terms of reduced dispersion and number of earthquake records, with a view to the use in subsequent repeated probabilistic safety calculations.

The modelling issue is afterwards analysed, with a brief mention to the sort of structural models currently employed for bridges and ways of accounting for material and geometrical nonlinearity. Special emphasis is put on the latter – different modelling alternatives for the material plasticity representation are scrutinized, a subject seen as quite pertinent.

The estimation of the structural response for the duly modelled structure, subjected to properly characterized seismic loading, which constitutes the next logical task, has been addressed by means of an extensive comparative parametric study of the two most commonly accepted approaching tools: nonlinear dynamic or nonlinear static analysis, featuring different sorts of seismic action input.

Finally, the intended safety verification is carried out probabilistically for a case study made up of a set of different bridge configurations, in length, regularity and structural type, together with an equally wide set of earthquake records, both already used for the previous calibration studies conducted for the different components of the safety assessment problem. Both capacity and seismic demand are characterized statistically, according to premises settled in the modelling and structural response estimation sections, respectively. Statistical characterization is managed through proper random simulation techniques, such as the employed Latin Hypercube Sampling scheme. Different alternatives to reach the failure probability, involving distinct uncertainty levels, are presented and compared, with the aim to conclude over applicability and accuracy of the methodologies, as well as the relative seismic safety of the tested configurations.



# Resumo

O trabalho apresentado nesta tese teve como principal objectivo percorrer as várias etapas do processo de verificação de segurança sísmica individual, num contexto probabilístico, de pontes existentes em betão armado. Presentemente, várias alternativas se encontram disponíveis para a abordagem ao problema de segurança sísmica e, por conseguinte, este trabalho pretende dar um contributo com a elaboração de uma perspectiva global do tema, sintetizando os aspectos mais relevante, com especial ênfase na análise de pontes. É proposta e aplicada uma metodologia de avaliação de segurança por cálculo da probabilidade de ruína da estrutura, com caracterização estatística das diferentes variáveis.

O trabalho conduzido começa por focar a caracterização da acção sísmica, reconhecidamente complexa e com elevada variabilidade, consequência natural da imprevisibilidade associada à ocorrência de fenómenos sísmicos. Desse modo, procura-se estudar a melhor maneira de definir tal acção, investindo na redução da dispersão e no número de acelerogramas reais a utilizar, com vista à sua utilização em aplicações praticas de verificação de segurança, envolvendo repetição de cálculos probabilísticos.

A temática da modelação é abordada fazendo referencia aos modelos estruturais correntemente utilizados para análise não linear de pontes bem como aos diferentes modos de ter em consideração a não linearidade material e geométrica. É dada especial atenção ao primeiro tipo de não linearidade enumerado, estudando a viabilidade de emprego de diferentes estratégias de modelação da plasticidade material, uma questão tida como particularmente pertinente na análise sísmica de estruturas.

A estimativa da resposta estrutural das pontes devidamente modeladas, quando submetidas a uma acção sísmica convenientemente caracterizada, é igualmente alvo de estudo com relativo detalhe por intermédio de um estudo paramétrico extenso de comparação das duas vias de análise tipicamente usadas: análise dinâmica não linear ou análise estática não linear, a que correspondem diferentes formas de representação da acção sísmica.

Finalmente, a verificação de segurança propriamente dita é efectuada para um caso de estudo constituído por diferentes configurações, em extensão, regularidade ou tipo de aparelhos estruturais, usando com um conjunto igualmente vasto de acelerogramas, igualmente utilizados na calibração das diversas componentes do processo da avaliação de segurança. A capacidade resistente e a exigência estrutural são caracterizadas estatisticamente de acordo com os resultados dos estudos sobre a acção sísmica, modelação e previsão da resposta. A caracterização estatística é conseguida por intermédio de técnicas de amostragem convenientemente aplicadas. São propostos e comparados diferentes procedimentos conducentes ao cálculo da probabilidade de ruína, com diferentes níveis de incerteza, com o objectivo de concluir quanto à sua aplicabilidade bem como da segurança sísmica das diversas pontes testadas.

# Résumé

L'objectif principal de cette thèse est de décrire l'ensemble du processus d'évaluation de la sécurité sismique de ponts existants en béton armé, dans un contexte probabiliste. Lorsque plusieurs méthodes possibles sont actuellement disponibles pour l'évaluation sismique avec l'inclusion du comportement des structures non linéaires, ce travail veut contribuer à une vision globale sur les aspects essentiels entourant toute la procédure d'évaluation de la sécurité, avec un accent particulier sur les structures de pont. Une méthodologie spécifique en utilisant la caractérisation statistique du problème d'évaluation, tenue à la probabilité de défaillance de calcul a été utilisé et optimisé.

Tout d'abord, un processus de caractérisation de l'action sismique a été réalisée, dans le but de représenter ce type de chargement, qui est bien connue pour sa complexité et la variabilité, provenant de la présence très imprévisible des risques naturels sismiques. En outre, la meilleure façon pour le chargement sismique à mettre en place est recherché, en termes de dispersion réduite et le nombre de dossiers tremblement de terre, en vue de l'utilisation répétée dans les prochains calculs probabilistes de sûreté.

La question de la modélisation est ensuite analysée, avec une brève mention de ce genre de modèles structurels actuellement employé pour les ponts et les moyens de la comptabilité pour le matériel et la non-linéarité géométrique. Un accent particulier est mis sur ce dernier – la modélisation de/sur différentes alternatives pour la représentation plasticité du matériau sont examinées, un sujet considéré comme tout à fait assez pertinente.

L'estimation de la réponse structurale de la structure modélisée dûment, soumis à des séismes de chargement bien caractérisé, qui constitue la prochaine étape logique, a été abordée par le biais d'une étude comparative approfondie des paramètres des deux outils les plus communément acceptés approche: dynamique non linéaire ou non linéaire analyse statique, avec différentes sortes d'entrées de action sismique.

Enfin, la vérification de sécurité destinée probabiliste est effectuée pour une étude de cas d'un ensemble de configurations différentes pont, dans la longueur, la régularité et le type de construction, avec une large série de documents tout aussi tremblement de terre, toutes deux déjà utilisées pour les études d'étalonnage précédente réalisée pour les différentes composantes du problème d'évaluation de la sécurité. Les deux capacités de la demande sismique sont caractérisées statistiquement, selon locaux installés dans les sections et structurelles réponse estimation de modélisation, respectivement. Caractérisation statistique est gérée par des techniques appropriées de simulation aléatoires, telles que l'échantillonnage par hypercubes latins régime des travailleurs salariés. Différentes alternatives pour atteindre la probabilité de défaillance, impliquant les niveaux d'incertitude distincts, sont présentés et comparés, dans le but de conclure sur l'applicabilité et la précision des méthodes, ainsi que la sismique de sécurité relative des configurations testées.

# Contents

<b>Acknowledgments .....</b>	<b>v</b>
<b>Abstract.....</b>	<b>vii</b>
<b>Resumo.....</b>	<b>ix</b>
<b>Résumé.....</b>	<b>xi</b>
<b>Contents .....</b>	<b>xiii</b>
<b>1. Introduction.....</b>	<b>1.1</b>
1.1 General.....	1.1
1.2 Motivation and goals .....	1.3
1.3 Thesis outline .....	1.4
<b>2. Seismic Assessment of Bridges.....</b>	<b>2.1</b>
2.1 Introduction.....	2.1
2.2 Recent earthquake events – major observations and lessons learned.....	2.3
2.2.1 Loma Prieta earthquake .....	2.4
2.2.2 Northridge earthquake .....	2.7
2.2.3 Kobe earthquake .....	2.9
2.2.4 L’Aquila earthquake .....	2.12
2.2.5 Haiti earthquake .....	2.13
2.2.6 Christchurch earthquake and Tōhoku earthquake and tsunami .....	2.15
2.2.7 Summary .....	2.17
2.3 The seismic action .....	2.19
2.3.1 Selection and scaling of real records .....	2.20
2.3.2 Number of records .....	2.24

2.4 Nonlinear seismic analysis – methods for structural response prediction .....	2.26
2.4.1 Nonlinear static analysis – pushover.....	2.28
2.4.2 Nonlinear dynamic analysis .....	2.31
2.4.3 Innovative displacement based approaches .....	2.33
2.4.4 Nonlinear response prediction of bridges .....	2.35
2.5 Nonlinear modelling overview.....	2.37
2.5.1 Material nonlinearity.....	2.38
2.5.2 Geometrical nonlinearity.....	2.41
2.6 Safety assessment methods .....	2.42
2.6.1 Deterministic assessment .....	2.42
2.6.2 Probabilistic assessment.....	2.43
2.7 Summary .....	2.44
<b>3. Seismic Input .....</b>	<b>3.1</b>
3.1 Accelerograms .....	3.2
3.2 Real accelerograms – selection of records .....	3.3
3.2.1 Initial considered set .....	3.3
3.2.2 A homogeneous base of records – Clustering analysis.....	3.5
3.2.3 Application to the set of selected records .....	3.6
3.3 Real accelerograms – scaling.....	3.8
3.3.1 Record quantities based intensity measures.....	3.9
3.3.2 Spectrum quantities based intensity measures .....	3.10
3.3.3 Comparative analysis of typical intensity measures .....	3.12
3.3.4 Response based intensity measures.....	3.14
3.3.4.1 <i>Preliminary Approach on a Displacement-Based Intensity Measure</i> .....	3.15
3.3.4.2 <i>Procedure</i> .....	3.16
3.3.4.3 <i>Structural application</i> .....	3.18
3.4 Artificial accelerograms.....	3.26
3.4.1 Algorithm of generation.....	3.27
3.4.2 Reference response spectrum for generation of records .....	3.28
3.4.3 Artificial ground motion records generation parameters .....	3.29

3.5 Comparison between real and artificial records – structural application.....	3.29
3.5.1 Structural description.....	3.30
3.5.2 Real records – original and homogeneous bases .....	3.31
3.5.3 Minimum necessary number of accelerograms .....	3.32
3.5.4 Artificial records .....	3.34
3.5.5 Comparison of results .....	3.35
3.6 Conclusions.....	3.37
<b>4. Nonlinear Modelling .....</b>	<b>4.1</b>
4.1 Material models .....	4.2
4.1.1 Concrete models .....	4.2
4.1.1.1 <i>Modified Kent-Park model</i> .....	4.4
4.1.1.2 <i>Mander-Priestley-Park model</i> .....	4.6
4.1.2 Steel models .....	4.7
4.1.2.1 <i>Giuffrè-Menegotto-Pinto model</i> .....	4.9
4.2 Material nonlinearity approaches.....	4.10
4.2.1 Lumped plasticity models (plastic hinges) .....	4.10
4.2.1.1 <i>Plastic hinge constitutive law – trilinear curve</i> .....	4.11
4.2.1.2 <i>Plastic hinge length and location</i> .....	4.12
4.2.2 Distributed plasticity models (fibres) .....	4.18
4.3 Case study .....	4.19
4.3.1 Selected bridges .....	4.19
4.3.1.1 <i>Piers</i> .....	4.22
4.3.1.2 <i>Deck</i> .....	4.24
4.3.1.3 <i>Abutments</i> .....	4.25
4.3.2 Seismic action .....	4.26
4.4 Comparative study .....	4.27
4.4.1 Elastic modal analysis comparison .....	4.28
4.4.2 Moment-curvature relationships .....	4.32
4.4.3 Pushover capacity curves .....	4.35
4.4.4 Structural response parameters .....	4.38
4.5 Conclusions.....	4.42

<b>5. Seismic Demand .....</b>	<b>5.1</b>
5.1 Nonlinear Static Analysis.....	5.2
5.2 Nonlinear Static Procedures.....	5.4
5.2.1 Capacity Spectrum Method (CSM).....	5.5
5.2.2 N2 Method .....	5.8
5.2.3 Displacement Coefficient Method (DCM) .....	5.10
5.2.4 Modal Pushover Analysis (MPA).....	5.11
5.2.5 Adaptive Capacity Spectrum Method (ACSM).....	5.13
5.2.5.1 <i>Damping-based spectral reduction</i> .....	5.17
5.2.5.2 <i>Ductility-based spectral reduction</i> .....	5.27
5.2.6 Adaptive Modal Combination Procedure (AMCP) .....	5.28
5.2.7 Method comparison.....	5.30
5.3 Parametric Study .....	5.31
5.4 Results.....	5.33
5.4.1 Results representation .....	5.33
5.4.2 Preliminary evaluation .....	5.35
5.4.2.1 <i>Capacity Spectrum Method</i> .....	5.35
5.4.2.2 <i>N2 Method</i> .....	5.38
5.4.2.3 <i>Modal Pushover Analysis</i> .....	5.43
5.4.2.4 <i>Adaptive Capacity Spectrum Method</i> .....	5.46
5.4.3 Comparative study results .....	5.53
5.4.3.1 <i>Global results</i> .....	5.53
5.4.3.2 <i>Intensity level results</i> .....	5.55
5.4.3.3 <i>Bridge configuration results</i> .....	5.57
5.5 Conclusions.....	5.62
<b>6. Safety Assessment .....</b>	<b>6.1</b>
6.1 Failure probability computation.....	6.2
6.1.1 Seismic action – intensity level probability density function .....	6.5
6.1.2 Capacity distribution .....	6.8
6.1.3 Latin Hypercube Sampling .....	6.9
6.1.4 Seismic structural effects .....	6.12



6.1.5 Failure probability with local uncertainty.....	6.13
6.1.6 Failure probability for a given intensity level.....	6.17
6.1.7 Failure probability with global uncertainty .....	6.19
6.1.8 Reliability index.....	6.21
6.2 Application to a set of bridges .....	6.22
6.2.1 Latin Hypercube sampling in capacity definition.....	6.23
6.2.2 Seismic action probability density function.....	6.29
6.2.3 Failure probability with traditional NSA approach .....	6.31
6.2.3.1 <i>Vulnerability function from nonlinear dynamic analysis</i> .....	6.31
6.2.3.2 <i>Vulnerability function from nonlinear static analysis</i> .....	6.37
6.2.3.3 <i>Structural effects and failure probability</i> .....	6.46
6.2.4 Failure probability with global uncertainty LHS approach .....	6.56
6.2.4.1 <i>Simulation process calibration</i> .....	6.56
6.2.4.2 <i>Structural effects and failure probability</i> .....	6.63
6.2.5 Comparison of methodologies .....	6.67
6.3 Conclusions.....	6.71
<b>7. Conclusions.....</b>	<b>7.1</b>
7.1 Concluding remarks .....	7.1
7.2 Future developments .....	7.9
<b>References.....</b>	<b>1</b>



# 1. Introduction

## 1.1 General

The occurrence of a major earthquake event is still seen as a catastrophe, with devastating consequences over human lives, buildings and transportation networks, causing a large scale impact in any society and multiple costs of different natures. Indeed, even if becoming particularly devastating to poor, underdeveloped countries, it equally greatly affects populations and several infrastructures in modern, industrialized countries, where, despite the advanced status of seismically designed structures, it is still possible to point out weakness points, such as historical or late XX century constructions, in need for retrofiting. From a more global picture, the occurrence of earthquakes can have an outcome which is reflected in affected country policies, during several years, given the deep changes in building philosophy or large investments in seismic design strategies.

A number of relatively recent earthquakes are typically referred to, due not only to their destructive impact but also to the lessons that were learnt, leading, sometimes, to profound changes or the establishment of turning points in seismic design philosophies. The San Fernando (1971), Loma Prieta (1989) or Northridge (1994) earthquakes in the USA; Kobe earthquake in Japan (1995); the 921 earthquake (1999), in Taiwan, are some of the examples of such important recorded events in the past few decades, together with other earthquakes that occurred in Turkey, Greece or China. The particular case of recent

earthquake events that stroke Italy in 2009 (L'Aquila earthquake); Haiti, in 2010; New Zealand and Japan, in 2011, denote essentially two different scenarios, both very pertinent. The first scenario, corresponding to the earthquakes that have occurred in so-called developed countries, with improved codes for seismic design, reveals how an earthquake can still cause severe damage, found in old, non retrofit constructions and in some new, supposedly seismic resisting, structures. On the other hand, the Haiti earthquake revealed the chaotic scenario that can be verified when the shaking takes place in poor, under development countries. Thousands of human losses occurred and several basic facilities became inoperable, mobilizing substantial international aid. The recognition of the importance of the role that earthquakes play in modern societies is, therefore, largely evident, in a much wider range of issues than sometimes thought.

There are two essential key intervening aspects, which any society needs to consider when drawing a response strategy to seismic hazard. The first is to develop efficiently enhanced building codes and guidelines, which become able, in the end, to assure that new constructions feature proper ductility characteristic, as well as energy dissipation mechanisms, allowing the structure to accommodate a much larger deformation demand, resisting and performing quite better, without collapsing, when facing earthquakes. The other intervention field is at the existing constructions assessment level. The number of existing structures that were built in the past, from hundreds to a few decades ago, with no regard for any seismic provisions is enormous. Such considerable portion of the total construction is extremely exposed to forthcoming seismic events, presents probably high vulnerability and needs, therefore, to be seismically assessed and, eventually, retrofit.

It is the author's belief, however, that effort has been more concentrated in the design of new structures side, rather than in the assessment of existing structures one. On that matter, considerable improvement has been made in the past few years, with the development of further refined methodologies, which include adequate consideration of relatively complex nonlinear structural models as well as highly refined probabilistic safety computation methods. Such approaches, seen as more accurate are, though, yet to become common procedure among practitioners. This is, in part, due to the several different methodologies that are available to reach a failure probability of an existing structure, as well as to the complexity of issues surrounding any possible safety assessment procedure. Moreover, detailed nonlinear analysis procedures continue to be complex, time-consuming and, for

that reason, common practice still majorly consists of elastically analysing the structures, with subsequent application of behaviour reduction factors. A summarizing work of the different approaches, stressing the relevant criteria, discarding unnecessary alternatives, in order to unify procedures and reduce the actual dispersion in methodologies is justified.

All of the drawn considerations become even more relevant on bridge structures, given that, traditionally, the majority of studies and frameworks have been focused on buildings, leaving space for a gap of knowledge that has, nonetheless, become less evident in the recent past. Even if typically highly resistant structures, many times protected by the deck's elastic behaviour, bridges are key elements in any region stricken by an earthquake and require therefore, special attention, due to their vital importance as connecting and transportation facilities. Indeed, in the immediate aftermath of an earthquake, closure of a bridge can impair emergency response operations.

The current challenge within the field of assessing existing structures, and therefore bridges, is to reach a failure probability, which takes into account the uncertainty of all the variables at stake. Furthermore, the applicability of such procedures in a current practice context is fundamental. To accomplish so, intermediate methodologies, less complex, but still improving with respect to the currently employed ones, by inclusion of simpler nonlinear features, can be considered within a transition process.

## **1.2 Motivation and goals**

The main goal of this work has been to probabilistically assess the seismic vulnerability of single existing reinforced concrete bridges to seismic action. Even if inevitably characterized by a certain level of ambiguity, the safety degree has been evaluated in a probabilistic fashion, i.e., through the computation of failure probability of single bridges, whose capacity features duly characterized uncertainty, when facing a specific seismic scenario, defined statistically as well. A deeper knowledge on different approaches for the collapse probability computation is sought and the influence of the different elements, or steps, of the safety assessment process is also studied in detail.

Indeed, the path to reach a final conclusion about the safety, or lack of, offered by a structural system is everything but straightforward and there is still no consensus among

the worldwide research community on a large number of aspects. As a result, this work aimed to look into as much detail as possible the different topics that need to be covered for the vulnerability evaluation, focusing on the particular case of bridge structures, trying to contribute to the exposure and clarification of the possible alternatives within each issue, providing as well, if possible, recommendations and guidelines for practitioners and future research. Such different issues include, from a macroscopic perspective, the definition of seismic input, which is naturally extremely variable, highly unpredictable, and able to be represented by different input modes; the structural modelling, featuring geometrical and material nonlinearity; the structural response estimation, which can be static or dynamic-based; and the final probabilistic computation itself, intersecting demand and capacity.

The study of each of the mentioned aspects has been systematically carried out by means of parametric studies, in which results were object of statistical treatment, in order to enable the covering of a high number of different structural configurations and earthquake records as well as to reach, as much as possible, generalized findings. An extensive battery of regular and irregular bridges, together with a relatively wide seismic input, is used to allow the fulfilment of the generalization purposes.

### **1.3 Thesis outline**

In order to fulfil the devised work objectives, each chapter of this thesis will go through every aspect considered to be relevant within a seismic assessment of bridges context, trying, as much as possible, to make it coincide with well defined steps of the natural path to follow within a full probabilistic vulnerability evaluation procedure. Most of the topics are strictly correlated and contribute to each others reciprocally, given that, structurally, everything is connected in some way. However, it would be impossible to present the work without sorting the topics in a predefined order, even if every choice would be arguable. The reader is hence asked to keep this in mind when going through the different chapters.

Firstly, an introduction to the seismic phenomenon is made in **Chapter 2**, featuring a brief description of the major earthquake events of the past decades, with the intent of stressing the importance and growing relevancy of the seismic assessment of existing structures, with special mention to bridges, as well as seismic design of new ones. Not only the devastating character of the ground shaking is highlighted but reference is continuously

made to specific structural damage occurring on bridges due to this sort of natural hazard. Afterwards, an initial approach to all the subjects involved in the process of assessing the seismic safety of bridges is presented, with the aim to summarize the state of knowledge and the main available paths for each of the tasks that need to be carried out towards the safety verification. The most significant advances in each theme are reviewed and topics still in need for further development are object of particular attention, hence, introducing the subsequent chapters.

The first of the aforementioned safety assessment process stages can be seen as the preparation of the seismic action to which the structure is expected to be subjected to. Accordingly, **Chapter 3** deals with the seismic action characterization, establishing a permanent correlation with the seismic analysis methods and its corresponding needs in terms of seismic input (Chapters 5 and 6). As a consequence, given the superior accuracy of nonlinear dynamic analysis, which is becoming more popular and disseminated within seismic assessment research, the main focus is on accelerograms, the most adequate input form of earthquake events. Aspects such as type of records, real or artificial, as well as selection and scaling techniques according to distinct intensity measures, when choice falls on the primer, are discussed and investigated, with a view to optimization. Based on a European integrated project, LESSLOSS, a brief case study, made up of a long, irregular viaduct, is parametrically analysed. An innovative intensity measure based on simplified pushover analysis is additionally proposed and preliminarily validated.

**Chapter 4** steps into the modelling topic, in which one of the most important issues is the inclusion of nonlinearity features. Indeed, nonlinear models are conspicuously needed for the employment of up to date methodologies, whether static or dynamic (reviewed in Chapter 5). An overview on geometrical and material nonlinearity is carried out, with emphasis on the latter. On such matter, the nonlinear material models, used for the characterization of reinforced concrete structures, are described, under monotonic and cyclic loading conditions. Furthermore, different ways of accounting for the material plasticity, namely through plastic hinges or fibres, are thoroughly evaluated by means of a detailed parametric study, which will enable the consideration of the most suitable type of model in extensive analyses in Chapter 6. The description of a case study of fourteen different bridge structures, as well as the seismic input, both used for the nonlinear modelling studies and within the subsequent subjects, is carried out.

After the seismic action and the nonlinear structural model are calibrated, the estimation of the structural response to such input, essential to the seismic demand definition, is the main scope of **Chapter 5**. Again, among the wide range of structural performance prediction possibilities, the analysis is centred in the comparison of the currently most considered as eligible tools: nonlinear static analysis or nonlinear dynamic analysis. Four commonly employed nonlinear static procedures are selected, individually calibrated and further statistically compared to nonlinear dynamic analysis, in terms of piers, deck and abutments different response parameters. Comparison is carried out for the case study and seismic input, both described in Chapter 4. The validity of using static approaches, when compared to dynamic counterparts, is investigated and relative performance of the different selected procedures is looked at as well.

The seismic safety assessment itself is at last dealt with in **Chapter 6**, making use of the previous chapters' conclusions. Featuring a deeply probabilistic nature, different methodologies are presented for the safety assessment, which foresee the failure probability computation. In order to accomplish so, as well as to duly incorporate the uncertainty associated to all the safety problem variables, both capacity and demand are statistically characterized by means of assumed and/or adjusted distributions, with the contribution of the findings and guidelines drawn in Chapters 3 and 4. Such statistical definition is carried out through the obtaining, when necessary, of random samples making use of the Latin Hypercube sampling technique, which is also thoroughly tested and calibrated. Furthermore, different ways of dealing with the uncertainty of the different variables, together with the use of different response prediction techniques, studied in Chapter 5, will yield distinct failure probability quantities. Distinction is essentially established between accounting for uncertainty local or globally and the use of static or dynamic vulnerability/fragility curves. Again, the different approaches are tested for the presented case study and observations are made towards the recognition of an optimum procedure, identifying patterns as a function of the bridge structural configuration.

Finally, in **Chapter 7**, a summary of concluding remarks, featuring a discussion of the most important findings of each subject, is presented. The level of accomplishment of the initial objectives of the work is appraised and future developments are suggested.



## 2. Seismic Assessment of Bridges

### 2.1 Introduction

Within the possible loading types to which a structure can be subjected to, seismic action is a highly unpredictable one, a characteristic that assumes an extreme importance and is widely recognized within the structural engineering field. For that reason, in situ post earthquake damage observation, experimental testing and probability based analysis methods are essential for an accurate seismic assessment procedure.

Unfortunately, the devastating effects of earthquakes that have been still affecting several populations in different countries for the past few years continue to be one of the disaster events that most uncover unexpected failure mechanisms and causes in structures subjected to such type of demand. Important advances in earthquake engineering of bridges have definitely been associated to the occurrence of intense seismic disasters, given that the observation of major seismic events allows the recognition of the structural damage extent, stimulating the development of more accurate and refined assessment methodologies as well as the definition of retrofitting solutions for the resisting elements, such as shear strengthening of the piers or improvements on the solutions for the foundations, pier-deck connection, amongst others. The initially observed damages were mainly related to the failure of the ground, whereas, as the bridges started to be built up of reinforced and

prestressed concrete, several different failure mechanisms, mostly the pier rupture kind of ones, appeared.

Additionally to the particular unpredictable character of the seismic action, bridge structures behave in a considerable different manner from building structures, something that has to do with the naturally irregular nature of the former sort of structures, highly vulnerable in the transverse direction, with respect to the development of the deck, as well as highly unknown, in terms of seismic behaviour, until the recent past.

Together with the experience that comes from observing the post-earthquake status of the structures, the thorough study of the seismic action itself is another fundamental issue, which has undergone intense development, mainly in the pursuance of an optimum way of selecting ground motion records and using them, so as to minimize the typically high dispersion that is found. Indeed, a major extent of the scatter that the results of any sort of nonlinear analysis present is frequently related to the irregularity characterizing the loading input.

At the same time, the techniques that are used to model the structure can equally lead to extensive debate, as a consequence of the considerable number of available alternatives, which go from geometrical to material modelling possibilities, including different degrees of elements discretization or hysteretic energy dissipation models as well. On such matter, the evolution along the past few years has definitely been outstanding, caused by a significant progress in the computational capacity, allowing more refined models to be considered and a greater amount of results data to be extracted from the analysis.

Any safety assessment process is carried out following a specific methodology that combines all the elements defining the capacity and the demand and, herein, the variety is even more pronounced, with a wide set of methods that can be used, from simplified, rough procedures to highly refined techniques. Several studies have been conducted, improving at the same time, methodologies with different detail levels, further and further, with the purpose of including them in current assessment, design and codes or guidelines. One of the greatest challenges has been the development of successively updated simple methodologies, yet credible and nonlinear, as the seismic action requires, for the use of practitioners and to be implemented in design codes. At the same time, more refined

alternatives have still continued to be calibrated until they become more user-friendly and the engineering community gets more familiarized with the sometimes complex concepts that are involved.

From a state-of-art point of view, within this chapter, a short review on the thematic of this work is intended, denoting the aspects of major relevance that are related to the seismic behaviour and safety assessment of bridges. Firstly, a few major earthquake events that have occurred in the recent past, which considerably affected reinforced concrete bridges, are mentioned emphasising the learned lessons and the critical issues that have lead to structural malfunction. Furthermore, with the recognition of the need for means to assess and identify vulnerable configurations, whether existing or new ones, a perspective on the different elements that are part of such endeavour and on what has been done in the past is carried out. The seismic action, a fairly complex one, is the first analysed element, in terms of types of representation, scaling techniques, amongst others. Indeed, the better characterized the seismic action is, the clearer and easier will the assessment process become. Structural modelling techniques, concerning nonlinear material models or energy dissipation, are another fundamental aspect, this one from the structure side. Finally, an overview on the typical ways of carrying out the safety assessment itself is presented, which will constitute no more than a contribute, given the wideness characterizing such matter.

Many of the concepts and notions that are herein presented are, in a certain way, universal, able to be implemented within the study of any sort of structures. It is well know, in addition, that the general knowledge in seismic behaviour of buildings, for instance, is quite superior than the one for bridges, which sometimes leads to the attempt of adapting some methodologies, developed bearing building frames in mind, to that sort of structures. According to such premises, the exposure that follows will consistently try to make the connection to the specific bridges case.

## **2.2 Recent earthquake events – major observations and lessons learned**

Bridges are a set of different elements working together in sometimes unexpected ways during earthquakes, rendering highly important the study of its behaviour during earthquakes. It has been relatively frequent that significant earthquakes have occurred and

strongly shaken populations all over the globe, affecting well developed, industrialized countries and less developed ones as well. The consequences are always significant and, sometimes, devastating, involving human lives and structures. In the past fifty years, approximately, the number of bridges, viaducts and special structures has increased hugely and so the effects of earthquakes have become more visible, calling the attention of the international community, even though not always to the desirable extent.

In previous studies on seismic behaviour of bridges (e.g., (Vaz, 1992; Delgado, 2009)) other authors pointed out the most relevant earthquake events in the twentieth century as well as more recent ones, in the past decade, recalling how undeniably topical seismic action is. It is not intended, therefore, herein, to be repetitive or exhaustive in describing the History around ground shaking but to provide the reader a context that enables better understanding of the importance of such matter and how the observation contributes to post-earthquake work guidance. The twentieth century has witnessed hundreds of earthquakes of magnitude 6 and above all over the globe. From a structural engineering point of view, the latter and the ones occurring in high building density regions, are more interesting, given that they have put to test a higher amount of bridges and viaducts, as well as more enhanced, up to date, seismic design criteria. On such basis, a set of the most representative earthquakes, having occurred in North America and Asia in the past thirty years, will be mentioned, mainly for their important contribute to bridges earthquake engineering. Furthermore, two major recent ground shaking events that took place in Europe and Central America will be briefly referred to, owing to their contemporaneity.

### ***2.2.1 Loma Prieta earthquake***

On such basis, the Loma Prieta earthquake, which shook the San Francisco Bay area of California in 1989, is a classical example of a natural disaster that largely affected a highly population density area, endowed with a vast highway transportation network. Causing a total of 63 casualties and near 4000 injuries, a particular aspect of this quake was that 42 of the casualties were due to the collapse of the two levels Cypress Street Viaduct of Interstate 880 in West Oakland, as illustrated in Figure 2.1. Nevertheless, less than five percent of the bridges exposed to ground shaking were damaged.

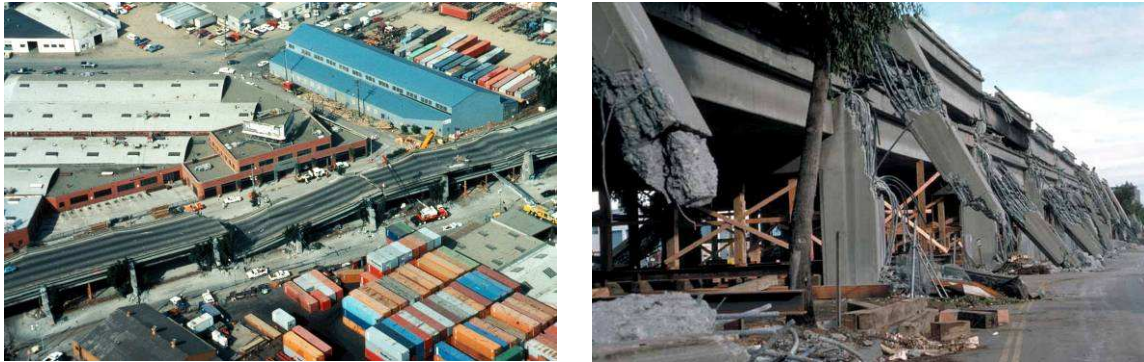


Figure 2.1 – Cypress viaduct collapse: *left* – aerial view; *right* – piers’ failure detailed view.

Two major factors, apart from soon after determined resonance effects, induced the collapse of the late 1950s-built viaduct: geotechnical issues and deficient reinforced concrete design. The upper and lower levels composing the structure were connected by two-column bents in a combination of cast concrete and four pin (shear key) connections. The upper deck in some sections was not securely fastened to the lower deck and, as the bridge vibrated during the earthquake, the pins connecting the levels also began to vibrate, causing the concrete surrounding the pins to crumble and break away. The lack of transverse reinforcement in the nodes connecting piers and deck was evident – see Figure 2.2 for detail. Indeed the connections of elements are often subjected to higher demand than the resisting elements themselves. The prediction of ductile connections was definitely not taken into consideration by the time the viaduct was built or strengthened.

As for geotechnical reasons, the viaduct was built on soft mud, weak soil, highly susceptible to liquefaction during an earthquake and exhibiting larger ground motion. Without the presence of concrete under the piers, those elements slid sideways under the weight of the upper deck and allowed a large portion of the upper deck to collapse (Yashinsky, 1998a). Several aspects of the design and construction of the structure have hence been suggested as contributing to its failure: inadequate transverse reinforcement in the piers, ineffective bent cap and pin connection design (Moehle, 1999) and improper compensation for the weak soil conditions (Yashinsky, 1998a).



Figure 2.2 – Cypress viaduct: lack of proper reinforcement in pier-deck connections.

The famous Oakland Bay Bridge, on the other hand, ended up suffering minor damage, as a section of the upper deck of the eastern truss portion of the bridge collapsed onto the deck below, indirectly causing one death. The satisfactory behaviour of such bridge has largely to do with the majority of the structure being made up steel, a material less vulnerable to seismic events than concrete, due to its inherently available ductility. The need for considerable attention to be paid to reinforced concrete bridges was, hence, confirmed.



Figure 2.3 – Oakland Bay Bridge: collapsed portion of the upper deck.

### ***2.2.2 Northridge earthquake***

The Northridge earthquake, named after a neighbourhood in the city of Los Angeles, California, occurred in 1994, lasting for about 45 seconds. With one of the highest ever measured ground accelerations in urban North America, in the range of 1.0g, it became one of the costliest natural disasters in the United States history, causing seventy two deaths and over 9000 injured.

After the Loma Prieta earthquake, in 1989, a retrofitting program was begun over Californian bridges and was yet to conclude when the Northridge earthquake took place. There were about 2000 bridges in the epicentral region; six of these bridges experienced failure and four others were so badly damaged they had to be replaced. The shaking was in the origin of considerable damage in the vast freeway network, with particular emphasis to the Santa Monica Freeway, which serves millions of commuters everyday, and the Antelope Valley Freeway, illustrated in Figure 2.4.



Figure 2.4 – Collapsed sections in Santa Monica freeway (*left*) and Antelope Valley Freeway (*right*).

The failure of those bridges was primarily due to the failure of the supporting columns that had been designed and constructed before 1971, a critical timing, given that after the San Fernando earthquake the standards for earthquake design began to be “toughened” considerably. The lack of proper concrete-core confinement, resulting in “birdcaging” effect of steel reinforcement, or poor behaviour of flared pier tops are some typical examples of column failure – see illustration in Figure 2.5.



The retrofitted bridges did not suffer serious damage, which consisted of, according to Yashinsky (1998b), minor cracks to the slope paving and settlement of the approach. In contrast, damage to unretrofit bridges at the same site was extensive.



Figure 2.5 – Failure of columns: insufficient confinement (*left*); shear failure of flared column with transverse reinforcement slipping (*right*).

Figure 2.6 illustrates the contrast between pier failure, due to lack of efficient reinforcement, and satisfactory behaving pier, provided with retrofitting (Cooper *et al.*, 1994).



Figure 2.6 – Failure of column due to failure of circular confinement steel (*left*); good behaviour of column retrofitted with steel jackets (*right*).

Indeed, bridges designed and built before 1971 performed worse than those designed according to most recent standards and piers were the most damaged components (Basoz and Kiremidjian, 1998). Still, the damage caused by the earthquake revealed that some structural specifications did not perform as well as expected, such as the case of two



bridges, both constructed shortly after the 1971 earthquake, on the Simi Valley-San Fernando Valley Freeway. These bridges presented severe column distress that resulted in bridge failure.

Other damage to bridges included spalling and cracking of concrete abutments, spalling of column-cover concrete, settlement of bridge approaches, and tipping or displacement of both steel- and neoprene-type bearings. Moreover, bridges with non-monolithic abutment types, discontinuous spans and single column bents performed poorly.

### ***2.2.3 Kobe earthquake***

The Great Hanshin earthquake, often referred to as Kobe earthquake, due to the city that was majorly stricken, occurred in January of 1995. It killed more than six thousand people, 4600 from the city of Kobe only. Even though experiencing ground shaking on a regular basis, this was Japan's worst earthquake since 1923. Comparison to the Northridge earthquake, which had occurred only one year before, was inevitable and less fortunate to the Kobe city side, given that damage was much greater than the one caused by the American quake. Such difference comes mainly from the type of ground beneath Kobe and the light, unreinforced construction type in masonry and wood.

The damage in highway bridges was one of the main post-earthquake images, coming from several different scenarios: substructure failure, originating from simple shear failure in reinforced concrete columns; premature shear failure at terminations of longitudinal bars with insufficient development lengths; extensive failure of steel columns, the first in the world; soil liquefaction, leading to settlements and tilting of foundations and substructures and lateral spreading of ground associated with soil liquefaction, causing movements of foundations.

One of the most impressive structural disasters was the collapsed eighteen spans in Fukae viaduct, inserted in Route 3, within the elevated Hanshin Expressway, illustrated in Figure 2.7.



Figure 2.7 – Collapsed Fukae Viaduct (*left*) and Premature Shear Failure of Reinforced Concrete Column, Fukae Viaduct (*right*) (Kawashima, 2007).

The viaduct was designed in accordance with the 1964 Design Specifications and was completed in 1969. The insufficient code provisions led to important problems in the design of the viaduct: the overestimated allowable shear stress, the insufficient development length of longitudinal bars terminated at mid-height and the insufficient amount of tie bars. The combination of these aspects originated the aforementioned extensive premature shear failure. Comparing the performance of this viaduct to the one of the parallel Route 5 viaduct of the same mentioned Expressway, completed in the early to mid-1990s, enhances the importance of the new seismic design stipulations, given that the latter behaved far better than the former, despite the potentially worse soil conditions.

Figure 2.8, taken from Kawashima's lecture notes (Kawashima, 2007), sketches the probable failure mechanism of the viaduct, where is extremely visible the importance of the proper reinforcement of the piers, especially at the base level, in order to assure a sufficient ductility level. To such extent, the adequate behaviour under high seismic demand will require good actual anchorage conditions.

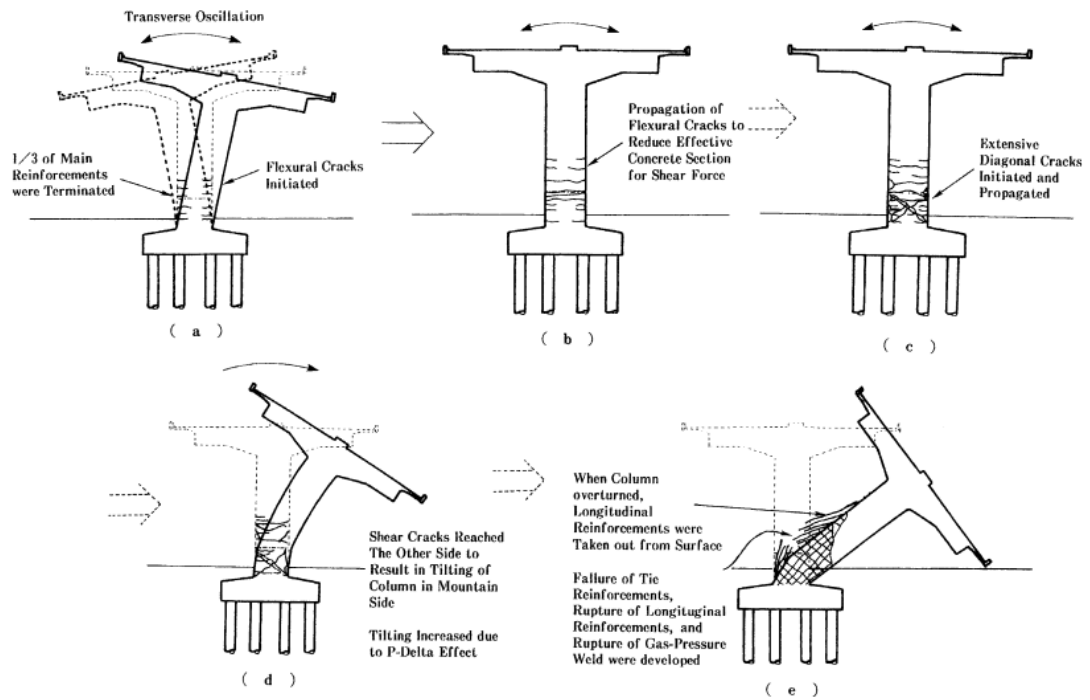


Figure 2.8 – Failure mechanism of Fukae Viaduct (Kawashima, 2007).

Soil failure was equally frequent as many of the bridges were founded on sand–gravel terraces (alluvial deposits) overlying gravel–sand–mud deposits at depths of less than ten meters, a condition which is believed to have led to site amplification of the bedrock motions. Several situations of liquefaction and lateral spreading, resulting in permanent substructure deformations and loss of superstructure support also occurred (Moehle and Eberhard, 1999). The collapse of the Nishinomiya-ko Bridge approach span, Figure 2.9, is good example of how the site conditions largely increased the vulnerability.



Figure 2.9 – Nishinomiya-ko Bridge approach span collapse (Kobe Collection, EERC Library, University of California, Berkeley).

Additional collapse of bridges resulted from damage of unseating prevention devices and from forces transfer through unseating prevention devices.

#### **2.2.4 L'Aquila earthquake**

In April, 2009, the L'Aquila earthquake occurred in the region of Abruzzo, in central Italy, featuring a magnitude of 6.3 on the Richter scale. Its epicentre was near L'Aquila, the capital of Abruzzo, which together with surrounding villages suffered most damage. The earthquake was felt throughout central Italy and 308 people are known to have died making it one of the deadliest earthquakes to hit Italy since the 1980. In spite of having occurred in a well developed country, with relatively advanced seismic regulation, the stroke effects were significant mostly because of the high number of medieval, historical constructions and unreinforced masonry buildings, known for being quite susceptible to the seismic action.

Not only medieval structures in L'Aquila suffered damage. Many relatively modern buildings, such as a local university dormitory, with nonductile concrete, soft-storey irregularities or new precast, suffered substantial damage as well. Damage extent even reached some buildings that were believed to be earthquake resistant. L'Aquila Hospital's new wing, which opened in 2000 and was thought capable of safely facing a strong earthquake, suffered extensive damage and had to be closed. This was, at some level, surprising, given that the event was moderate and the country modern. Failure was admitted as primarily due to the lack of consistent seismic design (Miyamoto *et al.*, 2009).

Nevertheless, transportation facilities, namely bridges, behaved reasonably, suffering minor damage. Indeed, major damage to such sort of structures would be expected for a higher magnitude earthquake or longer duration of strong ground shaking. The worst case corresponded to a short, 35 meters long, three-span, continuous reinforced concrete bridge, not far from the epicentre, which collapsed onto the riverbed, as visible in Figure 2.10.



Figure 2.10 – Bridge collapsed on the Aterno river, near Fossa (Grimaz and Maiolo, 2010).

The four reinforced concrete columns with hexagonal sections broke at the pier-slab connections, sliding sideways and penetrating the deck slab. Furthermore, it is believed that vertical downward motion was relevant to the failure of the bridge.

Other occurrences consisted of damage at the frame piers top of another three span continuous bridge, with additional damage of the superstructure by tensile cracking due to the movement of the piers towards the centre of the river, caused by movements of the embankment on both sides. A masonry arch bridge, which had collapsed before and was repaired by filling crashed limestone, collapsed again during the earthquake, due to probable movement of abutments, resulting in the loss of the arching effect. Finally, some of the viaducts within the A24 expressway near L'Aquila were affected by the earthquake, although the expressway itself did not collapse anywhere (Aydan *et al.*, 2009). Again, a major viewpoint is that, given the moderate nature of the ground motion, well seismic designed bridges should not have collapsed, which indicates a need for code review or a thorough existing structures safety assessment.

### ***2.2.5 Haiti earthquake***

The Haiti earthquake, one of the latest ground shaking events and probably one of the most catastrophic ones, took place in February, 2010, with massive human losses, taking the lives of more than 230 000 people. The consequences were devastating mainly due to the fact that there was a generalized lack of attention to earthquake-resistant design and construction practices and the poor quality of much of the construction. Indeed, the

historical pattern of earthquakes in Haiti indicates that an earthquake of high magnitude could strike southern Haiti near Port-au-Prince at any time.

According to field reports, it was not recognised any bridge failure due to the earthquake. Within Port-au-Prince, the majorly affected city, most of the crossings over streams were accommodated by box culverts, Figure 2.11, which did not appear to be damaged. In any case, these crossings can be hazardous in the future, given that large amount of garbage accumulated upstream such culverts may combine with silt and debris to prevent water from passing through the culverts (Eberhard *et al.*, 2010).



Figure 2.11 – Box culvert in Port-au-Prince (*left*); damage to shear key at intermediate support of bridge (*right*) (Eberhard *et al.*, 2010).

There were, anyway, river crossings on Nationale No. 2, most of them spanned by bridges with precast girders resting on cast-in-place reinforced concrete bents and supporting a cast-in-place deck. In two of such bridges damage was observed. One of them, the bridge over the Momance River presented minor pounding damage at the shear key at one of the intermediate supports that probably had not been adequately and/or properly reinforced. A similar bridge, in the Carrefour section of Port-au-Prince, suffered damage in the external shear keys at both intermediate supports, apparently caused by the lack of hook anchorage at the end of the top beam reinforcement.

One of the major findings of the scrutiny of Haiti's earthquake was that, even with the absence of seismographic stations during the main earthquake or its largest aftershocks, which could estimate accurately the intensity of ground motions, the indirect suggestion is that the earthquake did not produce ground motion enough to severely damage

well-designed structures. Several buildings and bearing-wall structures survived the earthquake with no signs of large deformation demands. Similarly, bridges near the epicentre suffered only minor damage and were able to function immediately after the earthquake. Such picture confirms, unfortunately, the lack of seismic-resistant conditions that still persist throughout the globe, with large incidence in poor countries.

### ***2.2.6 Christchurch earthquake and Tōhoku earthquake and tsunami***

The year of 2011 started early to feature severe earthquake disasters. Both events are herein presented together, not only for having taken place the same year but also because both occurred in so-called developed, wealthy countries, New Zealand and Japan.

The 2011 Christchurch earthquake was a 6.3-magnitude earthquake that struck the Canterbury region in New Zealand's South Island on 22 February 2011, causing widespread damage and multiple fatalities although no bridge collapses have been reported. It followed nearly six months after the 7.1 magnitude 2010 Canterbury earthquake that caused significant damage to the region but no direct fatalities. Analysts estimated that the earthquake could cost insurers US\$12 billion. Of the 3000 buildings inspected within the main avenues of the central city, around 45% have been given red or yellow stickers to restrict access because of safety problems and one thousand were expected to be demolished (around 25% of the total number of buildings). Many heritage buildings were also given red stickers after inspections but, in general, not many buildings have collapsed. Some examples include two six-storey buildings: the Canterbury Television building and the PGC Building, illustrated in Figure 2.12, a reinforced concrete building that had been constructed in 1963-1964, which drew significant amount of attention of the high vulnerability of pre-1970s mid- and high-rise buildings. The poor seismic behaviour of these buildings includes column shear failure, beam-column joint failure, onset of soft-storey failure, shear wall failure, etc. The 26-storey Grand Chancellor building, Christchurch's tallest hotel, was reported to be on the verge of collapse and was indicated for demolition pointed to be demolished over the following six months. While damage occurred to many older buildings, particularly those with unreinforced masonry and those built before stringent earthquakes codes were introduced, high rises built within the past twenty to thirty years performed well (Kam, 2011).





Figure 2.12 – The Pyne Gould Corporation (PGC) Building following the 2011 Christchurch earthquake.

The 2011 Tōhoku earthquake, officially named the Great East Japan Earthquake, was a 9.0-magnitude 9.0 undersea megathrust earthquake off the coast of Japan that occurred on March 11<sup>th</sup>. It was considered the most powerful known earthquake to have hit Japan, and one of the five most powerful earthquakes in the world overall since modern record-keeping began in 1900. The earthquake triggered extremely destructive tsunami waves, causing numerous casualties (approximately 14 616 deaths, 5278 injured and 11 111 people missing), destruction of infrastructures and a number of nuclear accidents. The overall cost could exceed \$300 billion. Structurally, over 125 000 buildings were damaged or destroyed, as well as roads, railways and bridges, and a dam collapsed.

Apart from the obviously numerous structural failure occurrences, such as the bridge failure illustrated in Figure 2.13, the 2011 Japan earthquake caused a serious nuclear accident, affecting, in the present and future years, the planet natural resources, as well as worldwide population.



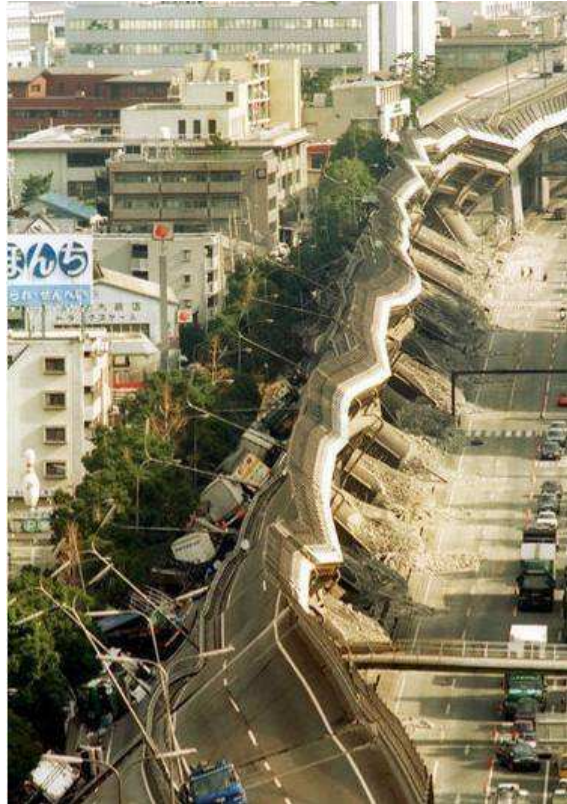


Figure 2.13 – Bridge collapse in 2011 Japan Earthquake and Tsunami.

The devastating way how ground shaking recently stroke New Zealand and Japan constitutes a sad, yet important, reminder of how vulnerable modern societies, even in relatively well-prepared countries, still are to seismic events.

### ***2.2.7 Summary***

The purpose of this section was to identify and briefly describe types of earthquake-induced damage to bridges and, where possible, to identify the causes of the damage. This is a task of recognized importance because of the obviously dramatic and severe consequences associated to bridge failure as well as the need for taking lesson from those disasters. It is not, however, a simple endeavour, given that damage process is complex and comes from the interaction of several contributing variables. Moreover, when damage is intense to the point of concealing detail and damage deformation itself, some speculative judgment may be needed for each particular collapse, being difficult to generalize the causes of bridge damage.

In the past, bridges responded to earthquakes in a very particular manner, each case depending on the characteristics of the ground motion at the particular site and the construction details of the specific bridge. Despite such individuality, it was still possible to learn from past earthquake damage, once that many types of damage occur repeatedly. With such observation, over the years, bridge seismic design practices evolved, largely reflecting lessons learned from performance in past earthquake events.

Within the North American situation, the rapid change in bridge construction practice following the 1971 San Fernando earthquake was evident (Hall, 1995). Prior to that, California design and construction practice was based on significantly lower design forces and less stringent detailing requirements compared with current requirements. With the 1989 Loma Prieta and the 1994 Northridge earthquakes, insightful study on bridge structural failure has gained strength, with the recognition for a needed review and update of seismic design, code and construction criteria. Indeed, major collapse situations due to the insufficient reinforcement of the piers, poorly designed connections between piers and deck, subjected to high demand, were observed, denoting a turning point towards more refined seismic specifications.

Moreover, although typically associated to older bridge rupture situations, soil failure still kept on being the cause of several collapses, influenced by proximity of the bridge to the fault and site conditions. Site conditions were clearly responsible for the bridge response in the 1989 Loma Prieta earthquake leading to the conclusion that local site conditions have significant impact on amplifying strong ground motion, and the subsequent increased vulnerability of bridges on soft soil sites. During the 1995 Kobe earthquake, significant damage and collapse likewise occurred in elevated roadways and bridges founded on alluvial deposits, which is believed to have led to site amplification of the bedrock motion.

In spite of the considerable effort that has been made in the past two or three decades in the improvement of seismic reinforcement and regulation, there are still disastrous events on a regular basis, compromising numerous existing structures as well as the lives of those who daily make use of them. Two of the most recent earthquakes that have been mentioned, L'Aquila and Haiti, prove how, in the past couple of years, it is still possible, not to say likely, for high structural and human damage to occur, even with modern construction and regulations. In such cases, failure took place because of the lack of attention in design and

construction to the possibility of earthquakes or poor construction practices. The Haiti case foresees probable future scenarios of huge metropolis being hit by earthquakes, suffering from massive destruction and human lives taking. The equally recent New Zealand and Japan earthquakes have again proved their destructive capacity, even if in presence of seismically prepared countries. The certainty that there is still a long path to run, with respect to seismic design and performance, is probably an equally important lesson to constantly keep in mind.

### **2.3 The seismic action**

As one of the key issues in any vulnerability analysis, the load definition requires considerable attention and sometimes, such as the case of the seismic action, thorough calibration. Moreover, reduction of dispersion is often needed given the high variability and uncertainty that characterizes earthquakes. The most logical and insightful way of representing the seismic action is by means of accelerograms, the time-history registration of the ground motion accelerations (eventually displacements or velocities) that are measured throughout the duration of the shaking. Depending on the sort of analysis that is being employed, other simplified representation possibilities, such as response spectra, that are usually implemented in code provisions or equally simplified methods, such as nonlinear static procedures, may be used. On the other hand, if a nonlinear dynamic analysis is intended, the use of accelerograms is fundamental and should be handled with care, given the disparity that often occurs within the several available types of records.

Accelerograms play an extremely important role when performing dynamic analyses, especially if nonlinear behaviour is considered. As an element which characterizes seismic action, it is possible to adopt accelerograms associated to different intensity levels and occurrence probability. At the same time, shape and energetic content characteristics of each record strongly influence any structural response. Thus, taking the pointed reasons in account, the importance of carefully evaluating the set of accelerograms to use is easily justified. A lot has been done in the recent past within this domain, particularly regarding selecting and scaling techniques, which is related to type of records and intensity level, respectively.

A very relevant aspect that can be deepened is the option between using real or artificial ground motion records, putting synthetic ones aside. This is actually the main issue: what sort of ground motion records is best to use? The choice for any of these types naturally involves each one's advantages and potentialities. At the same time, the interest remains on a practical and systematic analysis, a feature that may be associated to artificial records, but on the other hand one should avoid seismic records that may conduce to excessive structural effects, with loss of reality and overestimating design. Additionally, the sort of structure that is being object of analysis can be conditioning as well.

### ***2.3.1 Selection and scaling of real records***

The use of real records is naturally advantageous, given that the analysis will definitely become more genuine. Moreover, online databases of real ground motion records are becoming more and more available, for every typical spot of intense earthquake activity. It seems, hence, that an interesting combination of such a realistic as possible analysis, which is adequate, given the specific features of the seismic action, together with what is intended in a seismic analysis, arises with the use of real records, avoiding the need for generating artificial ones. Nevertheless, it is immediate to realise that the record-to-record variation associated not only to the real earthquake records parameters, such as duration, magnitude, epicentral distance, peak ground acceleration but to the subsequent structural engineering demand parameters median values as well, namely response spectra or ductility demand, will be higher in a great amount. Furthermore, not all the magnitude-distance-soil combinations are covered and spectra are generally not smoothed.

Although it is still not current practice, Eurocode 8 itself already considers the possibility of using real earthquake records. In fact, it recommends them, in Part 2 – Bridges (CEN, 2005b), comparing to the use of artificial ones, when performing nonlinear analyses, whereas for buildings, Part 1 (CEN, 2005a), no recommendation is given. With the choice for real records type in nonlinear dynamic analyses, a great number of other aspects arises, which has been the study target of quite wide research activity, with some considerable progress in the past few years.

In a logical proceeding order, the first step is to perform an initial selection of the accelerograms to use. Should it be randomly or based on geotechnical parameters or any

alternative techniques? Studies from Shome *et al.* (1998) or Bommer and Acevedo (2004) have addressed this issue whether selecting and cataloguing records based on magnitude and occurrence distance, in the case of the former, whether proposing a selection based on a code response spectrum matching procedure, minimizing the residual distance between the spectra.

After the initial selection of records, there is the need for a scaling technique to put them at a same level. The effectiveness of a certain technique may depend or not of ground motion parameters and should be verified on different structural systems. The majority of the past research studies were developed focusing intensity-based methods to scale ground motions, which keep the original non-stationary content and only modify its amplitude. Instead, spectral matching techniques that modify the frequency content or phasing of the record to match its response spectrum to the target spectrum can be considered.

Generally, two categories for intensity-based scaling techniques can be defined, according to the nature of parameters in which they are based. These can derive from records' inherent characteristics or from the corresponding response spectra. The first significant attempt to establish a comparison between several different intensity-based techniques was performed by Nau and Hall (1984). Such work has proved that scaling ground motions to match a target value of peak ground acceleration, which was the earliest approach, yielded inaccurate estimates with large dispersion. The study analysed six scaling techniques based on ground motion data and two based on response quantities used to normalize earthquake response spectra. The results seemed to show that traditional techniques, such as the ones considering peak ground reference values, tend to lead to high scatter, while spectrum intensities or Fourier amplitudes were considered as promising alternative scaling parameters. That study was, although, carried out considering only response spectra scaling, thus, effects on single-degree-of-freedom (SDOF) systems. The twelve selected records followed no particular criteria, such as the conventional seismologic properties, magnitude or epicentral distance, for instance. The purpose of covering a relatively wide range on those variables was sought, though. Similar findings can be found in work from Miranda (1993), Vidic *et al.* (1994) or Shome and Cornell (1998).

Later, Shome *et al.* (1998) looked at the use of real accelerograms from a different perspective, trying to address other issues, like the initial selection of records or the

appropriate number to use. The initial selection and cataloguing was based on the earthquakes magnitude and distance. Nevertheless, based on the nonlinear response of a five-DOF steel structure, the study ended up by concluding that those ground motions parameters do not have great influence. Different scaling techniques were once more tested. On this matter, conclusions pointed towards the consideration of spectral acceleration at the fundamental frequency of the structure as a better performing technique, recommending the use of peak ground acceleration to be disregarded. It is also noted by the authors that the conclusions were based on the analysis of the single multi-degree-of-freedom (MDOF) referred structure, highlighting the fact that, namely on scaling parameters, little work has been done on that sort of structures.

More recently, works conducted by Kappos and Kyriakakis (2000) and Kurama and Farrow (2003) revisited the natural records issue. The former presented some developments, mainly focusing on comparative analysis and new scaling parameters, and different seismotectonic environments on elastic or inelastic spectra, hence, SDOF systems. Also MDOF structures were analysed, particularly multi-storey frames. Conclusions on elastic spectral scaling indicated that generally, for intermediate and long period range, velocity-related parameters performed well, whilst, in inelastic conditions, spectrum intensity scaling produces better effects. Concerning effects on MDOF systems, spectrum intensity scaling continues to be the choice, either based on elastic spectra or inelastic pseudo-velocity spectrum. Similarly, Kurama and Farrow (2003), in their study, went back into ground motion scaling methods, analysing seven different techniques, insisting on different site conditions, such as soil profile and epicentral distance. SDOF and MDOF systems were tested with twenty records per soil profile. The study proposes another parameter to scale the records, which generally performs better across the considered site soil characteristics, for different structural types.

All the other scalar intensity measures, in general, have hence been found to be inaccurate and inefficient as well. Moreover, within most of the studies, with the exception of the work from Shome *et al.* (1998), none of the tested parameters considered any property of the structure to be analyzed. By including vibration data of the structure when scaling records to a target value of the elastic spectral acceleration, for instance, from a code-based design spectrum or PSHA-based uniform hazard spectrum at the fundamental vibration period of the structure, results became actually quite improved, nevertheless, for structures

whose response is dominated by their first-mode. When structures respond significantly in their higher vibration modes or far into the inelastic range, accuracy and efficiency decrease, as shown by the works of Kurama and Farrow (2003), Mehanny and Deierlein (2000), Alavi and Krawinkler (2004). There have been, though, approaches to scalar intensity measure parameters that consider higher modes response, combining spectral accelerations at the first two periods, developed by Bazzurro (1998) and Shome and Cornell (1999). In spite of improving accuracy, such measure remained inefficient for near-fault records with a dominant velocity pulse, as observed by Baker and Cornell (2006).

Alternative approaches, such as scaling earthquake records to minimize the difference between elastic response spectrum and target spectrum have also been followed, in some cases, implementing genetic algorithms (Alavi and Krawinkler, 2004; Kennedy *et al.*, 1984; Malhotra, 2003; Naeim *et al.*, 2004).

Intensity based measures can still be distinguished depending on whether they are based on the elastic response of the structure, relying on the structural period only, or they account for the inelastic features, taking structural strength into consideration. When the inelastic spectral deformation is significantly larger than corresponding elastic one, the elastic response based parameters, such as the ones that are tested in the studies previously mentioned, become less appropriate. The recognition of such situation led to the recent proposal of scaling parameters that are based on inelastic deformation spectrum, with improved estimates of median values and dispersion of control parameters (Bazzurro and Luco, 2006; Luco and Cornell, 2007). Studies carried out by means of dynamic analyses of generic frames subjected to different intensity levels, revealed promising results obtained when records were scaled with parameters defined as the inelastic deformation of the first mode equivalent single degree of freedom system, especially when compared to elastic response based ones (Tothong and Luco, 2007; Tothong and Cornell, 2008).

In terms of existing regulations, available American guidelines concerning building codes have addressed this issue prescribing methodologies to the scaling of ground motion records for a site-specific hazard. International Building Code (IBC) (ICC, 2006) and California Building Code (CBC) (CBSC, 2007) require earthquake records to be scaled according to the ASCE 7-05 provisions (ASCE, 2005). Provisions are established for 2D

analysis of regular structures, establishing that ground motions are scaled such that the average value of the 5%-damped elastic response spectra for a set of scaled motions is not less than the design response spectrum over a specific period range. Specific conditions are defined for structures having plan irregularities or without independent orthogonal lateral load resisting systems where 3D analyses need to be carried out.

Following the structural response based scaling parameters trend, a recent advanced method has been proposed by Kalkan and Chopra (2010), consisting of a modal-pushover-based scaling (MPS) technique to scale ground motions for use in nonlinear dynamic analysis of buildings and bridges. Ground motions are scaled to match (to a specified tolerance) a target value of the inelastic deformation of the first-mode inelastic single-degree-of-freedom system whose properties are determined by first-mode pushover analysis. The authors consider it appropriate for first-mode dominated structures, extending it, though, for structures with significant contributions of higher modes by considering elastic deformation of higher-mode SDOF systems in selecting a subset of the scaled ground motions. Within the application of the methodology, two bridges and six actual buildings, covering low-, mid-, and high-rise building types in California, were tested, confirming the accuracy and efficiency of the MPS procedure as well as its superiority over the ASCE 7-05 (ASCE, 2005) scaling procedure.

### ***2.3.2 Number of records***

Following the initial selection and scaling of records, in order to carry out the seismic analysis, the number of real records to use assumes critical importance. Basically, such issue has the underlying idea that one expects a certain number of different ground motion records to be able to estimate, trustfully, mean or median results, avoiding a cumbersome procedure, made of too many runs. Shome *et al.* (1998) dealt with the number of ground motion records to consider, in their aforementioned study, in a statistical way, through the definition of a confidence interval necessary to guarantee a dispersion level. That dispersion turned out as acceptable if seven records were used. Also the work from Bommer and Acevedo (2004) has addressed this issue, mainly from a qualitative point of view, analysing current design codes guidance and recent research on that matter. Their conclusions, in accordance with the existing variability in recommendations, tried to leave



the subject as flexible as possible, in a sense that each case should be considered individually, according to variables of multiple natures.

A recent work from Bradley (2011), estimated the seismic demand from seismic response analyses, from a probabilistic point of view, making use of the 84<sup>th</sup> percentile of the distribution of the sample mean seismic demand as the design seismic demand. That study took into account the number of ground motions considered, how the ground motions were selected and scaled and the differing variability in estimating different types of seismic response parameters, within a proposed simple three-step procedure suitable for routine design implementation.

From what has been mentioned, seems clear that using real earthquake records is no simple task, involving several aspects that conspicuously need to be looked at with some care. The advantages of using such genuine sort of records, and corresponding response spectra, to represent the seismic action has motivated intense research in the recent past, with the purpose of reducing the natural variation that is found. Some issues, such as scaling techniques, have been focused quite more thoroughly than others previously pointed out. Apart from that, the conducted studies until the moment are characterized by large heterogeneity, as far as topics and variables in the analyses or considered structural types are concerned. Moreover, the tendency has been to approach the problem by the inelastic structural effects side, rather than by the records' characteristics one, which will certainly be the basis of future code provisions.

As stated before, some studies considered geotechnical parameters while others denied their importance when selecting real accelerograms; some based their conclusions on the study of SDOF systems while others tried to call out results from MDOF systems; some follow certain criteria to initially select the records or try to reasonably define how many to use, others simply use an apparently sufficient number, in order to cover a considerable range of possibilities. Moreover, and moving forward within the use of accelerograms in seismic analyses, artificial records still represent a viable alternative and should therefore be eventually confronted to real records, something that seems not to have still been properly addressed. The option between one of the types, or even the possible indifferent choice for one of them, relating such option with the structural type that is being looked thorough, bridges in particular, is therefore a topic of clear significance.

## **2.4 Nonlinear seismic analysis – methods for structural response prediction**

Following the proper characterization of the seismic action, its multiple level uncertainties and dispersion, the seismic analysis itself, including the explicit consideration of the nonlinear effects, is an equally complex task, involving several aspects that need thorough concern. The main distinction between basic possibilities of approaching the problem has been, however, quite simple and immediate; the choice has laid on inelastic static analysis, typically recurring to pushover based algorithms, or inelastic dynamic analysis.

As noted by Elnashai (2002), inelastic static analysis is widely implemented in design office environment and is by far more familiar to practitioners than the dynamic alternative. Reasons such as complexity of time-integration algorithms or difficulties in defining damping, as well as the variation induced in acceleration and force related quantities by the combination of both issues, are pointed out by the mention state-of-art review to justify the still actual tendency. Other motives can be added, such as the significant amount of output information that nonlinear dynamic analysis yields, or the extensive number of parameters that need to be calibrated for the analysis to work out properly. Appropriate adjustment of such parameters may become a harsh task if the user has no experience or knowledge in advanced nonlinear analysis, which is probably the case of most of the design office structural engineers. Furthermore, the application domains of both sorts of analysis have not necessarily been crossing each other, something that has enabled a certain development in parallel. Static analysis has proven to represent dynamic response with a satisfactory accuracy level and has seen considerable progress, starting with quite simple attempts (Freeman *et al.*, 1975; Saiidi and Sozen, 1981; Kunnath *et al.*, 1992; Lawson *et al.*, 1994) but recently evolving to proposals of advanced pushover-based methodologies. Nevertheless, nonlinear static analysis is mostly useful and intuitive for the estimation of capacity. Structural effects, or demand, need to be determined later, through the inclusion of response spectra, not in a direct fashion, hence. Contrarily, dynamic analysis has the advantage of allowing structural members, with corresponding capacity duly modelled, to be submitted to the seismic action, knowing demand time-step by time-step, which again reinforces the idea that nonlinear dynamic analysis, despite possible complexity issues, has its place.

It is still not clear how the nonlinear analysis domain is to be shared between static or dynamic analysis. It seems clear that both domains tend to coexist and intersect each other. When static procedures are too simplistic for structures that demand higher accuracy, dynamic analysis will work as a complementing alternative, and vice-versa. There is no clear evolution trend when it comes to analysis types: in spite of being considered the most true and complete methodology, inelastic dynamic analysis is still not implemented and nonlinear static procedures, as well as other recent simplified alternatives, are nevertheless a great improvement over presently employed elastic evaluation procedures.

In the beginning of the past decade, Elnashai (2002) presented an interesting diagram, reproduced in Figure 2.14, illustrating the static and dynamic interaction domains, as function of strong-motion peculiarity and structural irregularity.

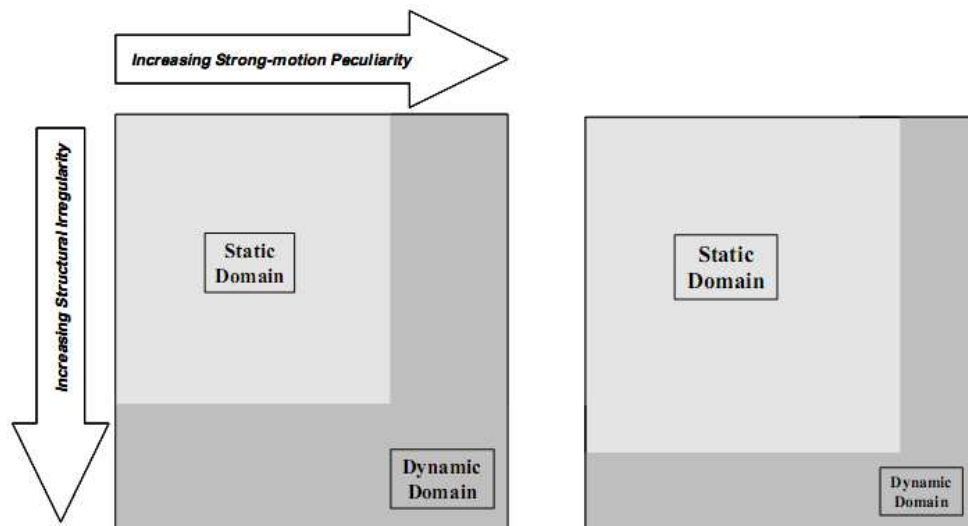


Figure 2.14 – Effect of development of advanced static analysis on model-input motion application domain (Elnashai, 2002).

Although it has been argued that static domain tends to expand as a consequence of higher refinement in nonlinear static procedures that have undergone, it is to the author's belief that such tendency merely reflects the actual analysis methodologies distribution within design office environment and that a future scenario will consist of increasing parity between such two major domains.

In what follows a brief discussion on the evolution and conditions of implementation of the different analysis alternatives is carried out.

### **2.4.1 Nonlinear static analysis – pushover**

The basic concept behind the technique of a pushover analysis has actually no rigorous theoretical basis and is to assume that, as referred in (Elnashai, 2002), “if a set of actions or deformations can be found such that a particular response mode, or a combination of modes, is represented statically, then the response of the structure under a monotonically increasing vector of actions or deformations may replace results from dynamic analysis”. The major assumption is simultaneously the main limitation of any pushover analysis, used to assess the capacity of the structure. In order to reach the structural effects caused by certain seismic action, the capacity curve must be intersected with the demand spectrum, which will define the performance point, often referred to by the corresponding target displacement. Herein, different possibilities have been suggested by different authors: Freeman (1998) proposed a method making use of elastic overdamped spectrum, whereas Fajfar (1999) was pioneering in implementing inelastic spectra in nonlinear static pushover procedures.

Other disadvantages of the pushover-based methods for estimating demand are the needed transformations of the MDOF structures under analysis into equivalent SDOF systems, which, understandably, carry a considerable degree of simplification. Once more, the formulation of such SDOF system is not unique, each author following a slightly different path, based on the common principle that the deformed shape of the structure is not excessively altered during the dynamic loading. Consequently, the inclusion of more than the first mode contribution to the analysis, which can play an extremely important part, has become one of the key challenges within recent proposals of pushover techniques. If bridge structures, of well known irregular and higher mode dependent behaviour, are kept in mind, the need for such endeavour becomes even more apparent.

Krawinkler and Seneviratna (1998) addressed the use of pushover analysis in seismic performance evaluation, summing up advantages and pitfalls, recognizing it as a valuable tool in today’s limited states of knowledge and practice. A pushover analysis used for demand prediction is certainly not highly accurate but neither the seismic action nor capacity estimates are. According to such review, the accuracy is essentially affected by the aspects around the estimation of the target displacement and the selection of load patterns that supposedly deform the structure in a similar way to expected when an

earthquake occurs. The authors emphasize difficulties and ambiguities around modifications needed to be applied to elastic demand spectrum, fundamental for target displacement location, to account for yield strength, stiffness degradation or pinching effect, strength deterioration, P-delta effects, viscous damping, among others. The load pattern is considered to be even more critical and is pointed out by the authors as probably the weakest point of the pushover analysis procedures, mainly if invariant patterns are used in long period structures with localized yielding mechanisms. Indeed, regardless the load pattern that is chosen, it will trigger certain deformation modes and miss others that are propelled by dynamic response and inelastic response characteristics. Major conclusions point towards the acknowledgment of the potential use of inelastic pushover analysis in demand prediction in many cases, able to provide information more relevant than static or dynamic analysis, mostly for structures that vibrate primarily in the fundamental mode.

As an attempt to overcome the mentioned drawbacks, namely the lack of higher modes contribution or the invariant nature of the load pattern, more advanced algorithms of pushover analysis have been proposed in the recent past, such as a Multi-Modal Pushover Procedure, by Paret *et al.* (1996), later improved by Moghadam and Tso (2002). A modal pushover analysis method, consisting of the repetition of single pushover analysis, corresponding to each relevant mode, with quadratic combination of results in the end, has been proposed by different authors Chopra in the beginning of the past decade (Chopra and Goel, 2001, 2002). This is probably the most intuitive way of considering higher mode effects, although not necessarily the most advantageous. Several improvements and application studies to probe the suitability of the method to different structural types have been presented thereafter (Chintanapakdee and Chopra, 2003; Chopra, 2005; Chopra and Chintanapakdee, 2004; Chopra and Goel, 2004; Goel, 2005; Goel and Chopra, 2004, 2005a, 2005b).

From a different perspective, other alternative procedures have been recently proposed, working on the type of pushover analysis that is employed. With the purpose of including higher mode effects, as well as better accounting for degradation characteristics with increasing loading and including the characteristics of the input ground motion, several authors, Bracci *et al.* (1997), Gupta and Kunnath (2000), Elnashai (2001), Antoniou and Pinho (2004) or Antoniou *et al.* (2002), proposed adaptive or fully adaptive pushover analysis techniques. Frequently applied together with spectrum scaling, it consisted of the

application of displacements, or forces, in an adaptive fashion, that is, with the possibility of updating the loading pattern according to the structural properties of the model at each step of the analysis, as in Figure 2.15, left. In such way, the structural stiffness at different deformation levels is considered in the evaluation of the new forces, the system degradation and period elongation can be accounted for and the alteration of the inertia loads during dynamic analysis for different deformation levels may be successfully modelled. The advantage in such procedure is to avoid the repetition of independent pushover analysis, as many as the relevant vibration modes, using a unique pushover analysis that, hopefully, includes all the relevant features neglected by the conventional analysis. The innovative algorithm proved to be numerically stable, even in the highly inelastic region, whereas the additional modelling and computational effort, with respect to conventional pushover procedures, is negligible. At most, it can be argued that additional complexity may come in terms of access to an efficient eigenvalue solver, scaling forces by spectral ordinates, updating applied forces or displacements vectors. Such possible complications are, however, on the programmer, rather than the user side, hence, no complexity is effectively added.

In Figure 2.15, right, results taken from work of the adaptive pushover authors show the proximity of response, using the adaptive technique for a building frame, to dynamic analysis, when compared to conventional pushover with two different load patterns.

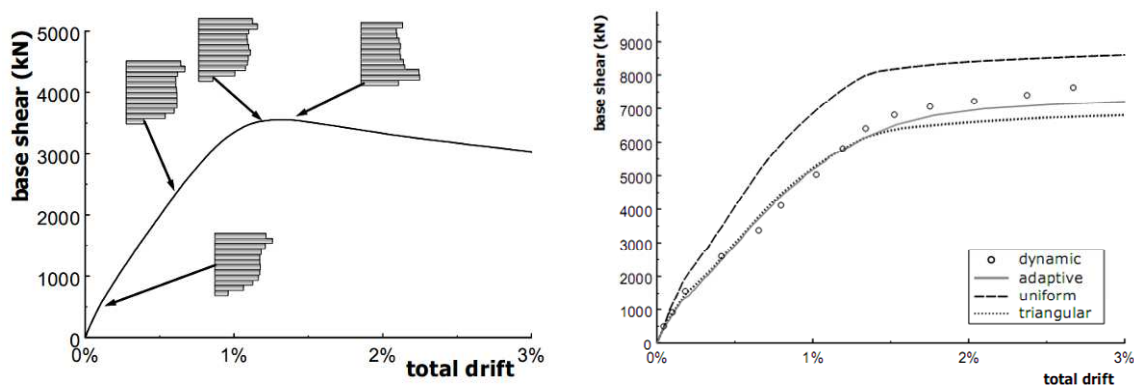


Figure 2.15 – Adaptive pushover: shape of loading vector updated at each analysis step (left) (Pinho and Antoniou, 2005); Adaptive vs. conventional pushover procedures (right) (Antoniou *et al.*, 2002).

Conventional pushover, regardless the load shape, seems to provide a certain envelope to dynamic analysis results whilst adaptive pushover is the one that gets closer.

Additional recent attempts to improve the results obtained by the nonlinear static procedures have been done by carrying out adaptive pushover analyses for each significant vibration mode, together with energy based modal capacity curves, such as the proposal of Kalkan and Kunnath (2006). Notwithstanding the value and benefits coming from further and further advanced procedures, it is important not to fall into a complexity level similar to the dynamic analysis one, losing the original purpose of simplicity of pushover based methods.

#### ***2.4.2 Nonlinear dynamic analysis***

Nonlinear dynamic analysis has always been seen as the most general and natural approach to predict the dynamic structural response, however, due to the large computational demand, its implementation within seismic analysis and design is yet to become usual practice. The requirements around the dynamic analysis, summarized by Elnashai (2002), in comparison to static pushover analysis, are substantially higher in number and complexity level, as reviewed in Table 2.1.

Table 2.1 – Comparison of requirements for static and dynamic analysis (Elnashai, 2002).

<b>Static Analysis</b>	<b>Dynamic Analysis</b>
Detailed models needed	Detailed models needed
Stiffness and strength represented	Stiffness and strength represented
No mass representation required*	Mass representation required
No damping representation required	Damping representation required
No additional operators required	Time integration operators required
No input motion required	Input motion required
Target displacement required	Target displacement is an output
Action distribution fixed*	Actions vary in time
Usually faster than dynamic analysis	Usually slower than static analysis

\*This may not be the case for advanced adaptive pushover

Essentially, dynamic analysis is widely recognized as the excellence tool for estimating seismic response, but is at the same time demanding, computationally and in terms of technical knowledge. It is still not common that practitioners experience covers all the needed parameters. The integration scheme is a crucial aspect and has been found to profoundly affect the results, as well as to compromise the analysis in several other

aspects, such as numerical stability or time step. Another critical parameter is the damping definition, elastic viscous or hysteretic, which is believed to cause variations of 50% or more in force response prediction (Elnashai, 2002; Priestley and Grant, 2005; Hall, 2006), as well as to contribute to numerical (in)stability. The input force itself, the ground motion, expressed in the form of one or more accelerograms, is a decisive and problematic issue itself, in terms of type of records, intensity or standardization, among others (see 2.3 for further detail).

The importance of the mentioned factors, is generally recognized, as summarized by Spacone *et al.* (2008), describing the unresolved issues within the use of nonlinear dynamic analysis as: the selection of an appropriate structural model, the selection of ground motions, the selection of a correct damping matrix, the heavy computational effort and the large volume of output quantities to be analysed.

Some indications are given as for the selection and nature of ground motion records within regulation codes, such as EC8 (CEN, 2005a). Moreover, it is commonly believed that recorded accelerograms are less demanding on the structures and should be used for actual design of structures. On the other hand, generated accelerograms present the opposite tendency and, therefore, are claimed by some to be used in research work to refine nonlinear methods of analysis. Given the extensive nature of the topic of nonlinear analysis, there are still no thorough studies and discussion is still going on in countries where dynamic analysis is starting to be applied broadly.

The damping issue is as important as controversial in nonlinear dynamic analysis. Hysteretic damping is usually responsible for the majority of the energy dissipation during the earthquake action. A remaining smaller amount of non-hysteretic or elastic viscous damping, the designation lacks consensus, resulting from physical phenomena involving structural and non-structural elements is also activated. Such portion has been traditionally considered by means of an equivalent viscous damping parameter, quantified by the Rayleigh damping model, as advocated by Clough and Penzien (1993) or Chopra (1995), believed to range from 1% to 8%, depending on several factors (Wakabayashi, 1986), or around 2% to 3%, always under 5% for an inelastic structure, as referred in (Spacone *et al.*, 2008). Generally, the more accurate the nonlinear structural model is, the lower the damping ratios should be (Panagiotou and Restrepo, 2007). The approach of using



equivalent viscous damping concept to represent energy dissipation sources that are not explicitly included in the model are admonished by authors such as Wilson (2002), but still supported by others, although with the recommendation for abandoning the Rayleigh damping model, which is proportional to mass and stiffness. A stiffness proportional only model is argued by many (Abbasi *et al.*, 2004; Hall, 2006; Pegon, 1996; Wilson, 2002) to avoid the spurious energy dissipation generated by mass proportional part. Particularly, tangent stiffness proportional damping has been seen as the most promising choice by Priestley and Grant (2005). The damping issue is rather complex and even difficult to solve, given that small changes in damping, mainly for very low damping, imply large variations in the results.

### ***2.4.3 Innovative displacement based approaches***

Recent developments in seismic behaviour assessment of bridges have focused the transition from force design philosophies to displacement based ones. In the present time, with a variety of new design approaches that require increased emphasis on displacement, rather than on strength, the most common approach has been to attempt to modify force-based design procedures, rather than to completely revise seismic design procedure in a more rational manner, as stated in (Calvi, 2004).

The evolution from forces (or accelerations) evaluation to displacements has been based in the recognition of a series of points, according to (Priestley, 1993, 2003): it is generally accepted that damage can be related to material strains, and that material strains can be related to maximum response displacements, but not to response accelerations; equal displacement approximation is known to be non-conservative for short-period structures. Priestley (2003) showed that all formulations are correct at some part of the period range of structural response, and all are wrong at other periods. New, displacement-based (some times referred to as performance-based), methods for design have therefore been developed recently, with emphasis to one of the approaches (Priestley and Calvi, 2003b), the Direct Displacement Based Design (DDBD), in which the fundamental difference from force-based design is that the structure to be designed is characterized by a SDOF representation of performance at peak displacement response, rather than by its initial elastic characteristics, based on the Substitute Structure approach (Gulkan and Sozen, 1974; Shibata and Sozen, 1976). Shortly, within the DDBD methodology, a structure is

designed/assessed based on its behaviour at maximum response, by determining the inelastic displacement pattern, characterizing the equivalent SDOF system, applying the displacement based design concept to the SDOF structure and determining the strength required to the structural elements. All the procedure, as well as the computed quantities, is defined for the structure to reach a predetermined displacement when subjected to an earthquake consistent with the design level event.

For the particular case of bridges, carrying out the first step, estimating the inelastic displacement pattern of the deck, compatible with the displacement at the top of the piers, will allow, in the end, the definition of the piers capacity, if design levels corresponding to increasing seismic intensity are considered. The critical pier can therefore be readily identified and, in most cases, will be the shortest one ruling the selection of the displacement pattern. Generally, the lateral displacements for bridge piers are based on a set of limiting longitudinal strains consistent with the desired damage level.

It is straightforward to compute the design displacement from strain limits, considering the strain profile at maximum deflection of a simple bridge pier under transverse response, defined by the maximum concrete compression strains,  $\varepsilon_c$ , and the maximum reinforcement tensile strain,  $\varepsilon_s$ , for the considered performance state. Accordingly, there are two possible limit state curvatures, based on the concrete compression and the reinforcement tension respectively. Plastic and yielding curvatures may be easily computed, enabling curvature ductility to be known. If ductility in displacements at the top of the pier intended, expressions including the pier height contribution ought to be used.

The use of such approach will definitely constitute a recently developed and greatly simplified alternative for the seismic analysis of bridges. It is certainly faster and less demanding than any nonlinear pushover based approach, not to mention nonlinear dynamic analysis. Some questioning may rise around the need for a SDOF substitute structure, which is, in any case, already considered in nonlinear static procedures or the task of associating a seismic intensity level to a specific performance level. Even though originally developed bearing design in mind, it can be used for assessment of existing structures purposes (Priestley *et al.*, 2007).

#### ***2.4.4 Nonlinear response prediction of bridges***

When it comes to bridges, it is commonly recognized that any of the aforementioned issues has been rather less scrutinized than for the case of building structures. Bridges have been designed by reference to acceleration response spectra, according to (Casarotti *et al.*, 2005), for the past 40 years at least, apparently for historical reasons, given that common practice has always dealt with other load types that not the seismic action: self-weight, traffic or wind. When structural design of bridges started to become routinely implemented, the first rough approaches consisted in procedures similar to the adopted for the case of wind loading, assuring that the structure would remain elastic for a portion of the vertical weight, applied as a uniform lateral force. There was no inelastic response being studied herein, the behaviour was fully elastic and, consequently, underestimation of deformation or deflections, together with overestimation of force, leading to the absence of significant strength degradation or insufficient reinforcement length (Priestley *et al.*, 1996; Kawashima, 2000), was widely verified during the occurrence of earthquakes (see 2.2).

Particularities regarding this sort of structures are often invoked to justify such different state of progress. To mention some, it can be pointed out that the superstructure, the deck, is designed to remain elastic and, hence, as long as piers enter their inelasticity range, the deformed shape of the structure will be essentially governed by the elastic behaving deck; effects of superior mode shapes, already highly pointed out, are more important for irregular bridges; complex torsional and distorsional effects are expected, due to the contrast between deck and piers element types.

In accordance with what has been just stated, standard and recently developed pushover procedures, as well, have been thoroughly tested for buildings, but not for less investigated typologies, such as bridges. The instant tendency would to extrapolate the procedures assessed with buildings, a practice that must be handled with care, due to the inherent mentioned differences between the two structural systems. Fischinger *et al.* (2004) even question the validity of traditional pushover procedures to bridges. Similarly, Spacone *et al.* (2008) argue that pushover procedures are still not readily applicable to irregular structures, where bridges fit in.

Nevertheless, and despite the unfavourable characteristics of bridge structural systems, there have been a few recent research studies indicating that nonlinear static procedures are possible to use within such configurations (Casarotti and Pinho, 2007; Isakovic and Fischinger, 2006; Lupoi *et al.*, 2007; Paraskeva *et al.*, 2006; Pinho *et al.*, 2007; Pinho *et al.*, 2009). Conclusions of the majority of such studies are drawn, though, towards the recommendation for using advanced, higher mode effects including nonlinear static analysis techniques.

With respect to nonlinear dynamic analysis, the application to bridges is frequently less demanding than for other sort of structures, such as buildings. Models are definitely less complex, with less structural elements, which make the dynamic analysis considerably more feasible. Typical discouraging issues, computational demand, analysis output or integration scheme, assume herein slightly lightened significance. Indeed, seismic assessment of important bridges is increasingly performed using dynamic analysis in the time domain. Nevertheless, some issues are traditionally pointed out as key simplifying assumptions when it comes to dynamic analysis of bridges response to appropriately selected and scaled time histories: the seismic motion that is transmitted to the structure through its supports is synchronous and identical for all piers and abutments; the local site conditions are accounted for in terms of site categorization and the superstructure is fully fixed at the pier base points (Sextos *et al.*, 2003). Such assumptions are important to avoid incorporating more complex models, which leads to often uneconomic and sometimes numerically sensitive analyses.

Damping stands, to what bridges are concerned, as an essential issue, assuming values that are typically lower, given that not only there are less non-structural elements, from where the so-called elastic viscous damping can appear, but also the structural hysteretic energy dissipation locations correspond to the base of the piers, only. The fluctuation of a bridge model response as a function of the damping can be extensive and calibration is frequently needed, as noted in (Carvalho, 2009).

The use and validation of Direct Displacement Based Design philosophy within bridges seismic analysis has been object of quite a few recent research studies (Alvarez, 2004; Dwairi and Kowalsky, 2006; Kowalsky, 2002; Priestley and Calvi, 2003a). The transverse response of bridges is especially more complex than the longitudinal response, requiring

careful consideration. Some aspects needing deeper attention have to do with: the definition of the displacement profile, which demands some consideration regarding the relative stiffness of the piers, when compared to the deck or the abutments; to this matter, Kowalsky (2002) and Dwairi and Kowalsky (2006) proposed the concept of effective mode shapes, whereas Priestley and Calvi (2003b) adopt more pragmatic approaches. Alvarez (2004) or Alfawakhiri and Bruneau (2000) use first mode based displacement shapes. System damping is another important issue although, given the simplified nature of the methodology, less complex of taking into account, as prescribed by the works of Kowalsky *et al.* (1995) and (1994) or Priestley and Calvi (2003a), both estimating damping in the individual elements, combining them later on according to the work or shear force, respectively, carried out by each member.

## **2.5 Nonlinear modelling overview**

The seismic action and nonlinear analysis methods have been seen to contemplate different characterizing possibilities, comprising several critical issues, to which sometimes corresponds significant uncertainty or dispersion. The modelling task, including material and geometric features, is equally not immune to different alternatives and need for choices and assumptions. Indeed, structural modelling for seismic evaluation becomes particularly noteworthy as a natural reflex of the complexity that is typically associated to such action.

The different structural modelling possibilities that are commonly seen as available can be classified according to the purpose of their use, as summarized by Spacone (2001). Global Models, or Lumped Parameters Models, feature the nonlinear response of a structure at specific degrees of freedom. Discrete Finite Element Models, also known as Member Models, Structural Elements Models or Frame Models, characterize a structure by connecting frame elements with duly modelled inelasticity. Finally, Microscopic Finite Element Models, using the Finite Element (FE) general method, approximate the solution of a problem in continuum mechanics by the analysis of an assemblage of two or three-dimensional FEs connected at a finite number of nodal points. The choice for each of the mentioned alternatives, reflecting the refinement level of the model, has plenty to do with the desired accuracy as well as with the computational effort that is implicated. Furthermore, the sort of analysis procedure that is being considered will definitely make a

difference, with the objective to avoid superposition of factors aggravating complexity of the whole process. It is, however, generally reasonable to assume that sophisticated FE models are more suitable for the study of structural details, which require high accuracy with bearable computational demand. At the same time, it is commonly accepted that frame models represent the best compromise between accuracy, provided by nonlinear FE modelled members, and simplicity, offering a sound enough view over the structural elements response.

Within a bridge structural system, frame models are typically used, with the nonlinearity engaged to the piers (the bearing structure), since deck and abutments are usually protected against collapse or severe damage, for reasons of cost and life safety (Casarotti and Pinho, 2006). The piers become therefore the fundamental elements (as recurrently stated) that need more detailed modelling of their nonlinear behaviour.

There are two major sources of nonlinearity: material and geometric. The former source has been definitely paid more attention over the years probably due to the fact that geometric nonlinearities become more important in a later phase of the structural response to high intensity, closer to the ultimate limit state.

### ***2.5.1 Material nonlinearity***

Material nonlinearity, regarding inelastic response of structures to seismic action, is typically accounted for by means of lumped or spread plasticity models.

Lumped plasticity models correspond to the use of linear elastic behaving elements, with the exception for certain, well defined, zones of the element, where the plasticity is admitted to be concentrated under the form of a plastic hinge, according to the observed typical concentration of inelasticity of RC frames at the extremities of the elements. As a consequence, the first approaches to model this type of behaviour considered nonlinear springs at the member ends (Clough and Johnston, 1966; Giberson, 1967; Takizawa, 1976), as referred in (Spacone, 2001). Plastic hinges have no standard implemented definition and its location, and mostly length, can be derived from several different approaches. Their definition, i.e., their constitutive law, can be specified using ad hoc plastic laws or more advanced fibre based cross section models (Spacone *et al.*, 2008). Many of them try to reproduce the effect of phenomena such as stiffness degradation in

flexure and shear (Clough and Benuska, 1967; Takeda *et al.*, 1970; Brancaleoni *et al.*, 1983), *pinching* under load reversal (Banon *et al.*, 1981; Brancaleoni *et al.*, 1983) or bar pull-out effects (Otani, 1974; Filippou *et al.*, 1983a). Modified versions of the previous have been developed as well, so as to include the different described issues, such as the one proposed by Costa and Costa (1987), later refined by Varum (1996), which considers stiffness and strength degradation and *pinching* all together. More contentious is the length along which the plastic the behaviour develops,  $L_P$ , needed to transform plastic rotations into plastic curvatures, and vice-versa. Again, there is no established formula or procedure to define such parameter, approaches have been refined over the years and several proposals have been made since the first approach by empirical expressions suggested by Baker and Corley, where the plastic hinge length is proportional to the distance from the critical section to the point of contraflexure, as mentioned by Park and Paulay (1975). Different proposals and refinements arose in the following years (Kappos, 1991; Paulay and Priestley, 1992; Priestley and Park, 1984), complemented by calibration and/or comparative studies by other authors, such as (Vaz, 1992; Guedes, 1997). The general conclusion has been to notice that no specific proposal stands out as outstandingly better or more accurate, given that a concentrated plasticity model itself is inevitably approximate. More simplified and expedite expressions do not, therefore, necessarily lead to worse estimates. This is actually the major drawback commonly associated to lumped plasticity models, the fact that structures are assumed almost totally elastic, although, at the same time, they are typically more employed within current commercial structural analysis computer programs (e.g., (Computers&Structures, 2006)). It is most likely an easier to grasp concept for inexperienced analysts (Spacone *et al.*, 2008). Other authors, though, counter this trend and call out the attention to the need for being careful when using a concentrated plasticity approach by users that are inexperienced in the calibration of the characterization of the constitutive laws (Casarotti and Pinho, 2006). Studies from Charney and Bertero (1982) or Bertero *et al.* (1984), amongst others, focused the limitations and pitfalls of employing lumped plasticity.

Spread plasticity models, commonly referred to as fibre models, consider the material nonlinearity in a totally distributed way, at each integration point. Considered to be more accurate when describing the continuous structural characteristics of RC members, with no inelastic regions definition, require simple geometric and material properties. The cross

section response is then estimated by classical plasticity theory in terms of stress and strain resultants or by explicitly discretizing the elements in fibres with uniaxial behaviour, with material inelasticity spread along the member longitudinal axis, which assures accurate estimation of damage even in the highly inelastic range. First approaches to distributed nonlinearity resulted in proposals by Aktan *et al.* (1974), Helleland and Scordelis (1981) or Marí and Scordelis (1984), the latter two making use of the classical stiffness method with cubic hermitian polynomials. Improved modelling algorithms, including axial force-bending moment interaction (Menegotto and Pinto, 1973), shear effects (Bazoant and Bhat, 1977) or alternative flexibility based formulations (Mahasuverachai and Powell, 1982; Kaba and Mahin, 1984; Zeris and Mahin, 1988, 1991) have followed. Implementation in commercial software, available for research or office design analysis and assessment is, however, relatively recent, with focus on OpenSees (McKenna, 1997; McKenna and Fenves, 2006), MIDAS (2006), SeismoStruct (SeismoSoft, 2008), among others, which allow the use of displacement-based or force-based elements.

In the end, both sorts of models use the same cross section constitutive laws, at an integration point level, for spread plasticity models, or at a plastic hinge level, for lumped plasticity ones. The concrete and steel material models are, hence, the basic input source, which admit, as well, different refinement and subsequent complexity levels. Amongst numerous available steel models, the bilinear, the Menegotto and Pinto (1973) and the Monti and Nutti (1992) proposals are frequently used, whereas for concrete there are current tri-linear (more simplified) or nonlinear with constant or variable confinement, such as the models from Kent and Park (1971), Scott *et al.* (1982) or Mander *et al.* (1988b), just to mention some.

FE fibre models are, nevertheless, the most developed and up to date, given the ability to directly take into account phenomena such as interaction between axial and bending forces or shear effects, through the entire length of the element with no need for distinction between elastic and inelastic sub-elements, as in plastic hinges based models. Furthermore, due to its exact integration nature, fibre models are commonly seen as more accurate and precise but, to some extent, more delicate to use, according to Spacone *et al.* (2008), particularly when sections of structural elements feature softening; in such cases, deformations will occur concentrated in the extreme sections with solution objectivity loss, which somehow recalls a plastic hinge scenario. In fact, contributions from the two



modelling possibilities may be reconciled, using plastic hinge typical lengths for discretization of elements within fibre based models (Casarotti and Pinho, 2006; Calabrese *et al.*, 2010).

As far as bridges are concerned, the relative positioning of the two modelling types is at least interesting. On the one hand nonlinear behaviour of bridges is deemed to occur at well defined structural elements, the piers, which, in turn, witness quite concentrated, delimited, plasticity effects at the bottom or, at most, at the top, depending on the connection to the deck. This set of aspects will easily induce the suitability of lumped plasticity models. On the other hand, given the relative simplicity that characterizes bridge structural systems, and keeping in mind that nonlinear modelling will be restricted to the main bearing substructure (the piers), the argument of high computational demand and analysis complexity loses relevance and finite fibre-based elements modelling becomes more appealing.

### ***2.5.2 Geometrical nonlinearity***

There is not much experience in modelling geometric nonlinearity in frame analysis, in spite of being generally recognized their importance during earthquake-induced ground motion, as the structures may experience considerable lateral drifting. Different sources, local and global, are usually admitted for geometric nonlinear behaviour, corresponding to beam-column effects and large displacements or rotations, respectively. Quoting Spacone *et al.* (2008), when displacement-based elements are used, contemplation of P- $\Delta$  effects or large displacements and moderate rotations is a “well established field” whilst, for force-based elements, general co-rotational formulations have been posed (Crisfield, 1990; Sandhu *et al.*, 1990; Neuenhofer and Filippou, 1998; Izzuddin, 2001; Felippa and Park, 2002; Scott and Filippou, 2007). Recent work from Correia and Virtuoso (2006) allows generalized accounting for large displacements/rotations and large independent deformations relative to the frame element's chord (the P- $\Delta$  effects), through the employment of a total co-rotational formulation.

The importance given to this matter within design codes is relative, such as the example of EC8, which does not include specific guidelines on geometric nonlinearity, indicating only when and how to consider the phenomenon, in an approximated way. Second order effects

will be taken or not into account, depending on an approximate formula for interstorey drift.

According to Priestley *et al.* (1996), concerning bridge response, lateral displacements during an earthquake event are typically small, with regards to the piers height and cross section dimension, which generally allows nonlinear geometric effects to be neglected. For the case of highly flexible bridges or slender or very tall piers, geometrical nonlinearity may become significant, especially when combined with considerable vertical load, and must therefore be included. Nevertheless, second-order (P- $\Delta$ ) effects consideration, instead of full, large-deformation nonlinear geometric behaviour, will be enough.

## **2.6 Safety assessment methods**

Several paths can be followed with the purpose of evaluating the seismic safety of bridges, when properly modelled, subjected to duly characterized seismic loading. The main distinction that can be made is between deterministic and probabilistic methods. Both of the approaches within this basic division can recur to the same tools for characterizing the seismic input (response spectra, accelerograms), estimating structural capacity or predicting structural effects (fibre or plastic hinges modelling approaches, nonlinear static or dynamic analysis) but the main difference will be in the way uncertainty (of the seismic input, capacity models and analysis procedures) is taken into account and how it is reflected in the final assessment output.

### **2.6.1 Deterministic assessment**

The deterministic assessment is currently the most employed tool, mainly if one considers the design office environment. It is basically given by the crude comparison of the capacity, member-by-member, with the corresponding demand, when the structure is submitted to seismic forces. The capacity, as prescribed by many codes (e.g., EC8) is often affected by empirical reduction coefficients, applied to the mean or characteristic values, so as to account for uncertainty. For the case of the seismic input, a minimum number of records is also frequently prescribed in order to guarantee a good average or maximum demand. The safety verification will then be typically carried out according to predefined limit states, currently associated to specific return periods, which will govern the way of

considering the seismic input and computing the capacity and demand for further comparison.

### ***2.6.2 Probabilistic assessment***

The employment of probabilistic methods is, on the other hand, far from large dissemination among the professional engineering community, even though they have been rather well-established in the recent past (few decades). Their main practical application has been actually the calibration of the deterministic approaches used in codes, based on the use of partial safety factors. The reason that is mostly pointed out for such state of the art is the abstractness, mathematical complexity and much greater consciousness on the actual physical terms of the problem, unlike the traditional design procedures, which offer clear-cut guidance, as stated by Pinto *et al.* (2007). A new wave of probabilistic methods, developed over basic probabilistic concepts has come up in the past decade, especially in the US. Their “simplicity” with respect to theoretical background makes them more easily approachable by engineers and, thus, more appealing to the community. Their popularity has reached the state of use as complement to code-based design, assessment of existing structures or even design of new ones. Even if “simple” any probabilistic procedures requires a substantial amount of different information, in comparison to the deterministic ones, to characterize the uncertainty in the structural safety problem. Such data includes probabilistic characterization of seismic action, as well as description of the capacity and structural demand, accompanied by a measure of the corresponding variability.

According to (Pinto, 2001) probabilistic assessment of structures is usually simulation-based, FORM-based (First Order Reliability Methods) or response-surface based. Several different proposals for implementation are available in literature within each category but it generally recognized that the seismic risk subject is still in considerable development and definition, due to the growing awareness of the international community of the need for including probabilistic measures in seismic assessment practice.

## **2.7 Summary**

This chapter featured the main goal of providing a background to this work, regarding the current status of the different steps within probabilistic seismic assessment of bridges, calling the attention out to the vital importance of considering the seismic events in bridge engineering as well as summarizing the different topics in discussion and in need for improvement. Based on such considerations, Chapters 3 to 6 will focus the different identified subjects, which will allow, in the end, the obtaining of a consistent probabilistic safety measure.

## 3. Seismic Input

The definition of the seismic input is probably the primary step within any seismic assessment analysis and is sometimes assumed as a straightforward task, which can be highly misleading. Effectively, seismic action has been proved as complex, unpredictable, allowing several different representation modes, each with considerable dispersion coming from natural variation. The way how seismic loading is accounted is deeply related to the employed analysis method: accelerograms are used for nonlinear dynamic analysis whereas response spectra are typically utilized for nonlinear static procedures.

The use of accelerograms is definitely more realistic, given that it enables the application time-step by time-step of the dynamic loading, becoming more suitable than response spectra for multi-degree-of-freedom (MDOF) structures. It is, however, understandable that such advantageous use of accelerograms carries a corresponding fair amount of complexity, usually requiring preliminary treatment. Response spectra, on the other way, are usually more consensual and information is generally represented in a more smoothed way, especially if within code or guidelines applications. The immediate disadvantage is that, by definition, response spectra refer to single-degree-of-freedom (SDOF) structures which will require MDOF systems to be converted to equivalent SDOF ones, if analysis through such sort of seismic action representation is intended.

The substantial differences concerning the complexity surrounding the mentioned approaches indicate that, clearly, a higher number of calibrating issues are associated to accelerograms. Moreover, nonlinear dynamic analysis is becoming more and more popular, given the advances in current computational capability. Consequently, the main focus of this chapter will be on the use of accelerograms for seismic analysis.

### **3.1 Accelerograms**

Several aspects are worth considering within the process of setting up real or artificial records for the use in nonlinear dynamic analysis. A brief overview is herein intended, as a contribution to this matter, especially regarding the application to bridge structures. Much of the work within this topic has been carried out under the European Project LESSLOSS (2004a), which considered the application of seismic risk assessment methodologies of several research teams of different institutions to the analysis of two distinct structures: a building frame, named ICONS and a viaduct, named LORDO.

Starting with the scaling and selection issue, a set of twenty records was initially considered, serving as the original base of records, within a certain range of magnitude, epicentral distance and soil profile types. Several different scaling techniques were compared using elastic acceleration response spectra, therefore, results of SDOF systems. Simultaneously, a double selection is performed, one related to the scaling parameters that markedly perform better and the other based on the disregarding of accelerograms which, due to their inflated effect, increase greatly the scatter among the records, forming a reduced base. This selection is performed by means of a statistical grouping technique, which is based on clusters – groups of elements with similar characteristics or effects, formed by likeness measuring. The records are afterwards used, scaled according to the best performing previously found procedures, to the nonlinear seismic analysis of the two mentioned case study MDOF structures: the building frame and the bridge. Furthermore, analyses with artificial accelerograms, matched to the response spectra of the real records, are also carried out. Results, namely ductility in displacements, are used to: i) check the stability effect of the clustering selection; ii) search for a minimum number of records necessary and sufficient to reach the same mean/median result that the global set would

provide; iii) compare scaling techniques, previously filtered based on response spectra; iv) confront performance of real and artificial accelerograms.

### 3.2 Real accelerograms – selection of records

#### 3.2.1 Initial considered set

The study on real records was carried out over a set of twenty accelerograms selected from the European Strong Motion Database (Ambraseys *et al.*, 2002). The records have been selected from firm soil sites, free-field, including large and distant, large and close, moderate and close as well as intermediate earthquake records, in an attempt to cover a sufficiently representative range of distances and the expected range of magnitude in Europe. Figure 3.1 illustrates the range of magnitudes and epicentral distances across the initially considered base of records, where it can be observed how the chosen accelerograms are spread out within the four quadrants, although scenarios of simultaneously high or low magnitude and distance are prominent. Figure 3.2, in turn, represents the cumulative distribution of the measured magnitudes and epicentral distances. The cumulative distribution shape is a good indicator of how homogeneously the parameter varies within its range: a slope close to 45 degrees would be the ideal situation.

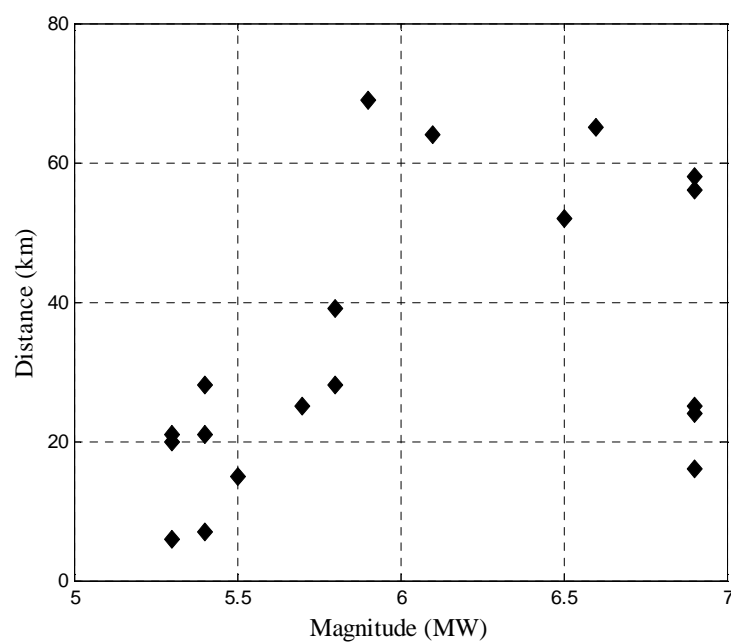


Figure 3.1 – Magnitude-Distance used pairs of values.

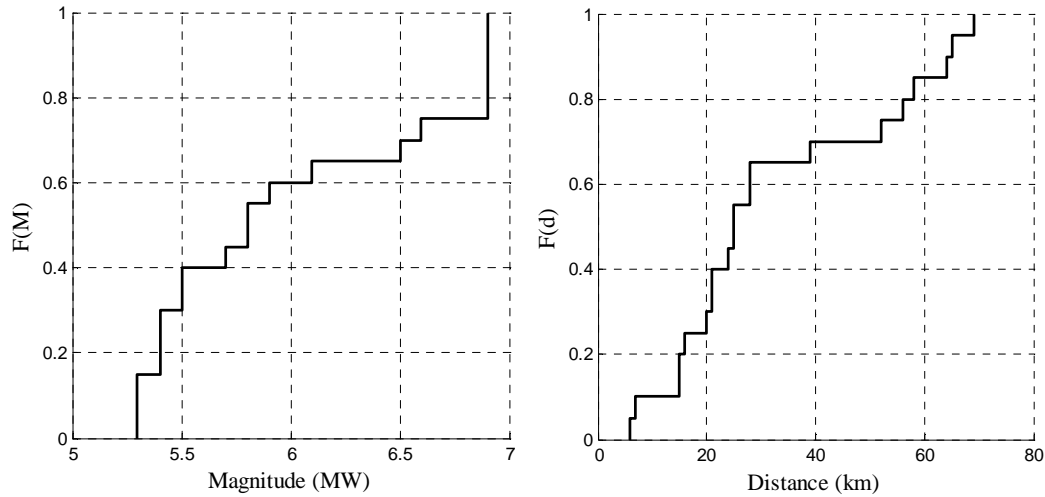


Figure 3.2 – Magnitude and distance cumulative distributions.

Table 3.1 briefly presents the main seismotectonic characteristics of the twenty initially selected records.

Table 3.1 – Selected real records – main features

	Earthquake Name	Date	Magnitude (MW)	Epical Distance (km)	Fault Distance (km)	Duration (s)	Peak Horizontal Acceleration (m/s <sup>2</sup> )
1	Montenegro	1979	6.9	56	46	15.94	0.572
2	Campano Lucano	1980	6.9	58	41	13.04	0.532
3	Erzincan	1992	6.6	65	58	18.56	0.297
4	South Iceland	2000	6.5	52	50	21.58	0.692
5	Montenegro	1979	6.9	25	12	48.23	4.453
6	Montenegro	1979	6.9	24	9	48.22	2.88
7	Campano Lucano	1980	6.9	16	13	45.54	1.725
8	Friuli (aftershock)	1976	5.3	21	15	7.19	1.701
9	Friuli (aftershock)	1976	5.5	15	17	23.82	2.273
10	Friuli (aftershock)	1976	5.5	15	17	86.06	0.898
11	Friuli (aftershock)	1977	5.4	7	6	48.98	2.365
12	Dursunbey	1979	5.3	6	6	18.31	2.824
13	Preveza	1981	5.4	28	7	14.93	1.402
14	Etolia	1988	5.3	20	12	21.88	0.584
15	Etolia	1988	5.4	21	6	30.50	0.383
16	Umbria Marche	1997	5.7	25	25	46.33	0.519
17	Valnerina	1979	5.8	39	37	38.41	0.386
18	Lazio Abruzzo	1984	5.9	69	64	23.21	0.171
19	Potenza	1990	5.8	28	29	20.38	0.944
20	South Aegean	1994	6.1	64	–	35.00	0.565



Earthquake duration is quite variable, ranging from 7.19 to 86.06 seconds, as well as peak ground acceleration values, which go from 0.01g to 0.46g. A scaling parameter based on earthquake duration has been considered, and will be presented further on, so as to provide some information on the importance of the variability associated to that parameter.

### ***3.2.2 A homogeneous base of records – Clustering analysis***

Starting from the initial set, a selection procedure is thought to be advantageous in the sense that extremely severe or particularly peculiar earthquakes may be segregated with benefits to the consistency of the analysis. Consequently, a homogeneous base of records is intended to represent a smaller set of earthquake records, based on the original ones, made up by removing those having very distinct characteristics, without loss of identity of the initial base. This representativity is assured by grouping elements with largest similarities, which has been measured, at a first stage, using response spectra. Afterwards, also displacement ductility demand quantities have been object of clustering procedure, applied, therefore, to structural effects. The methodology used to aggregate the original real ground motion records into groups, based on similarity measures, is called Clustering Analysis.

Clustering analysis can be seen as a collection of statistical techniques that can be used to classify objects, resulting in a size reduction of the available data. Given that it is possible to measure similarity and dissimilarity in a number of ways, data classification will depend upon the method being used, such as distance measuring, e.g., (Everitt *et al.*, 2001). Elements that are significantly different from others will be grouped into clusters of a single element, which reflects the fact that the association degree is strong between members of a same cluster and weak between members of different clusters. Clustering analysis classification is based on placing objects into more or less homogeneous groups, in a way that the relationship degree between groups becomes more perceptible. The application of this methodology is based on the two following steps: (i) measuring distances or evaluating the similarity between objects and (ii) grouping objects based on such distances or similarity measures.

There are two major clustering techniques, corresponding to hierarchical and non-hierarchical algorithms. The hierarchal procedure involves putting up a hierarchy tree defining the relationship among individuals, whilst, when a non-hierarchical algorithm is

used, the position in the measurement is taken as the central place and distance is measured from that central point. Currently, the non-hierarchical method has been less considered, due to the difficulties in choosing an ideal reference central point. To what hierarchical clustering is concerned, the technique can be divisive or agglomerative. A divisive method begins with all cases in one cluster, which is gradually split up into smaller clusters. On the other hand, the agglomerative technique starts with (usually) single member clusters that are gradually merged until one large cluster is formed.

When carrying out a clustering analysis, the first step is to establish distance measurements (e.g., Euclidean, squared Euclidean or Chebychev distances) or similarity measurements (e.g., Pearson's correlation, Russell, Rao or Jaccard coefficients) matrixes, in which the linkage degree between each two units of analysis (response spectra or displacement ductility for different intensity levels, for instance) will be evaluated, disposed in both columns and rows and where the cell entries are the measure of similarity or distance for every pair of cases. Distance measures indicate how distinct two observations are from each other, in a way that cases which are considered to be alike will correspond to low distance amounts.

The following task is the definition of a clustering method that will determine the way how clusters will be combined at each step (e.g., nearest neighbour, further neighbour or centroid method). Once several objects have been put together these methods define the distances between those clusters and the remaining elements, creating eventual new clusters (Everitt *et al.*, 2001). Output results can be either graphical representations (e.g., dendograms or icicle plots) or tables (e.g., cluster membership table or agglomeration schedule). It should be noted that clustering analyses can be performed using easily available commercial statistical software.

### ***3.2.3 Application to the set of selected records***

In order to assess the similarity of the 20 initially selected ground motion records, characterized in 3.2.1, elastic response spectrum ordinates were used as the variable herein submitted to agglomerative hierarchical clustering analysis, a rather simple procedure. Within clustering analysis, all the previously referred distance and similarity measures differ on the distance definition itself as well as on the way of evaluating it. For this

specific case, a likeness measure, the Pearson's correlation, was chosen, given that it allows comparing the linkage between each two variables (different response spectra). The chosen clustering combination method was the "nearest neighbour", which groups objects based on the minimum aforementioned distance between them. Table 3.2 indicates, for specific numbers of considered clusters, 3 to 8, which are the similar variables, i.e., the ones that are grouped in a same cluster.

Table 3.2 – Cluster definition and homogeneous base

Case/Record	8 Clusters	7 Clusters	6 Clusters	5 Clusters	4 Clusters	3 Clusters
1	1	1	1	1	1	1
2	1	1	1	1	1	1
3	1	1	1	1	1	1
4	2	2	2	2	2	2
5	3	2	2	2	2	2
6	4	3	3	3	3	3
7	5	4	4	4	1	1
8	6	5	5	4	1	1
9	1	1	1	1	1	1
10	7	6	2	2	2	2
11	3	2	2	2	2	2
12	2	2	2	2	2	2
13	2	2	2	2	2	2
14	3	2	2	2	2	2
15	3	2	2	2	2	2
16	3	2	2	2	2	2
17	1	1	1	1	1	1
18	1	1	1	1	1	1
19	1	1	1	1	1	1
20	8	7	6	5	4	2

Homogeneous base	1	2	3	4	5	9	11	12	13	14	15	16	17	18	19

For instance, if 8 clusters are considered, i.e., if one wants to divide the 20 records into eight groups by means of the predefined similarity measures, according to Table 3.2, records 1, 2, 3, 9, 17, 18 and 19 would belong to Cluster No. 1; records 4, 12 and 13 to Cluster No. 2; records 5, 11, 14, 15 and 16 to Cluster No. 3; whereas records 6, 7, 8, 10 and 20 would constitute the single-element clusters No. 4, 5, 6, 7 and 8, respectively. As an example, a schematic illustration of the records division, when defining 8 Clusters, is provided in Figure 3.3. Records 6, 7, 8, 10 and 20 are defined as the most "different" from all the rest, according to the adopted criteria, given that the clustering analysis determined that they should be in single-element clusters.

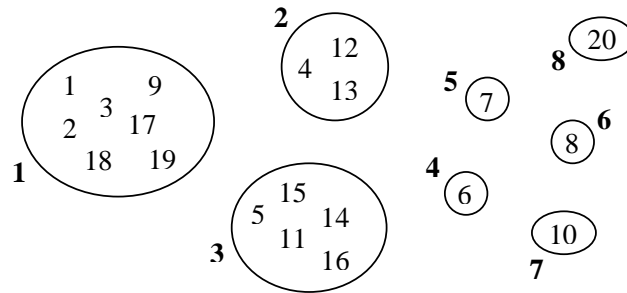


Figure 3.3 – Records distribution when defining 8 clusters.

Analogously, the same interpretation can be made for the case of 7 to 3 clusters, identifying the records that are considered individually (shadowed cells in Table 3.2). Clearly, records 6 and 20 are consistently individuated, whereas records 7, 8 and 10, are highlighted if the lower boundary of 6 or 7 clusters is considered. Based on such results, the selection was made to group variables into 7 clusters, for which members 6, 7, 8, 10 and 20 are not alike, hence defining five clusters of one member only. By segregating the corresponding five response spectra from the original set, a homogeneous reduced set of ground motion records, with the remaining 15 elements, was defined.

### 3.3 Real accelerograms – scaling

Considering accelerograms exactly as they were recorded, significant differences come up, a natural feature on the use of real records. Subsequently, a seismic analysis involving different real records requires the accelerograms to be put at a ‘same’, or at least comparable, intensity level. In practice, what has been typically considered is the imposition that different records share a specific characteristic, which can be an exceeding probability for a predefined hazard level or a ground motion parameter, such as peak ground or spectral acceleration in order to enable the average or median representation of results. The immediate consequence is that accelerograms will necessarily be modified through the application of an appropriate scaling factor.

The main goal, when selecting an appropriate scaling technique, related to a specific standardizing parameter, is to reduce, ideally minimizing, the associated scatter. Recalling what has been said in 2.3, several scaling methodologies have been studied in previously published work and have been traditionally divided in two major groups: scaling factors

obtained from the characteristics of the accelerogram or from corresponding response spectra.

The scaling parameter to choose may be closely related to eventual structural safety verification, if the work is being developed within a probabilistic framework, depending on the safety assessment selected method. If a failure probability is intended, recurring to the statistical characterization of the capacity and the demand, the exceeding probability density function for the selected scaling parameter is needed, and its availability has to be taken into account when that choice is made. For such reason, some parameters have been tested and emphasis has been given to those presenting a well-known or easily obtainable exceeding probability density function.

### ***3.3.1 Record quantities based intensity measures***

Based on the accelerogram itself, simple quantities can be computed and considered as scaling parameters. Among several possible ones, the following were selected for testing.

- **Peak ground acceleration (*pga*)**  
Each accelerogram is scaled in order to have its maximum acceleration equal to a predefined level.
- **Square Ground Motion (*s*)**  
Integral of the square ground acceleration.
- **Root-square ground motion (*rs*)**  
Square root of the square ground motion.
- **Mean-square ground motion (*ms*)**  
Mean square value of the ground acceleration history for the time interval corresponding to the attainment of 5% and 95% of the record's energy.
- **Root-mean-square ground motion (*rms*)**  
Square root of the mean-square ground motion.

### 3.3.2 Spectrum quantities based intensity measures

Including effects on SDOF systems, response spectrum, either in acceleration or pseudo-velocity, of each record can be the base of certain scaling procedures. Additionally, power spectrum may be used with the same purpose, bringing out a total of three other possible scaling parameters.

- **Spectrum intensity ( $si$ )**

Integral of the pseudo-velocity between 0.1 and 2.5 seconds.

- **Spectral acceleration ( $sa$ )**

Accelerograms are scaled to have the same spectral acceleration at the fundamental period of the structure.

- **Power spectrum area ( $psa$ )**

Area under the power spectrum

For each scaling technique, the adopted normalization procedure was to establish a record as a reference (the first one in Table 3.1 was herein considered) and scale all the others to match the reference value of the considered scaling parameter for that reference record. Figure 3.4 shows the set of scaled response spectra according to one of the scaling parameters, with the purpose of illustrating the existing dispersion within the initial set of real earthquake records.

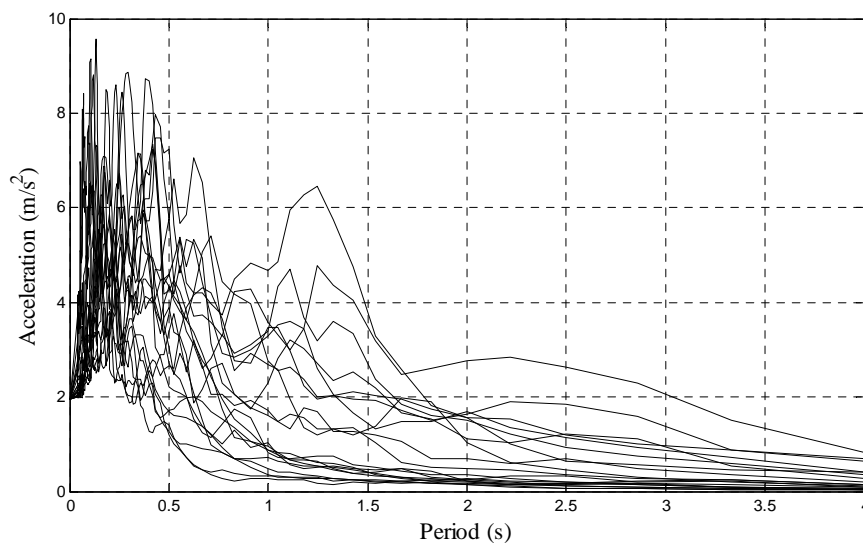


Figure 3.4 – Scaled response spectra according to peak ground acceleration

The considerable heterogeneity level among the initial set can be relevant to check if any of the alternative scaling parameters is actually particularly advantageous, given that a highly homogeneous set of records may not put in evidence the real differences on the performance of the different parameters.

Figure 3.5, in turn, stands for the average response spectrum for each scaling technique. The *ms* technique yields a median response spectrum outstandingly different from all the others, which denotes inappropriateness regarding the use of this parameter. For that reason, a new plot of the average response spectrum for each scaling technique, featuring not the *ms* technique, is presented in Figure 3.6.

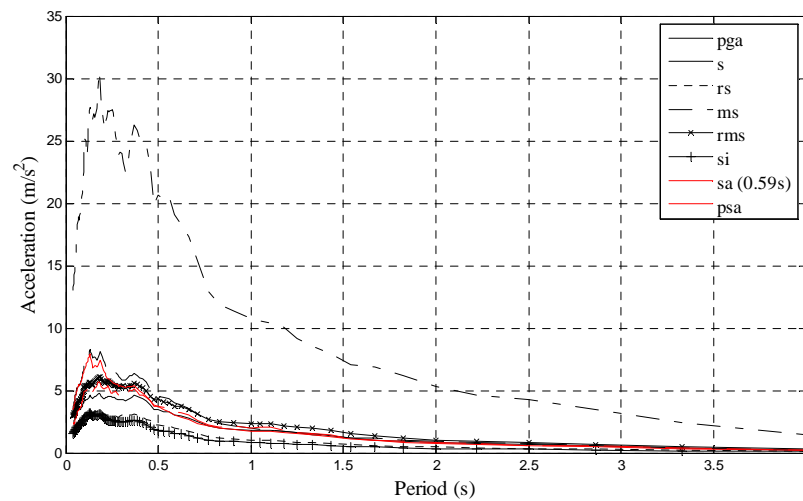


Figure 3.5 – Mean response spectrum to each of the scaling techniques

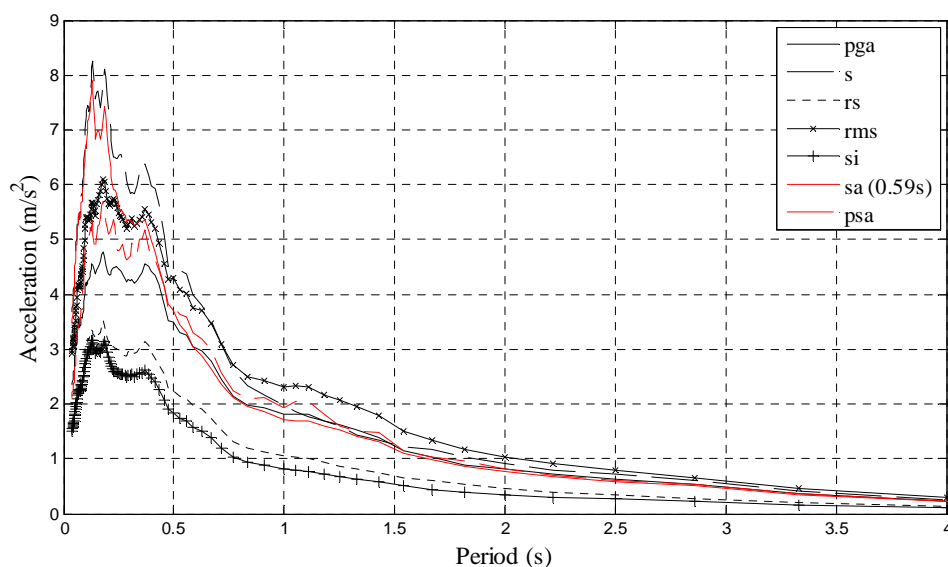


Figure 3.6 – Mean response spectrum to each of the scaling techniques (without *ms*)

In spite of a similar general shape on the spectra, differences are significantly higher for periods under 1s, the range of interest, mainly at the first half of the interval. Furthermore, no significantly distinct trend between record quantities based and response spectrum based scaling techniques has been encountered, which denotes a clear need for a more thorough analysis in terms of dispersion among the selected ground motion records (by means of coefficients of variation).

### 3.3.3 Comparative analysis of typical intensity measures

Comparison of techniques has been carried out by computing a simple statistical measure, the coefficient of variation (COV), referring to the ordinates of the twenty response spectra normalised to each of the reference scaling parameters. The coefficient of variation, along with the period or frequency, is presented in Figure 3.7 and Figure 3.8, respectively, for the eight scaling procedures. Spectral acceleration technique is employed for a matching period of 0.59 seconds, which corresponds to the case study of Lordo viaduct, considered within the research project referred in Section 3.1.

In agreement with the markedly different behaving mean spectrum that has been observed, the *ms* technique performs generally worse than the others. It features the largest coefficient of variation across almost the whole range of periods. Similarly, other parameters based on the square of the acceleration tend to introduce no noticeable reduction in the dispersion levels: the *s* technique performs rather poorly, comparatively to *ms*; with *rs* and *rms* better results are achieved, mainly for low periods, whereas at the opposite side, such improvement does not stand. Velocity-based parameter, *si*, assumes the best behaviour for periods over 0.5 seconds (or frequencies under 2.0 Hz).

Regarding the other parameters, as expected, scatter is small around the considered structural fundamental frequency, when using the spectral acceleration matching technique, *sa*, but average to poor results are obtained elsewhere. If one focus on the frequency-dependent plot, scaling procedure based on peak ground acceleration, *pga*, the typically most employed parameter, performs fairly well, when compared to the other parameters, except for low frequencies (high periods), where its performance is surpassed by other techniques.



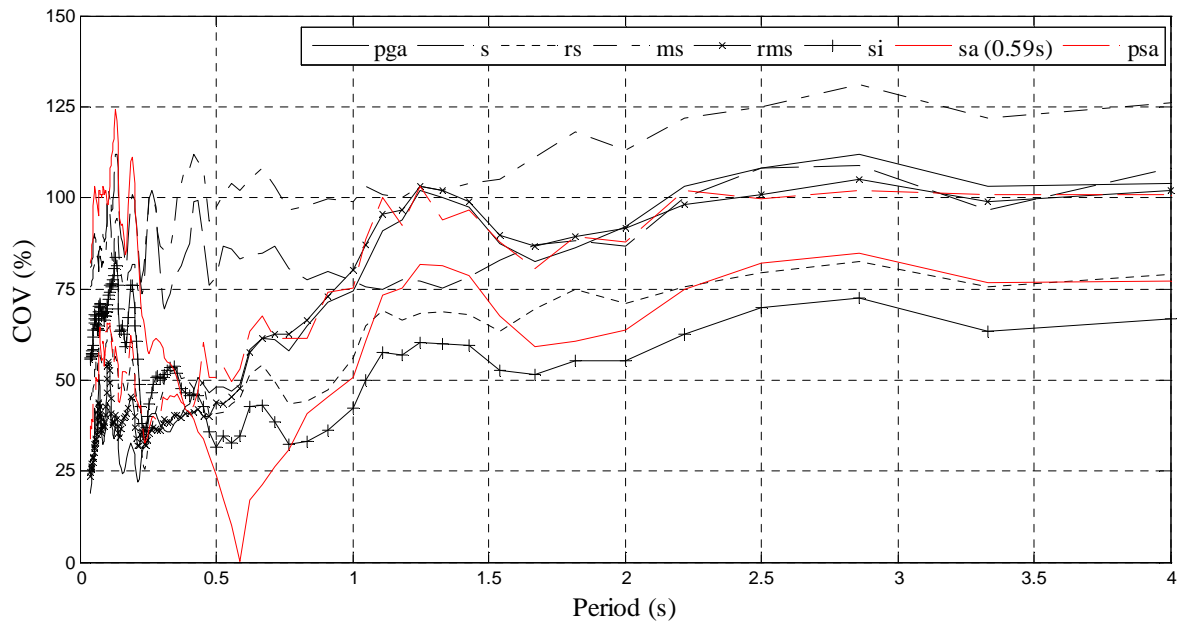


Figure 3.7 – Response spectra ordinates coefficient of variation for each scaling technique (period dependent)

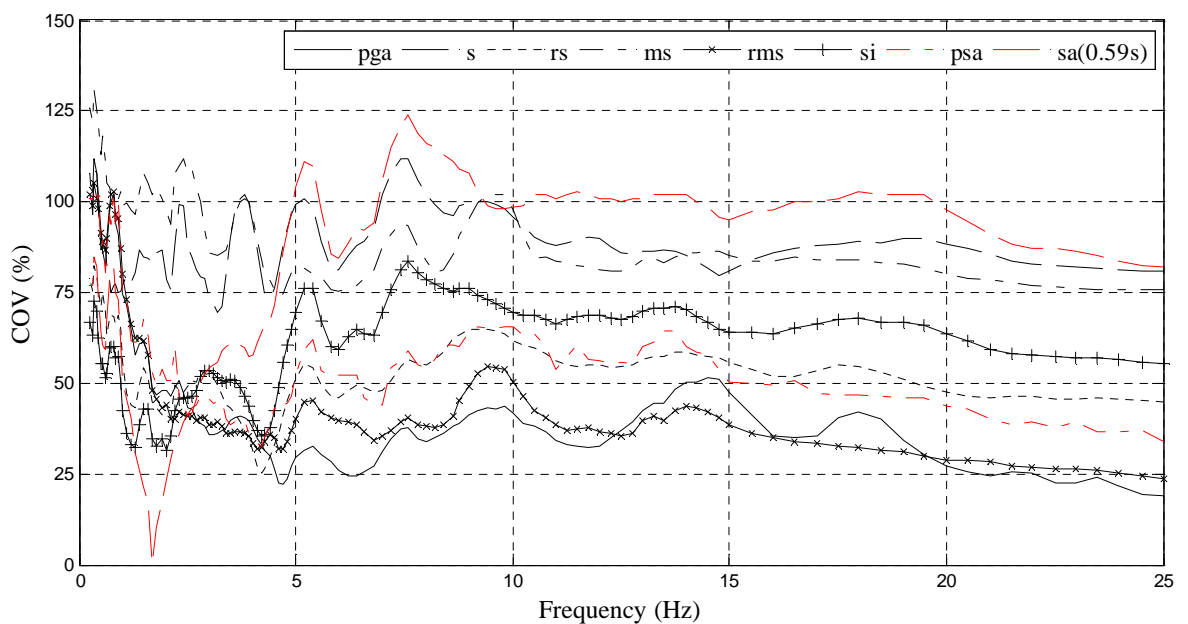


Figure 3.8 – Response spectra ordinates coefficient of variation for each scaling technique (frequency dependent)

The standardization by means of the area under the power spectrum, *psa*, a different parameter regarding its nature, has a constantly median performance, therefore, not worth the use. In general, it may be said that, considering the entire range of frequencies, *pga* and *rms* techniques are the best, though for low frequencies (<1.0 Hz) *si* and *rs* techniques

yield somewhat better results. Furthermore, if the structure under analysis is particularly considered, the spectral acceleration matching procedure assumes great relevance in the region of the fundamental period. According to the exposed, *pga* and *sa* techniques were assumed for the rest of the seismic action characterization study. Such choice has been based on two important aspects: first, if a full-range efficient technique is intended, *pga* performs well, whilst the others have shown a less steady performance. Furthermore, the use of a different parameter, instead of the traditional, well known peak ground acceleration, seems, therefore, not worthy. Secondly, if a procedure that is calibrated for the specific structure being assessed is sufficient, spectral acceleration technique behaves extremely well, as previously demonstrated.

### ***3.3.4 Response based intensity measures***

Within probabilistic seismic demand analysis, the choice for the intensity measure (IM) to be adopted relies not only on its ability to harmonize the seismic input, reducing the scatter levels around response of SDOF or MDOF systems but on its characteristics of practicality, sufficiency (i.e., the structural response does not depend on other ground motion features given the IM), efficiency (i.e., the structural response is well correlated with the IM) and hazard computability as well, as discussed in (Padgett *et al.*, 2008). Up to a relatively recent past the focus on intensity measures has been on the ground motion parameters or the response of SDOF structures side, through the use of response spectra, as detailed in the previous sections. Typically, peak ground acceleration (PGA) or spectral acceleration ( $S_a$ ) at a specific period or the fundamental period of the structure have been used in most of the bridge engineering applications (Shinozuka *et al.*, 2000; Mackie and Stojadinovic, 2004; Nielson and DesRoches, 2007). The task of selecting appropriate or optimal IMs to condition the demand and serve as basis to structural fragility curves has been object of improvement and new approaches have been recently developed, given that the choice of an optimal IM is still a subject in need for further addressing, as far as classes of bridges are concerned. Such new approaches include denser formulations, such as the inclusion of simplified static analysis of the structure to take into account accurate estimates of its period and stiffness characteristics. It is actually recognized in the work by Padgett *et al.* (2008), how structurally based IMs are challenging to implement in a regional risk assessment context because often there is no sufficient available information to estimate structural parameters, such as fundamental period.

An alternative approach has been studied so as to eventually replace the need for running nonlinear dynamic analysis with pre-scaled accelerograms, through the establishment of a new displacement based intensity measure, developed from simplified displacement based principles, applied to bridges.

### 3.3.4.1 Preliminary Approach on a Displacement-Based Intensity Measure

A nonlinear static analysis (*pushover*) based procedure has been adopted, using the results afterwards in a displacement based fashion, characterizing an equivalent SDOF system and determining the bridge performance through the consideration of specified limit states. The main goal was to seek for the relationship between the responses coming from a simplified procedure and the result coming from nonlinear dynamic analysis, represented by a specific number of accelerograms.

The procedure starts by carrying out a nonlinear static analysis of the structure, which enables the characterization of the structural system. Three different limit states, which are identified and located in the *pushover* curve, have been considered: the yielding limit state (LSy) and two post-yielding ones (LS2 and LS3). The post-yielding limit states have been defined in accordance with the displacements at which the first element reaches pre-defined strains in the steel or concrete. The strains in the steel and concrete have been taken as the ones admitted by Bal *et al.* (2008) as 0.35% for the concrete and 2% for the steel for the second limit state (LS2) and 0.75% in the concrete and 3.5% in the steel for the third limit state (LS3). Secant yield and post-yield periods have been defined accordingly. Equivalent SDOF properties are defined and the displacement for each limit state is computed from all the locations of the structure (for a bridge structure, all the deck nodes at piers location will be considered), hence, in a Displacement Based fashion, according to Equation (3.1), depending, therefore, on the actual load factor corresponding deformed shape of the deck,  $d_i$ .

$$d_{SDOF} = \frac{\sum m_i \cdot d_i^2}{\sum m_i \cdot d_i} \quad (3.1)$$

### 3.3.4.2 Procedure

The procedure used to estimate the intensity measure for a given structure and the calculation of the engineering demand parameter from nonlinear dynamic analyses, for calibration, is summarised in the following steps and should be carried out for each of the considered accelerograms.

1. Calculate the displacement response spectra (5% damping);
2. Run the nonlinear dynamic analyses for the bridge using tangent stiffness proportional damping;
3. From a static nonlinear analysis calculate the displacement capacity for each limit state as described in 3.3.4.1 and using Equation (3.1);
4. Calculate the effective periods of vibration and the equivalent viscous damping for each limit state. Several different proposals can be assumed in this step;
5. Obtain the spectral displacement demand for each limit state, based on the effective period and equivalent viscous damping, and compare it with the displacement capacities to estimate which limit state the bridge is predicted to exceed; the intensity measure (IM) can thus be estimated. If the bridge does not exceed the first limit state, the first limit state demand is used as the intensity measure; if the bridge falls between the first and second limit state the second limit state demand is used as the intensity measure; if the bridge falls between the second and third limit state the third limit state demand is used as the intensity measure and if the bridge is assumed to collapse then no intensity measure is assigned and the results are removed;
6. According to the deformed shape associated to the Limit State that the structure is not exceeding, a representative reference location,  $x_{ref}$ , is defined employing Equation (3.2), where  $x_i$  is the distance measured along the deck, measured from one of the abutments. The engineering demand parameter (EDP) herein considered is the maximum displacement at the reference location of the bridge ( $D_{dyn}$ ), which is obtained from the nonlinear dynamic analysis for the specific record;

$$x_{ref} = \frac{\sum x_i \cdot m_i \cdot d_i}{\sum m_i \cdot d_i} \quad (3.2)$$

### 7. Plot IM against EDP.

A flowchart representing the procedure is presented in Figure 3.9.

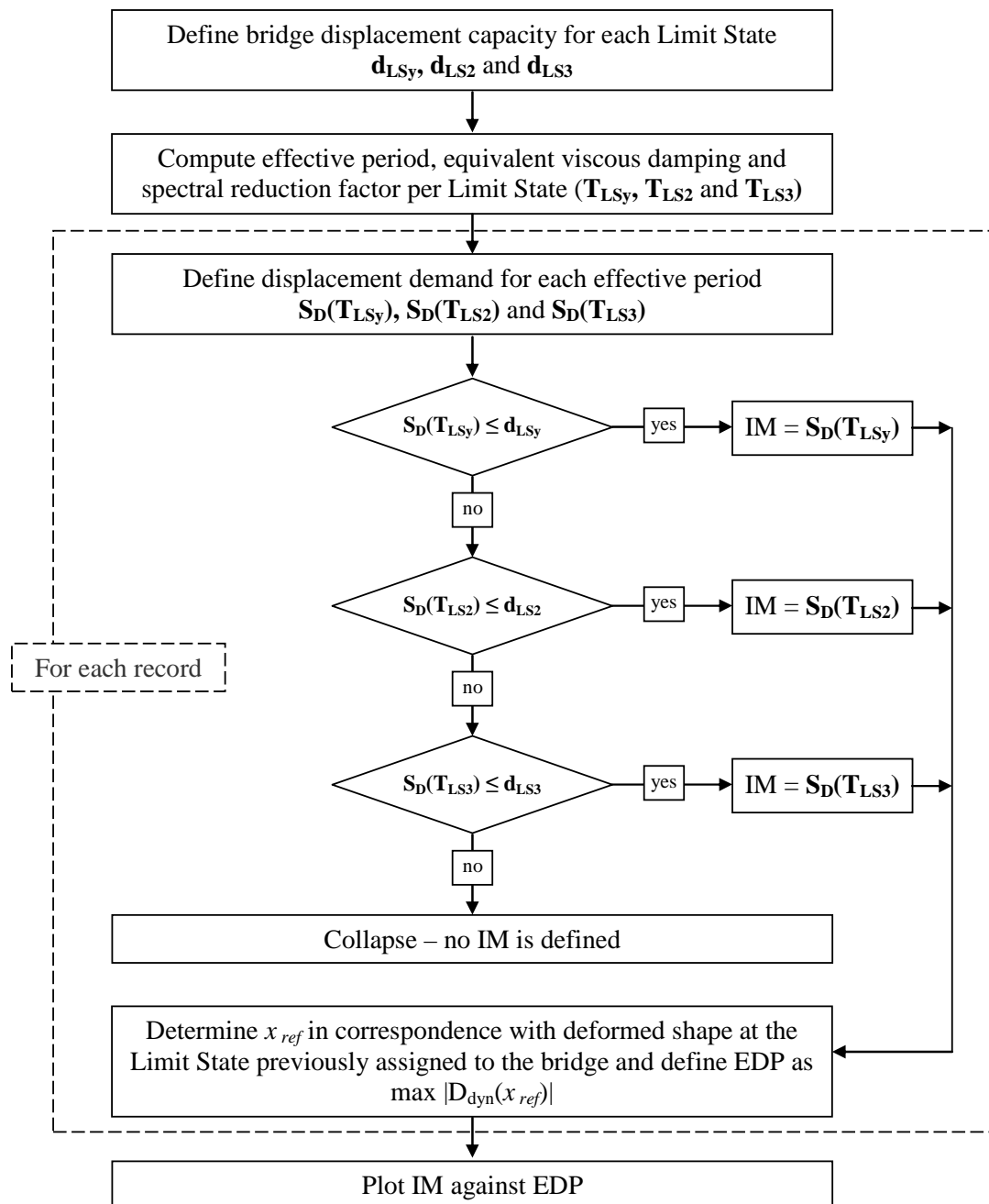


Figure 3.9 – Bridge displacement-based intensity measure procedure.

### 3.3.4.3 Structural application

A case study consisting of fourteen well-known bridges, used for application in other studies (Casarotti and Pinho, 2007), has been adopted, comprising two bridge lengths (with regular, irregular and semi-regular layout) and two types of abutments. The complete description and detailed information on the selected bridge configurations is carried out in Section 4.3. Three different types of pushover analysis for each bridge have been carried out: (i) adaptive displacement-based pushover; (ii) conventional pushover, with 1<sup>st</sup> mode proportional load shape; (iii) conventional pushover, with uniform load shape. Further details on nonlinear static analysis can be found in Chapter 5. Regarding the definition of the limit states, within the reported framework, the yield limit state of the structure has been considered to occur as soon as the steel on the first pier yields. Figure 3.11, referring to one of the analysed structural configurations (Figure 3.10), illustrates the limit states definition for the adaptive pushover curve computation case. The first pier to yield is P2, the central one, in which Limit States 2 and 3 occur before the yielding of the third pier.

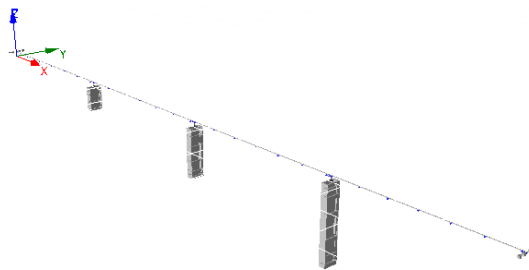


Figure 3.10 – A123 configuration.

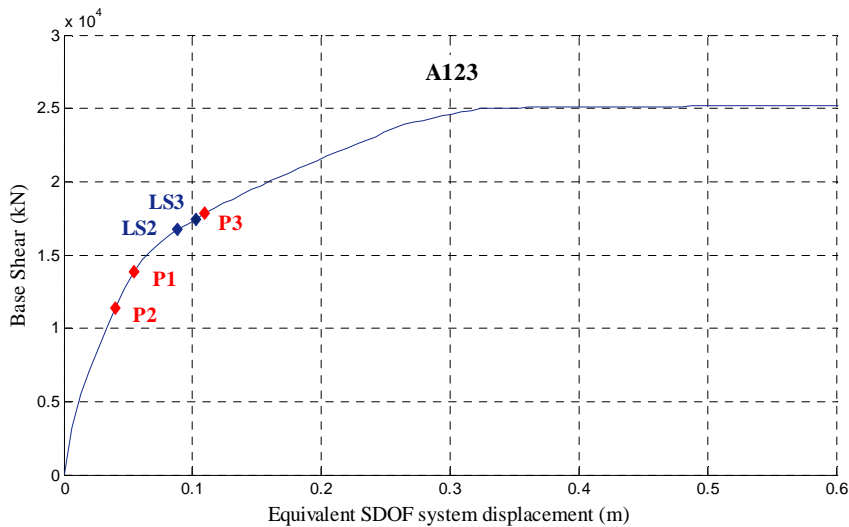


Figure 3.11 – Adaptive pushover curve and limit states for A123 bridge.

With respect to the computation of the equivalent damping, effective period and spectral reduction factor, two proposals, Priestley *et al.* (2007) and FEMA-440 (ATC, 2005) will both be considered. According to Priestley *et al.*, the effective period can be obtained using the expression in Equation (3.3), the equivalent viscous damping is given by Equation (3.4) and the correction factor applied to the displacement spectrum is given by Equation (3.5), where  $T_y$  is the yield period,  $\mu_{LS}$  is the ductility at a given limit state,  $\xi_{eq}$  is the equivalent viscous damping and  $\eta$  is the correction factor.

$$T_{LS} = T_y \sqrt{\mu_{LS}} \quad (3.3)$$

$$\xi_{eq} = 0.565 \frac{(\mu_{LS} - 1)}{\mu_{LS} \cdot \pi} + 0.05 \quad (3.4)$$

$$\eta = \sqrt{\frac{7}{2 + \xi_{eq}}} \quad (3.5)$$

Effective period, equivalent viscous damping and correction factor proposed in FEMA-440 guidelines are as presented from Equations (3.6) to (3.8), respectively.

$$T_{LS} = T_y \{0.2(\mu_{LS} - 1)^2 - 0.038(\mu_{LS} - 1)^3 + 1\} \quad (3.6)$$

$$\xi_{eq} (\%) = 4.9(\mu_{LS} - 1)^2 - 1.1(\mu_{LS} - 1)^3 + 5 \quad (3.7)$$

$$\eta = \frac{5.6 - \ln(\xi_{eq})}{4} \quad (3.8)$$

The nonlinear dynamic analyses were carried out using ten earthquake real records from the SAC Project (SAC, 1997), scaled to match the 10% probability of exceedance in 50 years (475 years return period) uniform hazard spectrum for Los Angeles. Detailed description of the seismic records ensemble can be found in Section 4.3.

Applying the procedure described in Figure 3.9 for the 14 bridges and 10 earthquake records, the preliminary plots with the relation IM–EDP, shown in Figure 3.12, are obtained. The effective periods have been calculated using Equations (3.3) and (3.6), the equivalent viscous damping using Equations (3.4) and (3.7) and the correction factor applied to the displacement spectrum using Equations (3.5) and (3.8).

The black line in the plots in Figure 3.12 shows the linear regression of the data ( $y=ax$ ). It should be noted that the slope of the linear regression is a measure of the bias in the data and  $\sigma$  is a measure of its efficiency (a low level of dispersion denotes an efficient intensity measure). On average, the intensity measure underpredicts the maximum displacement response at the reference location of the bridge.

The data dispersion,  $\sigma$ , calculated as the standard deviation of EDP/IM has been found to be roughly from 0.4 to 0.6. The use of FEMA-440 approach improves the efficiency, given that dispersion is usually 0.1 less. However the same does not happen with the bias, which is between 1.2 and 1.3 for the closest to one situation, the adaptive pushover one. The improvement in the scatter does not seem very surprising considering that in FEMA-440 equivalent linear parameters (i.e., effective period and damping) were determined *through a statistical analysis that minimizes, in a rigorous manner, the extreme occurrences of the difference (i.e., error) between the maximum response of an actual inelastic system and its equivalent linear counterpart*. The scatter around the IM is larger for higher intensity levels.



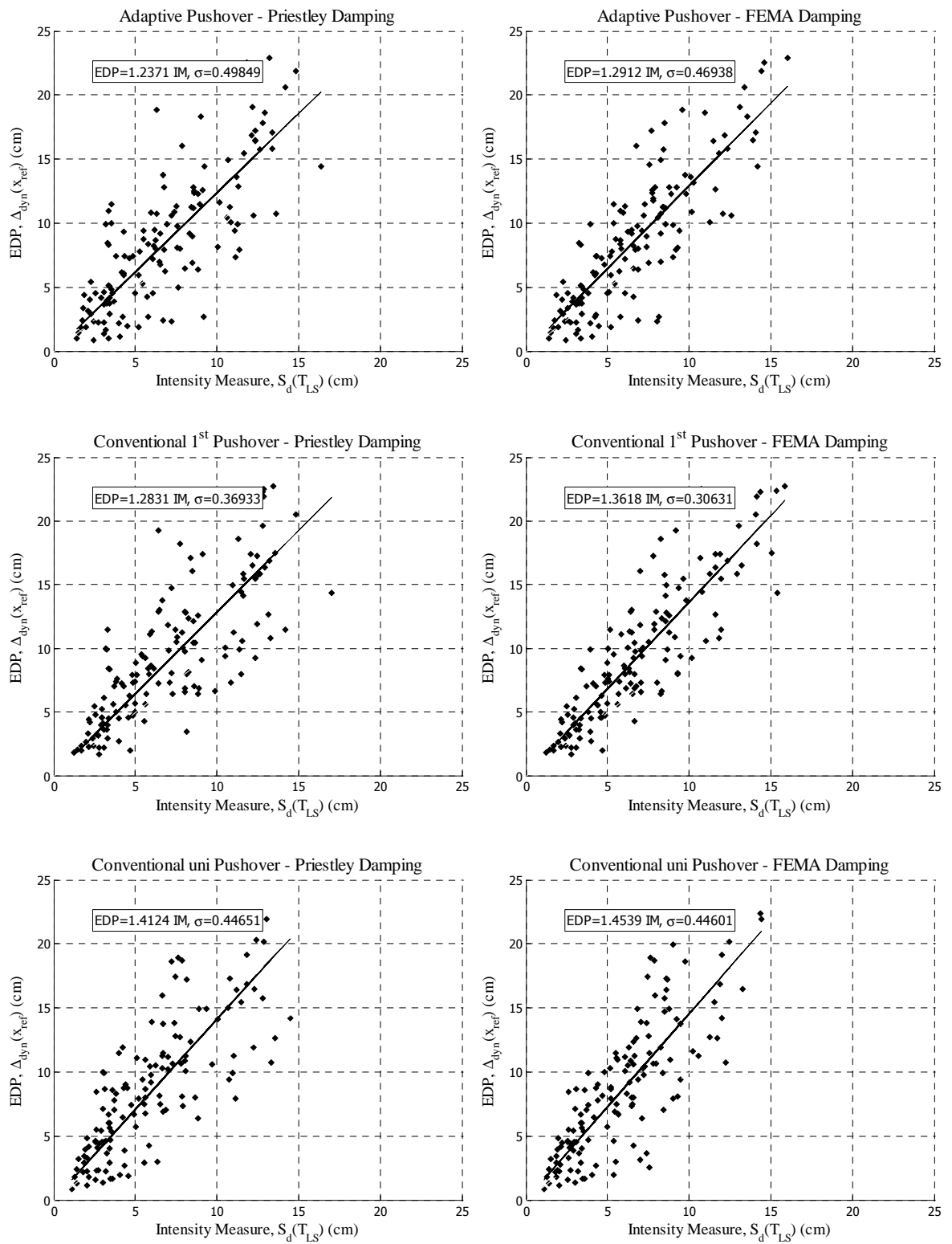


Figure 3.12 – Intensity measure vs. EDP.

In order to look at whether a procedure based on the increase in the period of vibration with limit state displacement is meaningful, the response period of vibration from each

nonlinear dynamic analysis has been calculated through the Fourier Amplitude Spectrum of the response history at the reference location of the bridge. The period of vibration obtained in this way for each dynamic analysis is plotted against the EDP, the dynamic analysis results for the reference location, in Figure 3.13.

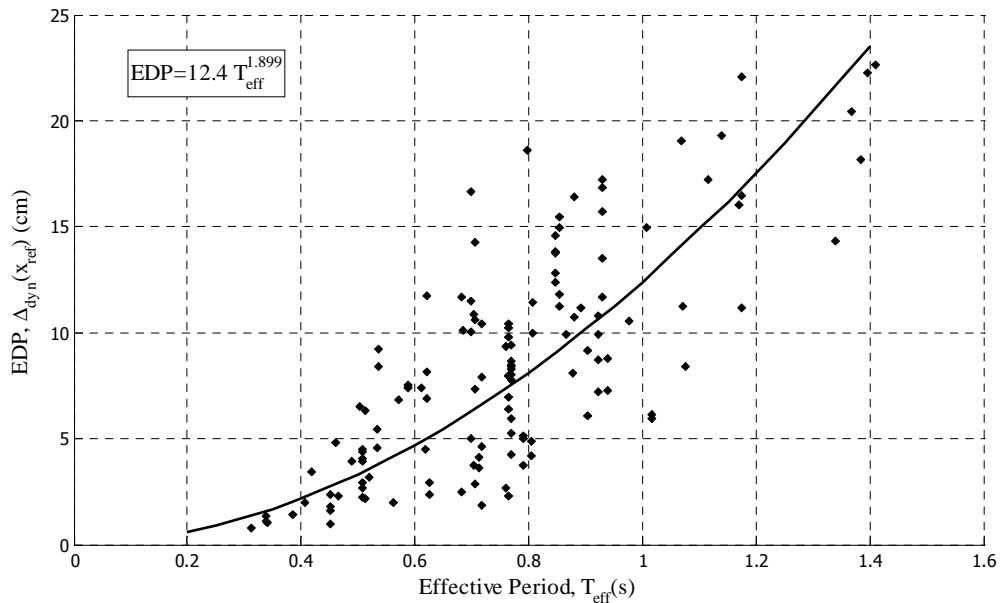


Figure 3.13 – Response period of vibration versus EDP.

There seems indeed possible to establish some kind of trend between the effective period and the respective EDP measure. Furthermore, Figure 3.14 shows how these periods compare with the effective periods proposed in FEMA-440, which have been calculated using Equation (3.6) where the ductility is based on the results of the pushover analysis (Figure 3.11). It appears that these limit effective periods are, for a significant number of cases, upper bounds to the actual periods of vibration recorded.

In order to investigate whether a closer relationship between the intensity measure and the displacement at the reference location can be obtained using these periods of vibration, the intensity measure has been recalculated using the effective periods shown in Figure 3.13, with the ductility being estimated as  $\text{EDP}/\Delta_{\text{LSy}}$ , where  $\Delta_{\text{LSy}}$  is obtained as described in Sections 3.3.4.1 and 3.3.4.2. The updated IM vs. EDP plots are presented in Figure 3.15.

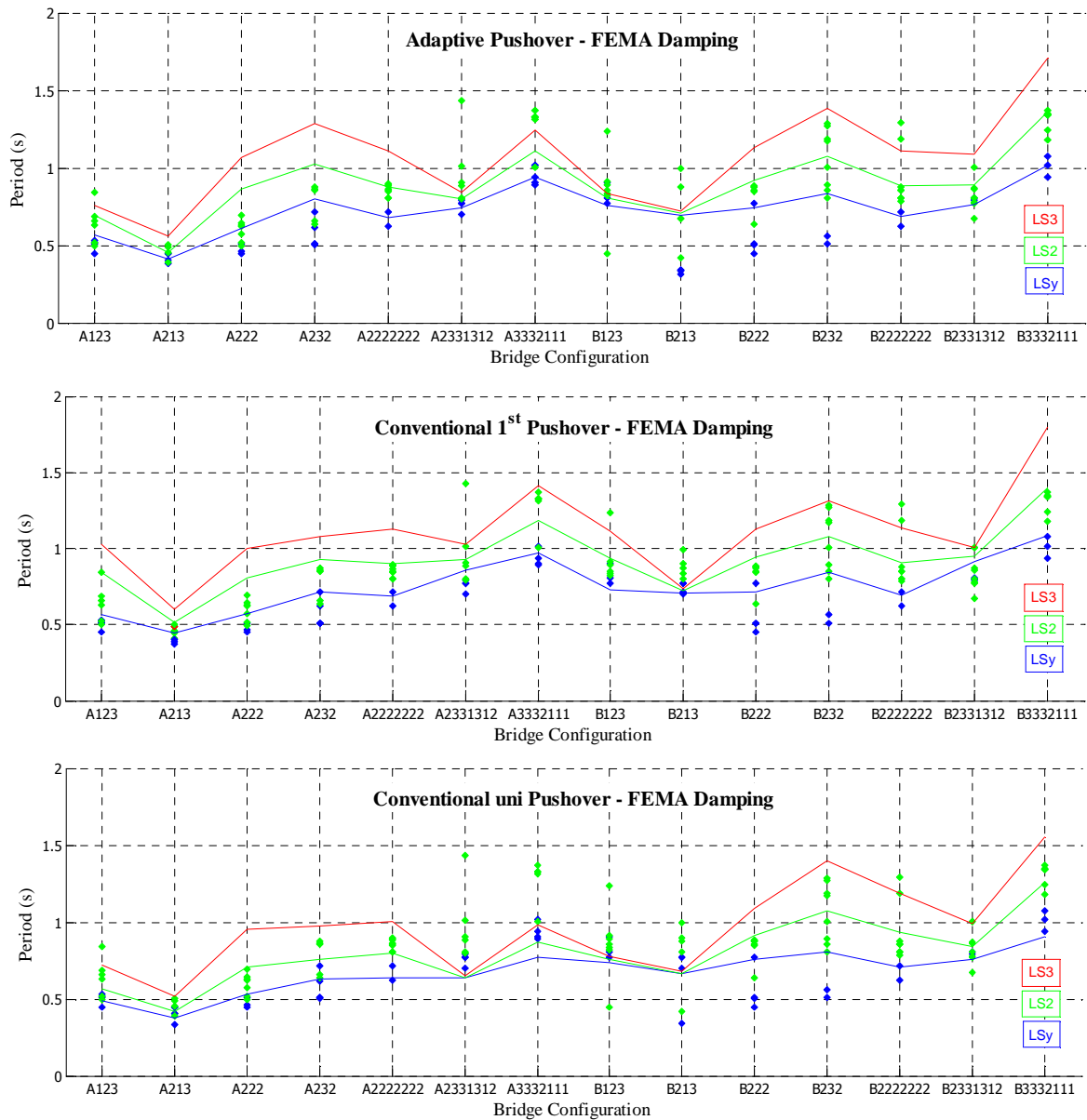


Figure 3.14 – Response periods of vibration and corresponding effective periods of vibration from Equation (3.6) for different bridge configurations and types of pushover analysis.

It can be seen that the underprediction given by the intensity measure has increased. The use of the effective measured periods does not seem indeed to improve the procedure. Indeed, even though the clouds of points do seem to have become slimmer, the number of outliers has apparently increased as well. Nevertheless, adaptive pushover based procedure is the less underpredicting one. FEMA-440 approach for the equivalent viscous damping and spectral reductions factor keeps on leading to closer to EDP estimates and lower dispersion.

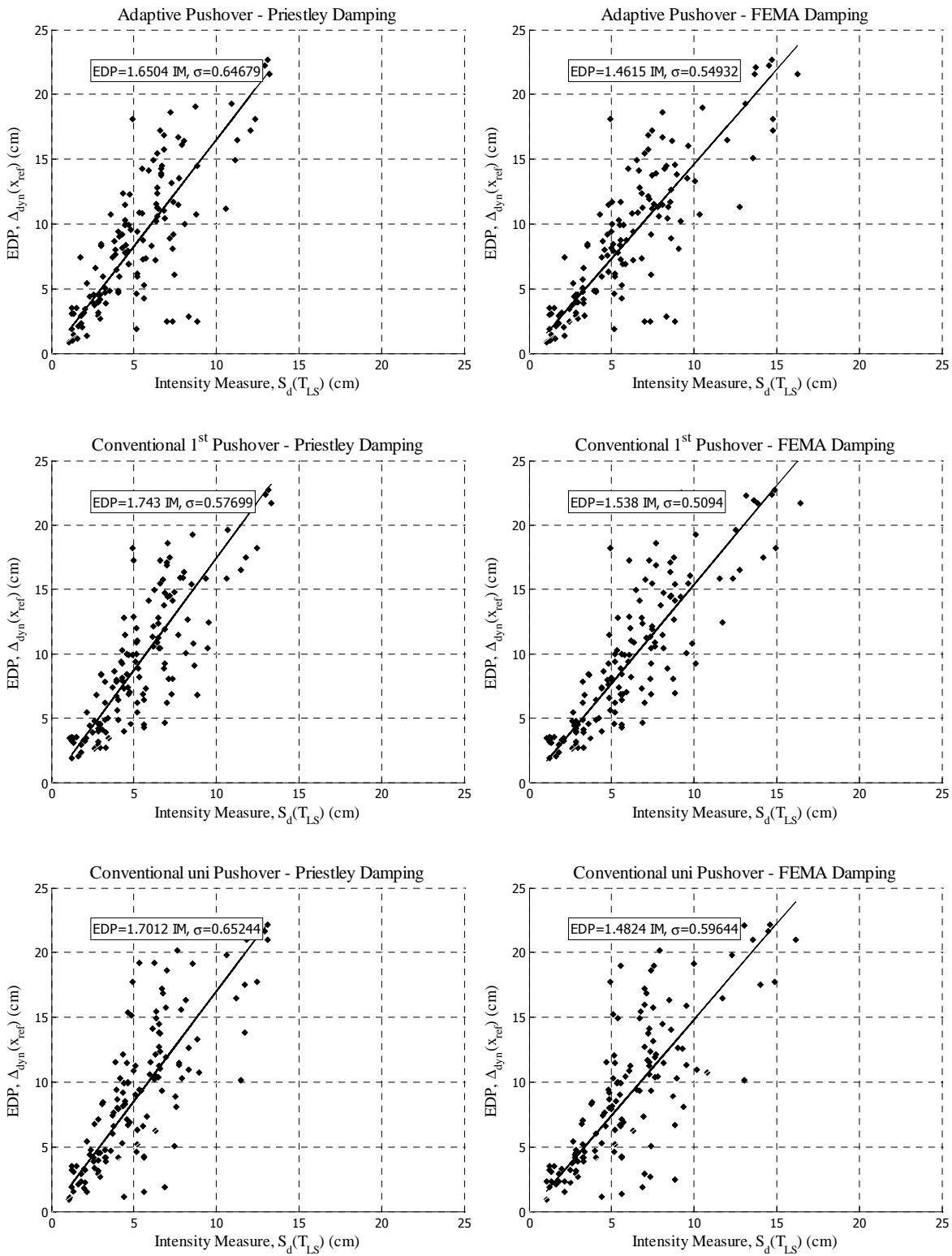


Figure 3.15 – Intensity measure vs. EDP using dynamic analysis-measured  $T_{eff}$  and ductility.

Some of the assumptions that have been made to streamline the procedure can be discussed and revisited:

- 
- The Limit State strains considered for concrete and steel may be reviewed, or adjusted, since this is fundamental data for the displacement capacities of the structure, within the intensity measure procedure; the fact that yielding and subsequent Limit States are assumed in the structure as soon as they occur in one of the piers, may as well influence the procedure in a relevant manner. A possibility would be to try an approach similar to what is typically followed for buildings, where the yielding displacement is taken as the one corresponding to 75% of the maximum base shear. However, this may not be easy, since it can be seen that the first pier reaches LS2 and LS3 shortly after yielding. Additionally, the definition of the maximum base shear is not clear for all the bridge configurations;
  - The equivalent SDOF displacement is another important issue, which has been defined according to Equation (3.1). A possible alternative is to use the displacement corresponding to the reference location,  $x_{ref}$ , shown in Equation (3.2). For the buildings case, the effective height is used, which seems to be a simpler approach. An approach simply using the deck central node as reference, as proposed in EC8 and other codes and guidelines within nonlinear static procedures, seems therefore worth a try;
  - The relationship of the effective measured periods with actually observed Limit State in the dynamic analysis, as well as with the effective LS periods coming from Priestley or FEMA approaches, is still missing. This may be important to justify the use of such effective periods instead of the empirical proposed ones;
  - The use of a reference node which is dependent on the displacement shape renders also somewhat difficult the evaluation of dynamic analysis results. The displacement shape at the Limit State that the bridge was considered not to exceed was used, in agreement with the determined intensity measure. For that shape the reference location was computed and response of that node was submitted to Fourier analysis to get the effective period. Moreover, EDP results from the first run had to be used to estimate the measured ductility  $EDP/LS_y$  used on the second run, given that EDP results depended on the Intensity Measure which was still being computed. This seems to suggest an iterative procedure. Anyhow, EDP used

to estimate ductility and EDP obtained in the new run proved not to be very different.

### **3.4 Artificial accelerograms**

It has been discussed, up to now, the use of real accelerograms as well as additional needed procedures, such as selection and scaling, which come from the mentioned and observed dispersion level among this sort of records. Consequently, at this point, the consideration of artificial accelerograms starts to gain relevance. The use of artificial accelerograms is no innovative, yet relevant, tool, especially if the difficulty in assuring a representative real ground motion records base is considered. From a design code point of view the use of artificial records is taken into account, namely on Eurocode 8, which considers their use as much as recorded accelerograms. The use of simulated accelerograms, as they are referred to for the analysis of buildings, shall be adequately qualified with regard to the seismogenetic features of the sources and to the soil conditions appropriate to the site. Also for bridges, appropriate simulated accelerograms may be used in case the required number of recorded ground motions is not available. The choice for this type of records is surrounded by several issues, as previously introduced, being that the main disadvantage lies exactly on their nature, and the possibly associated lack of authenticity, whereas its major argument is the overcoming of the complexity allied to the use of real records.

The term artificial is herein employed with a wide meaning and one can argue that the general designation non-real or synthetic records should be used, instead. Briefly, these can refer to spectrum compatible artificial earthquake records, which are based on random vibration theory and wavelets and make use of spectral density function and random phases (e.g., SIMQKE (Gasparini and Vanmarcke, 1976)) or non-stationary stochastic vector processes (e.g., TARSCTHS (Papageorgiou *et al.*, 2001)) or to synthetically simulated records, which are generated through complex numerical simulation of source and travel path mechanism of a seismic event. Engineering applications of these models are still few at the present, whereas much progress is being achieved on the models and on their calibration (Hwang and Huo, 1994; Lam *et al.*, 2000), which contextualizes the consideration of artificial records in this study. Therefore, the goal of this section consists mainly on scrutinizing the advantages that can be found when using artificial

accelerograms compatible with the set of selected real records, by direct comparison of the structural response.

### 3.4.1 Algorithm of generation

The frequency is the varying parameter along the duration of the time history. The chosen process of coming up with artificial accelerograms consisted on generating earthquake time-histories compatible with an elastic velocity response spectrum, based on the methodology proposed by Gasparini and Vanmarcke (1976), later improved by Barbat and Canet (1994). The procedure is based on the definition of the ground motion records,  $\ddot{a}(t)$ , by a superposition of series of sinusoidal waves, as in Equation (3.9). Frequency, amplitude and phase angle, are therefore the main varying parameters, according to the same equation.

$$\ddot{a}(t) = I(t) \cdot \sum_{i=1}^n A_i \sin(\omega_i t + \Phi_i) \quad (3.9)$$

$A_i$  represents the amplitude,  $\omega_i$  each angular frequency and  $\Phi_i$  is the phase angle. Essentially, by generating different arrays of phase angles, different ground motion records can be generated.  $I(t)$  is an intensity envelope function. The algorithm starts by setting  $n$  frequencies ( $\omega_i$ ) equally spaced and  $n$  phase angles randomly generated (between 0 and  $2\pi$ ). A group of amplitudes ( $A_i$ ) is obtained by using the simplified relation, Equation (3.10), with the power spectral density function ( $S_{\ddot{x}}$ ), which can be determined according to Gasparini and Vanmarcke (1976), as in Equation (3.11).

$$A_i \approx \sqrt{2 \cdot S_{\ddot{x}}(\omega_i) \cdot \Delta\omega_i} \quad (3.10)$$

$$S_{\ddot{x}}(\omega_i) \approx \frac{1}{\omega_i \cdot \left( \frac{\pi}{4\nu_{te}} - 1 \right)} \cdot \left[ \frac{\omega_i^2 \cdot S_v^2(\omega_i)}{\zeta_{p,te}^2} - \int_0^{\omega_i} S_{\ddot{x}}(\omega) \cdot d\omega \right] \quad (3.11)$$

In Equation (3.11),  $\zeta_{p,te}$  represents the peak factor, defined as a function of the duration of the generated motion,  $t_e$ , and of a probability level,  $p$ . Numerical research has shown that for a value of  $p = 0.367$  (corresponding to  $\ln(p) = -1$ ) rather good results are obtained, for relatively short ground motion signals.  $S_v$  is the velocity response spectrum and  $\nu_{te}$  is the fictitious time-dependent damping factor, a fraction of the artificial critical damping factor. Equation (3.11) has been employed by using the smallest natural frequency,  $\omega_1$ , with which the integral in the right becomes zero. The adjustment between provided and the generated spectrum is best for larger values of the duration,  $t_e$ .

### 3.4.2 Reference response spectrum for generation of records

Recalling one of the main goals of this section, to establish the comparison of the structural response coming from the use of real and artificial ground motion records, in order to do so, equivalent/comparable properties for both types need to be established. Hence, the generation of artificial records has been based on equal probability response spectra and knowledge of the corresponding Hazard distribution (Delgado *et al.*, 2006). By considering a specific exceeding probability level it is possible to define a reference response spectrum, which can be in terms of peak ground acceleration (PGA) or spectral acceleration ( $S_a$ ).

Defining the reference spectrum in terms of PGA consists in imposing the same peak ground acceleration for the mean real response spectra, obtained by the peak ground acceleration (**pga**) scaling technique (Section 3.3), and for the isoprobable response spectrum. On the other hand, when defining the reference spectrum as a function of spectral acceleration, the characteristics of the structure being analysed, namely the fundamental vibration period, are taken into account. Taking the mean real response spectrum, the corresponding exceedance probability level can be taken from the isoprobable spectrum. That mean response spectrum is then scaled to match the spectral acceleration of the isoprobable at the structure's period.



---

Once the reference response spectrum is defined, the evaluation of the scatter levels concerning the response of the analysed structures when subjected to real and artificial records.

### ***3.4.3 Artificial ground motion records generation parameters***

The generation code established that the response spectra of the artificial records are compatible with the reference one for a scatter (measured in terms of COV) lower than 20%. The main characteristics of the artificial ground motions records are related to the duration, the intensity envelope function's type, the time step and the peak ground acceleration. As there are no criteria established in design codes for the duration, the recommendation of a value not lower than 10 seconds was followed (CEN, 2005a). All the signals were generated with 10 seconds and a time step of 0.01 seconds, assumed as detailed and stable enough. A trapezoidal envelope function was adopted for the intensity, for which the beginning and ending time of the constant function value had to be prescribed.

## **3.5 Comparison between real and artificial records – structural application**

It has been stated that scatter effects caused by the use of real records have different meaning and proportion whether if SDOF or MDOF systems are to be considered. The initial analysis on response spectra dispersion has shown scatter levels associated to different scaling techniques. Subsequently, structural effects on MDOF structures, which probably constitute the case of major interest on this kind of analyses, should be further addressed. The role associated to nonlinear features on different structures makes the nature of accelerograms and eventual scaling procedure much more relevant. Herein, a MDOF structure (RC viaduct) has been considered as case study. The structure has been subjected to the selected real records, scaled to peak ground or spectral accelerations, as well as to comparable artificial accelerograms. Nonlinear analyses have been carried out using PNL software, which is based on plastic hinges models. The algorithm, developed in the eighties, has been extensively validated, supported on experimental testing, for the past few years. More information may be found in (Costa and Costa, 1987; Costa, 1989; Varum, 1996). Studied nonlinear response effects refer to ductility in curvature for critical

sections. Statistical analysis has been applied, characterizing different results in terms of average and standard deviation/coefficient of variation as dispersion measures.

### 3.5.1 Structural description

The structure that has been object of several dynamic nonlinear analyses consisted of the Lordo viaduct, located on a mountainous area of high seismicity in Southern Italy, region of Reggio Calabria, which has been studied within the European Integrated project LESSLOSS (2004a). The structure is defined by two independent and parallel viaducts corresponding to two motorways, with slight curvature in plan – Figure 3.16.



Figure 3.16 – Lordo viaduct (LESSLOSS, 2004a).

The analysis will focus the south viaduct, defined by piers 1 to 10 and abutments A and B, hence, eleven spans with variable length between 40 and 110 meters, as shown in the longitudinal profile in Figure 3.17. The deck is a continuous beam composed by a hollow composite steel-concrete girder of rectangular cross-section, strengthened by diagonal braces, struts, flanges and transverse stiffeners and diaphragms along span and at abutments. The deck cross section has constant height over the major part of the spans. Regarding the piers, they present polygonal hollow section with two different types. For the piers 2 and 3 the cross-section was set for hydrodynamics reasons, therefore, these are the only piers with hexagonal cross-section (6m deep and 3m wide); the remaining ones feature rectangular hollow section with central sept (6m deep and 2m wide), as in Figure 3.17. Piers 2 to 5 are supported on piles, whereas the other piers have direct foundations.

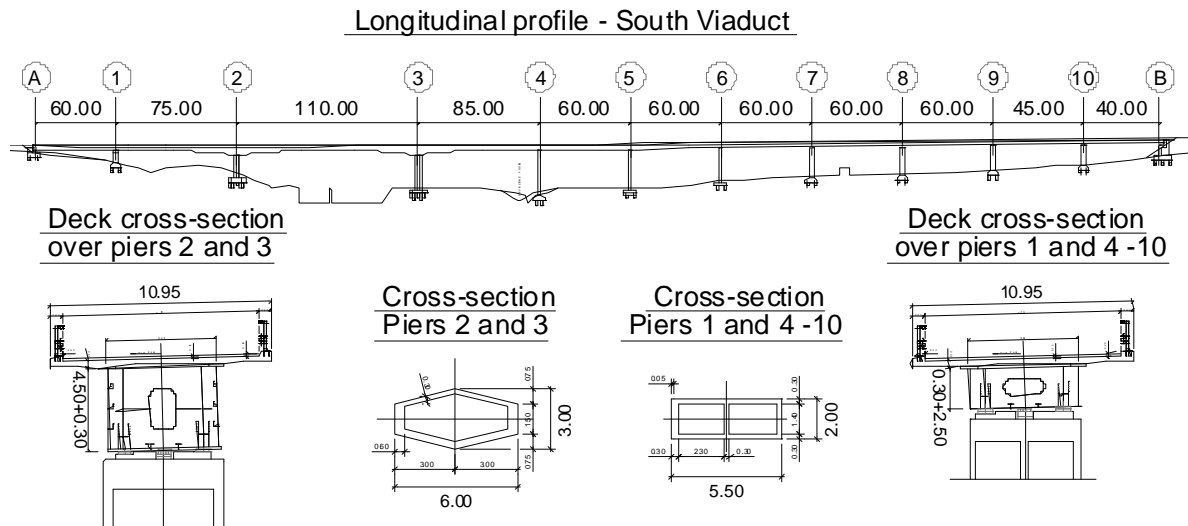


Figure 3.17 – Lordo Viaduct – South viaduct longitudinal profile and cross section of the piers (LESSLOSS, 2004a).

The structure is schematically illustrated in Figure 3.18 and the critical sections in terms of ductility demand, defined from preliminary analyses, are marked. For the subsequent applications, due to similar ductility demand levels, only the P3-related results will be presented.

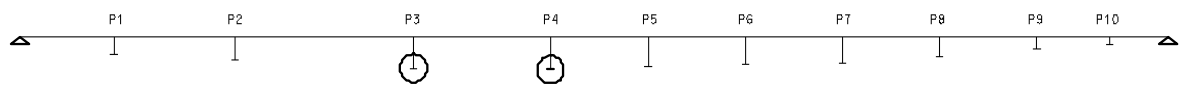


Figure 3.18 – Lordo viaduct – critical sections: P3 and P4.

### 3.5.2 Real records – original and homogeneous bases

Effects of the original set of accelerograms on the structure are represented in Figure 3.19, left. As expected, the original, unprocessed set of records yields quite scattered results, across all intensity levels (each line represents a level). The graphical representation enables the expedite conclusion that peaks are associated to accelerograms causing instability, which advocates for the use an aggregating technique similar to the one performed for response spectra in Section 3.2.2. As described in that section, a new cluster analysis was therefore carried out. Linear dependence between variables was not evaluated but Euclidean distances were measured instead. The cluster analysis highlights similar elements, which allows disregarding records causing the major scatter effects, hence, leading the original set of results to a higher homogeneity level, as illustrated in the same

figure, on the right. The new reduced set of results corresponds to 15 of the initially selected records.

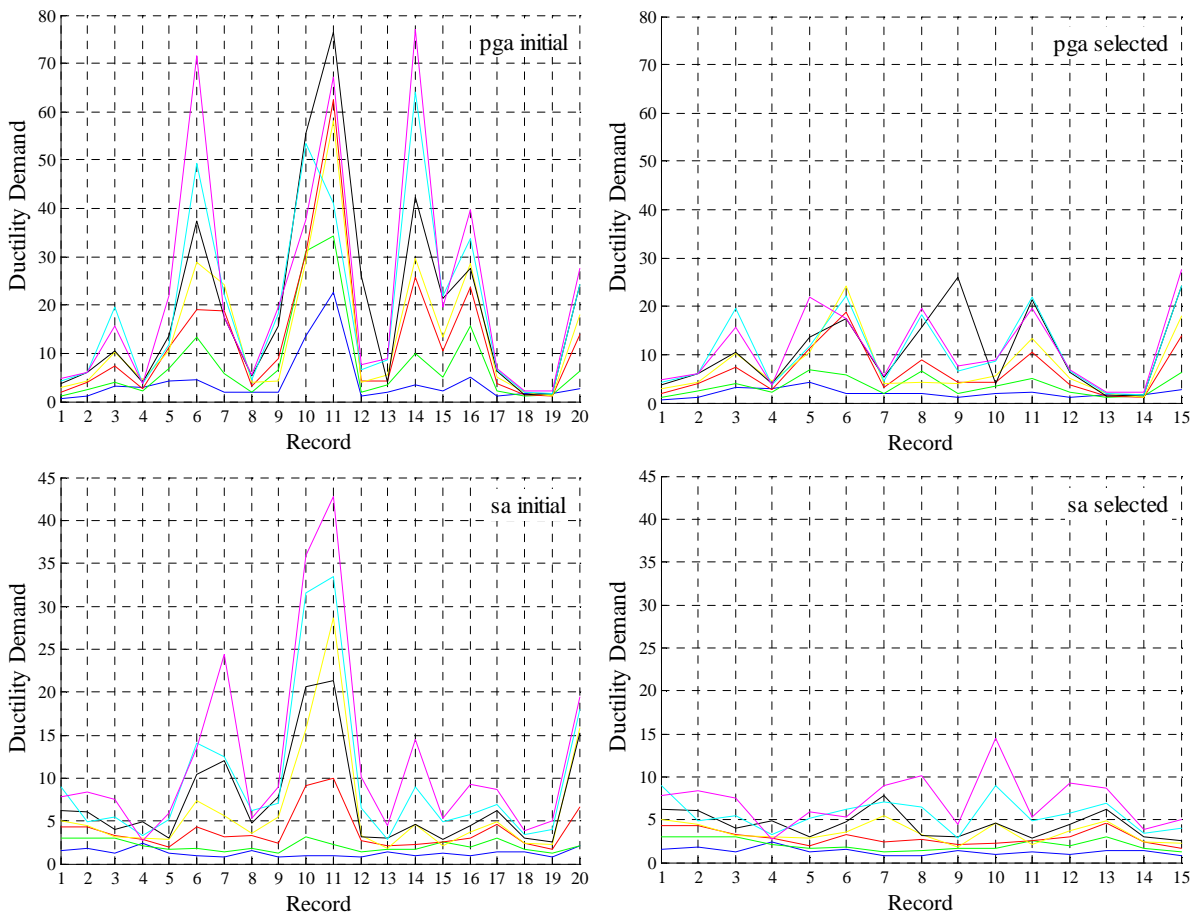


Figure 3.19 – Ductility demand at LORDO viaduct for the original (left) and reduced (right) base of real records, for the different records, scaled according to peak ground or spectral acceleration (Pier P3).

### 3.5.3 Minimum necessary number of accelerograms

The initial set of records includes twenty accelerograms whereas the homogeneous base has been set with fifteen accelerograms. When carrying out nonlinear dynamic analyses, the use of whether twenty or fifteen records will definitely be more representative and advantageous in the assessment of the scatter around the structural performance predictions. However, twenty accelerograms imply an equal number of different, dense and often time-consuming analyses, possibly leading to low feasibility levels. The number of records to use for seismic analysis will not necessarily have to be that large, given that it is expected that the engineering demand parameter at stake, such as ductility demand, will

stabilize, for a given tolerance, around a specific value. It can then be worthwhile to look into the possibility of reducing the number of records to a minimum able to adequately represent the whole set and produce the same mean/median structural response.

A former reduction procedure on the number of records has already been applied to the original set of twenty accelerograms by removing the most diverging ones through cluster analysis, as detailed in Section 3.2.3. It is thought to be possible to again reduce the fifteen records from the homogeneous base and still achieve the same mean structural response (ductility demand). The adopted procedure to study this intended reduction was based on quite simple considerations, although other studies have gone through this matter on the basis of confidence intervals (see Section 2.3.2). Samples of 3, 4 and so on, up to 10 accelerograms, were defined randomly. The  $n$  possible number of distinct samples of a certain size  $p$ , is thus given by combinations of  $n$ ,  $p$  to  $p$ . For each sample, the mean ductility demand,  $X_i$ , and the coefficient of variation (COV) to the “real” mean value,  $X$ , taken from all the 15 elements, is computed, according to Equation (3.12).

$$COV = \frac{\sqrt{\frac{1}{n} \sum_{i=1}^n (X_i - X)^2}}{X} \quad (3.12)$$

Representing COV as a function of the sample dimension, one may expect to identify a number of accelerograms that guarantees a satisfactory low distance to the “real” value, which refers herein to the average result coming from the homogeneous non reduced set of records. Figure 3.20 presents the curves obtained to the critical piers cross sections, for several seismic intensity levels. The results for the remaining piers have been found to be similar.

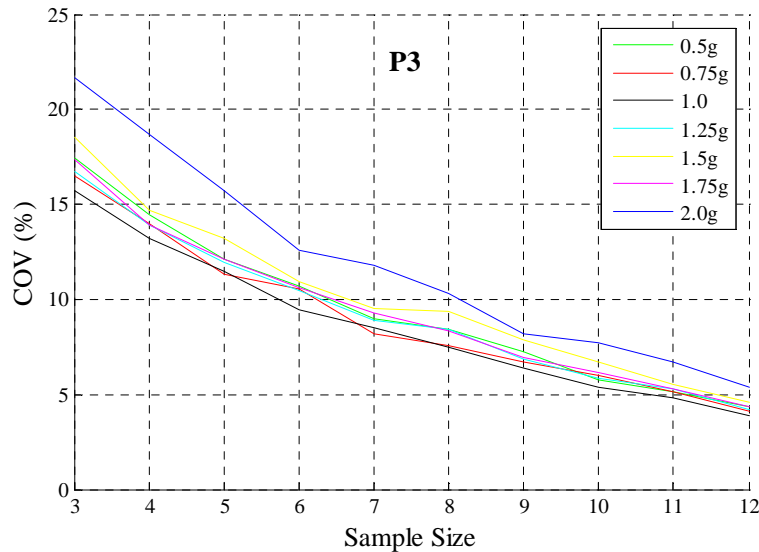


Figure 3.20 – Ductility demand COV according to sample size (Pier P3).

General scatter increases with the increase in nonlinearity, i.e., intensity level, which is an expected feature, even though major differences come up for peak ground acceleration of 2g, only. Moreover, it can be observed how the decrease rate along with the sample size is rather constant and, hence, it is difficult to define a number of records complying with the defined goal. Notwithstanding the difficulties in interpreting the results, a deceleration in the COV decrease is slightly visible from 6 records on and it is interesting to notice how the dispersion level with respect to the real mean value can be seen as reasonably low – mostly below 20%. If at least 6 records are considered, the COV lies around 10%. Using 7 records, instead, that amount is never reached.

The number of seven records is actually mentioned by the EC8 (CEN, 2005a) as the minimum necessary for the average of the individual responses to be used, which is reassuring, especially when the focus is on real records. In case less than seven nonlinear dynamic analyses are carried out, the maximum response should be used.

#### 3.5.4 Artificial records

Considering the conclusions just drawn on the suitable number of accelerograms to carry out nonlinear dynamic analysis, the use of seven artificial ground motion records seems a rational option, at least for a starting point. Most likely, and due to expected increased homogeneity, less than seven artificial accelerograms will be enough to obtain a stable median result. The ductility demand for each of the seven records, over the different

intensities, is represented in Figure 3.21, for the critical pier cross section. As expected, the scatter characterizing results is much lower despite the fact that one of the records still falls relatively out of the general panorama of the *pga*-based artificial accelerograms. The effect of one outlier will be, however, easily absorbed by the mean or median value.

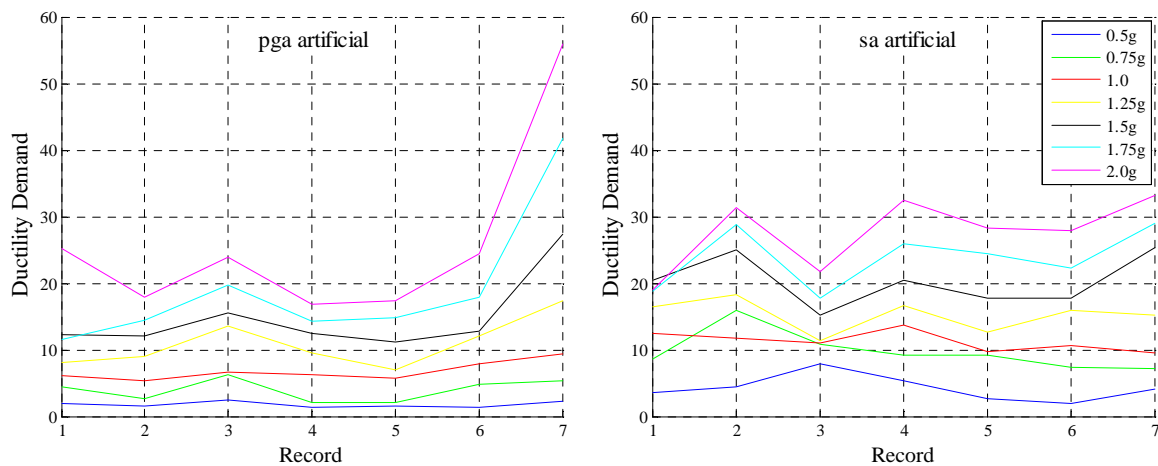


Figure 3.21 – Ductility demand at pier P3 for the artificial records base, for different intensity levels.

### 3.5.5 Comparison of results

The use of artificial records as an alternative to real accelerograms, or vice-versa, is still matter of discussion, hence, the comparison of engineering demand parameters (ductility demand) mean values as well as the associated scatter, when using both types of records is pertinent. The initial set of real accelerograms (initial real) and also a new set involving only the most similar 15 accelerograms (selected real) were used for analysis and comparison. For the purpose of comparing the performance of real and artificial records, the minimum number of 7 records has not been used given that, apart from the 10% residual, the outcome is the same. Furthermore the comparative endeavour was developed for the two scaling techniques previously selected, peak ground acceleration (*pga*) and spectral acceleration (*sa*). Artificial records were generated in agreement, as well.

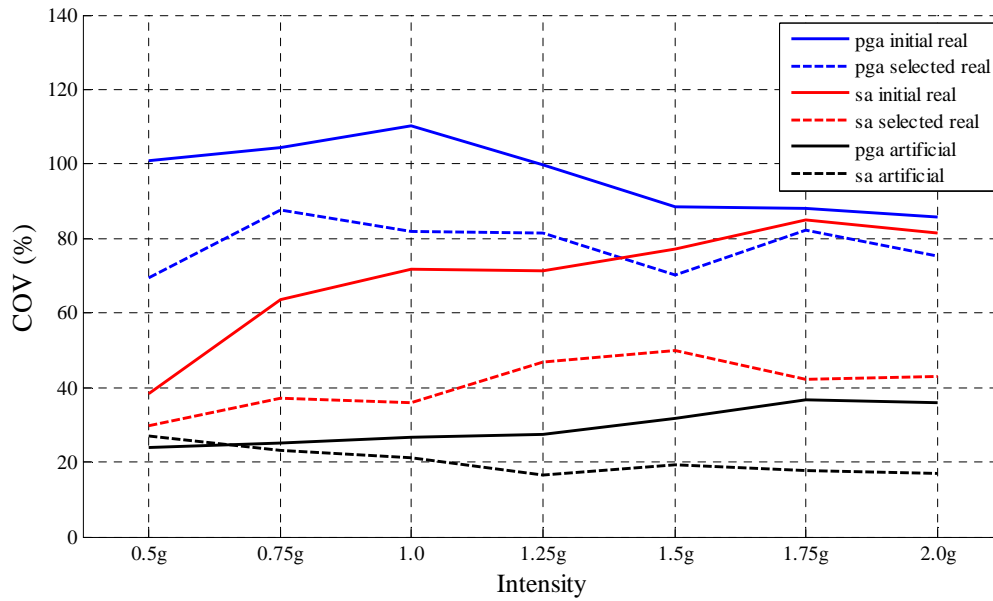


Figure 3.22 – Coefficient of variation for the ductility demand, according to the different scaling techniques and types of accelerograms.

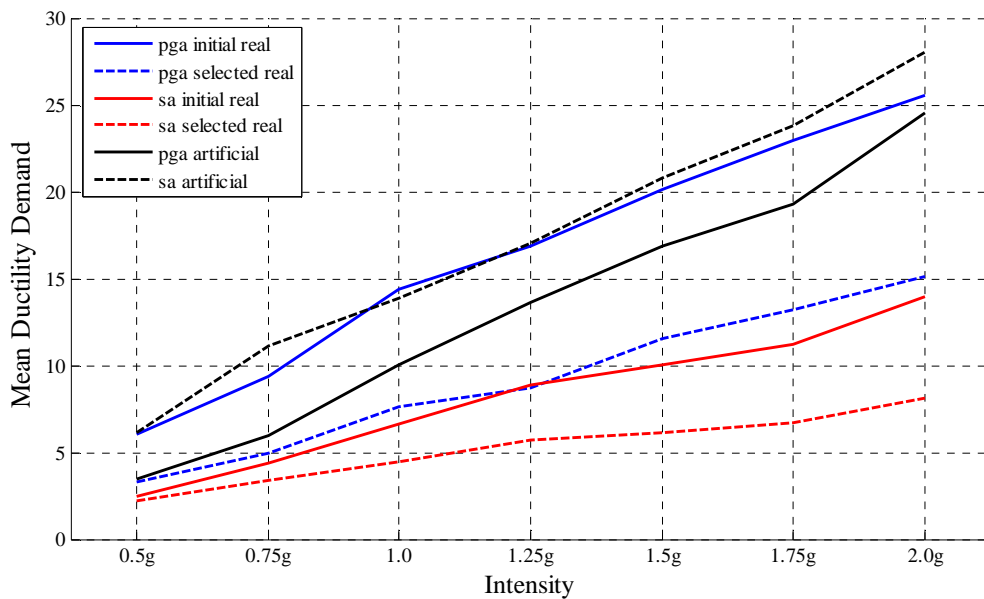


Figure 3.23 – Mean ductility demand for different scaling techniques and types of accelerograms.

According to Figure 3.22 real accelerograms scaled according to peak ground acceleration (*pga*) yield the highest scatter levels, even if considering the selected base of records. The same happens for the case of *pga*-scaled artificial records, when compared to *sa*-scaled ones. Nevertheless, artificial accelerograms, as expected, feature the lowest dispersion. When using real records scaled by means of spectral acceleration at the structural period (*sa*) the coefficient of variation lies between the two mentioned categories. If the selected



---

real base is used, instead, the dispersion associated to *pga* scaled records moves closer to the one obtained with *sa* scaling technique applied to the initial set of accelerograms.

With respect to the mean ductility demand, Figure 3.23, considerably higher mean values are obtained when using *pga* scaled records and the initial base whilst rather lower ones (around 50% of the maximum *pga* numbers), and the lowest at the same time, come from the use of *sa* scaling technique, which yields similar results to both initial and selected base of records. Employing artificial records, instead, again, intermediate or close to *pga* initial real values for the ductility demand are obtained, which may denote an underestimating trend for the *sa* results. Typically, all the alternative approaches tend to differ more among each other, in terms of median values, as the intensity level increases, whereas, considering COV, the difference tends to reduce, which can be advantageous from a collapse or near-collapse limit states analysis point of view. The ductility demand estimates obtained when carrying out the analysis with artificial records are generally in between the ones coming from initial and reduced set of *pga* scaled accelerograms, which accounts for validity in the use of artificial records, involving a lower number of analyses, as an alternative input to nonlinear dynamic analysis.

### 3.6 Conclusions

The definition of the seismic action, together with all of the subsequent issues, is related to the type of analysis. If nonlinear dynamic analysis is considered, seen as the most accurate way of estimating the structural response, the seismic action is represented by accelerograms; their selection, in number and type, scaling or homogenization has proven to be no straightforward task. This chapter intended to provide a contribution, firstly, to the matter of choosing between real ground motion records or artificial accelerograms. Approaches to deal with the scatter, usually large, associated to the real records have been addressed, as well as the topic of how many records to consider. A revisiting of traditional scaling techniques, also seen as intensity measures, has been carried out focusing on records or response spectrum base quantities. More advanced, yet preliminary, displacement-based intensity measures have also been proposed. Finally, a comparison between the use of artificial and real records, based on the structural response of a bridge

MDOF system, has been presented. The main observations and conclusions are discussed next.

- A first approach to the consideration of real records issue has again emphasized the considerable existing scatter, through the analysis of a database of real accelerograms. A “filtering” technique, based on statistical clustering analysis, has been applied to the initial set of records, in order to harmonize the database, eliminating the individuals considered to be statistically out of the group. The technique revealed itself easy to apply, making use of proper statistical tools and the so called homogeneous base was then obtained.
- Apart from selecting the most significant records for analysis, having eliminated the most “distant” ones, the most efficient parameter to use when standardizing them to a comparable level has been looked for, revisiting the typical used measures, adding some less used ones. The comparative study considered eight parameters, based on records or corresponding response spectrum quantities: peak ground acceleration; square ground motion; root-square ground motion; mean-square ground motion; root-mean-square ground motion; spectrum intensity; spectral acceleration and power spectrum area. The dispersion around the spectral ordinates, measured in coefficient of variation, was evaluated for the correspondingly scaled accelerograms. In general, all the parameters behaved similarly and it has been observed that, given a relatively heterogeneous database of 20 ground motion records, the traditionally used peak ground and spectral acceleration intensity measures performed superiorly, with respect to reducing the scatter around spectral ordinates. Such observation features two positive aspects; firstly, it goes along with most of past research work on this matter; furthermore, despite the development of more refined intensity measures, recently proposed by some authors (please refer to Section 2.3), the availability of Hazard data for such measures is very limited, if not inexistent (this does not happen with peak ground or spectral acceleration, which have been widely used). The latter becomes particularly important within a probabilistic vulnerability assessment framework, such as the one carried out in Chapter 6, which requires the seismic action to be defined probabilistic. Indeed, typically, the probability density functions for the

seismic action are available for the peak ground acceleration (or spectral acceleration, sometimes) intensity measure.

- Moving forward in the intensity measures subject, an advanced formulation, yet simplified in terms of analysis, has been studied. The proposed spectral displacement-based intensity measure was based on the establishment of limit states (defined through material behaviour) and corresponding secant periods, determined by means of nonlinear static analysis. Different pushover analysis types, as well as damping-based reduction factors, have been tested in an ensemble of fourteen bridge structures and ten ground motion records. Interesting trends between the results of nonlinear dynamic analysis and intensity measure have been encountered, although further development will be needed, so as to improve its efficiency. Indeed, some difficulties have been found in the definition of displacement based theory simplified quantities for generalized bridges, such as reference node location, which is somewhat expected, given that bridges are well-known for its potentially high irregular behaviour, in height and plane. Nevertheless, the experienced shortcomings have not prevented the proposed measure from revealing itself as promising.
  
- A structural application to investigate the viability of using artificial accelerograms, when compared to real records, with respect to the structural effects (engineering demand parameter considered as the ductility in curvature at the piers) in an irregular viaduct has been carried out. Artificial records constitute a very attractive alternative for two main reasons, which motivated the study. Firstly, the (complex) process of selection and scaling of real records would be avoided. In addition, within a safety assessment procedure based on nonlinear dynamic analysis, such as the one in Chapter 5, the number of records to assure accurate results would be less, with respect to real accelerograms, enabling therefore significant savings in computational demand. The clustering technique was therein applied to the ductility demand coming from the use of the initial base of accelerograms, leading to the homogeneous base of records. Such procedure was actually something new, given that a selection on the basis of a MDOF system response was employed.

- In order to avoid numerous nonlinear dynamic analyses, a simple parametric study was carried out to determine the minimum number of real accelerograms that would lead to the same results of the homogeneous base (within a specified tolerance). It has been observed that 7 records would represent a good compromise between feasibility and significance. To summarize, starting from a 20-record set, a homogeneous base of 15 records has been derived from clustering analysis and, in the end, a 7-record database could be used, assuring acceptable representativeness.
- A simple algorithm of generation of artificial records was then selected and 7 accelerograms have been obtained, following the conclusions of the study on the number of records. The comparison with real records (original and reduced set) scaled in the two traditional intensity measures that performed best (peak ground acceleration and spectral acceleration) was then carried out. The major conclusions pointed the use of artificial records as valid, yet conservative, with logically much lower scatter levels, standing between the median effect of the original set of accelerograms, scaled by mean of peak ground acceleration and spectral acceleration.

Once duly characterized, the seismic input will be applied to a proper nonlinear model of the structure. As certainly not exempt from discussion, the structural nonlinear modelling task will be addressed in the following chapter.

## 4. Nonlinear Modelling

The structural modelling topic is typically known for comprising a high number of challenging issues, some necessarily calling out for assumptions to be made and some in need for further development. Apart from the choice for the sort of model to use to represent the bridges to study, the option between fibres or plastic hinges as the mode of characterizing the material nonlinearity, the most important within bridge analysis (see 2.5), is another determinant aspect.

This chapter will consist, therefore, of detailing modelling aspects surrounding the work that has been carried out. A brief mention to the type of models that have chosen to represent a set of bridges is initially carried out, distinguished in accordance with the sort of material nonlinearity that is respectively considered, the computation tools and analysis procedures that are available. The used material models, concrete and steel, are afterwards contextualized and described, highlighting the potentialities that lead to their choice. Finally, and recognizing it as one of the current key issues, a parametric study is carried out to compare the use of lumped (plastic hinges) or distributed (fibre models) plasticity for the nonlinear material modelling.

The models that have been considered, in terms of spatial configuration, were selected considering different criteria. Regarding the computation available tools, the lumped plasticity models were idealized using software SAP2000 (Computers&Structures, 2006),

defining the plastic hinge constitutive law by means of a fibre based cross section model in BIAX (Vaz, 1992), whereas fibre models were built up using SeismoStruct (SeismoSoft, 2008). Both of the computer programs enable 3D frame models, which are, as stated in (Casarotti and Pinho, 2006), currently the best compromise between simplicity and accuracy, providing reasonable insight on the seismic response of both members and global structure.

#### **4.1 Material models**

A brief discussion on the concrete and steel models that have been used to characterize the bridge piers cross sections is in what follows. Whereas steel has been defined recurring to the same base model, concrete behaviour, more complex and less standardized, has been characterized through different approaches, depending on if plasticity is concentrated or distributed.

##### ***4.1.1 Concrete models***

Several concrete models are available in the literature, with different sophistication levels. The importance of highly refined concrete models in the moment-curvature response of reinforced concrete cross sections has been confirmed as not too relevant, in accordance with analytical studies conducted by Aktan and Ersoy (1979). This is most likely due to the fact that the expected ductile behaviour of RC sections will rely essentially on the steel contribution, rather than the concrete one. This main feature will be of great importance when carrying out, ahead, comparison parametric studies that make use of distinct concrete models.

The typical concrete monotonic behaviour goes through relatively well defined different damage stages, from initial cracking to rupture. The stress-strain diagram has a first approximately linear region which lasts until around half of the maximum compressive strength is verified. From that point on, a nonlinear behaviour stage follows, classically assumed as parabolic, caused by the considerable stiffness reduction due to cracking. The end of the 2<sup>nd</sup> degree polynomial branch corresponds to the peak compressive strength, which can be more or less evident, depending on whether the strength level is high or low. After the stress peak, the resisting compressive stress diminishes significantly until the

ultimate strain is reached, corresponding generally to about 20% of the compressive peak stress. That last descending portion is modelled as linear. Tensile concrete strength may be assumed, typically between 10 and 20% of the compressive strength. As very low contributing to the behaviour under bending forces, the tensile strength turns out to be generally neglected.

Early proposals for concrete model constitutive stress-strain relationships came up in the mid-late 1960s, by Shina *et al.* (1964) and Karsan and Jirsa (1969), both based on experimental tests of a large number of concrete cylinders or cubes, subjected to uniaxial compression. These were considerably preliminary models, which were, nevertheless, useful to study and recognize cyclic loading and unloading path features of the concrete material. Afterwards, from the decade of 1970 on, the number of proposals continued to increase, together with several variants and modifications, as summarized in a work by Yeh *et al.* (2002), referring to seismic performance of rectangular hollow bridge piers, which considered nine different stress-strain rectangular reinforced concrete models and found no significant dispersion in different model predictions, in particular for the moment-curvature plots. The selection included well known and widely spread out model from Kent and Park (1971), in its unconfined and confined versions; the modified Kent and Park model by Park *et al.* (1982); a model proposed by Muguruma *et al.* (1978), similar to the confined Kent and Park model with a different stress-strain curve shape and ultimate confined concrete strain; the Sheikh and Uzumeri model (Sheikh and Uzumeri, 1980, 1982), similar to the modified Kent and Park model, except for a flat ultimate strength within a strain range; the popular Mander *et al.* approach (Mander *et al.*, 1988a; Mander *et al.*, 1988b), which makes use of a confining pressure to affect the shape of the stress-strain curve; a proposal from Fujii *et al.* (1988), a model that is similar to the Muguruma *et al.* (1978) model except for different control parameters; a modification of the modified Kent and Park model with effective confining pressures of the rectangular cross section in both directions, presented by Saatcioglu and Razvi (1992) and a model from Hoshikuma and Nagaya (1997), which does not use effectively confined core area and suggests a residual strength of half of the peak compressive strength at large strain.

The lumped plasticity models, carried out in SAP2000, using a RC cross section constitutive trilinear law defined in BIAX (Vaz, 1992), make use of the modified Kent-Park model, whilst the fibre-based finite element models idealized in SeismoStruct

considered the Mander-Priestley-Park model. Both of them are described in higher detail, as follows.

#### 4.1.1.1 Modified Kent-Park model

The concrete nonlinear behaviour proposed by Park *et al.* (1982) is basically the modification of the originally presented by Kent and Park (1971), approximately one decade before. Such initial model takes into account the confinement effect in the concrete ductility, provided by the transverse reinforcement steel but not the corresponding increase in the compressive strength. The modification carried out by Park *et al.* consisted of introducing a confinement factor,  $k$ , which accounts for the confinement phenomenon when predicting the compressive strength, as well as the corresponding strain. Additionally, it features a reduction in the slope of the descending branch in the tension-strain diagram, reproducing the improvement in the concrete ductility provided by the confinement. The stress-strain diagram is represented in Figure 4.1, where three distinct branches, defined from points A to D, are distinguished as follows.

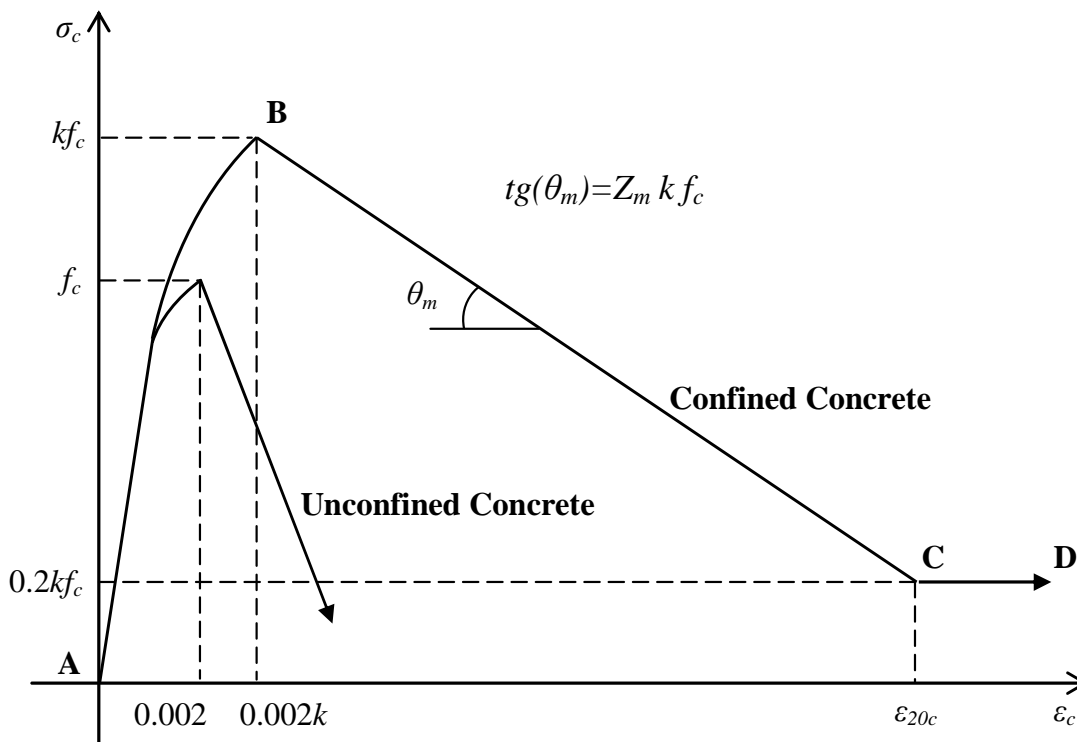


Figure 4.1 – Modified Kent-Park model – confined concrete stress strain envelope diagram for monotonic loading.



- A–B ( $\varepsilon_c < 0.002k$ )

$$\sigma_c = k f_c \left[ \frac{2\varepsilon_c}{0.002k} - \left( \frac{2\varepsilon_c}{0.002k} \right)^2 \right] \quad (4.1)$$

- B–C ( $0.002k \leq \varepsilon_c < \varepsilon_{20c}$ )

$$\sigma_c = k f_c [1 - Z_m (\varepsilon_c - 0.002k)] \quad (4.2)$$

- C–D ( $\varepsilon_c \geq \varepsilon_{20c}$ )

$$\sigma_c = 0.2k f_c \quad (4.3)$$

The confinement factor,  $k$ , is given by Equation (4.4);  $Z_m$ , related do the slope,  $\theta_m$ , of the descending branch B–C, is defined in Equation (4.5);  $\varepsilon_c$  is the longitudinal concrete strain,  $\sigma_c$  is the concrete compressive stress, (in MPa);  $f_c$  is the unconfined concrete compressive strength (in MPa);  $\varepsilon_{20c}$  is the concrete strain corresponding to 20% of the maximum compressive strength, in the branch B–C;  $f_{syt}$  is the yielding stress of the transverse reinforcement steel (in MPa);  $\rho_v$  is the ratio between the transverse reinforcement steel volume and the confined concrete volume;  $h$  is the confined concrete width and  $s$  is the transverse reinforcement steel spacing.

$$k = 1 + \frac{\rho_v f_{syt}}{f_c} \quad (4.4)$$

$$Z_m = \frac{0.5}{\frac{3+0.29f_c}{145f_c-1000} + \frac{3}{4}\rho_v\sqrt{\frac{h}{s}} - 0.002k} \quad (4.5)$$

The specific rules to model the concrete behaviour under repeated loading were originally proposed by Park *et al.* (1972) but it has been foreseen that alternative rules from Thompson and Park (CEB, 1983) are more realistic and were hence employed together with the stress-strain model.

#### 4.1.1.2 Mander-Priestley-Park model

The most interesting feature of the model proposed by Mander *et al.* (1988b) is probably that it is fairly generalist. Indeed, it is possible to explicitly consider the sort and arrangement of the transverse reinforcement steel, within a similar procedure to the one adopted by Sheikh and Uzumeri (1979), when developing their model under monotonic loading. The stress-strain constitutive relationship is illustrated in Figure 4.2 and is given by the expression in Equation (4.6), in which the variables assume the following indicated meanings.

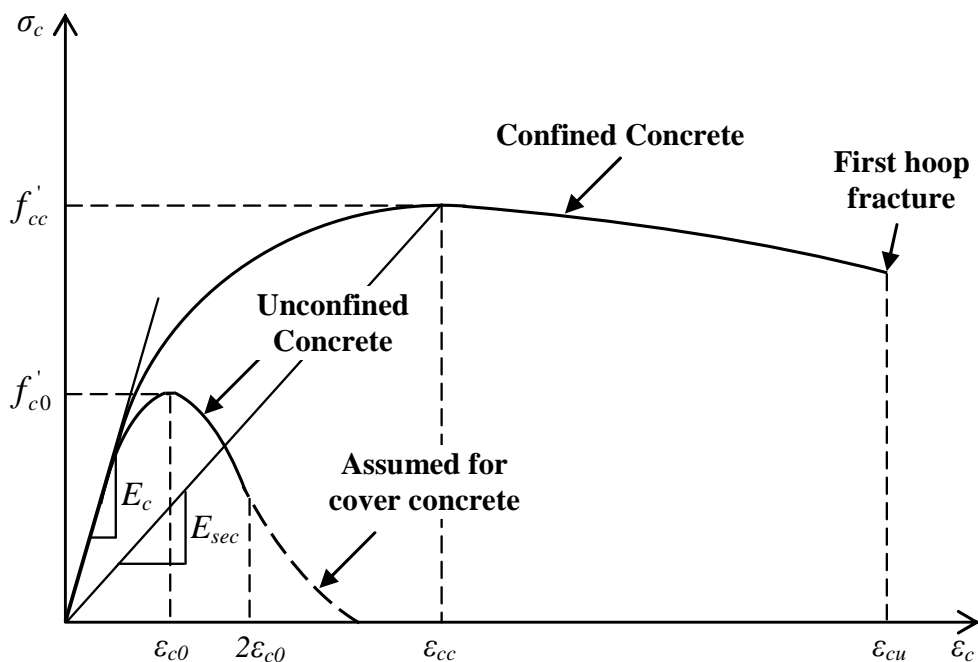


Figure 4.2 – Mander *et al.* stress-strain model for confined concrete under monotonic loading.

$$\sigma_c = \frac{f'_{cc} x r}{r - 1 + x^r} \quad (4.6)$$

$f'_{cc}$  is the confined concrete compressive strength;  $\epsilon_c$  is the longitudinal concrete strain;  $f'_{c0}$  is the unconfined concrete compressive strength;  $\epsilon_{c0}$  is the concrete strain corresponding to  $f'_{c0}$ ;  $x$  is the ratio between  $\epsilon_c$  and  $\epsilon_{cc}$ , given by Equation (4.7);  $r$ , in turn, is defined in Equation (4.8).

$$\epsilon_{cc} = \epsilon_{c0} \left[ 1 + 5 \left( \frac{f'_{cc}}{f'_{c0}} - 1 \right) \right] \quad (4.7)$$

$$r = \frac{E_c}{E_c - E_{sec}}; \quad E_c = 5000 \sqrt{f'_{c0}} \quad \text{and} \quad E_{sec} = f'_{cc} / \epsilon_{cc} \quad (4.8)$$

Within the fibre modelling that has been carried out the cyclic rules proposed by Martinez-Rueda and Elnashai (1997) have been used. The confinement effects provided by the lateral transverse reinforcement were, in turn, incorporated through the rules proposed by Mander *et al.* (1988b) whereby constant confining pressure is assumed throughout the entire stress-strain range. The model considers, additionally, tensile strength, even if evidently residual, which depends on the compression strain behaviour. It is assumed that for  $\epsilon_c > \epsilon_{cc}$ , or as soon as cracking occurs, for the following loading cycles, the tensile strength becomes null.

#### 4.1.2 Steel models

Steel is, by nature, a less complex than concrete behaving material, which will be reflected in the number and sophistication level of available models. Indeed, the steel monotonic behaviour can be essentially divided in three stages: a first branch, linear, where stress is constantly proportional to the strain; a second, where the stress is practically constant for increasing strain, the yielding plateau; and a final, where the stress increases again until

rupture occurs. Such typical behaviour refers to hot rolled steel, whereas cold rolled steel does not exhibit the yielding plateau, with higher tensile strength and lower deformation capacity. Some of the steel models are developed on the basis of material constitutive theories; however, the majority of those are phenomenological models that characterize the macroscopic response on the basis of experimental data. The fundamental characteristics of the steel response are relatively simple, thus, the appropriate material model not only predicts such response with reasonable level of accuracy but is also calibrated to fit experimental data with relative ease.

A number of models characterizing the response of reinforcing steel subjected to reversal cyclic loading on the basis of microscopic material response were identified and discussed by Cofie (1984).

More representative models for the response of reinforcing steel subjected to reversing cyclic loading can be achieved through the use of phenomenological models in which nonlinear equations are calibrated on the basis of experimental data. Several models on such basis have been proposed, since one the first approaches, in 1943, from Ramberg and Osgood (1943). Bertero and Popov (1976) presented a model consisting of a monotonic stress-strain law defined by seven points; Atkan-Karlson-Sozen (CEB, 1983) proposed stress-strain relationships made up of four zones, between tow consecutive loading reversals; Pinto and Giuffrè (1970) came up with a more complex behaviour model, including asymptotic representation of hardening and Bauschinger effects. Shortly after, Menegotto and Pinto (1973) applied the Giuffrè-Pinto model, systemizing a set of nonlinear equations describing steel behaviour, which served as a base for a bunch of other improving models: Stanton and McNiven (1979) improved computational efficiency; Filippou *et al.* (1983b) worked better on the unloading response, with both reasonably accurate prediction of response and relatively simple implementation and calibration; sophisticated Chang and Mander (1994) model accounted for cyclic strain hardening, providing quite accurate predictions of steel response.

Both lumped and distributed plasticity models have been defined taking the same Giuffrè-Menegotto-Pinto steel model, eventually applied with further refinement for the case of the SeismoStruct fibre models. A more detailed description of the main aspects of such model is carried out next.

#### 4.1.2.1 Giuffrè-Menegotto-Pinto model

The Giuffrè-Menegotto-Pinto model, used to describe the cyclic behaviour of the steel was originally elaborated by Pinto and Giuffrè (1970) and later improved by Menegotto and Pinto (1973). It manages to model the changes in stiffness and strength of the steel, due to the inversion during cyclic loading, through curves developed within four asymptotes, such as illustrated in Figure 4.3: two, parallel, with slope  $E_s$ , based on the elastic branch of the monotonic diagram, and two other, parallel as well, with slope  $E_{s1}$ , corresponding to the post-yield hardening stiffness.

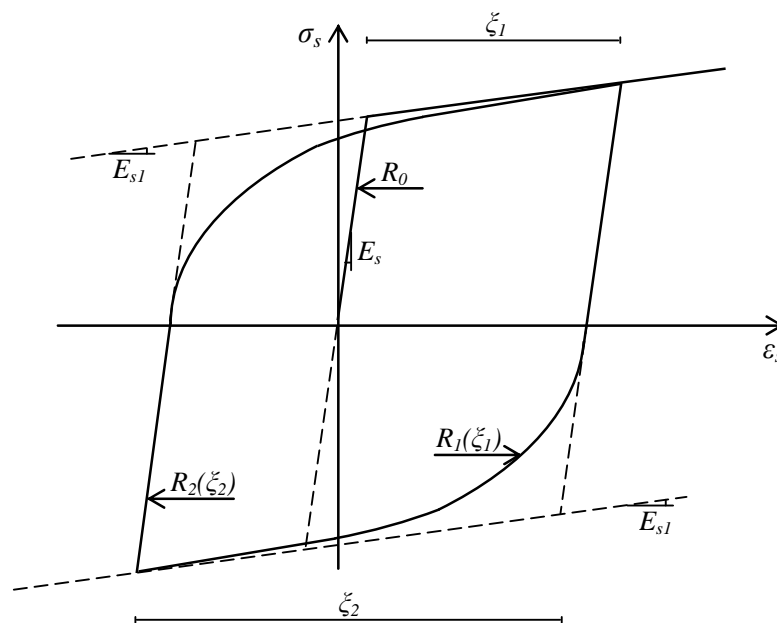


Figure 4.3 – Menegotto and Pinto stress-strain model for steel under cyclic loading.

Loading and unloading paths are completely involved by the monotonic loading bilinear behaviour law. The general expression for the stress-strain relationship is given by Equation (4.9), where effective strain and stress ( $\sigma^*$ ,  $\epsilon^*$ ) are function of the unload/reload interval;  $b$  is the ratio of the initial to post-yield tangent stiffness and  $R$  is a parameter that defines the shape of the unloading curve, representing the Bauschinger effect.

$$\sigma^* = (1-b) \frac{\epsilon^*}{\left(1 + \epsilon^{*R}\right)^{1/R}} + b\epsilon^* \quad (4.9)$$

Within the fibre modelling, computation implementation carried out by Monti *et al.* (1996), initially performed by Yassin (1994), was used, together with the modification introduced by Filippou *et al.* (1983b), to include isotropic strain hardening. This is actually considered to be one of the most accurate and convenient models to use, combining computational efficiency and very good agreement with experimental results.

## 4.2 Material nonlinearity approaches

Two main ways are currently followed when the purpose is to account for the nonlinear material features: lumped and distributed plasticity models. Within this topic, in the section that follows, each of the alternatives is looked into higher detail, with particular emphasis on critical issues. A few calibration studies were carried out, prior to the comparison of bridge response, obtained using each of the plasticity models.

### 4.2.1 Lumped plasticity models (plastic hinges)

When considering a concentrated plasticity model, the nonlinear behaviour of the bar elements is located in a rotational spring in both extremities of the elastic behaviour part of the element. Indeed, and regarding the particular application to bridges, studies carried out in the recent past have shown that bridge piers have a clear tendency to assume a nonlinear behaviour in well defined regions, which somewhat enables the plastic hinge approach illustrated in Figure 4.4 (Monteiro *et al.*, 2008b).

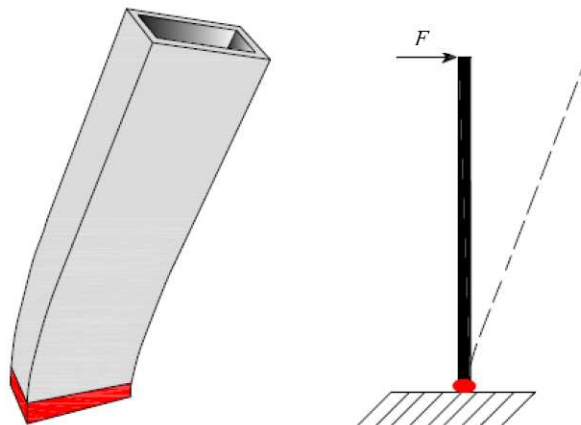


Figure 4.4 – Plastic hinge development at the bottom of a pier subjected to horizontal load.

Nevertheless, this kind of simplified model should be handled with care given that accuracy of the results may be compromised when the user does not have reasonable know-how on calibration of inelastic elements parameters. The assumption of the concentrated plasticity zones for the structural elements, with corresponding plastic hinges formation is currently used to estimate the real deformation capacity, taking duly account of the material nonlinear behaviour. Using this kind of approach, the nonlinear analysis process becomes greatly simplified, namely to what concerns the numerical data processing. The deformation capacity of the element depends on the ultimate curvature and plastic hinge length; different criteria used for the definition of these parameters may imply a different deformation level. Within the current work, different possibilities for the definition of the plastic hinge length were considered in a short complementary parametric study. Moreover, the characterization of a plastic hinge requires a moment-curvature diagram to be defined, or other “equivalent” one, which is obtained from the monotonic loading of the cross section. The carried study has used, for the plastic hinge models analyses, the bar finite element program SAP2000 (Computers&Structures, 2006) and BIAX (Vaz, 1992), developed at University of Porto, for the moment-curvature constitutive laws.

#### ***4.2.1.1 Plastic hinge constitutive law – trilinear curve***

The plastic hinges constitutive law, commonly expressed in terms of moments-curvatures, is probably the crucial contributing element within a lumped plasticity model analysis. That law, representing the behaviour of reinforced concrete sections subjected to bending, usually exhibits a trilinear approximate format, defined by cracking, yielding and rupture (Park and Paulay, 1975). Its definition has been typically achieved by means of a fibre discretization of the cross section of the element being considered, from which the nonlinear behaviour characterization is intended. Such is the methodology employed by the aforementioned fibre analysis algorithm BIAX, used and improved for hollow bridge pier sections in (Delgado, 2000). The section is therefore discretized in fibres with longitudinal uniaxial behaviour, which are analysed for biaxial bending, for a given axial compression force, but neglecting shear effects. Fibre detailing distinguishes unconfined and confined concrete and steel. Figure 4.5 illustrates the fibre modelling of the cross section of the bridge piers under study.

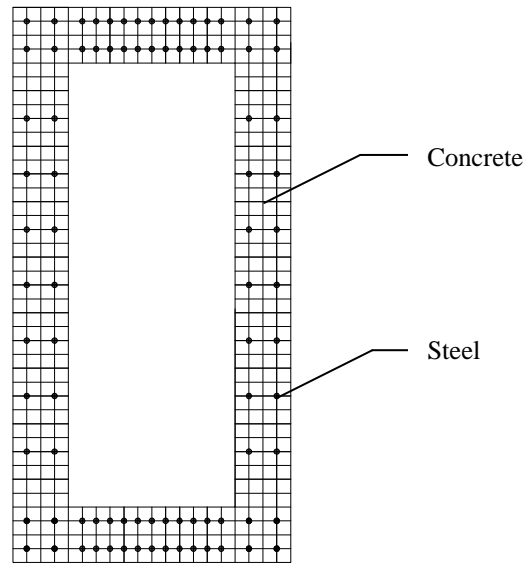


Figure 4.5 – Pier cross section fibre discretization

The plane sections hypothesis is assumed, catering for the strain at each fibre to be easily computed, as well as corresponding tension, making use of the employed material stress-strain relationships for the monotonic loading.

Alternatively, the moment-curvature diagram under monotonic loading can be obtained through a mechanistic procedure, in which the three characteristic point of the referred curve, cracking, yielding and ultimate points, are computed using steel and concrete stress-strain models, as defined, together with geometric characteristics of the section. Arêde and Pinto (1996) carried out an efficient implementation of this procedure for a generic T-shape reinforced concrete section, which can become rectangular, given that the algorithm is general. The characteristic moments and curvatures are obtained by applying imminent state conditions (known strains or stresses) along with elementary static principles, provided the external axial force is known. This sort of monotonic loading trilinear curve definition is particularly useful, within the context of such global section models, particularly when dynamic calculations with several loading steps, are needed in a large number, as has been done for probabilistic safety assessment – see Chapter 6.

#### **4.2.1.2 Plastic hinge length and location**

The plastic length is equally fundamental within a lumped plasticity approach. The accuracy of the element behaviour, when admitting that nonlinearity is concentrated in its



extremity portions, where curvature are assumed to be constant, depends on a correct estimation of the development extent of such behaviour. When duly characterized, the limitation of the plastic effects to a delimited portion will enhance major computation effort savings. The definition of the mentioned length is not, however, straightforward, given the theoretical and physical complexity of the phenomenon.

The plasticity length to be considered is majorly defined according to the extent where the longitudinal reinforcement bars have yielded. There are, nevertheless, other important phenomena that occur, such as the yield penetration, illustrated in Figure 4.6, corresponding to an additional rotation at the base support of the element, due to the physical inability for the curvature to go from zero to its maximum value in an infinitesimal length, leading to an extra rotation. Additionally, the plastic hinge length can be “spread out” as a consequence of the shear forces cracking, when the plane sections theory loses validity and steel deformation becomes larger than the computed one.

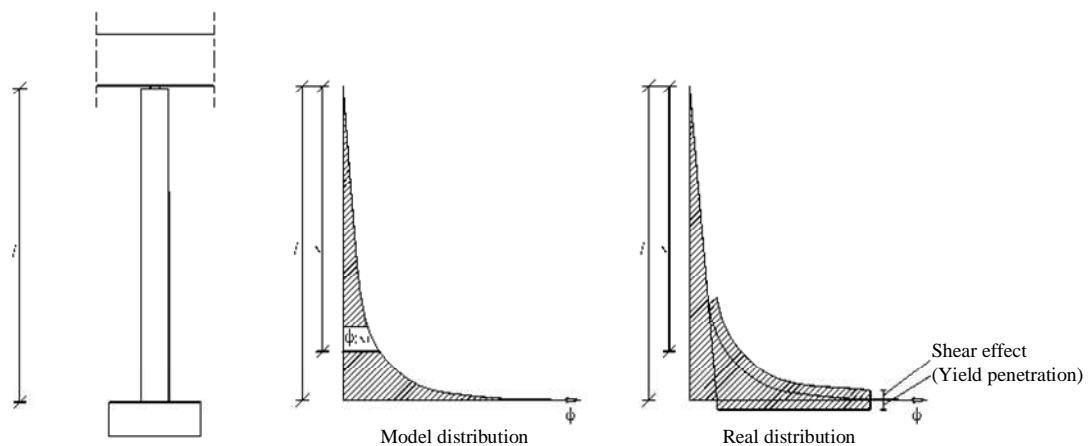


Figure 4.6 – Idealization of curvature distribution (*left*) and real curvature distribution, accounting for yield penetration and shear effect (*right*).

Several empirical expressions have been proposed over the years for the plastic hinge length,  $L_P$ , since the first approaches from Baker, Corley or Sawyer, as documented by Park and Paulay (1975), in which it was essentially assumed that the such length is proportional to the distance of the critical point to the point of contraflexure. More recently, Priestley and Park (1984), supported by a large number of experimental tests, pointed out for the plastic hinge length to be reasonably estimated by half of the element cross section height,  $h$ , according to Equation (4.10).

$$L_p = 0.5h \quad (4.10)$$

A few years later, Kappos (1991), based on experimental tests from Canterbury University as well, resented the expression in Equation (4.11), for the plastic hinge length, based on the element length,  $l$ , and longitudinal reinforcement steel bars diameter,  $d_b$ .

$$L_p = 0.08l + 6d_b \quad (4.11)$$

Paulay and Priestley (1992) refined the proposal from Kappos and came up with Equation (4.12), which includes the steel yielding strength,  $f_{sy}$ .

$$L_p = 0.08l + 0.022d_b f_{sy} \quad (4.12)$$

The more recent version of this approach ended up being presented by Priestley *et al.* (2007), re-including the distance to the point of contraflexure,  $L_C$ , as in the expression of Equation (4.13), where  $f_{su}/f_{sy}$  is the ratio of the ultimate tensile strength to yield strength of the flexural reinforcement.

$$L_p = kL_C + L_{SP} = 0.2 \left( \frac{f_{su}}{f_{sy}} - 1 \right) + 0.022 f_{sy} d_b \quad (4.13)$$

If the ratio is high, plastic deformations are expected to spread away from the critical section as the reinforcement strain-hardens, whereas a low value will correspond to concentrated plasticity close to the critical section, leading to lower hinge length.

Eurocode 8, in Part 2 – Bridges (CEN, 2005b), prescribes as well an expression for the estimation of the length of a plastic hinge occurring at the top or the bottom junction of a

pier with the deck or the foundation body, with longitudinal reinforcement of yield stress  $f_{sy}$  and bar diameter  $d_b$ , as in Equation (4.14).

$$L_p = 0.10l + 0.015f_{sy}d_b \quad (4.14)$$

As demonstrated, the number of different proposals for the length quantification of the plastic hinges is high and, therefore, a small parametric study has been carried out with the purpose of selecting one of the approaches for both comparative study with fibre models and subsequent nonlinear dynamic analysis (see Chapter 6). The study consisted of performing a simple pushover analysis of a single pier supported at the bottom, corresponding to one of the piers of the considered case study, described in Section 4.3. The pier is 14 meters high, discretized in seven elements with rectangular hollow cross section outer dimensions of 2.0x4.0m and constant width of 0.4m, as in Figure 4.7.

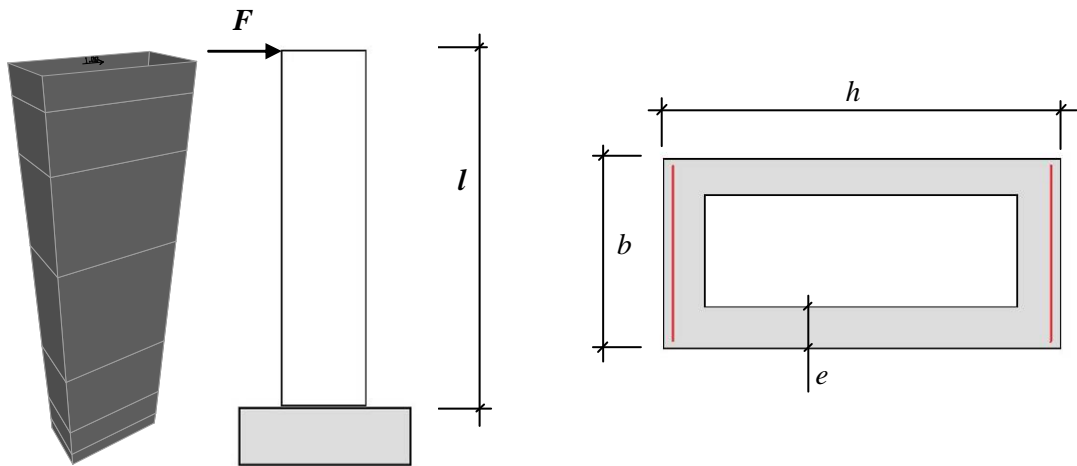


Figure 4.7 – Single pier used to calibrate the plastic hinge length (*left*) and corresponding cross section (*right*).

From the presented alternatives for the plastic hinge length, three have been selected for comparison: Kappos, Priestley and EC8, corresponding to Equations (4.11), (4.13) and (4.14), which represent the most recent/improved versions of the different authorships. The length obtained for the different tried versions ( $L_{p1}$ ,  $L_{p2}$  and  $L_{p3}$ ) is presented in Table 4.1,

whilst the corresponding base shear-top displacement curves, obtained with SAP2000, are plotted in Figure 4.8.

Table 4.1 – Plastic hinge length for different versions.

Equation	Plastic hinge length (m)	Designation
(4.11)	1.24	$L_{p2}$
(4.13)	1.55	$L_{p3}$
(4.14)	0.77	$L_{p1}$

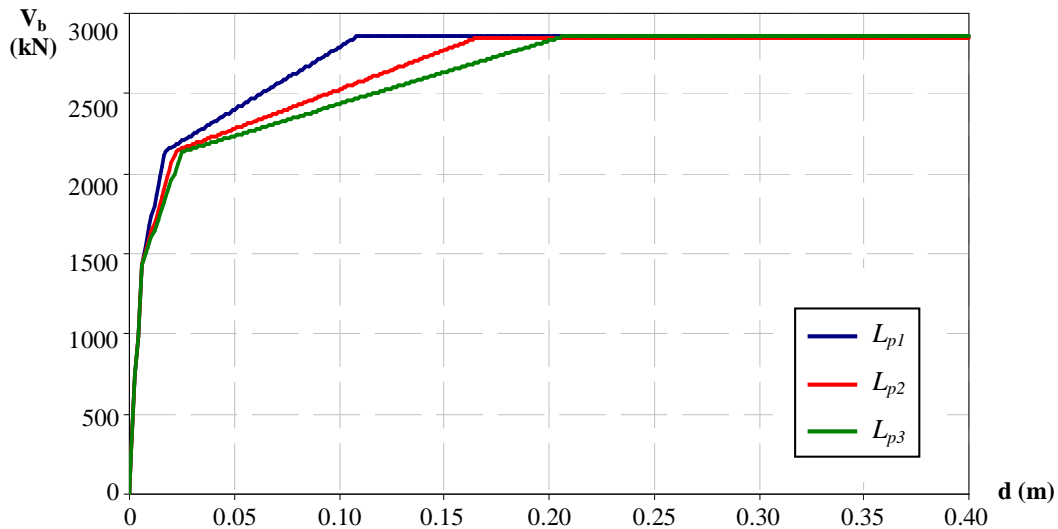


Figure 4.8 – Capacity curves for different plastic hinge lengths.

The numbers in Table 4.1 feature considerable dispersion, with the proposal from Priestley consisting of a plastic hinge length that is approximately the double of the EC8 one. Nevertheless, as expected, the results in terms of capacity curves do not differ much, especially for what concerns the ultimate base shear. On the other hand, the use of different plasticity lengths passes on to the displacements evolution, when the structure enters the inelastic field. The size of the difference between approaches increases with the inelasticity level: the yielding plateau is reached much later when using Priestley’s approach, which corresponds to the longest plastic hinge.

Another relevant parameter, from this concentrated plasticity perspective, is the plastic hinge location in the element, which, according to the used software package, SAP2000, can be at any position within the ending portion of the discretized bar. A study to on this location parameter has been conducted, analogously to the plastic hinge length one. Three location points have been tested, corresponding to the bottom ( $ph0$ ), half ( $ph0.5$ ) and top

( $phl$ ) of the bottom element of the pier, which is 0.7m long. The plastic hinge length has been estimated according to the formula proposed by Kappos, which provided intermediate results. The capacity diagrams, illustrated in Figure 4.9, reveal that the plastic hinges-based computation assumes the nonlinearity features completely concentrated in the specified location, using the plastic hinge length to determine the rotation for that specific location. Indeed, if the plastic hinge constitutive law is introduced in moments-rotations format, the specification of its length is exempt.

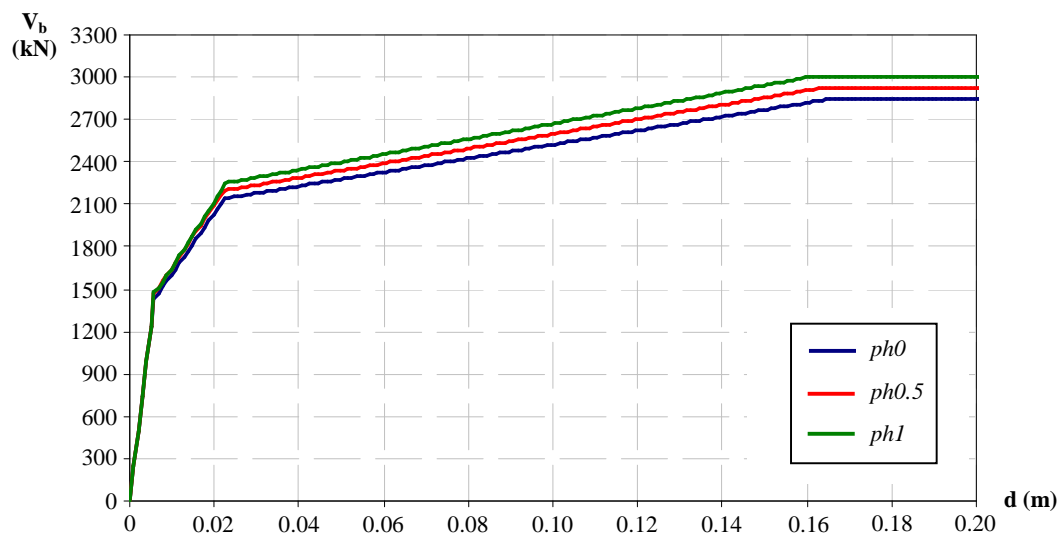


Figure 4.9 – Capacity curves for different plastic hinge locations.

The plastic hinge is “triggered” as soon as the force that is being controlled (usually bending moment) reaches the first inelastic moment defined in the plastic hinge constitutive law. From that step on, deformation is controlled by that constitutive law. Consequently, by shifting up the location of the plastic hinge along the bottom pier element, supported at the base, according to the triangular moments’ diagram that is installed, the base shear activating the plastic hinge behaviour is reached later. The closer to the base the plastic hinge is located, the lower the global force able to trigger it will be. Such finding justifies the differences found in Figure 4.9, which have been found, apart from being negligible (variation in maximum base shear less than 5%), to be mainly related to the maximum attainable base shear capacity rather than the curve shape itself.

#### **4.2.2 Distributed plasticity models (fibres)**

A structural model that includes material nonlinearity in a distributed fashion, using finite fibre elements, is able to characterize in higher detail the reinforced concrete elements and thought to capture more accurately response effects on such elements. Geometrical and material properties are the only required ones as input. According to Casarotti and Pinho (2006) a fibre model manages to represent the propagation of the nonlinear effects over the cross section of the element as well as along its extension. Consequently, higher accuracy in the structural damage estimate is attained, even for the case of high inelasticity levels. Fibre based analysis may have numerical solution using a stiffness or flexibility-based formulation. Differences between the two possibilities have been studied in Papaioannou *et al.* (2005) and the choice for the classic formulation based on the stiffness matrix developed by Izzuddin (2001) has been made. For this kind of models analysis, the fibre-based finite elements software package SeismoStruct (SeismoSoft, 2008), which basically performs 3D finite element modelling, with behaviour prediction for high displacement levels of structures subjected to static or dynamic loading, has been chosen. Material nonlinearity and second order effects are taken into account. A stiffness based cubic formulation is used to represent the development of the inelasticity along the element, together with axial load and transverse deformation interaction. Numerical integration makes use of two Gauss points per element, and the reinforced concrete cross section is discretized in fibres, as shown in Figure 4.10.

One of the main advantages of the use of fibre models is precisely the fact that there is no need for calibration regarding input variables, which are limited to the material and geometrical properties of the elements. Indeed, within a uniaxial 2-node finite element formulation, the variables that might be adjusted would be mainly the number of fibres or the elements' subdivision. The ideal number of section fibres, enough to assure an adequate reproduction of the stress-strain distribution across the element's cross-section, varies with the shape and material characteristics of the latter, depending also on the degree of inelasticity to which the element will be forced to. A number of fibres between 100 and 200 is currently used; the latter, or more, is usually adopted for more complicated sections, subjected to high levels of inelasticity.

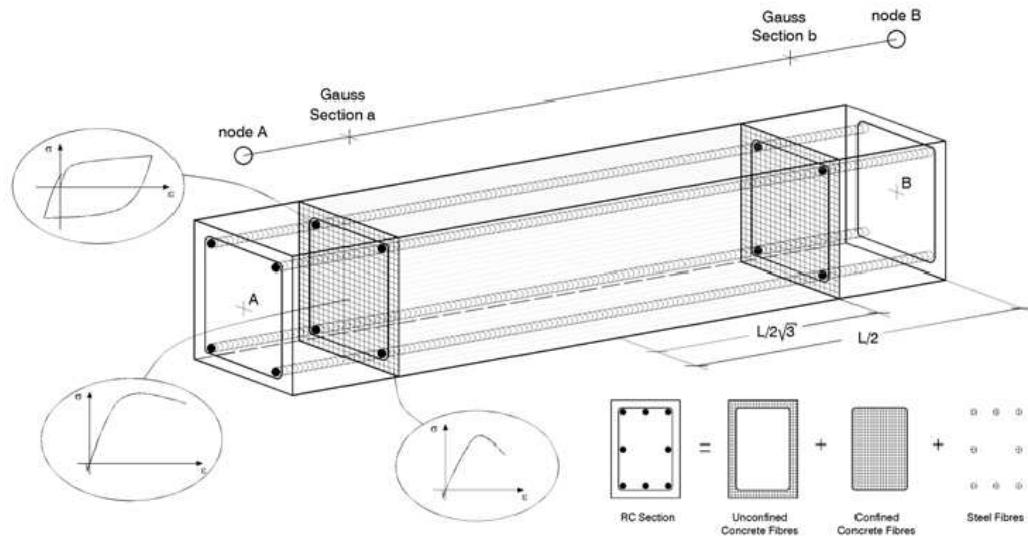


Figure 4.10 – Reinforced concrete element discretization – fibre modelling approach (Casarotti and Pinho, 2006).

Given the characteristics of the cross section of the piers, which is double-material, and of the analysis taking the structures to high nonlinearity, 200 fibres have been used. Regarding the number of elements, the extremities of the piers are the location for potential plastic hinges, therefore, a possible approach is to adopt a discretization that roughly follows such phenomenon. The adopted subdivision was, hence, to use five elements corresponding to 15%, 20%, 30%, 20% and 15% of the structural length of the pier.

### 4.3 Case study

An extensive parametric study has been conducted over several topics, namely, material plasticity modelling issues, nonlinear static procedures or probabilistic safety assessment, using a set of bridges, differing in regularity level, in terms of piers' heights and deck length, and abutment types.

#### 4.3.1 Selected bridges

The bridges selected for application were obtained by reformulation of the configurations used in the former research project PREC8 – Bridge Research Programme (Pinto *et al.*, 1996; Guedes, 1997), a program launched to cover topics of the European standard design code EC8 that needed to be clarified (in terms of structural regularity, evaluation of behaviour factors improvement of methods of analysis and of capacity design procedures).

The referred venture worked over two basis configurations, one regular and the other irregular, designated Bridge 232 and Bridge 213, respectively. The label numbers 1, 2 and 3 stand for pier heights of 7, 14 and 21 meters, respectively, as represented in

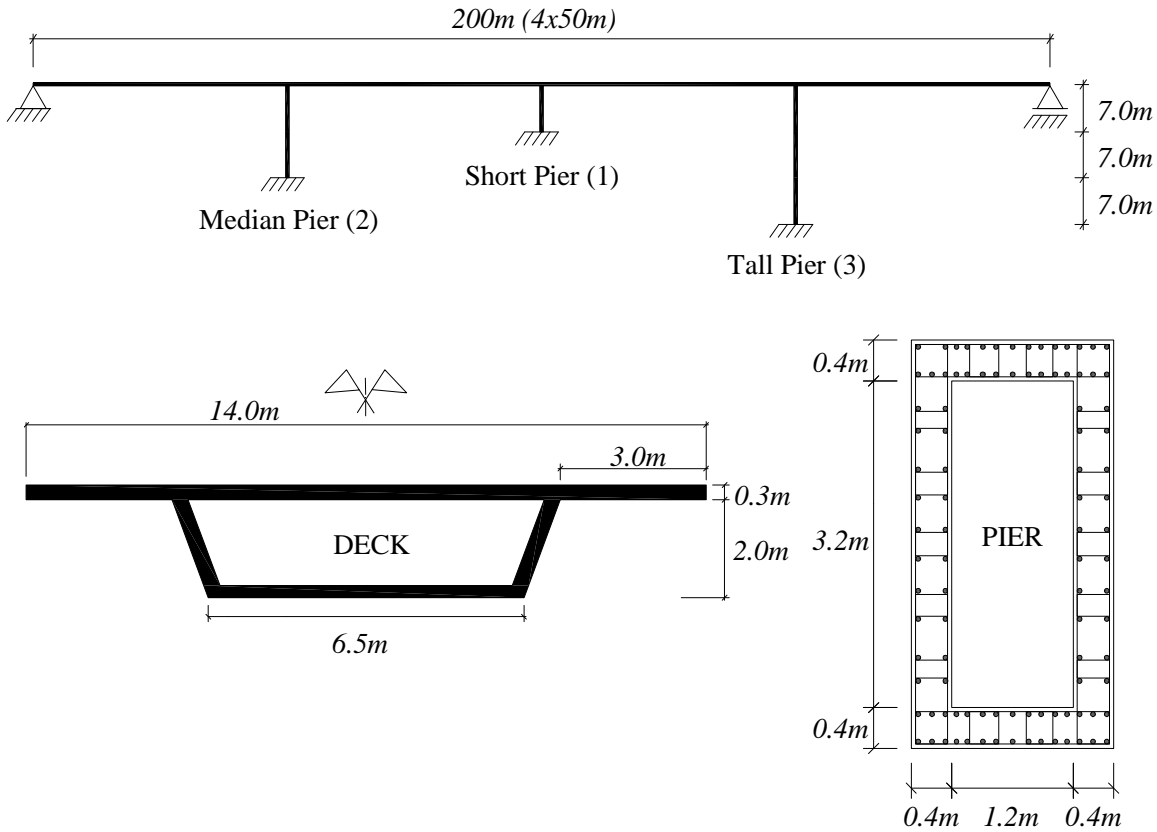


Figure 4.11, which illustrates the initially defined configuration 213, together with the structural elements that are common to the rest of the bridges. Different versions based on such geometrical configurations were considered by altering reinforcement features of the piers as well as existence/distribution of isolating/dissipating devices.

The bridges have been designed for a peak ground acceleration of 0.35g, according to (Calvi, 1994; Calvi and Pinto, 1995), in average soil conditions, following EC8 provisions. A minimum reinforcement steel ratio equal to 0.5%, half of the 1% prescribed by the code, has been adopted for the piers, in order to avoid highly forces to be attracted to the piers. The deck has been assumed as elastic behaving for all the bridges.



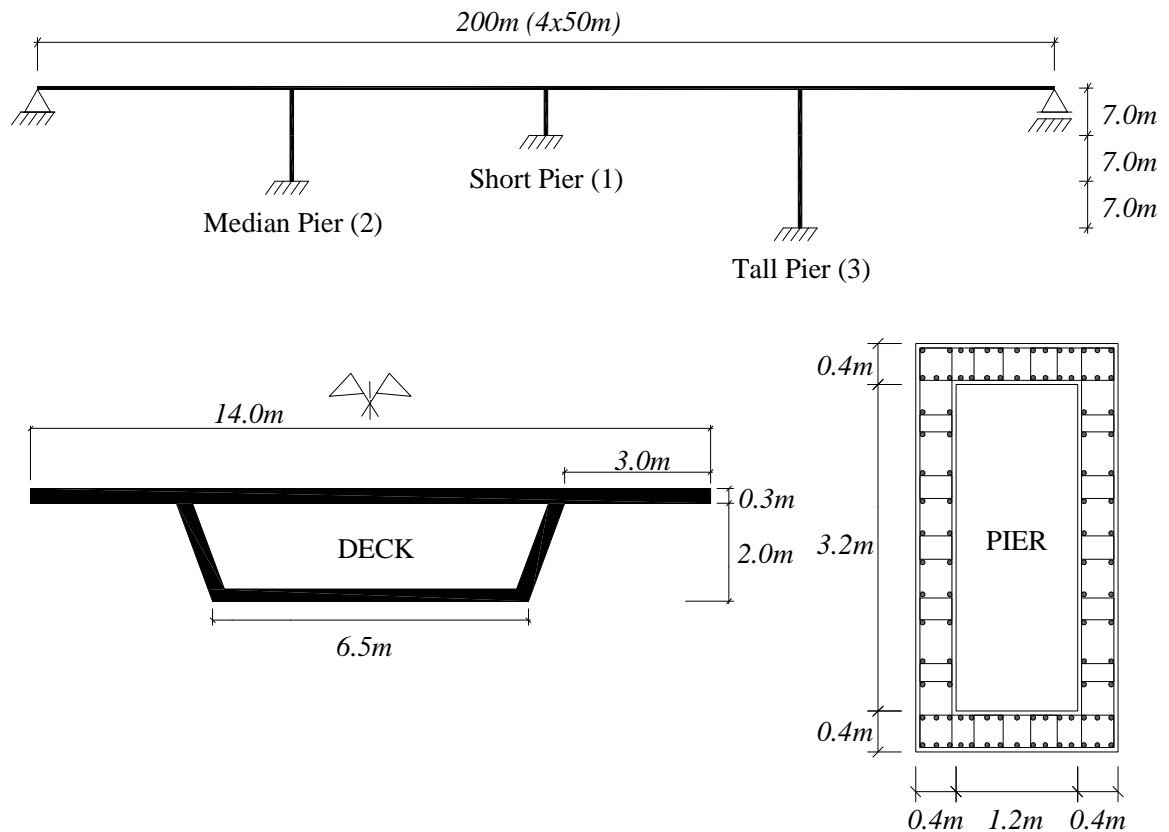


Figure 4.11 – Geometrical configuration of Bridge 213 and of the different structural elements, constituting the studied bridges.

Using the aforementioned bridge 232 and 213 configurations, Casarotti *et al.* (2005), extended the set to include deck lengths of 200 and 400 meters, with different configurations as well, analysing the additional 123, 222, 2222222, 2331312 and 3332111 configurations. The parametric studies carried out within the work herein described were based on the resulting final set of seven different bridge configurations.

Two bridge lengths have hence been considered (viaducts with four and eight 50m spans), with regular, irregular and semi-regular layout of the piers' height and with two types of abutments; (i) continuous deck-abutment connections supported on piles, with bilinear behaviour (type A bridges), and (ii) deck extremities supported on linear pot bearings (type B bridges). The total number of bridges is thus fourteen, as implied by Figure 4.12.

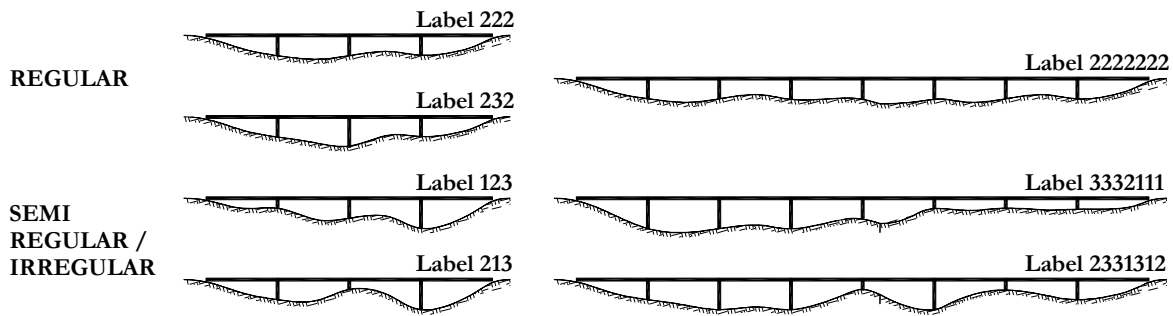


Figure 4.12 – Considered bridge configurations.

The fundamental period of vibration (see Table 4.2) ranges approximately from 0.3 to 0.5 seconds in short configurations and from 0.6 to 0.8 seconds in long ones.

Table 4.2 – Fundamental transverse periods of vibration (seconds)

Configuration	123	213	222	232	2222222	2331312	3332111
Type A abutments	0.46	0.40	0.41	0.51	0.59	0.65	0.71
Type B abutments	0.40	0.32	0.42	0.53	0.60	0.67	0.77

#### 4.3.1.1 Piers

The piers are made up of hollow reinforced concrete cross sections, as illustrated in Figure 4.13, in which the reinforcement details are included as well. The concrete and steel constitutive laws are considered as described in Section 4.1 and the corresponding defining parameters are presented in Table 4.3 and Table 4.4.

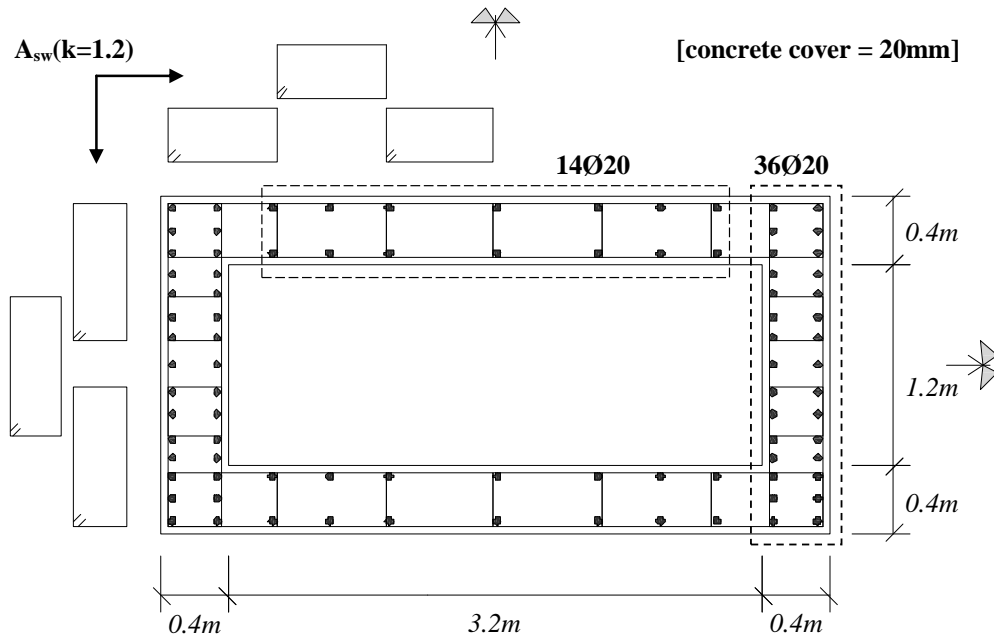


Figure 4.13 – Piers cross section

Table 4.3 – Concrete properties.

Parameter	
Young's Modulus (GPa)	30.5
Compressive stress (MPa)	42
Tension stress (MPa)	residual
Strain at the peak compressive stress	0.002
Confinement factor	1.2
Specific weight (kN/m <sup>3</sup> )	24

Table 4.4 – Steel properties.

Parameter	
Young's Modulus (GPa)	200
Yielding stress (MPa)	500
Strain hardening parameter	0.005
Transition curve initial shape parameter	20
Transition curve shape calibrating coefficients (a <sub>1</sub> , a <sub>2</sub> )	18.5, 0.15
Isotropic hardening calibrating coefficients (a <sub>3</sub> , a <sub>4</sub> )	0, 1
Specific weight (kN/m <sup>3</sup> )	77

The modelling of the piers has featured particular attention to its bottom and top regions, next to the ground and the deck, where the nonlinear behaviour will be concentrated. According to Priestley *et al.* (1996), depending on the footing/connection conditions, the plastic hinge regions should occur within an extent from 1/10 to 1/20 of the element's length. On the other hand, the length of the elements should not be very small, when compared to the cross section depth, which is four meters. Bearing such considerations in

mind, the piers have been divided in seven elements of length corresponding to 15%, 20%, 30%, 20% and 15% of the height, featuring, hence, higher refinement degree at the edges.

**4.3.1.2 Deck**

The deck has been assumed as elastic behaving, which is commonly accepted within design codes, due to its considerable flexibility or even to the fact that it is typically prestressed, not allowing plastic deformations. Furthermore, many times, isolating devices are employed with the purpose of protecting the deck from damaging movement of the soil. For the particular case of the bridges herein considered, the deck has been modelled by means of an elastic beam 3D element accounting, nevertheless, for second order geometrical nonlinear phenomena. The geometry of the deck is illustrated in Figure 4.14 and the corresponding mechanic characteristics are listed in Table 4.5, analogously to the 1:1 scale tested model at ISPRA (Guedes, 1997). The assumed Young’s and shear moduli are 25GPa and 10GPa ( $\nu=0.25$ ). Each span of the deck is divided in eight elements, with higher refinement in the regions over the piers and next to the abutments, only, given that elastic elements will certainly not require large discretizing amount. Moreover, the bar element representing the deck is shifted from the top of the piers of 1.508 meters, a height corresponding to its cross section centre of mass (see Figure 4.14).

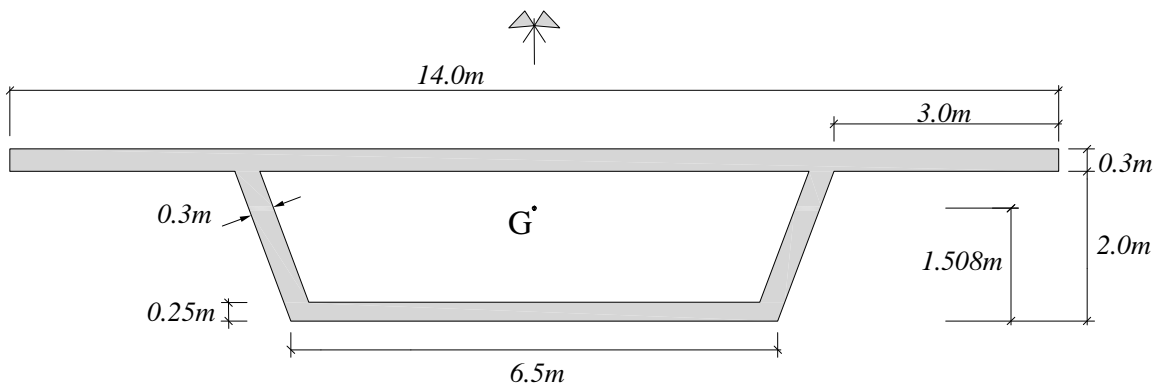


Figure 4.14 – Deck geometry

Table 4.5 – Deck properties.

Parameter	
EA (kN)	$1.74 \times 10^8$
$EI_2$ (kN.m <sup>2</sup> )	$1.34 \times 10^8$
$EI_3$ (kN.m <sup>2</sup> )	$2.21 \times 10^9$
GJ (kN.m <sup>2</sup> )	$1.17 \times 10^8$
Mass (ton/m)	17.4

The connection between piers and deck is assured by rigid link elements, of residual mass, which guarantee that only shear and axial forces are passed to the piers, so as to simulate the shear keys supporting the deck, as schematically represented in Figure 4.15, taken from SeismoStruct model.

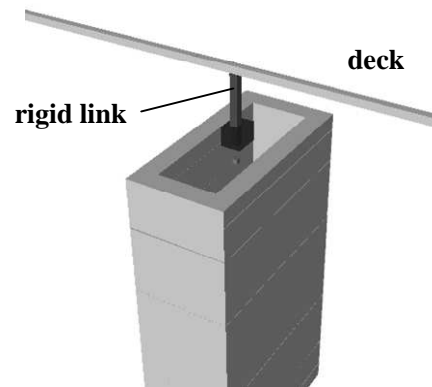


Figure 4.15 – Pier-deck connection through rigid link elements

It is worth noticing that the employed elastic element deck modelling does not take into account shear contribution to the deformation.

#### **4.3.1.3 Abutments**

The abutments are essentially modelled through springs that intend to represent whether the supporting on pot bearings or piles, whereas the piers are fully restrained at the bottom. Bridge abutments design is usually carried out for serviceability limit states and afterwards verified for the seismic demand. The use of elastic spring elements to model this sort of structural element is common when analysing bridges, given the easiness in incorporating the dynamic behaviour of the ground adjacent to the abutment, the different structural features of the abutment and the soil-structure interaction (Casarotti *et al.*, 2005). Further detail and approaches on the modelling of abutments can be found in studies from Goel and Chopra (1997), Megally *et al.* (2003), Bozorgzadeh *et al.* (2006) amongst others.

Adopting the modelling in the work carried out by Casarotti *et al.* (2005), based on iterative procedures or simplified approaches, the definition of the abutments consisted of quantifying the stiffness of the different springs. For the selected configurations, two sorts of abutment have been defined for testing: continuous deck-abutment connections supported on piles (type A), with assumed bilinear behaviour, and deck extremities simply

supported on pot bearing (type B), which feature linear response. Both cases are modelled by means of four springs in parallel, which represent either the soil or the bearings, connected through rigid arms, as shown in Figure 4.16.

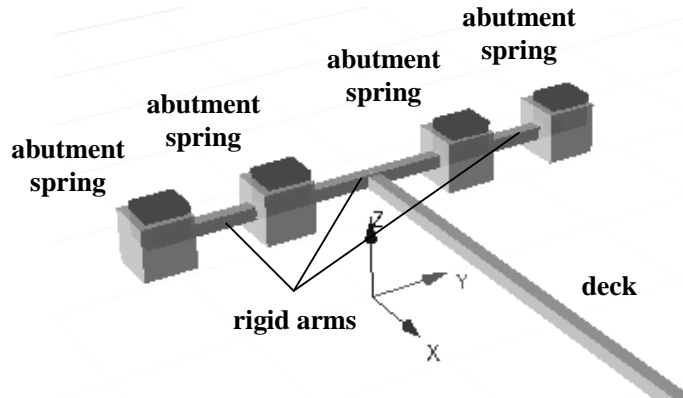


Figure 4.16 – Abutments modelling scheme.

#### **4.3.2 Seismic action**

The employed set of seismic excitations is defined by an ensemble of ten records selected from a suite of historical earthquakes (SAC, 1997) scaled to match the 10% exceeding probability in 50 years (475 years return period) uniform hazard spectrum for Los Angeles, which corresponds, in the current endeavour, to the intensity level 1.0. Figure 4.17 illustrates pseudo-acceleration and displacement spectra for the selected earthquake records, with damping ratio of 5%, together with the median spectrum in thicker line.

Additional intensity levels, linearly proportional to the latter by a factor of 0.5, 0.75, 1.5, 2.0 and 2.5, have been also considered, with the purpose of allowing an overview on how results evolve with increasing seismic intensity.

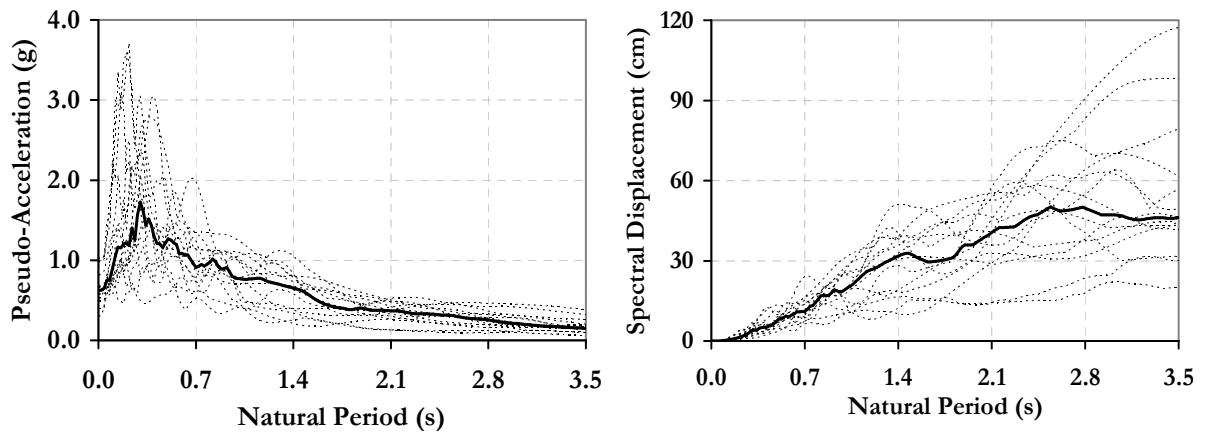


Figure 4.17 – Elastic pseudo-acceleration and displacement spectra.

The ground motions were obtained from California earthquakes with a magnitude range of 6-7.3 recorded on firm ground at distances of 13-30 km; their significant duration (Bommer and Martínez-Pereira, 1999) ranges from 5 to 25 seconds, whilst the PGA (for intensity 1) varies from 0.23 to 0.99g, which effectively implies a minimum of 0.11g (when intensity level is 0.5) and a maximum of 2.5g (when intensity level is 2.5). The demand spectrum was defined as the median response spectrum of the ten records.

#### 4.4 Comparative study

In the previous sections, both the modelling possibilities have been discussed and duly calibrated, regarding the typically relevant parameters of each approach. The next step is to look into the differences taking place when a nonlinear analysis is carried out, which, ideally, would be insignificant or at least very low, regardless the type of model being used for the analysis. In order to put away possible sources of divergence coming from the use of dynamic nonlinear analysis, considered the most accurate analysis method, yet definitely more complex, the employment of nonlinear static pushover analysis has been decided. Furthermore, pushover-based procedures have been gaining ground as valid methods for response estimation, when compared to dynamic analysis, mostly for buildings, in the past few years. In addition, their suitability to the case of bridges has been thoroughly investigated and confirmed in this work (Chapter 5). The comparative study has focused the case study configurations described in the previous section. For the sake of simplicity, and keeping in mind that material plasticity will be developed essentially at the piers, only the first type of abutments, type A, has been considered. The comparison is,

hence, based on a total of seven different configurations. A preliminary eigenvalue study on the vibration modes of the different configurations has been carried out, with a view to calibrate both analysis software programs models, in terms of stiffness and mass, assuring the structural elastic validity of the subsequent comparisons.

The first comparison of material nonlinearity approaches that has been carried out was in terms of the moment-curvature law obtained within the use of both of the computation versions: the BIAX obtained one, used for the Plastic Hinge Model (**PHM**) in SAP2000, and the one ‘internally’ considered by SeismoStruct, within a Fibre Model (**FM**). Such initial comparison is due to the fact that for the capacity curve computation, the main output of a pushover analysis, the need for an accurate consideration of the behaviour of the piers’ cross sections is obvious, given that the piers will be the bridge elements with nonlinear behaviour.

Two different cross sections, hollow and solid, submitted to three different axial loading forces, have been tested and the moment-curvature behaviour given by both of the approaches (plastic hinge or fibre based) have been compared. Pushover analyses were subsequently carried out for the seven different considered bridge configurations, presented in Section 4.3, followed by direct graphical comparison of pushover curves and statistical parametric comparison of distinct response quantities: deck displacements, deck bending moments, pier shear forces and abutment shear forces.

#### ***4.4.1 Elastic modal analysis comparison***

The first three eigenmodes for the seven bridge configurations, computed for both structural modelling versions, fibre based SeismoStruct (FM) and plastic hinges based SAP2000 (PHM), are presented from Table 4.6 to Table 4.12.



Table 4.6 – Vibration modes for configuration 123 – Fibre vs. Plastic Hinge Modelling.

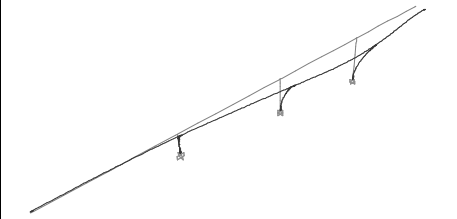
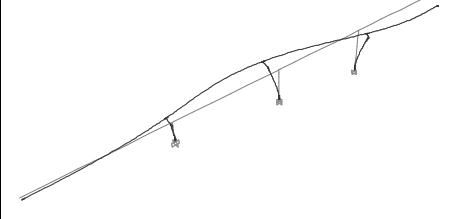
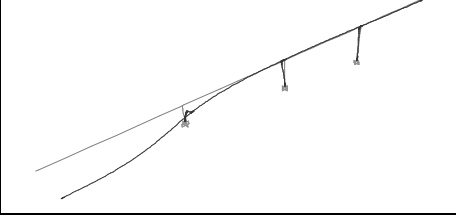
Bridge 123 transversal vibration modes		Period (s)	
		Fibre Model	Plastic Hinge Model
1 <sup>st</sup>		0.4596	0.4597
2 <sup>nd</sup>		0.2989	0.3006
3 <sup>rd</sup>		0.2441	0.2450

Table 4.7 – Vibration modes for configuration 213 – Fibre vs. Plastic Hinge Modelling.

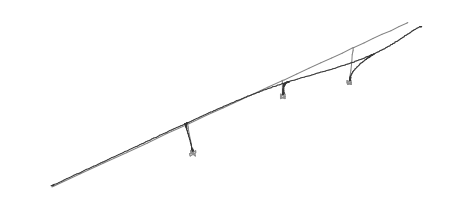
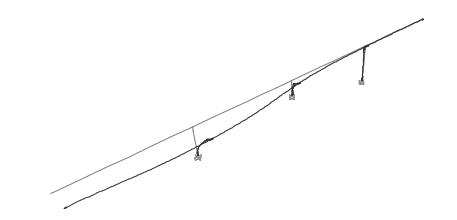
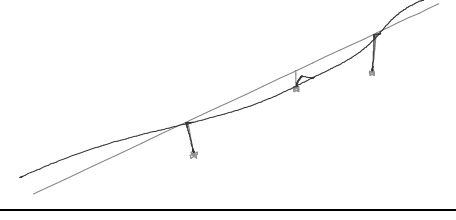
Bridge 213 transversal vibration modes		Period (s)	
		Fibre Model	Plastic Hinge Model
1 <sup>st</sup>		0.4004	0.4012
2 <sup>nd</sup>		0.3373	0.3377
3 <sup>rd</sup>		0.2302	0.2321

Table 4.8 – Vibration modes for configuration 222 – Fibre vs. Plastic Hinge Modelling.

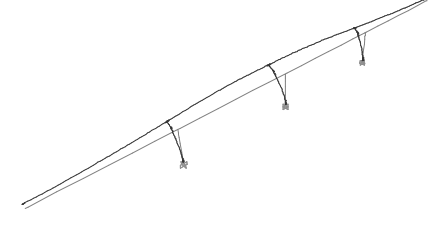
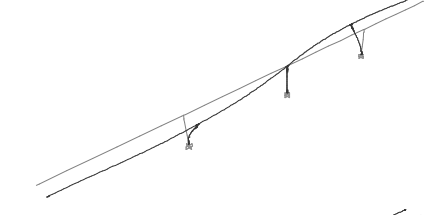
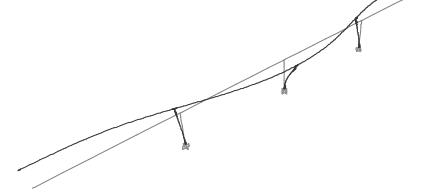
Bridge 222 transversal vibration modes		Period (s)	
		Fibre Model	Plastic Hinge Model
1 <sup>st</sup>		0.4147	0.4149
2 <sup>nd</sup>		0.3312	0.3319
3 <sup>rd</sup>		0.2729	0.2748

Table 4.9 – Vibration modes for configuration 232 – Fibre Model vs. Plastic Hinge Model.

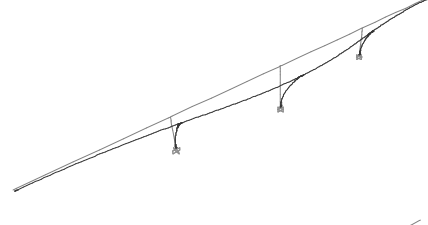
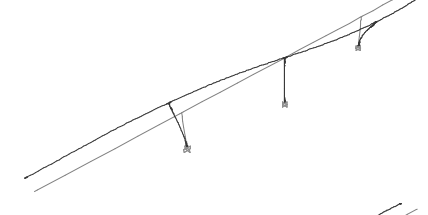
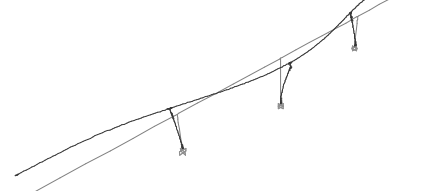
Bridge 232 transversal vibration modes		Period (s)	
		Fibre Model	Plastic Hinge Model
1 <sup>st</sup>		0.5053	0.5060
2 <sup>nd</sup>		0.3312	0.3319
3 <sup>rd</sup>		0.2842	0.2858

Table 4.10 – Vibration modes for configuration 2222222 – Fibre vs. Plastic Hinge Modelling.

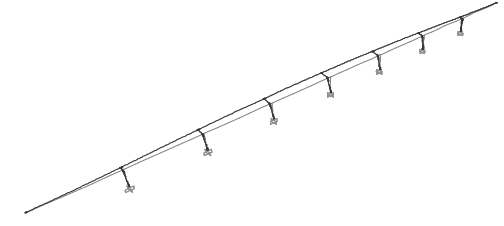
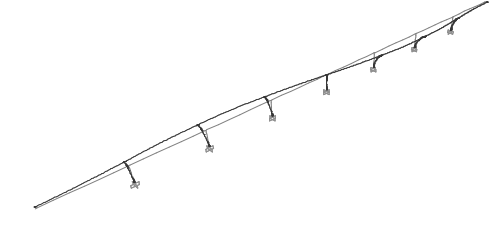
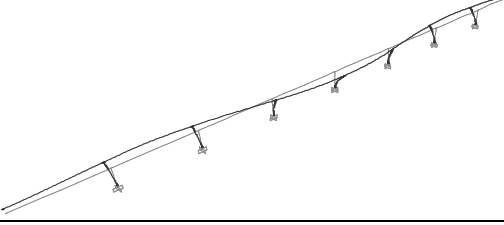
Bridge 2222222 transversal vibration modes		Period (s)	
		Fibre Model	Plastic Hinge Model
1 <sup>st</sup>		0.5886	0.5884
2 <sup>nd</sup>		0.4254	0.4258
3 <sup>rd</sup>		0.3699	0.3707

Table 4.11 – Vibration modes for configuration 2331312 – Fibre vs. Plastic Hinge Modelling.

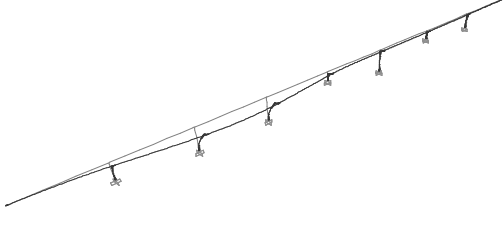
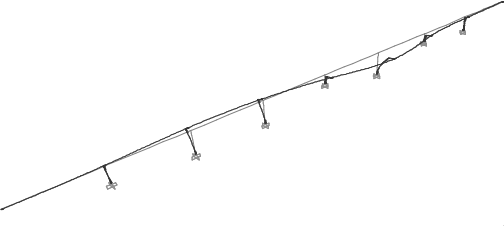
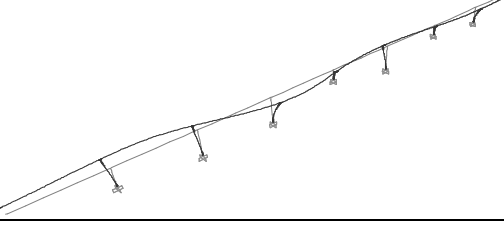
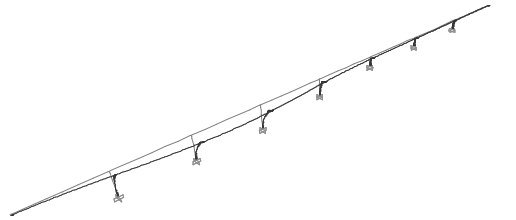
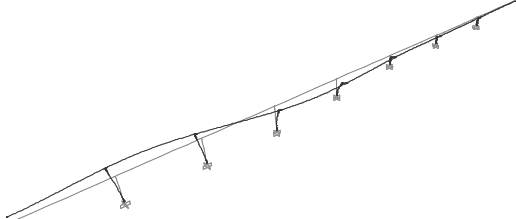
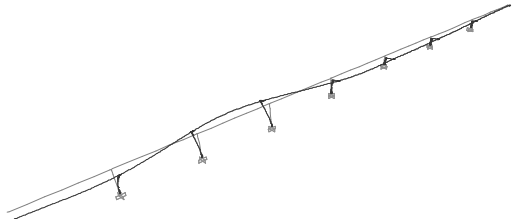
Bridge 2331312 transversal vibration modes		Period (s)	
		Fibre Model	Plastic Hinge Model
1 <sup>st</sup>		0.6522	0.6527
2 <sup>nd</sup>		0.4741	0.4751
3 <sup>rd</sup>		0.3604	0.3619

Table 4.12 – Vibration modes for configuration 3332111 – Fibre vs. Plastic Hinge Modelling.

Bridge 3332111 transversal vibration modes		Period (s)	
		Fibre Model	Plastic Hinge Model
1 <sup>st</sup>		0.7069	0.7071
2 <sup>nd</sup>		0.4776	0.4787
3 <sup>rd</sup>		0.3700	0.3712

The observation of the elastic modal analysis plots indicates a clear agreement between the two models for each and every bridge configuration, given that whether the mode shape (comparison omitted for the sake of simplicity) and the eigenvalues match quite perfectly. The slight differences may be partially, at least, associated to the fact that the mass matrix considered by SAP2000, as opposed to SeismoStruct, is diagonal and does not take into consideration the mass contribution from the rotational degrees of freedom.

#### 4.4.2 Moment-curvature relationships

Two reinforced concrete cross sections have been considered defining a 14 meters high pier: solid rectangular, 0.5mx1.0m, and hollow rectangular, the same used for the plastic hinge calibration (see Section 4.2.1.2), corresponding to the cross section of the piers of case study bridges. Figure 4.18 illustrates the two tested elements. In spite of the fact that the case study bridges feature hollow sections only, the presence of several solid section piers in the existent bridges portfolio motivated the its inclusion in this calibration exercise.

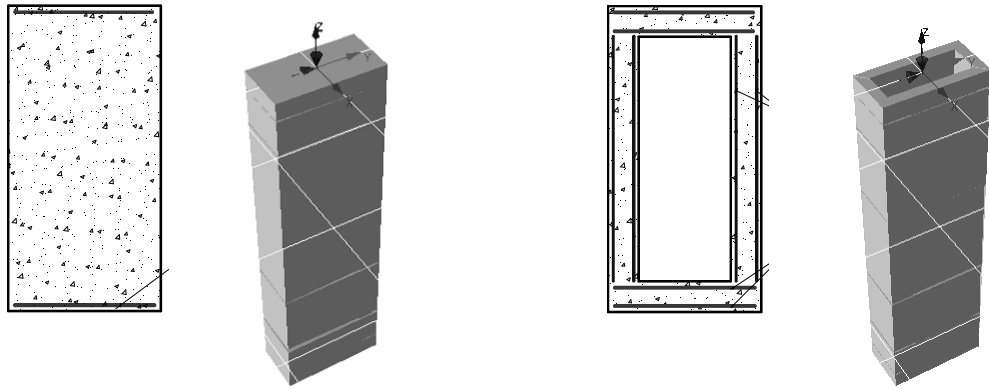


Figure 4.18 – Solid (*left*) and hollow (*right*) reinforced concrete cross section piers.

Three axial loading levels have been applied, according to Table 4.13, in order to observe the matching of approaches for different bearing conditions.

Table 4.13 – Tested axial load forces (N) and axial load ratio ( $\nu$ ) for each cross section.

Designation	Solid cross section		Hollow cross section	
	N (kN)	$\nu$	N (kN)	$\nu$
<i>N1</i>	0	0	0	0
<i>N2</i>	500	0.024	3000	0.017
<i>N3</i>	1500	0.071	9000	0.052

Figure 4.19 and Figure 4.20 plot the moment curvature laws obtained for use within plastic hinge or fibre models, using BIAX and SeismoStruct, respectively, for a solid and a hollow cross section bridge pier. Whereas the BIAX computer module works with the cross section characteristics as the only input, moment-curvature behaviour, using SeismoStruct, has been determined through the application of an increasing loading force at the top of the pier, recording data of interest at the closest to the base Gauss point.

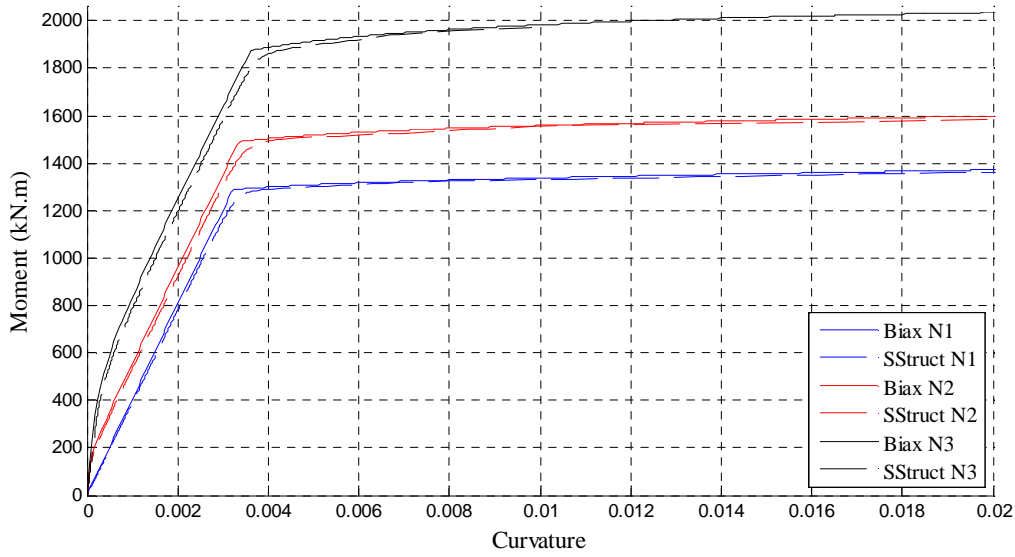


Figure 4.19 – Moment curvature constitutive laws, obtained for the solid cross section, with different axial loading.

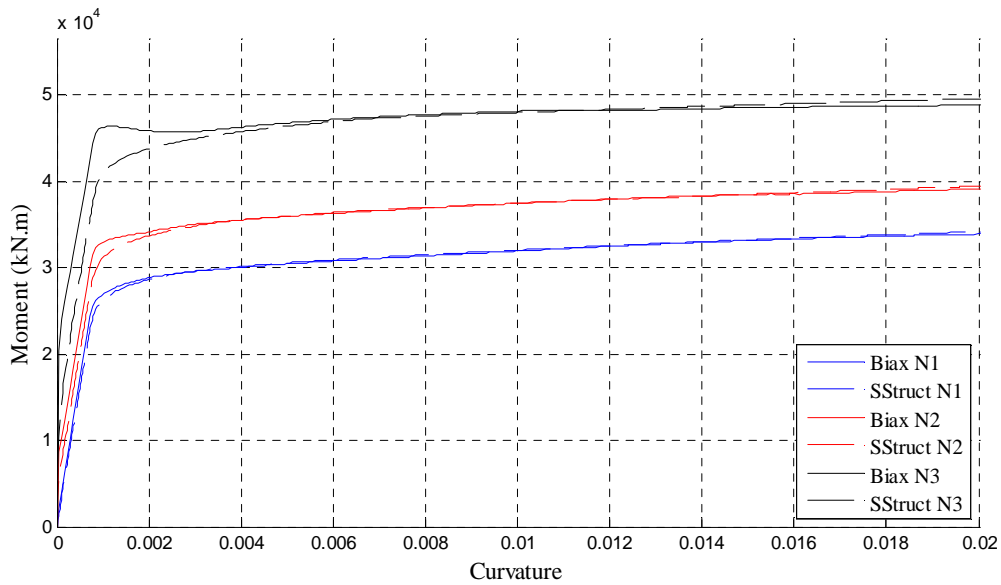


Figure 4.20 – Moment curvature constitutive laws, obtained for the solid cross section, with different axial loading.

A first observation to make from the two sorts of cross sections is that both computation approaches have given little relevance to tensile strength of the concrete, given that constitutive laws are nearly bilinear when the axial load is inexistent. The first branch of the trilinear behaviour for the rest of the situations will correspond, therefore, to the ‘elimination’ of the compressive axial load.

For the case of the simple, solid cross section, moment-curvature relationships are extremely similar, with no differences noteworthy, besides the softer yielding showed by SeismoStruct. With respect to the hollow cross section, for low axial load, there is again no worth mentioning divergence, whilst, for a high axial loading scenario, there is some difference until the yielding plateau is reached, with higher moments being recorded in the BIAX analysis, and a higher stiffness initial branch. In any case, global similarity is evident, which indicates how both computation tools are in agreement regarding cross section constitutive laws.

#### ***4.4.3 Pushover capacity curves***

The nonlinear static analysis of each of the bridges considered within this study has been carried herein using two different deck loading patterns, uniform or 1<sup>st</sup> mode proportional, as recommended by EC8. Regarding the node of control, two alternatives have been admitted as well, for the case of the modal loading pattern: the centre of mass of the deck and the maximum modal displacement node. The uniform loading pattern has been tested with the centre of mass of the deck as reference node. Further detail on pushover-based nonlinear static procedures can be found in Chapter 5. Within both the model analysis, the control node of short bridges has been pushed until 0.75m, along 750 load steps, whereas, for long bridges, the target displacement of the control node was 1.5m, divided in 1500 load increments.

The crude observation of the plots that follow, regardless the sort of bridge configuration, bridge length, load shape or reference node, leads to the conclusion that there is a generally good agreement between the capacity curves for both of the material plasticity models, neither regarding the shape of the curve, nor the maximum base shear.

For short, irregular bridge configurations, Figure 4.21, the correspondence between the **Plastic Hinge Model (PHM)** and **Fibre Model (FM)** based pushover curves, in the pre-yield and post-yield regions, is notorious and independent from the loading pattern or the reference node. A slightly higher difference in the transition of such two zones may be found for the use of the first mode proportional load vector, which is, nevertheless, probably a reflex of the same type of difference encountered in the moment-curvature constitutive laws (Section 4.4.2).

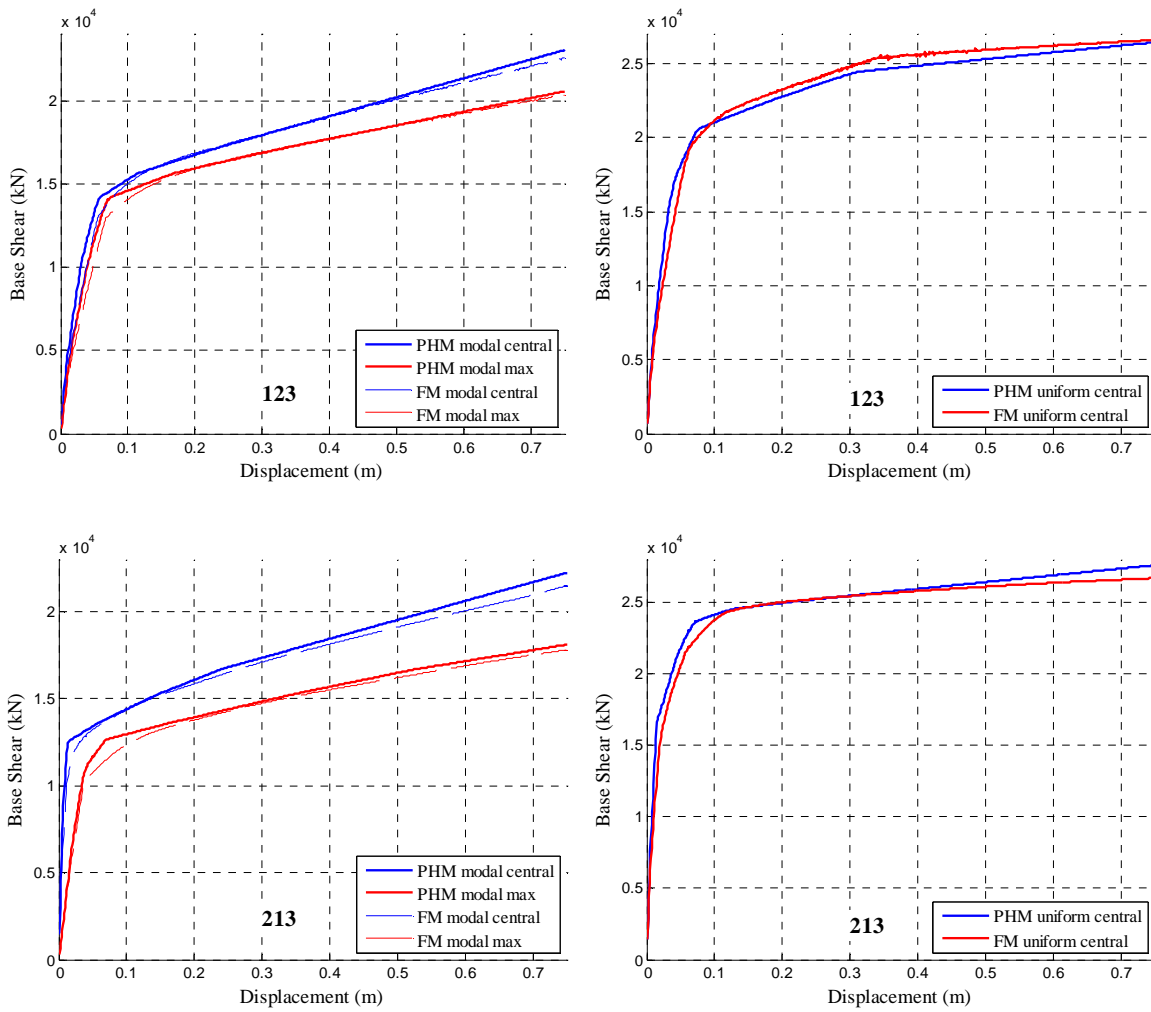


Figure 4.21 – Capacity curves for short, irregular configurations 123 and 213.

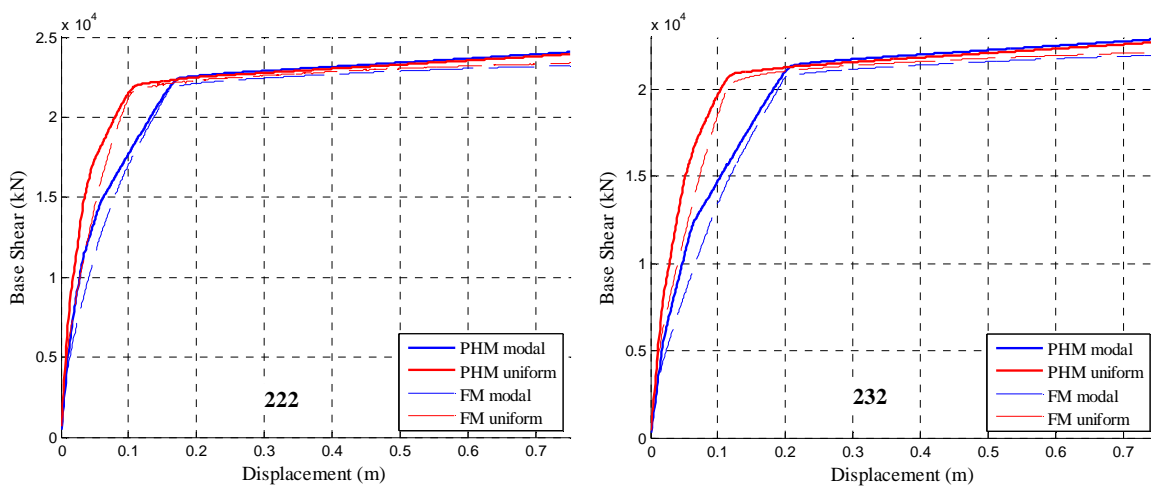


Figure 4.22 – Capacity curves for short, regular configurations 222 and 232.



With respect to short, regular configurations, the main trend is fairly similar to the irregular ones, as documented in Figure 4.22. The difference between the two approaches within the first branch (pre-yield) is however slightly more pronounced.

Regarding long configurations, though, the general picture changes a little, according to the plots in Figure 4.23. For irregular long bridges the difference between the curves, prior to the yielding, tends to diminish, whereas the post-yield slope can differ to a larger extent, in contrast to what happened for short configurations.

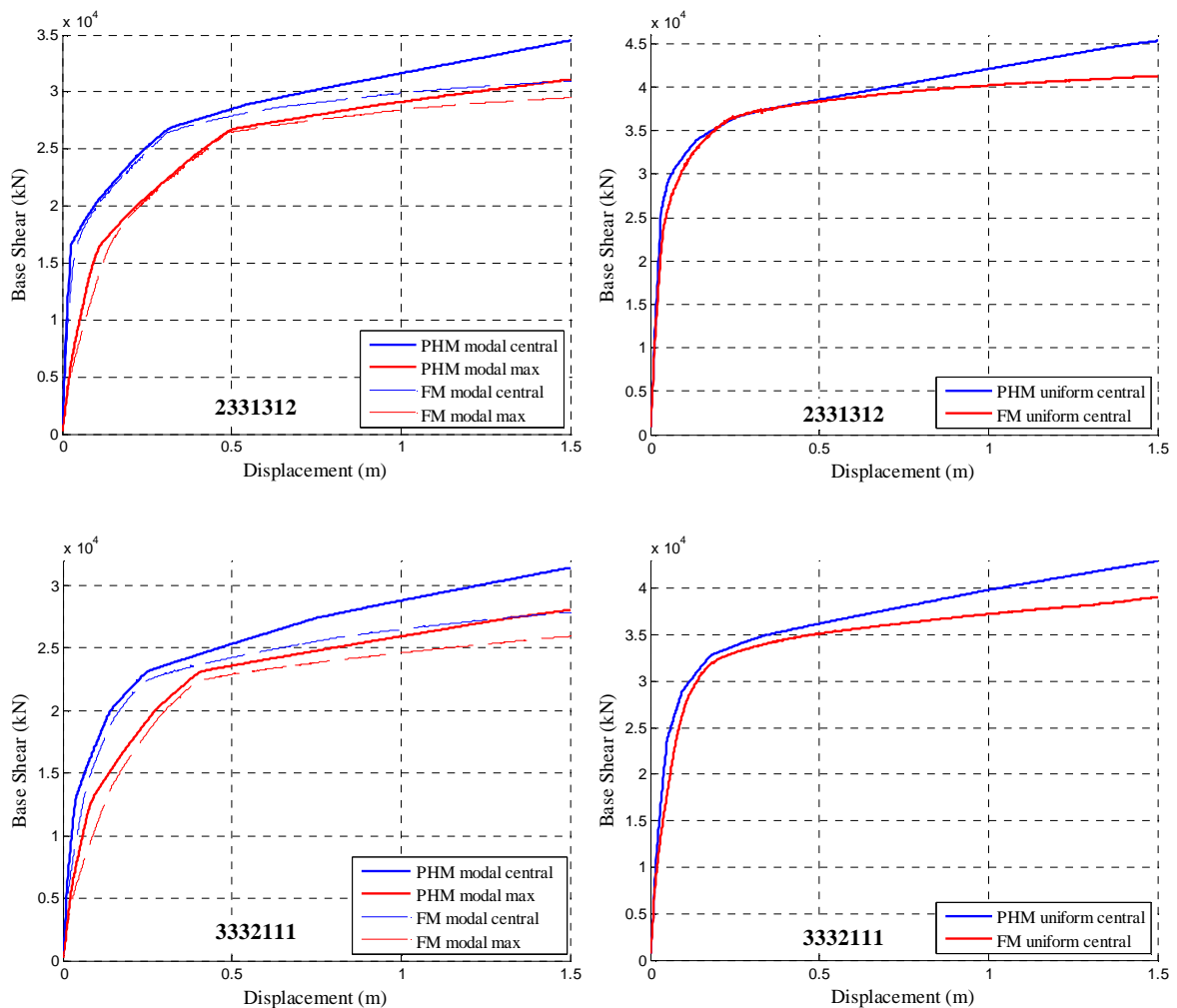


Figure 4.23 – Capacity curves for long, irregular configurations 2331312 and 3332111.

Finally, for the tested long regular configuration, Figure 4.24, the differences are equally distributed along the entire domain of the capacity curves, with no relevant distinction between the pre- and post-yield branches.

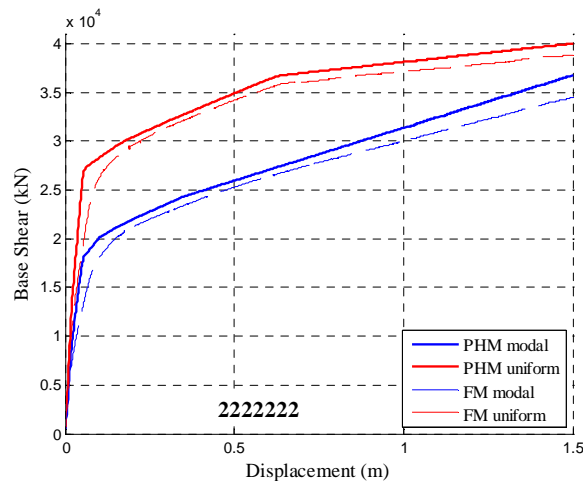


Figure 4.24 – Capacity curves for long, regular configuration ‘2222222’.

In addition, it is worth to mention that plastic hinges models yielded consistently higher shear capacity than the fibre models, for each end every studied bridge configuration, load pattern or reference node. Such scenario was not always verified for the moment-curvature comparison carried out for the two analysis computer programs, which indicates that, indeed, the way of accounting for material plasticity plays an important part.

#### 4.4.4 Structural response parameters

In addition to the comparison of the evaluation of the modelling possibilities when assessing the structural capacity, herein carried out by means of the pushover curve, the agreement level of the structural response, individuated in different parameters, for the different approaches has been looked at as well. In correspondence with the pushover-based capacity evaluation, the structural response comparison has made use of a nonlinear static procedure, N2, prescribed in EC8 (CEN, 2005a, 2005b). Response data corresponding to four parameters, measured in seven bridge configurations, across six intensity levels, have been statistically processed. The four response parameters have been deck displacements, deck bending moments, pier shear forces and abutment shear forces, measured at each relevant location, which are, logically, the pier locations for the first three parameters and the abutments for the latter.

A statistical parameter, Bridge Index (BI), has then been defined, corresponding to the median of the ratio of Plastic Hinge Model (PHM) and Fibre Model (FM) responses, across the relevant locations, as in Equation (4.15), written for a general response

parameter,  $\Delta$ . The ratio is computed for the piers location, with the exception for the abutment shear forces, which is measured at the two obvious locations. An ideal agreement between the two sorts of plasticity modelling would, therefore, correspond to a unitary Bridge Index.

$$BI = \text{median} \left( \frac{\Delta_{PHM,i}}{\Delta_{FM,i}} \right)_{i=1:npiers} \quad (4.15)$$

Furthermore, if the median BI is computed across the different configurations, for each intensity level, one will obtain plots with PHM–FM matching evolution trends as function of the intensity level, as presented in Figure 4.25. On the other hand, if the median of the Bridge Indexes is computed across the intensity levels, for each bridge configuration, the evolutions of the results according to the sort of bridge will be obtained, illustrated in Figure 4.26. For the sake of simplicity, only global median results will be presented, instead of the detailed bridge-by-bridge median BI across different intensity levels.

The observation of results as a function of intensity level indicates, first of all, that, generally, in median terms, the agreement between the two plasticity models' predictions is rather good. Deck displacements and bending moments' predictions tend, however, to be less steady than shear estimates, along the intensity increase and, for such situation, the use of modal loading shape leads to better agreement between the modelling possibilities, rather than uniform pattern. Displacements estimates are larger for the case of fibre models, given that the ratios are mostly under unity, which does not happen, at least not so evidently, for the rest of the parameters. Finally, it is noteworthy the fact that the modelling approaches seem to get closer for higher inelasticity levels, a more visible scenario for the case of shear forces and deck displacements.

In terms of bridge configuration, the results do not differ much. Deck bending moments are particularly unstable for short, regular configurations, something that has already happened for low intensity levels, although not to such extent in that representation mode. The advantage in going for a 1<sup>st</sup> mode proportional loading pattern is not so explicit and relative positions between the two loading shapes do tend to invert, along the different

configurations. Again, agreement is definitely higher within shear predictions. No significant correlation between similarity of nonlinear approaches and bridge configuration has been detected.

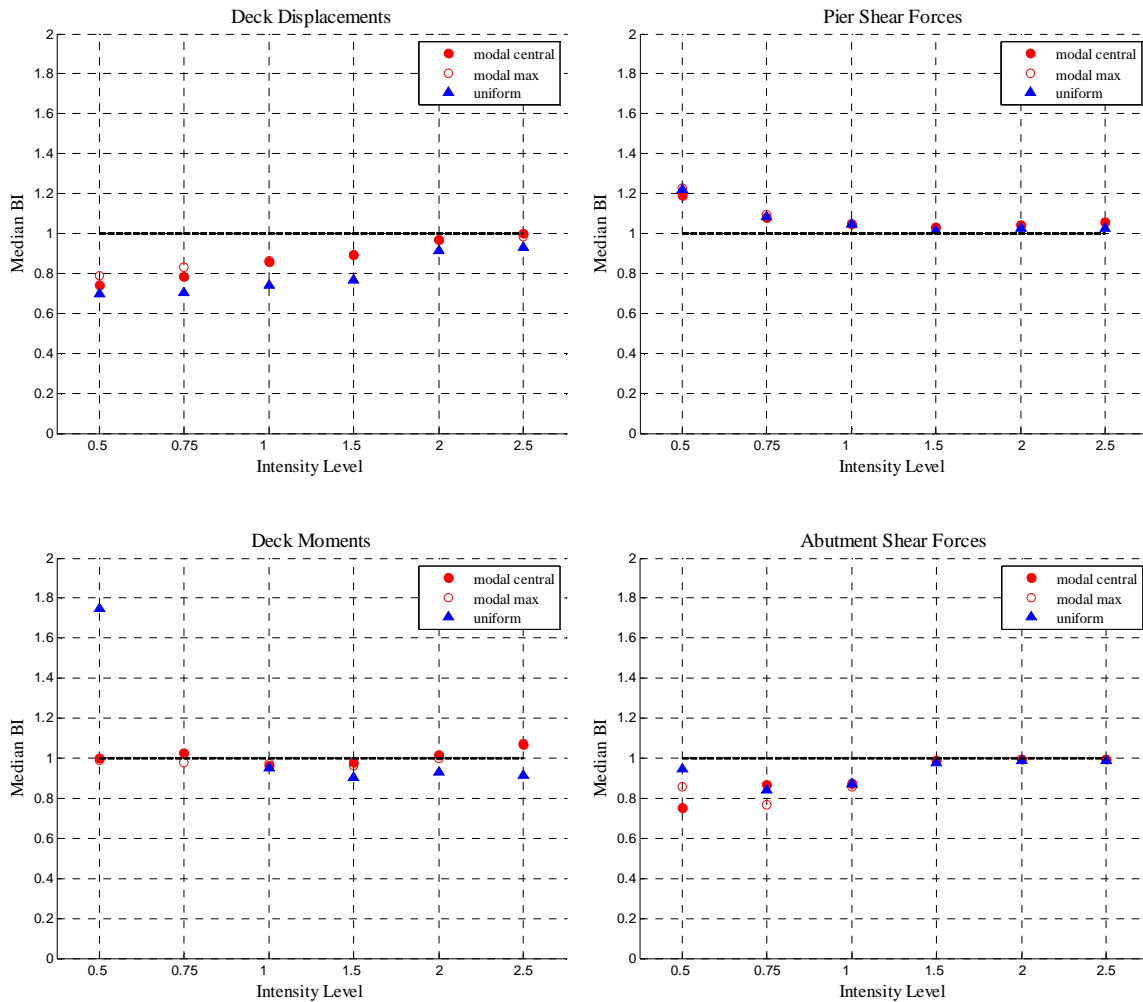


Figure 4.25 – Median Bridge Index (BI) for different response parameters, according to intensity level.

A structural response comparison in terms of median indexes is interesting to assess the matching extent of plastic hinges and fibre models predictions, across the entire bridges (all locations) and intensity levels. In any case, from a design or safety assessment perspective, the quantities of main interest will eventually be the maximum deformations and/or forces. Based on such hypothesis, it would probably be of interest, or even more accurate, within a safety assessment context, the analysis of the coherence of different modelling strategies in terms of maximum demand. In order to do so, plots have been

redrawn, considering that, for each bridge configuration, the Bridge Index is not defined as the median of the BIs at the piers locations, Equation (4.15), but as the ratio of the maximum demand value for the structural parameter at stake, when using the plastic hinges model and the corresponding value, when using the fibre model.

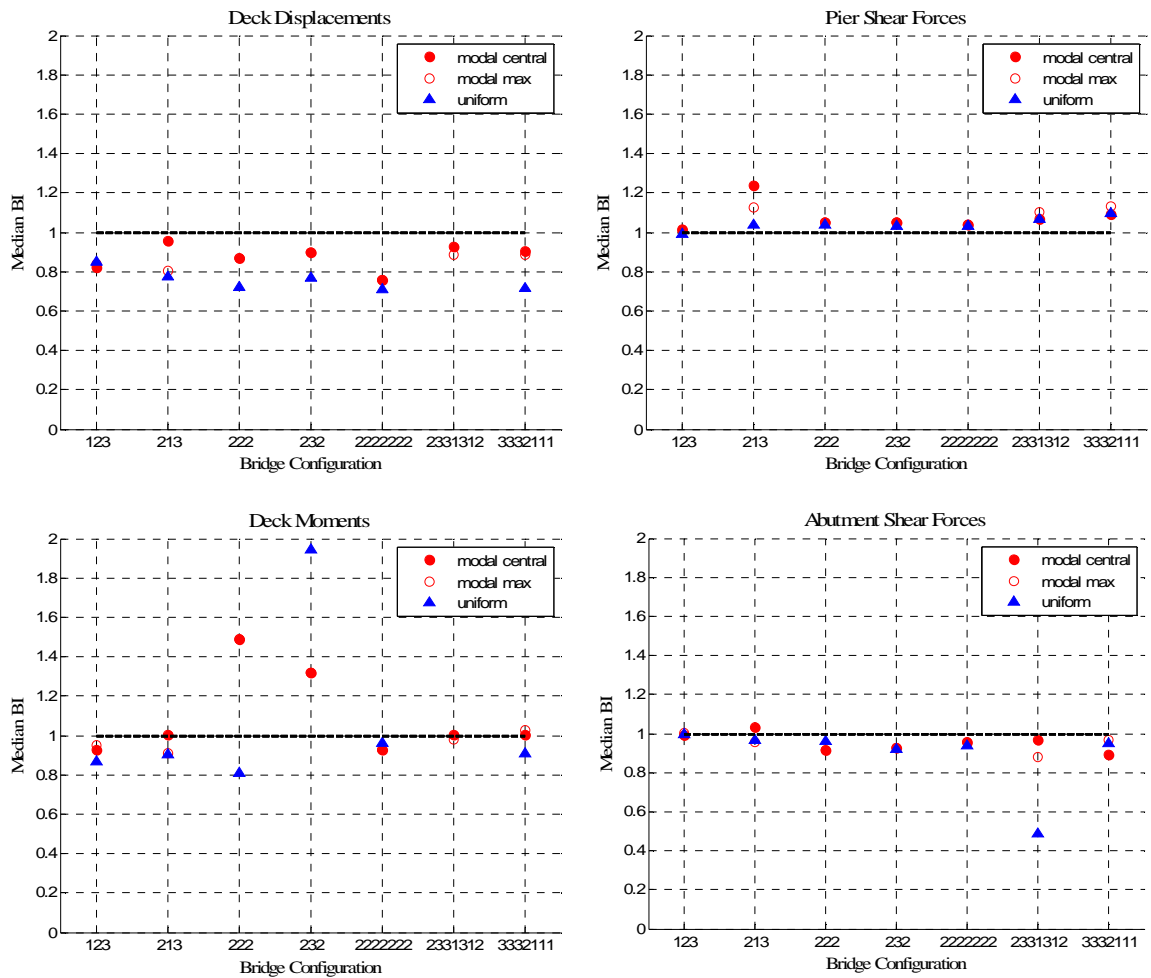


Figure 4.26 – Median Bridge Index (BI) for different response parameters, according to bridge configuration.

This alternative way of looking into results has, nevertheless, the limitation of eventually being comparing maximum demand quantities coming from different locations, if the response pattern differs greatly from lumped to distributed plasticity models. Results have proven to be extremely similar to the ones obtained with the median indexes and are, hence, not presented. Such fact contributes to the reassurance of the similarity of both modelling techniques.

## **4.5 Conclusions**

The work that has just been presented had as main target the focus on the main issues within the nonlinear modelling of reinforced concrete bridges in a seismic safety assessment endeavour context. Structural modelling has been carried out by means of 3D frame elements, using two available structural analysis software tools, able to include geometrical and material nonlinear features.

Typically seen as less relevant when it comes to bridge structural systems, geometrical nonlinearity requires, moreover, less calibration and admits less variation in the mode of being accounted for. Material nonlinearity, on the other side, assumes greater importance, representing one of the major points of energy dissipation during seismic response and therefore has been looked into with higher care. Material models, for concrete and steel, have been initially described, pointing out some of the several available alternatives and detailing the ones that have been considered for the study. Furthermore, material nonlinearity is typically modelled in a lumped way, through plastic hinges, or in a distributed way, using fibre models. Recognizing this as a critical issue in the present seismic analysis, a comparative study has been carried out with the purpose of identifying the eventual convergence between the two possibilities. Comparisons have been based on simple pushover-based nonlinear static analysis, a less complex structural analysis methodology than dynamic analysis, for instance, which, hopefully, induced less dispersion factors affecting the modelling comparison itself.

For the use of lumped plasticity models, a first calibration study has been carried out on the characterization of the plastic hinge constitutive law. Different parameters have been tested, such as length or location of the plastic hinge within the element, according to different formulations, within a single pier pushover analysis. Three plastic hinge lengths and locations have been tested and the results have proven that the influence of such parameters is of limited significance, mainly on the maximum capacity and yielding deformation. Major differences between the considered approaches for the plastic hinge length occur in the elastic-cracked behaviour region only. It is therefore expected that no considerable divergence occurs when the structure is under large deformation conditions. Regarding plastic hinge location in the element, a specific feature of some computer

program algorithms, such as the used SAP2000, it has been seen that its relevance is negligible.

The comparison between lumped and distributed plasticity models itself has been carried out for a relatively large set of bridge configurations, regular, semi-regular and irregular, for a wide range of intensity levels, in three different components. Firstly, the moment-curvature constitutive laws used by both sorts of models have been compared for different axial loading levels found in the tested bridge configurations. Subsequently, the structural response, using both types of modelling, obtained through the employment of a nonlinear static procedure, was compared, in terms of pushover capacity curves and response parameters, namely deck displacements and bending moments and pier and abutment shear forces. Main observations on such three aspects are as follows:

- The moment-curvature constitutive laws, the essential input source for the definition of the nonlinear behaviour of structural elements, have been found to be rather similar, whether the obtained independently for plastic hinge characterization or the ones intrinsically considered by the fibre model analysis software. Slight differences have been found in the elastic pre- and post-cracking phases, which is probably due to the formulation assumed within the used tools. For plastic hinges definition, the employed BIAX algorithm makes use of equilibrium equations to determine internal forces, whereas SeismoStruct works under interpolation between Gauss points. The axial loading effect proved to be extremely important for the maximum available bending moment, particularly when dealing with hollow cross sections, a typical situation for bridges.
- The capacity curve, as the main output result of a pushover analysis, has been obtained for each of the modelling versions, according to different loading patterns and reference nodes: 1<sup>st</sup> mode proportional load shape, tested with the centre of mass of the deck or the maximum modal displacement as reference nodes, and uniform load shape, carried out with the centre of mass of the deck as reference node only. The pushover curves have turned out quite in agreement, regardless the type of loading pattern, reference node or bridge configuration. Slight found differences were probably due to the corresponding divergences previously encountered in the reinforced concrete cross section constitutive laws.

- Finally, it has been studied the influence of the differences in the pushover curves with different load shapes and reference nodes, representing the structural capacity, in the structural demand, through four response parameters statistical comparison, based on the definition of a median index parameter – the Bridge Index. The EC8-recommended nonlinear static procedure has been used in order to obtain the performance point at each of the six intensity levels, for each studied configuration. The global observation of results points to the conclusion that, generally, both lumped and distributed material plasticity models match in every of the analysed parameters: displacements, bending moments and shear forces, at deck, piers and abutments. The median Bridge Indexes were recurrently quite close to unity, across the different intensity and regularity levels. Despite such similarity, it may be stated that plastic hinge models tend to lead to higher shear force predictions, when compared to fibre models, whereas the opposite scenario is verified for deck displacements. Deck bending moments have presented a less constant trend. Estimates obtained by means of pushover analysis with 1<sup>st</sup> mode proportional loading pattern have been found generally more agreeing. For the majority of the configurations and intensity levels, the maximum modal displacement node used as reference led as well to more consistent estimates between the two approaches. Agreement between the models has been found at its best when assessing shear forces, even and mostly for high inelasticity levels. Disparity found for low/median intensity levels may have to do with the employed nonlinear static procedure, which carries out a bilinearization of the capacity curve, using equal areas criteria. Such bilinear curve simplification can amplify dissimilarities in the pushover curves of the different models for low to median seismic demand, where the behaviour is deemed to be linear elastic. Under such conditions, displacements BIs are above unity and shear forces BIs present the opposite trend, therefore, overestimated by plastic hinge models, which indeed present higher initial elastic stiffness, when compared to fibre models.

The adopted modelling technique and the included nonlinear features constitute a particularly important step, given that it will largely influence capacity and structural demand, the two fundamental variables within a seismic safety assessment procedure. From the material models, under monotonic and cyclic loading, to the way of considering



plasticity characteristics of the structural members, different versions may be regarded as eligible. Amongst the possible alternatives, with respect to the various issues that are involved in the modelling task, special focus was given to the pertinent option between concentrated or spread plasticity, given that, to the author's opinion, the other aspects are less controversial, at least for the time being. It has been interestingly verified that the option for a more refined fibre model over a more 'simplified', in the assumptions sense, plastic hinges model does not necessarily lead to more accurate evaluation of the seismic behaviour of bridge structures. Such conclusions must be handled with relative care, given that simplified nonlinear static analysis has been carried out, with no cyclic loading, such as the one introduced by nonlinear dynamic analysis. Further studies, using more complete analysis procedures, would provide a valuable contribute to this matter.

Accordingly, in the future, and in the rest of this work as well, the option for one or other sort of model may be more influenced by other parameters such as computational effort or model complexity, without expected limiting loss of accuracy. In particular, in Chapter 6, the verified agreement between nonlinearity approaches will be used to carry out numerous nonlinear dynamic analyses, within a simulation-based probabilistic context.

Firstly, though, in the following chapter, structural response prediction tools, the next step when seismic input and structural model are characterized, will be discussed, from a bridge application perspective.



## 5. Seismic Demand

Estimating the seismic effects in a structure subjected to earthquake loading is definitely one of the key issues within the global structural safety assessment problem. Even if naturally depending on the structure's characteristics and the seismic action itself the main differences, or not, arise from the nature of the approach, either static or dynamic, each comprising different concepts, techniques and procedures. The distinction here will be established between nonlinear dynamic analysis and nonlinear static analysis.

The main advantage in using nonlinear dynamic analysis is naturally the fact that the real phenomenon is directly reproduced when the acceleration is applied to the ground connections leading, therefore, to more accurate results. Nevertheless, several drawbacks may be pointed out when considering this sort of analysis, starting with the seismic action being particularly defined by an accelerogram. The ground motion records, the structural modelling (including the reproduction of damping phenomena, the post-elastic behaviour and corresponding energy dissipation, during loading and unloading periods) are all important issues within nonlinear dynamic analysis and have been extensively debated in Chapters 3 and 4. In addition, attention must also be paid to time/computational demand. It is well known that dynamic analysis may require considerable amount of time to be carried out, this being due to the analysis method itself, to a complex structural model, which will typically not occur when assessing bridges, or to the long duration of the input ground motion record.

The most commonly employed alternative to nonlinear dynamic analysis is the nonlinear static analysis. Typically, this kind of approach is based in a pushover analysis carried out on the structure, with the main goal being to somewhat envelope all, or at least a considerable part, of the possible dynamic analysis results at each intensity level. This sort of outcome is accomplished through the application of an increasing lateral force or displacement vector to the structure. An example of a pushover curve, representing base shear versus displacement of a reference node, is illustrated in Figure 5.1. The main drawback to be found here is the assumed level of simplification, given that one expects that the structural behaviour obtained from horizontal loading is able to replace the one coming from the dynamic analysis.

This chapter looks into the way of estimating the seismic demand on bridges subjected to such horizontal action. The main focus is the validation of static nonlinear simplified procedures, which are directly compared to dynamic analysis. Several possibilities are taken into account and a thorough parametric study is carried out on such validation.

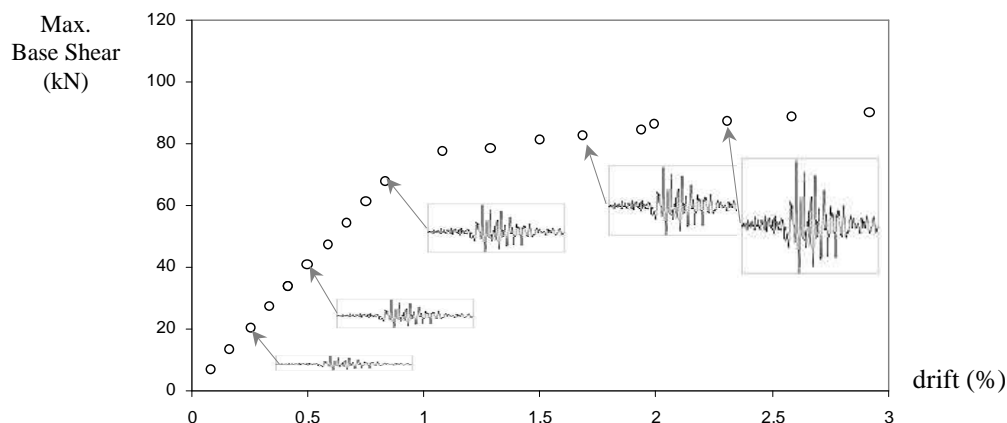


Figure 5.1 – Nonlinear static analysis: concept (Pinho, 2011).

## 5.1 Nonlinear Static Analysis

For the last few years, a considerable effort has been put in research of simplified, but credible, methodologies to assess the seismic behaviour of structures. The so-called Nonlinear Static Procedures (NSP) have therefore been developed and recognized for application in some guidelines, such as the ATC-40 (ATC, 1996), FEMA-273 (ATC, 1997) or the European Code (CEN, 2005a, 2005b). This type of procedure is extensively spread within the earthquake engineering community, mainly due to its simplicity and potentially

easy application when assessing a large number of structures. Although these methods were initially thought having the application to buildings in mind, their extension to bridge structures is full of interest and there is actually no reason for not doing it. Indeed, bridges have the advantage of being, in general, structurally simple when compared to buildings. Some very recent endeavours have dealt with the application to bridges of this kind of procedures (e.g., (Isakovic and Fischinger, 2006; Paraskeva *et al.*, 2006; Casarotti and Pinho, 2007; Lupoi *et al.*, 2007)). However, those studies were carried out for a specific NSP, which was not scrutinised in several possible application ways, a gap that this chapter tries to fill.

The aforementioned methods are based on the computation of the pushover curve, a representation of the nonlinear force-deformation behaviour of the structure. With the use of appropriate transformation relationships, the capacity curve of the single-degree-of-freedom (SDOF) system equivalent to the original multi-degree-of-freedom (MDOF) structure may be obtained. At this point the main differences between the proposed methods arise, such as the contemplation or not and choice for a reference node, the way of reducing the demand spectrum so as to account for the hysteretic energy dissipation, the consideration of higher modes of vibration, on the way to determine the displacement demand for a given ground motion.

There are quite a few possible procedures to carry out a nonlinear static analysis, essentially depending on the sophistication level and time of appearance. From truly simplified methods, based on correcting coefficients, to others, more complex, including nonlinear and modal effects in a refined way, the choices are plenty.

Corresponding to the earliest attempts to propose a static method that would quickly lead to accurate results, a first group of NSPs may be considered, including the pioneering Capacity Spectrum Method (CSM), introduced by Freeman (1998) and implemented in ATC-40 guideline, and N2 method, (Fajfar and Fischinger, 1988) included in the recommended simplified procedures of European Code (CEN, 2005a). These first proposals are appealing mainly for the simplicity of the method and usually consider either the first mode proportional or uniform load distribution for the pushover curve computation. Recently, an improved version of CSM method has been presented in FEMA-440 guidelines (ATC, 2005), mainly consisting of the update of the prescribed

empirical relations to determine both the equivalent viscous damping and spectral reduction factor.

Not much later than the ATC-40-adopted CSM, the Displacement Coefficient Method (DCM) (ATC, 1997) has been proposed within the NEHRP Guidelines for the Seismic Rehabilitation of Buildings. Whereas ATC-40 referred only to concrete structures, DCM is applicable to a wide range of structural systems and computes the elastic response, which is then tuned by a series of coefficients that account for the nonlinear behaviour. DCM assumes, therefore, a certain empirical character, which distinguishes it from the previous ones.

An additional group of procedures includes more recent approaches to nonlinear static analysis, such as the Modal Pushover Analysis (MPA) (Chopra and Goel, 2002), the Adaptive Modal combination Procedure (AMCP), by Kalkan and Kunnath (2006) or the Adaptive Capacity Spectrum Method (ACSM), developed by Casarotti and Pinho (2007). All of them come up with some improvements, mainly the inclusion of higher modes contribution or, as in the ACSM, an alternative way of addressing the reference node issue. The application of methods which try to implement new features, i.e., the ones belonging to this group, may generate some controversy and it may be argued that effortlessness is being left behind, towards to a complexity level increasingly similar to dynamic analyses. Such perspective is relative. Indeed there may be so-called advanced NSPs, MPA or AMCP, which foresee several repeated steps, whereas others, such as ACSM, carry no additional effort to the analysis, since higher modes are included in the analysis all together when working out the pushover curve. The importance of an increase in the computational effort will depend, anyhow, on the corresponding difference in the performance.

## **5.2 Nonlinear Static Procedures**

The six aforementioned procedures are briefly discussed in what follows, going through the fundamental aspects of a nonlinear static analysis within the context of bridge structures, such as loading pattern, equivalent SDOF system computation or eventual spectral reduction technique, among others.

Herein, each of the referred methods is studied individually, scrutinised in several possibilities, according to its settlement variables. With this preliminary approach, an optimisation of each procedure is looked for and a best performing way is chosen for comparison. A confront of the four selected NSP is subsequently carried out, with the purpose of emphasizing relative advantages and disadvantages or, eventually, coming up with the choice for one of them as noticeably better. An extensive parametric study, covering fourteen different bridge configurations, ten earthquake records scaled to six intensity levels, and four control variables (deck displacements and flexural moments and piers and abutments shear forces), was carried out in order to make a full comparison of the four major available methods. The predictions accurateness evaluation is made by means of confront with dynamic analysis results.

### ***5.2.1 Capacity Spectrum Method (CSM)***

The Capacity Spectrum Method was initially introduced by Freeman *et al.* (1975) in the early seventies as a methodology to rapidly evaluate seismic vulnerability of buildings, with the basis idea of getting a reasonable approximation of the elastic and inelastic limits for the structure's behaviour. Basically it consists in the intuitive, and rather rational, graphical comparison of the capacity with the demand, represented by over-damped response spectrum. Such graphical nature gives the engineer the opportunity to visualise the relationship between demand and capacity. The capacity spectrum is given by the displacement of a reference node and base shear, coming from the nonlinear pushover curve, in the spectral displacement and acceleration (ADRS) format. The pushover curve is obtained applying a lateral load distribution proportional to the fundamental vibration mode shape of the structure. Linear elastic response spectra, scaled to account for the energy loss due to hysteretic cyclic behaviour, are used to characterize the demand in an inelastic response spectrum fashion. The reduction factors are based on effective viscous damping levels that may be computed using Newmark-Hall relationships for damping and ductility or according to idealized hysteretic parallelogram loops. The intersection of the two curves is then considered to be the performance point of the structure.

The method has been included in ATC-40, a document that emphasizes the use of nonlinear static procedures in general, such as Displacement Coefficient Method, but focusing on CSM. The document includes step by step procedures to determine capacity,

demand and performance. Capacity is represented by a pushover curve, generally constructed to represent the first mode response of the structure, which is based on the assumption that the fundamental vibration mode is predominant. Demand is represented by 5% damped response spectrum, reduced in terms of effective damping, and performance point is attained according to three methodologies, different in terms of their dependency on analytical versus graphical techniques.

Two important aspects should be noted: classical CSM uses the fundamental mode shape when computing the pushover and capacity curves and depends on a reference node, usually considered the top floor, for buildings, or the deck centre of mass, in the case of bridges. For the latter case, this a very particular issue because the accuracy of the deck central node when representing the structure is quite dependent on the piers configuration. In what concerns the demand curve, the response spectrum is reduced considering the equivalent viscous damping, obtained summing the elastic viscous damping (recommended by ATC-40 to be 0.05) with the hysteretic damping.

To summarize, according to what is prescribed in ATC-40, the Capacity Spectrum Method can be applied taking the following steps:

8. Create a computer model of the structure and apply lateral forces to the structure in proportion to the product of the mass and fundamental mode shape, including gravity loads.
9. Calculate and record the base shear and reference node displacement, constituting the pushover curve of the structure.
10. Convert the obtained capacity curve to the capacity spectrum, a representation of the base shear-displacement curve in Acceleration-Displacement Response Spectra (ADRS) format (spectral acceleration  $S_a$  versus spectral displacement  $S_d$ ), using first mode quantities to make the transformation.
11. Construct a bilinear representation of the capacity spectrum, for a first trial displacement and acceleration, estimate effective damping, combining viscous damping inherent to the structure and hysteretic damping, and appropriate reduction of spectral demand. The hysteretic damping is considered to be related to the area inside the loops of the base shear-structural displacement diagram during



the earthquake occurrence. It is obtained using an approach based on the energy dissipated by the structure in a single cycle of motion (Chopra, 1995). The spectral reduction factors use, in turn, the relationships developed by Newmark and Hall (1982), and are defined and limited according to the structural behaviour type (A, B or C), which depends on the shaking duration and the quality of the primary elements of the seismic resisting system.

12. Intersect capacity spectrum and reduced demand spectrum, build new bilinear capacity spectrum for that point and update effective viscous damping and spectral reduction factor;
13. If the updated damping acceptably matches the previously determined/assumed one, the Performance Point (PP) of the structure is found, otherwise, iteration is carried out until convergence is reached.

Recently, FEMA-440 guidelines (ATC, 2005), within the ATC-55 Project, performed an evaluation of current Nonlinear Static Procedures, which included a review of the Capacity Spectrum Method, prescribed in ATC-40. The document constitutes an effort to assess current NSPs for the seismic analysis and evaluation of structures as well as to present suggestions developed to improve such procedures for practical application in the analysis of both existing and new structures. The improved recommendations rely on the original procedure, with most of the process remaining intact. New expressions to determine the effective damping and period are introduced as well as a new technique to modify the resulting demand spectrum to coincide with the familiar CSM technique of using the intersection of the modified demand with the capacity curve to obtain the performance point of the structure. The suggested new expressions are set by type of hysteretic model – bilinear or stiffness degrading – and post-yielding stiffness parameter  $\alpha$  and its parameters vary according to the ductility achieved by the system. Additionally, general expressions, independent from the structural system type, are proposed.

According to the previously exposed, CSM was tested, further on this study, using its original configuration as well as considering the FEMA-440 improving recommendations, with expressions independent from structural system. Additionally, the reference node has been tried either as the deck centre of mass or maximum modal displacement node, yielding a total of 4 distinct variants.

### **5.2.2 N2 Method**

A simple Nonlinear Analysis Method for Performance Based Seismic Design was formally proposed in the late nineties by Fajfar (1999), combining pushover analyses of a MDOF model with the response spectrum analysis of the equivalent SDOF system. The method is named N2, where 'N' stands for its nonlinear analysis character, and '2' for the use of two separate mathematical models, the application of the response spectrum approach and pushover analysis. With such methodology, a satisfactory balance between reliability and applicability for everyday use is intended, along with a contribution to new trends in seismic design, even if eventually originally restricted to the planar analysis of new or existing building structures. Similarly to CSM, N2 method is formulated in the acceleration-displacement format, providing a visual interpretation of the procedure. The main difference is that N2 makes use of inelastic spectra rather than elastic spectra with equivalent damping and period.

The nonlinear procedure has been considered and implemented in Eurocode 8 (CEN, 2005a) for application either to building or bridges. In order to come up with the MDOF model pushover curve at least two load distributions are recommended: a uniform one, in which the shape factor is unitary along the building's height or deck and a first mode proportional shape. The most essential assumption of the method becomes, therefore, the time-independent lateral displacement shape, notwithstanding that the method's results are believed not to be excessively sensitive to changes in the assumed displacement shape. An additional possibility, which has effectively been considered in this framework, is the envelope of those two load shapes, a sort of a filtering technique that would try to capture the best of each loading profile. The capacity curve is represented plotting the base shear force as a function of the reference node displacement coming from the pushover analysis.

N2 is, conceptually, another procedure where higher modes will hardly be taken into account properly, being therefore recommend for the application of building structures oscillating predominantly in a single mode, even if irregular. If not, demand quantities are expected to be underestimated. Solutions for this drawback, based on appropriate dynamic magnification of selected quantities, are being sought, though. The method is equally dependent on the choice of a control node, recommended to be the top floor of the building or the centre of mass of the deformed deck. The design point is determined throughout the

computation of the target displacement of the SDOF system, the performance point of the structure, obtained through expressions that vary with the range where the equivalent period falls in, short or medium-long. Those expressions are fundamentally based on the ductility achieved by the system and on the spectral acceleration for the equivalent period.

The application of N2 procedure, according to EC8, consists on the following steps:

1. Create a computer model of the structure and apply lateral forces in proportion to the product of the mass and a shape factor, which should be considered, for the deck, as constant or proportional to the first mode shape, and for the piers, proportional to the height above the foundation of the individual pier.
2. Build the capacity curve, given by the relation between base shear force and control node displacement, which should be the centre of mass of the deformed deck.
3. Transform the MDOF structure to an equivalent SDOF system, computing the equivalent mass,  $m^*$ , force,  $F^*$ , and displacement,  $d^*$ .
4. Determine the idealized elasto-perfectly plastic force-displacement relationship, defined for the plastic mechanism point in such a way that the areas under the actual and the idealized force-deformation curves are equal. At this point, a maximum displacement,  $d_m^*$ , the one corresponding to the formation of the plastic mechanism, may be assumed, in order to proceed with the bilinearization.
5. Determine the period,  $T^*$ , of the idealized equivalent SDOF system, based on the idealized bilinear capacity curve.
6. Find the displacement target,  $d_t^*$ , depending on the comparison of the equivalent period with the code spectral period,  $T_C$ , i.e., depending on whether the structure is in the short-period range or in the medium and long-period range.
7. If  $d_t^*$  is very different from  $d_m^*$ , assumed in the bilinear capacity curve, iteration may be optionally carried out, re-bilinearizing the capacity curve for  $d_t^*$ .

Three different loading possibilities have been considered for the application herein carried out of N2 method: uniform load distribution, first mode load distribution and their envelope. Because of the method's reference node dependency, each of the three modalities was repeated changing the reference node to the maximum displacement one

instead of the centre of the mass of the deck. This way, N2 method was applied in 6 different versions.

### ***5.2.3 Displacement Coefficient Method (DCM)***

The Displacement Coefficient Method is another method that has been proposed in a document prepared by the Applied Technology Council, within the ATC-33 Project, funded by the Federal Emergency Management Agency, FEMA 273 publication. Such document, dated of 1996, had as major goal the development of technically sound guidelines for the seismic rehabilitation of buildings and proposed four distinct analytical procedures, linear or nonlinear, static or dynamic. DCM is the document's considered Nonlinear Static Procedure and consists in pushing the structure to a target displacement, expected to be equivalent to the experienced one during the earthquake event. The target displacement corresponds to the displacement obtained using the equal displacements approximation, then modified by various coefficients.

The methodology, mainly the tabled coefficients, is based on statistical analysis of dynamic analysis of SDOF models of different types and provides a direct numerical process for calculating the displacement demand, not requiring any conversion of the capacity curve to spectral coordinates. It is recommended to be applied to all buildings, new or existing, that are regular and do not have adverse torsional or multimode effects.

The structural model, directly incorporating inelastic material response is displaced by monotonically increasing lateral forces until the target displacement, controlling corresponding internal forces and deformations, or the building collapses. The displacement target is, similarly to other procedures, referred to a control node, assumed by FEMA-273 guidelines to be the centre of mass at the roof. The lateral load pattern should be tested according to two possibilities, uniform or modal, proportional to total mass at each floor level. Computing the effective fundamental period in the direction under consideration and effective lateral stiffness, the displacement that the elastic-behaving structure would have can be determined. Four coefficients are then applied to adjust that displacement, considering the relation between spectral displacement and the building roof's displacement, the relation between expected maximum inelastic displacements to

displacements calculated for linear elastic response, the effect of hysteresis shape on the maximum displacement response and the dynamic P-delta effects.

The Displacement Coefficient Method is, due to the empirical expressions previously developed, quite simple to apply, completing the following steps, as prescribed by FEMA-273:

1. Create a computer model of the structure and apply lateral forces using at least two distributions, uniform and modal.
2. Establish the relation between base shear force and lateral displacement of the control node, the capacity curve.
3. Construct a bilinear representation of the capacity curve considering that the pre-yielding branch passes through the point corresponding to a base shear of  $0.6V_y$ , where  $V_y$  is the yielding shear.
4. Calculate the effective fundamental period from the bilinear capacity curve.
5. Calculate the target displacement by the elastic behaving structure spectral displacement, affected by a set of four coefficients,  $C_0$  to  $C_3$ , which take into account nonlinear response of the structure.

Displacement Coefficient Method was not formulated having application to bridges in mind. Indeed, FEMA-273 guidelines state that the procedures have not been tested for each and every structural type, particularly those that have generally been covered by their own codes or standards, such as bridges. For that reason and due to its substantial empirical nature, this nonlinear static procedure will not be included in the comparative study.

#### ***5.2.4 Modal Pushover Analysis (MPA)***

The Modal Pushover Analysis was introduced by Chopra and Goel (2002) and consists in the repeated application of a given nonlinear static analysis procedure for each of the significant vibration modes of the structure, followed then by an adequate combination of the results. Self claimed as a procedure based on structural dynamics theory, retaining the conceptual simplicity and computational attractiveness of current procedures with invariant force distributions, has been proposed and widely spread up in the past recent years. The main reason for such acceptance was the awareness of the accuracy lack that pioneering

simplified methods, such as CSM in ATC-40, would many times provide. This is thought to be mainly due to disregarding higher modes contribution to the response or the redistribution of inertia forces because of structural yielding and associated changes in the vibration properties, aspects deemed to assume a greater meaning when analysing bridges.

The whole procedure is actually quite similar to the one pursued by the other methods. It starts with the computation of a number of MDOF pushover curves, each of which obtained employing a load distribution that is proportional to the individual modes of vibration being considered. The equivalent SDOF capacity curves are then determined by transforming and bilinearizing the modal pushover-derived base shear-displacement relations, making use of the  $n^{\text{th}}$  modal quantities and the reference node displacement. The main step, estimating the peak deformation, i.e., the performance point, can be done by means of (i) response history analysis (RHA), (ii) inelastic design spectrum or (iii) empirical equations for the ratio of deformations of inelastic and elastic systems. Response history analysis consists in performing a nonlinear dynamic analysis of the equivalent SDOF system for each significant mode, characterized by the bilinearized pushover curve. Finally, a quadratic combination rule (e.g., through SRSS or CQC) is employed to combine the responses obtained for each modal analysis.

Several improvements, with respect to its original formulation, have been carried out within the Modal Pushover Analysis proposed procedure. The authors have focused on a new way of computation of member forces, given that the initial quadratic combination of results could lead to miscellaneous estimates, comparing them to the actual shear member capacity. Additionally, other features have been included, such as inclusion of P- $\Delta$  effects for all modes, different way of computing beam plastic rotations as an iterative procedure to solve dependency on selected ground motion record for RHA.

More recently, a Modified Modal Pushover Analysis methodology, MMPA, has been suggested as well, as a new, faster, MPA. Higher modes are considered with the structure as elastic-behaving, which corresponds to a single nonlinear pushover analysis, the first mode one, and, therefore, less computational effort.

The original procedure, together with the recent adjustments, widely found in available literature (Chopra and Chintanapakdee, 2004; Chopra and Goel, 2004; Goel and Chopra,

---

2004; Chopra, 2005; Goel, 2005; Goel and Chopra, 2005b, 2005a), can be summarized in the following steps:

1. Compute the  $n$  natural frequencies and modes for the linearly elastic vibration of the structure.
2. For the first mode, develop the base shear-roof displacement pushover curve for force distribution proportional to the mass and mode shape.
3. Idealize the pushover curve as a bilinear curve and convert it, computing the first mode inelastic SDOF system quantities.
4. Compute the peak deformation of the first mode inelastic SDOF system defined previously using nonlinear response history analysis, inelastic design spectrum or empirical equations for the ratio of deformations of inelastic and elastic systems.
5. Compute the dynamic response due to the first mode combining the effects of lateral and gravity loads.
6. Compute the dynamic response due to higher modes under the assumption that the system remains elastic, performing a classical modal analysis of a linear MDOF system, skipping the need for additional pushover analysis.
7. Determine the total response combining the peak modal responses using SRSS rule.

As for the conventional NSPs, the MPA method relies on the choice of a given reference node, hence two variants have once again been considered in the study that will follow, one using with the central deck node as a reference and the other selecting the reference in correspondence to the point of maximum deck deflection. It is also noted that the inelastic-elastic response ratios approach was adopted in this work for the determination of the performance point.

#### ***5.2.5 Adaptive Capacity Spectrum Method (ACSM)***

Recent studies (Pinho *et al.*, 2007; Monteiro *et al.*, 2008a; Pinho *et al.*, 2009) reported the viability of employing Displacement-based Adaptive Pushover (Antoniou and Pinho, 2004) to estimate seismic response of bridges. Contextually, an equally adaptive NSP has been proposed, and preliminarily verified, by Casarotti and Pinho (2007). The proposed approach combines elements from the Direct Displacement-based design method (e.g.,

(Priestley and Calvi, 2003a)) and the Capacity Spectrum Method (ATC, 1996; Freeman, 1998), maintaining a spectrum-based approach which employs the substitute structure methodology to model an inelastic system with equivalent elastic properties philosophy, but elaborated and revised within an “adaptive” perspective, for which reason it can also be viewed as an Adaptive Capacity Spectrum Method (ACSM). The procedure essentially consists in deriving an adaptive SDOF capacity curve and plotting it versus the Acceleration-Displacement Spectrum of the design earthquake, appropriately over-damped, thus obtaining the design intersection. For that intersection, the Performance Point, a model for the relationship between the hysteretic energy dissipation and equivalent viscous damping is used, explicitly accounting for the ductility achieved by the system, and iterations are carried out until convergence in damping is found.

The proposed method is therefore distinct from the original Capacity Spectrum Method, making use of: (i) more reliable displacement-based adaptive pushover curves, (ii) equivalent SDOF curve without reference either to any given elastic or inelastic mode shapes, but calculated step by step based on the actual deformed pattern, either than invariant elastic or inelastic modal shape, and not built on a modification of the capacity curve referred to the displacement of a specific physical location. As a consequence, all the ‘equivalent SDOF quantities’ even though of same ‘format’ of the corresponding modal quantities, are also calculated step-by-step based on the actual deformed pattern at each analysis step, which, together with the fully adaptive pushover algorithm, stands for the double adaptiveness of the procedure.

The procedure’s algorithm may be summed up in the following steps:

1. Perform a reliable pushover analysis on a nonlinear model of the MDOF structure and derive, step-by-step, the equivalent SDOF adaptive capacity curve.
2. Apply the demand spectrum to the SDOF capacity curve, determining their intersection, the performance point, for an assumed damping.
3. Bilinearize the capacity curve at the performance point and calculate corresponding system damping.



4. Determine if the actual damping matches the assumed one. If so, the performance point is established, otherwise, update damping and repeat steps 2 to 4 until convergence is found.

With respect to the demand spectrum reduction to account for the hysteretic energy dissipation ability of the structures, several possible scenarios have been considered and evaluated, nine damping-based and two ductility-based spectral reduction modalities, seeking for an optimal way of applying ACSM, as described in (Casarotti *et al.*, 2009).

For what seismic assessment of structures is concerned, the use of pushover-based simplified procedures is considered as a useful alternative to the more rigorous nonlinear dynamic analyses, if and when all relevant variables and effects are suitably taken into account. Those variables include, namely within the Adaptive Capacity Spectrum Method, amongst others, the hysteretic damping associated to the energy dissipation capacity that a structure inherently presents during an earthquake. One of the main concerns, when applying such procedure, is thus the definition of a demand spectrum that features ordinates appropriately scaled-down to take due account of the aforementioned capacity of structures for dissipating seismic energy through hysteresis.

Reduction of spectral ordinates may be carried out through the use of either over-damped elastic or constant-ductility inelastic spectra. The former make use of equations that estimate, as a function of ductility, values of the so-called equivalent viscous damping which is then used as input into another set of expressions that provide the spectral scaling factor. In alternative, the use of constant-ductility inelastic spectra, although perhaps less commonly, has also been proposed as a means to estimate seismic demand within the scope of nonlinear static assessment of structures (Chopra and Goel, 1999; Fajfar, 1999).

There are a relatively large number of past parametric studies dedicated to the derivation and/or validation of different approaches to estimate spectral reduction factor values (e.g., (Miranda, 2000; Miranda and Ruiz García, 2002)), however such studies seem to have focused mainly, if not exclusively, on SDOF systems. It seems, therefore, that verification on full structural systems is conspicuously needed in order to verify the adequacy of using existing SDOF-derived relationships in the assessment of MDOF systems. In the present work, the case of bridges was considered together with, as previously mentioned, eleven

different approaches for taking into account, through spectral scaling, the energy dissipation capacity of such systems.

As already mentioned, spectral Reduction Factors (RF) can be roughly divided in two groups: damping-based and ductility-based. Roughly, the first family consists of all those methods which, through the application of a reduction factor  $B$  based on the equivalent viscous damping (elastic viscous plus hysteretic), reduce by the same amount both displacement and acceleration spectral ordinates (see Equation (5.1) and Figure 5.2 left). To the second category belong all those approaches which make use of a 5%-damping elastic response spectrum and then reduce the spectral acceleration ordinates by a factor defined as a function of ductility (Equation (5.2) and Figure 5.2 right). The spectral reduction within ductility-based methods is not exactly vertical, given that displacements are modified as well, however, for the range of periods considered in this work,  $R \approx \mu$ . A few hybrid methodologies have also been proposed, as discussed subsequently.

$$\begin{aligned}
 S_{a,damp} &= B \cdot S_{a,el-5\%} \\
 S_{d,damp} &= B \cdot S_{d,el-5\%} \\
 S_{d,damp} &= \frac{S_{a,damp}}{\omega^2}
 \end{aligned}
 \tag{5.1}$$

$$\begin{aligned}
 S_{a,duct} &= \frac{S_{a,el-5\%}}{R} \\
 S_{d,duct} &= \frac{\mu}{R} S_{a,el-5\%} = C \cdot S_{d,el-5\%}
 \end{aligned}
 \tag{5.2}$$

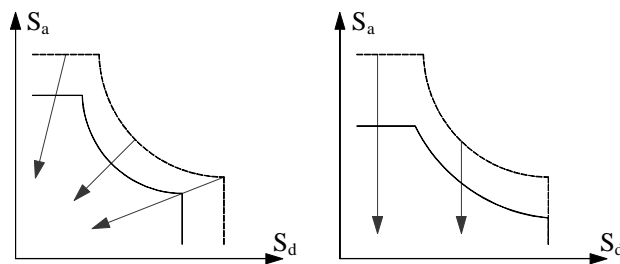


Figure 5.2 – Spectral reduction methods: damping-based (left) and ductility-based (right).

### 5.2.5.1 Damping-based spectral reduction

With regard to damping-based spectrum scaling methods, a combination of different ways of calculating the (i) equivalent viscous damping  $\xi_{eq}$  and (ii) corresponding spectral reduction factor B are available. Some of the most commonly used ones are presented and reviewed in what follows.

#### Equivalent viscous damping models

In the following equations,  $\xi_0$  stands for the so-called elastic viscous damping and  $\mu$  for ductility (which was a variable of the work, given that it varied with the intensity level and the characteristics of the response of each bridge).

#### A) ATC-40, based on the modified Rosenblueth and Herrera model (herein termed *ATC40*)

This proposal by Rosenblueth and Herrera (1964), and subsequently adopted by ATC-40 (ATC, 1996), was the first equivalent linear method to suggest the use of secant stiffness at maximum deformation as the basis for considering inelastic response. In such approach, if one considers a bilinear system with a post-yield stiffness ratio  $\alpha$ , the viscous damping for the equivalent linear elastic system is given by Equation (5.3), where  $\kappa$  is an empirical parameter that takes account the degree to which the hysteresis response cycle resembles a parallelogram or not; three possibilities are defined (A, B or C), depending on structural system configuration and duration of ground shaking.

$$\xi_{eq-ATC40} = \xi_0 + \kappa \frac{2}{\pi} \left[ \frac{(1-\alpha)(\mu-1)}{\mu - \alpha\mu + \alpha\mu^2} \right] \quad (5.3)$$

#### B) Kowalsky, based on the Takeda hysteretic model with post-yield hardening (herein termed *TakKow*)

Kowalsky (1994) derived an equation for equivalent viscous damping ratio that was based on the Takeda hysteretic model. For a thin response mode (empirical parameter  $b=0$ ) with

unloading stiffness factor of 0.5 and a post-yield stiffness ratio  $\alpha$ , the equivalent damping ratio is given by Equation (5.4).

$$\xi_{eq-TakKow} = \xi_0 + \frac{1}{\pi} \left[ 1 - \frac{(1-\alpha)}{\sqrt{\mu}} - \alpha\sqrt{\mu} \right] \quad (5.4)$$

**C) Gulkan and Sozen, based on the Takeda model without hardening (herein termed *TakGS*)**

Gulkan and Sozen (1974) used the Takeda hysteretic model and experimental shaking table results of small-scale reinforced concrete frames to develop empirical Equation (5.5) to compute equivalent viscous damping ratio values.

$$\xi_{eq-TakGulSoz} = \xi_0 + 0.2 \left[ 1 - \frac{1}{\sqrt{\mu}} \right] \quad (5.5)$$

**D) Iwan (herein termed *Iwan*)**

Iwan (1980) derived empirically equations to estimate the equivalent viscous damping ratio, Equation (5.6), using a hysteretic model derived from a combination of elastic and Coulomb slip elements together with results from dynamic analyses using 12 earthquake ground motion records.

$$\xi_{eq-Iwan} = \xi_0 + 0.0587(\mu - 1)^{0.371} \quad (5.6)$$

**E) Dwairi *et al.* (herein termed *Dwairi* or *DwaKowNau*)**

Dwairi *et al.* (2007) recently developed new equivalent viscous damping relations for four structural systems, defined as a function of ductility and effective period of vibration. With the latter, the authors claim to having managed to significantly reduce the error in

predicting inelastic displacements and minimize the scatter of results. Considering the structural system that best fits the case of continuous deck bridges, the equivalent viscous damping relation is that shown in Equation (5.7), where  $C_{ST}$  is a parameter dependent on the effective period, ranging from a minimum of 0.3 to a maximum value of 0.65.

$$\xi_{eq-DwaKowNau} = \xi_0 + \frac{C_{ST}}{\pi} \left( \frac{\mu-1}{\mu} \right) \quad (5.7)$$

#### F) Priestley *et al.* (herein termed *Priestley*)

The approach proposed by Priestley *et al.* (2007) can, in a somewhat simplified manner, be represented by Equation (5.8). Actually, the equation should be applied to each individual pier, and then a weighted average based on shear forces and response displacements would be used to estimate the overall damping of SDOF system. Herein, for reasons of simplicity and congruency with the employed NSP, the simplification of applying Equation (5.8) directly to the full system is carried out.

$$\xi_{eq-Priestley} = \xi_0 + 0.444 \left( \frac{\mu-1}{\mu\pi} \right) \quad (5.8)$$

Figure 5.3 plots the six previously listed approaches for equivalent viscous damping estimation. It is noted that ATC-40 results are computed for a structural type B (the most appropriate for the structures considered), no post-yield hardening was considered for ATC40 and TakKow approaches, and Dwairi's estimates are plotted for two representative values of 0.4 and 0.5.

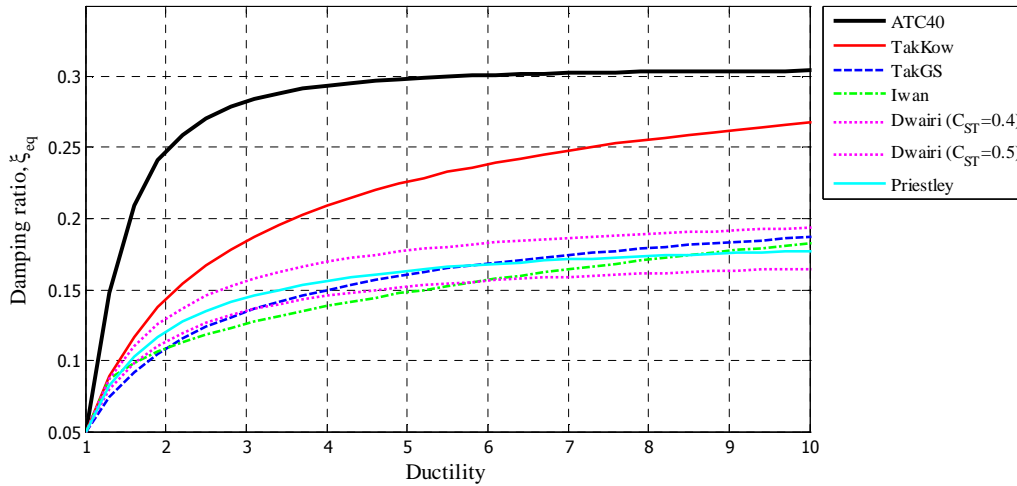


Figure 5.3 – Considered damping models.

It is readily observed that whilst ATC40 and TakKow models distinguish themselves from the rest by providing significantly higher equivalent viscous damping estimates, the remaining four approaches (TakGS, Iwan, Dwairi and Priestley) yield results that are very close. With the latter in mind, and considering its relative contemporariness with the work of Gulkan and Sozen (1974), the expression proposed by Iwan (1980) will not be considered on the subsequent parametric study, also because, in opposite to the other relationships, it does not feature an upper bound limit. Such rationale could also have led to the exclusion of one the two proposals from Dwairi *et al.* (2007) and Priestley *et al.* (2007), however in this case both were kept in the parametric study given their diverse nature in terms of application.

### Damping-based reduction factors

As previously discussed, the computation of  $\xi_{eq}$  is then followed by the calculation of the corresponding spectral reduction factor B. Different approaches may again be considered.

#### A) Newmark-Hall and ATC-40 (herein termed *NH-ATC40*)

In the well known method proposed by Newmark and Hall (1982), the damping reduction factors  $B_{NH}$  for median estimates of response (i.e. 50% probability of exceedance) are given by Equation (5.9).

$$\begin{cases} B_{NH(acc)} = \frac{3.21 - 0.68 \ln(100 \xi_{eq})}{2.21}, & T_b \leq T < T_c \\ B_{NH(vel)} = \frac{2.31 - 0.41 \ln(100 \xi_{eq})}{1.65}, & T_c \leq T < T_d \\ B_{NH(displ)} = \frac{1.82 - 0.27 \ln(100 \xi_{eq})}{1.39}, & T \geq T_d \end{cases} \quad (5.9)$$

The data of Newmark and Hall were limited to viscous damping ratios of 20% and are obtained from a limited number of earthquakes prior to 1973. In addition they were derived from the displacement response spectrum or pseudo-acceleration response spectrum. It is noted that, for damping ratios higher than 5%,  $B_{NH(acc)} < B_{NH(vel)} < B_{NH(displ)}$ .

The method has been adapted by most of the American design codes and guidelines, such as the ATC-40 (1996), among others, where  $B_{ATC40}$  is defined by  $SR_A$  and  $SR_V$ , corresponding to constant acceleration and velocity regions, respectively:

$$\begin{cases} SR_A = \frac{3.21 - 0.68 \ln(100 \xi_{eq})}{2.21} \geq \overline{SR}_A & T < T_c \\ SR_V = \frac{2.31 - 0.41 \ln(100 \xi_{eq})}{1.65} \geq \overline{SR}_V & T \geq T_c \end{cases} \quad (5.10)$$

In Equations (5.9) and (5.10) a period  $T_{c'}$ , given by Equation (5.11), should be applied in order to guarantee continuity conditions with respect to the corner period.

$$T_{c'} = \frac{B_{(vel)}}{B_{(acc)}} T_c \quad (5.11)$$

The constraints imposed by Equation (5.10), referring to Table 5.1, depend on the aforementioned ATC-40 structural typologies (A, B or C), and imply maximum admitted damping ratios of 37-40% for type A, 28-29% for type B and 19-20% for type C. Analogously,  $SR_A < SR_V$ .

Table 5.1 – Maximum allowable  $SR_A$ ,  $SR_V$  (ATC-40) and  $SR_D$  (present study) values.

Structural Type	$SR_A$	$SR_V$	$SR_D$
A	0.33	0.50	0.59
B	0.44	0.56	0.66
C	0.56	0.67	0.73

In the present study, an approach blending the proposals of Newmark and Hall (1982) and ATC-40 (1996) is taken into account. The original NH formulation is therefore complemented by considering the lower limits introduced by ATC-40 for the velocity and acceleration zones, and introducing a factor  $SR_D$  (see Table 5.1) with a limitation similar to  $SR_A$  and  $SR_V$ , i.e., maximum admitted damping ratios of 40%, 29% and 20%, for types A, B and C respectively.

**B) Eurocode 8 (herein termed EC8)**

Eurocode 8 (CEN, 2005a) recommends the use of the spectral reduction factors given in Equation (5.12), with a minimum of 0.55.

$$B_{EC8} = \begin{cases} 1 - (1 - \eta) \frac{T}{T_b} & 0 \leq T < T_b \\ \eta & T \geq T_b \end{cases} \quad (5.12)$$

$$\eta = \sqrt{\frac{10}{5 + 100 \xi_{eq}}} \geq 0.55$$

**C) Ramirez *et al.* (herein termed Ramirez)**

Ramirez *et al.* (2002) proposed a bilinear relationship – Equation (5.13) – between the reduction factor  $B_{short}$  and equivalent damping ratio  $\xi_{eq}$ , valid up to damping ratios of 50%. Exceeding that value the relation becomes trilinear and dependent on  $B_{long}$  – Equation (5.14).  $T_b$  and  $T_c$  are the first and third spectral characteristic/corner periods, whilst  $B_{short}$  and  $B_{long}$  can be found in Table 5.2.



$$B_{Ram} = \begin{cases} 1 - (1 - B_{short}) \frac{T}{T_b} & 0 \leq T < T_b \\ B_{short} & T \geq T_b \end{cases} \quad (5.13)$$

$$B_{Ram} = \begin{cases} 1 - (1 - B_{short}) \frac{T}{T_b} & 0 \leq T < T_b \\ B_{long} - (B_{short} - B_{long}) \frac{(T - T_b)}{(T_c - T_b)} & T_b \leq T < T_c \\ B_{long} & T \geq T_c \end{cases} \quad (5.14)$$

Table 5.2 – Reduction factors for Ramirez *et al.* approach.

Equivalent damping, $\xi$ (%)	$B_{short}$	$B_{long}$
5	1.00	$B_{short}$
10	0.83	$B_{short}$
20	0.67	$B_{short}$
30	0.59	$B_{short}$
40	0.53	$B_{short}$
50	0.45	$B_{short}$
60	0.43	0.38
70	0.43	0.34
80	0.42	0.30
90	0.41	0.27
100	0.40	0.25

#### D) Lin and Chang (herein termed *Lin-Chang*)

In a recent study, Lin and Chang (2003) proposed a period-dependent reduction factor, Equation (5.15), based on an extensive dynamic analysis parametric study of linear elastic SDOF systems, using real USA records. Such RF has the advantage that, whilst still following the general trend of the others with respect to the structural period  $T$ , it is inherently continuous, hence not requiring the addition of any other type of continuity constraints or conditions.

$$B_{LinChang} = 1 - \frac{a \cdot T^{0.3}}{(T+1)^{0.65}} \quad (5.15)$$

$$a = 1.303 + 0.436 \ln(\xi_{eq})$$

**E) Priestley *et al.* (herein termed *Priestley*)**

Recently, Priestley *et al.* (2007) proposed the application of Equation (5.16), which was included in earlier versions of Eurocode 8, but was then subsequently abandoned.

$$B_{Priestley} = \left( \frac{0.07}{0.02 + \xi_0} \right)^{0.5} \quad (5.16)$$

Figure 5.4 presents results obtained with the above-listed spectral reduction equations for values of response period from three representative spectral regions; constant acceleration zone ( $T=2T_b$ ), constant velocity zone ( $T=2T_c$ ), constant displacement zone ( $T=1.5T_d$ ).

It is observed that those approaches that feature a lower bound limit (i.e. NH-ATC-40, EC8 and Priestley) tend to yield the higher spectral reductions for low damping ratios (Priestley across the entire period range, EC8 in the displacement zone and NH-ATC-40 in the acceleration zone). On the other hand, for higher values of damping (larger than 0.25-0.36) Ramirez and Lin-Chang equations provide the higher spectral reductions. The dispersion among the different proposals also increases with damping ratio.

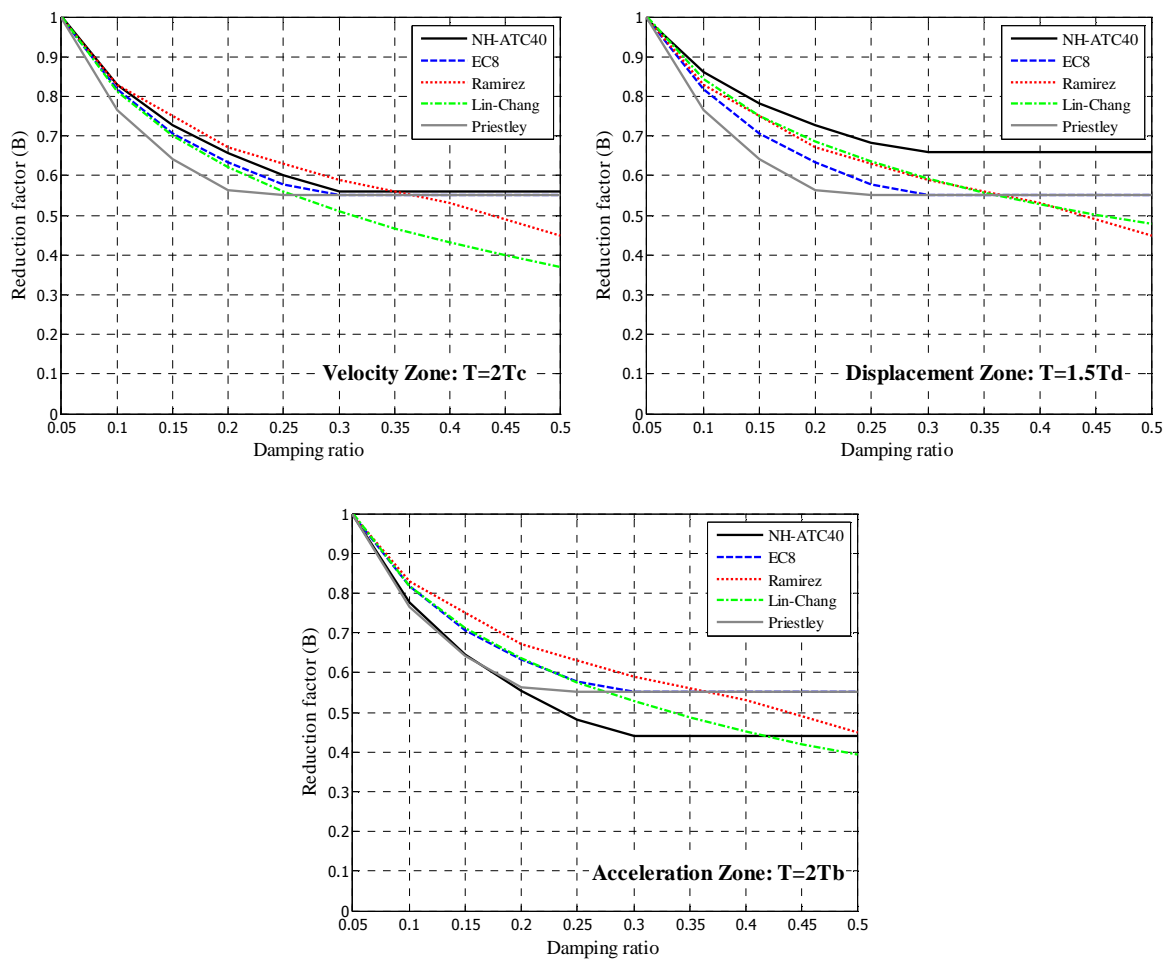


Figure 5.4 – Reduction factor variation with damping in the three spectral regions.

Finally, it is perhaps also noteworthy to see that the NH-ATC-40 formulae is highly sensitive to period values; if one considers a constant high value of damping (e.g.,  $\xi_{eq}=0.3$ ), the spectral reduction factor may vary from 0.44 to 0.67, depending on the response period of the structure. To shed further insight into this latter issue (i.e. period dependency of spectral reductions), Figure 5.5 has also been produced.

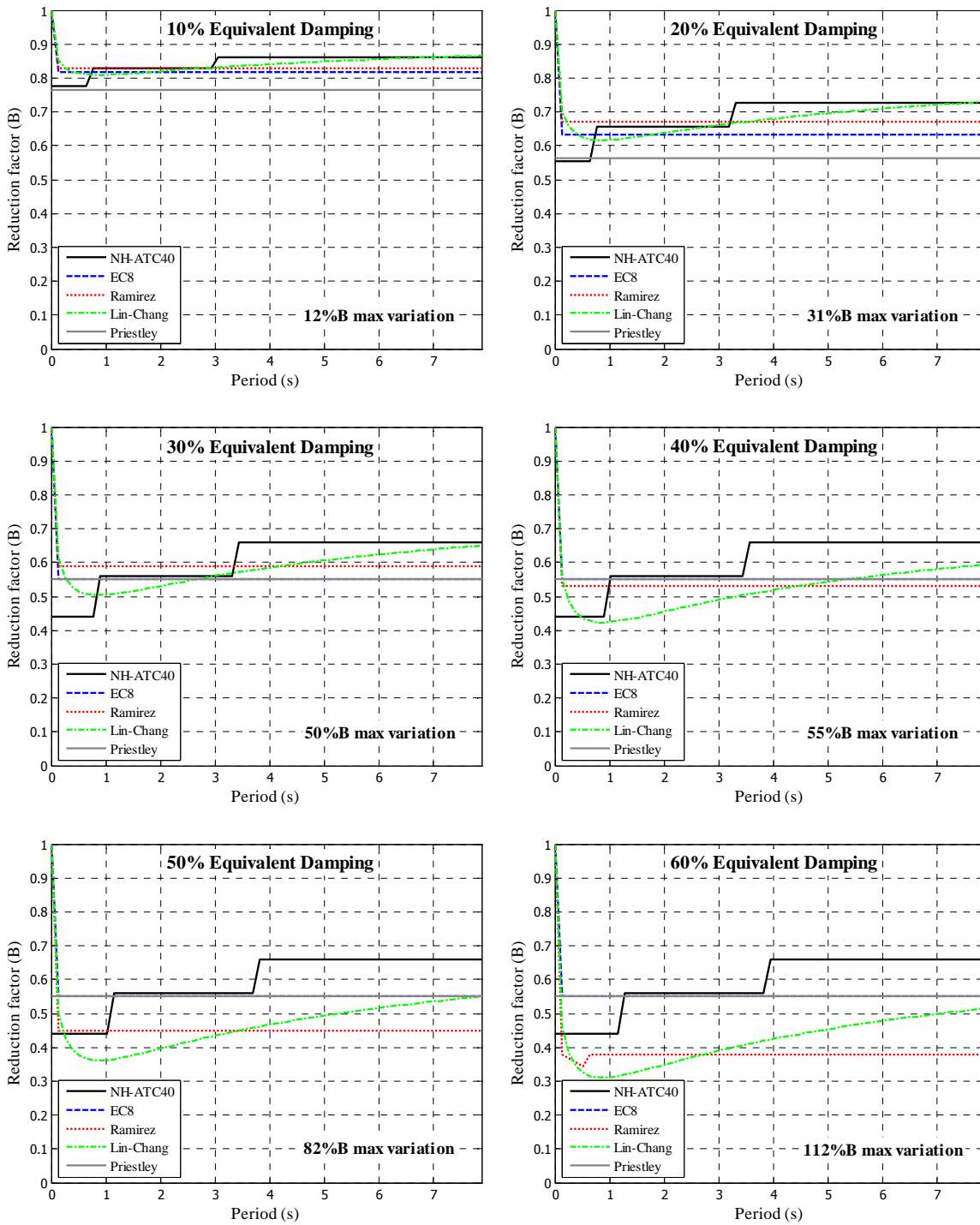


Figure 5.5 – Reduction factor variation with period for different damping ratios.

It is observed that the dispersion among the several RF approaches, indicated in the plots as a percentage of the maximum RF, increases with the damping ratio. It is also noted that the NH-ATC-40 variant generally yields the highest reduction factor, especially for periods higher than 3 or 4 seconds.

In the parametric study described subsequently, three out of the above-listed five possible reduction factor approaches have been selected: (i) Lin-Chang (Equation (5.15)), (ii) Priestley (Equation (5.16)), (iii) a combination of EC8 and Ramirez (Equation (5.17)). This last hybrid approach, herein termed EC8Ram, aimed especially at creating a more simplified version of EC8 and Ramirez proposals that would nonetheless envelop the general period-dependent trend of RF; EC8 is employed for low periods where it yields lower RF estimates and Ramirez is considered for the high period range where it provides high RFs.

$$B_{EC8\_Ram} = \begin{cases} B_{EC8} & 0 \leq T < T_{dd} = T_d \frac{B_{Ram}}{B_{EC8}} \\ B_{Ram} & T \geq T_{dd} \end{cases} \quad (5.17)$$

The somewhat cumbersome trilinear NH-ATCH40 relationship was not considered further, whilst the equation by Priestley *et al.* (2007) was employed only in tandem with the equivalent viscous damping equations proposed by the same authors (Equation (5.8)).

#### 5.2.5.2 Ductility-based spectral reduction

As mentioned before, the reduction of the spectral ordinates may also be achieved by an alternative type of approach, whereby a reduction factor, directly dependent on ductility, is used. Amongst the different approaches present in literature, two have been considered in the current work:

##### **A) Miranda (2000) for firm soils (herein termed *Mir2000*)**

Miranda (2000) observed that, for sites with average shear-wave velocities higher than 180 m/s in the upper 30 m of the soil profile (typically soil types A-B-C-D in ATC and FEMA guideline documents), inelastic displacement ratios are not significantly affected by local site conditions, nor by changes in earthquake magnitude, nor by changes in epicentral distance (with the exception of very near-field sites that may be influenced by forward directivity effects). As a result, the displacement modification factor expression, in Equation (5.18), was proposed:

$$C_{Mir} = \left[ 1 + \left( \frac{1}{\mu} - 1 \right) \exp(-12T \mu^{-0.8}) \right]^{-1} \quad (5.18)$$

### B) Vidic *et al.* (herein termed *VidFajFish*)

Vidic *et al.* (1994) suggested a relationship for a ductility-based reduction factor, with a corner period  $T_{c'}$  dependent of the characteristic spectral period  $T_c$ , Equation (5.19):

$$C_{VFF} = \begin{cases} \mu \left[ 1.35(\mu-1)^{0.95} \frac{T}{T_{c'}} + 1 \right]^{-1} & T \leq T_{c'} \\ \mu \left[ 1.35(\mu-1)^{0.95} + 1 \right]^{-1} & T > T_{c'} \end{cases} \quad (5.19)$$

$$T_{c'} = 0.75\mu^{0.2}T_c \leq T_c$$

In the parametric study that follows, a number of diverse spectrum scaling approaches will be employed, considering combinations of different equivalent viscous damping models and damping-based scaling factors, together with ductility-based scaling equations. With reference to the nomenclature introduced above, the eleven cases considered are hence: ATC40 - EC8Ram, ATC40 - LinChang, TakKow - EC8Ram, TakKow - LinChang, TakGS - EC8Ram, TakGS - LinChang, DwaKowNau - EC8Ram, DwaKowNau - LinChang, Priestley, Mir2000, VidFajFish.

#### 5.2.6 Adaptive Modal Combination Procedure (AMCP)

The Adaptive Modal Combination Procedure, proposed by Kalkan and Kunnath (2006), is fundamentally based on the adaptive pushover procedure of Gupta and Kunnath (2000) in which the main feature is the modification of the applied lateral loads according to the changes in the modal attributes of the structure, as well as the system's response during the inelastic phase, as the earthquake load carries on. Such new lateral load configuration, using factored modal combinations, enhances an alternative scheme to represent realistic lateral force demands, managing to incorporate inherent advantages of CSM and MPA, yet

avoiding the need for a pre-estimated target displacement. Indeed the procedure makes use of a displacement-controlled method, in which the demand is determined by individual adaptive pushover analysis using inertia distribution of each mode, continuously updated.

With respect to the equivalent single degree of freedom system definition, the corresponding displacement, abscissa of the ADRS format capacity curve, is obtained at each step through an energy-based approach, computing the work done therein by the lateral force pattern. The performance point is determined in a Capacity Spectrum Method similar fashion with the difference of using inelastic spectra, computed for a set of ductility levels, skipping a preliminary estimate for the target displacement. This so-called dynamic target point is, therefore, the intersection of the equivalent SDOF capacity curve with the inelastic demand spectrum corresponding to the global system ductility, which contributes to a more realistic representation of demand. The match will be better as the ductility refinement used for computation of inelastic spectra increases. The procedure is carried out separately for each of the  $n$  relevant modes and the total response, similarly to what is done in Multimodal Pushover Analysis, is simply determined by combining peak modal responses with an adequate rule (SRSS or CQC). In the end,  $n$  individual mode contribution adaptive pushover analyses and corresponding target point determination processes (with inelastic spectra computed for possible several levels) will be required within this procedure.

The following steps synthesize the procedure:

1. Compute modal properties of the structure at the current state of the system.
2. For the  $n^{\text{th}}$  mode, construct the adaptive lateral load pattern proportionally to the mass and mode shape; recomputed the load distribution for every step or at a set of predefined steps.
3. Evaluate the next incremental step of the capacity curve for each equivalent SDOF system using the energy based approach.
4. If the response is inelastic for the  $i^{\text{th}}$  step of the  $n^{\text{th}}$  mode pushover analysis, calculate the approximate global system ductility and post-yield stiffness ratio, using a bilinear representation.

5. Generate the capacity spectra in the ADRS format for a series of predefined ductility levels and plot it together with the inelastic demand spectra at different ductility levels. The dynamic target point will be the intersection of the equivalent SDOF system modal capacity curve with the inelastic demand spectrum corresponding to the global system ductility. The match will be as better as higher the ductility levels' refinement is.
6. Repeat steps 1 to 5 for as many modes as deemed essential for the system under consideration and combine peak modal results using the SRSS combination scheme.

Several difficulties have been found throughout the implementation of the procedure on bridges, concerning the computation of the adaptive pushover curves with individuated modes' contribution. Additionally, the authors themselves do not claim it eligible for this sort of structures, potentiating the decision of not to include the AMCP in the endeavoured parametric study.

#### ***5.2.7 Method comparison***

As stated along the description, from the six more popular proposed Nonlinear Static Procedures only four have been selected for bridge application: CSM, N2, MPA and ACSM. The other two were discarded given their low rationality or applicability to this sort of structures. All the four methods were applied with the main purpose of making a comparison of current NSPs, a task that represents an inedited study. Additionally, each method was preliminary studied in different versions in order to select its best performance, selecting them for the confronting. Table 5.3 presents a summary of the main considerations in each of the four methods, in order to clarify the conditions in which the comparative study was carried out.



Table 5.3 – Summary of studied Nonlinear Static Procedures

	<b>ACSM</b>	<b>CSM</b>	<b>N2</b>	<b>MPA</b>
<b>Pushover analysis type</b>	Adaptive displacement-based	Conventional force-based		
<b>Load pattern</b>	Displacements loading	1 <sup>st</sup> mode	1 <sup>st</sup> mode	All significant
<b>Capacity curve</b>	Base shear vs. Displacement computed from all nodes, including higher modes contribution	Base shear vs. Displacement of a reference/control node, usually recommended as the centre of mass of the deck		
<b>Demand curve</b>	Equivalent viscous damping reduced spectra		Inelastic ductility-based reduced spectra	
<b>Number of studied versions</b>	<b>Eleven:</b> Different demand spectrum reduction possibilities	<b>Four:</b> Original CSM and FEMA improved with central or maximum displacement reference node	<b>Six:</b> 1 <sup>st</sup> mode, uniform loading pattern or envelope with central or maximum displacement reference node	<b>Two:</b> Central or Maximum displacement reference node

### 5.3 Parametric Study

The investigate the applicability of nonlinear static procedures, as well as their individual calibration, a set of bridge structures has been selected going through different regularity levels, in terms of piers' heights and deck length. Further details on the considered case study can be found in 4.3.

The seismic demand on the bridge models is evaluated by means of nonlinear dynamic analyses (NDA), assumed to constitute the most accurate tool to estimate the 'true' earthquake response of the structures, using the fibre-based finite elements program SeismoStruct (SeismoSoft, 2008). The same software package was employed in the running of the force-based conventional pushovers (used in CSM, N2 and MPA methods) and of the displacement-based adaptive pushover analyses (Antoniou and Pinho, 2004) that are required by the ACSM procedure.

Results are presented in terms of different response parameters: the estimated displacement pattern (D) and flexural moments (M) of the bridge deck at the nodes above the piers, and the shear forces at the base of the piers (V) and abutments (ABT). Then, in order to appraise the accuracy of the NSPs results obtained with the different approaches, these are normalized with respect to the median of the corresponding response quantities obtained

through the incremental NDAs; this provides an immediate indication of the bias for each of the four procedures. Equation (5.20) shows, for a generalized parameter  $\Delta$  at a given location  $i$ , how the results from the incremental dynamic analyses (IDA), run for each of the ten records considered, are first processed.

$$\hat{\Delta}_{i,IDA} = \text{median}_{j=1:10} [\Delta_{i,j-IDA}] \quad (5.20)$$

The aforementioned results' normalization consists thus in computing, for each of the parameters and for each of the considered locations, the ratio between the result coming from each NSP and the median result coming from NDA, as illustrated in Figure 5.6 and numerically translated into Equation (5.21). Ideally the ratio should be unitary.

$$\bar{\Delta}_i = \frac{\Delta_{i,NSP}}{\hat{\Delta}_{i,IDA}} \dots \xrightarrow{\text{ideally}} 1 \quad (5.21)$$

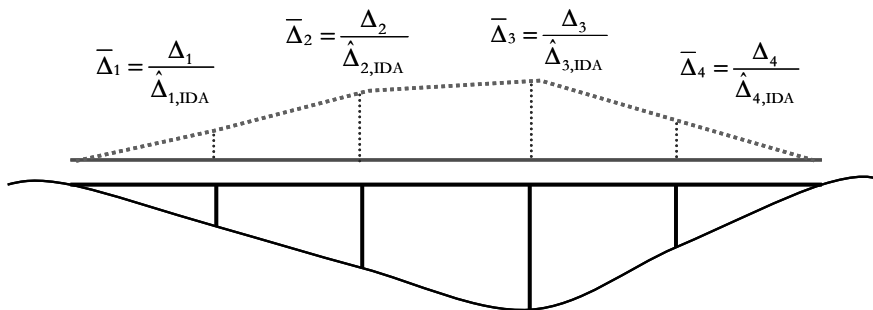


Figure 5.6 – Normalized transverse deformed pattern.

This normalization renders also somewhat “comparable” all deck displacements, moments and shear forces, since all normalized quantities have the same unitary target value, thus allowing in turn the definition of the aforementioned Bridge Index (Pinho *et al.*, 2007). Recalling the definition presented in Section 4.4.4, the bridge index (BI) is computed as the median of normalized results for the considered parameter over the  $m$  deck locations: deck displacements ( $BI_D$ ), deck moments ( $BI_M$ ) or shear forces at the piers and abutments ( $BI_V$  and  $BI_{ABT}$ ), as shown in Equation (5.22). The standard deviation STD measures, on

the other hand, the dispersion with respect to the median, for each of the procedures' tested versions – Equation (5.23).

$$BI_{\Delta, NSP} = \text{median}_{i=1:m} [\bar{\Delta}_{i, NSP}] \quad (5.22)$$

$$STD_{\Delta, NSP} = \left[ \frac{\sum_{i=1}^m (\bar{\Delta}_{i, NSP} - BI_{NSP})^2}{m-1} \right]^{0.5} \quad (5.23)$$

## 5.4 Results

In this section, the results obtained from the aforementioned parametric study are scrutinized and interpreted, with a view to evaluate the accuracy of the different NSPs considered (recalled in Table 5.3). However, before passing onto a direct comparison between the four procedures, a preliminary study was carried out to identify which of the variants of the CSM, N2, MPA and ACSM methods, discussed in previous sections and summarized in Table 5.3, would lead to the attainment of best results.

### 5.4.1 Results representation

The relative performance of possible variants within each procedure, or the comparison of the methods itself, is evaluated in detailed fashion with respect to two variables: intensity level and bridge configuration. According to such formula, the intensity level of results consists of the median Bridge Index over the 14 bridge configurations whereas a bridge configuration level of results represents, for each bridge configuration, the median Bridge Index across the 6 intensity levels. While an intensity level detail of results will show how procedures behave when the structure enters the nonlinear range, a bridge configuration detailed level of results enables the analysis of the influence of symmetry, regularity, length, abutments type, among other variables. Finally, a global overview may be put up where the bridge index over all the 14 bridges and 6 intensity levels is computed. In other words, the median bridge index over all bridge configurations and intensity levels represents the median of the single BI of every considered bridge configuration, at every

intensity level. The same sort of compound approach can be carried for standard deviation as well. Figure 5.7 schematically presents the different types of detailing level of results.

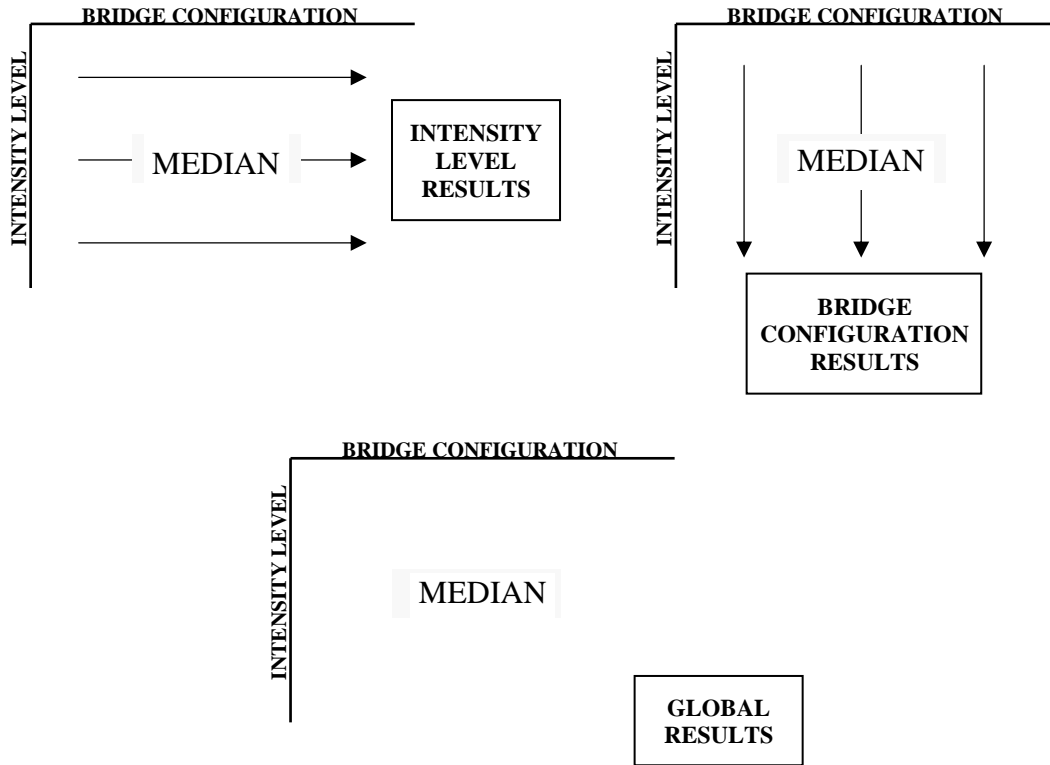


Figure 5.7 – Types of approaches for results: intensity level detailed (*top left*), bridge configuration detailed (*top right*), global (*bottom*).

The importance, and relevance, of such multiple approaches to represent results is easily understandable. If a general comparison is intended, especially if the purpose is to elect a specific procedure or variant of the same method, then an overall perspective may be needed for the sake of simplicity and clearness of interpretation, making use of statistically-based reduction. However, the Bridge Index that is computed over all configurations and intensity levels will certainly conceal significant information that may help to clarify general results. The observation of prediction in greater detail, from intensity level or bridge configuration point of view, or even across different locations inside a specific bridge, is the mean to better understanding and warranty that miscellaneous judgement is not taken.

## 5.4.2 Preliminary evaluation

### 5.4.2.1 Capacity Spectrum Method

Figure 5.8 illustrates the graphical results for one of the short irregular configurations (A213) for the different versions of the method, at the end of the iterative procedure, at two distinct levels of seismic intensity. The plots are in the ADRS format (Acceleration Displacement Response Spectrum) and two distinct pushover curves are presented due to the two possible reference nodes. The response spectrum, in turn, is reduced according to ATC-40 or FEMA-440 and intersected with the two possible capacity curves, rendering four performance points.

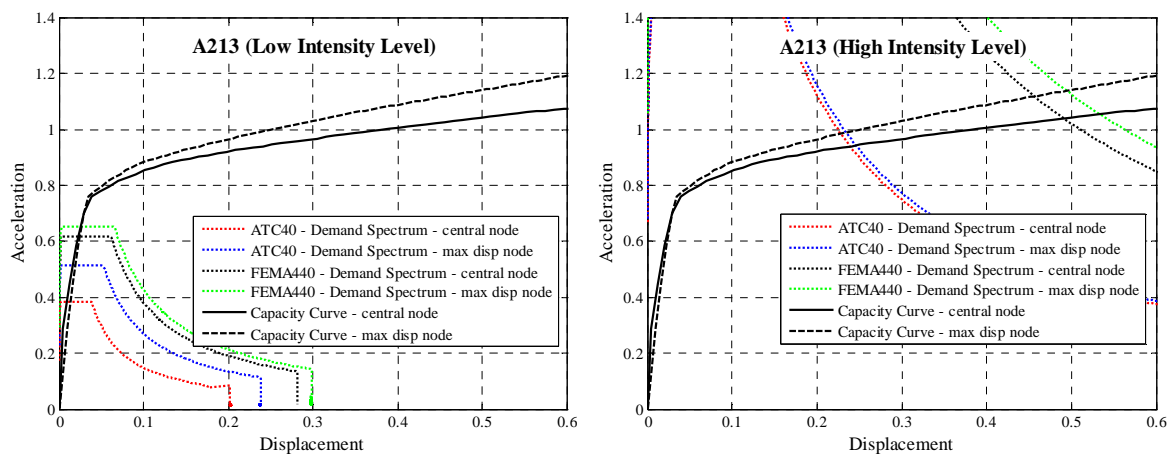


Figure 5.8 – CSM performance points for bridge A213: low and high intensity levels.

It is immediately noticeable that the influence of the reference node position in the capacity curve is not outstanding. The curves tend to move away from each other as the structure goes further into the nonlinear range. The performance points will be, thus, more or less different depending on the region where the demand intersects the capacity. On the other hand, the effect caused by the employment of the new damping equations proposed in the FEMA-440 report is quite more pronounced, as well as the corresponding spectral reduction, which is clearly observed in the plots, especially for high intensity levels. Therefore, regarding this issue, noteworthy differences in the predictions are expected.

Figure 5.9 and Figure 5.10 show values of Bridge Index and Standard Deviation, with respect for the median BI, for each intensity level, which is the median across the entire set of bridges.

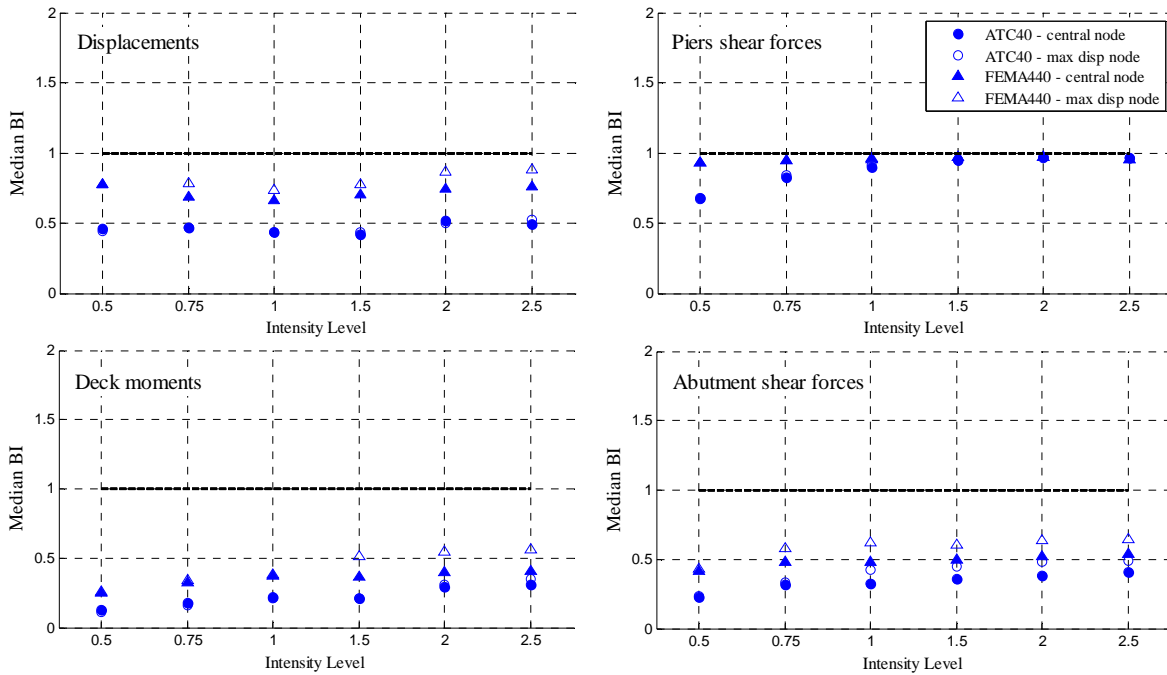


Figure 5.9 – CSM median Bridge Index (BI) per intensity level.

The improvements introduced by the FEMA-440 report are clearly observed, especially in the estimations of displacement, deck moments and abutment shear forces, where results obtained using the spectrum scaling procedures suggested in FEMA-440 are much closer to unity (which means NSP estimates equal to NDA predictions) than those obtained using the ATC-40 equations. Nevertheless, both approaches seem to overestimate the equivalent viscous damping, hence, the corresponding spectral reduction, as well, which renders moderate to heavy underestimation of displacements. On the other hand, if shear forces estimates at the piers are considered, the improvement introduced by FEMA-440 guidelines is barely noticeable, except for the lowest intensity levels, given that predictions are generally very good, i.e., fairly matching the nonlinear dynamic analysis' ones. The use of the location of maximum displacement node as reference will generally yield higher estimates for nearly all the parameters, thus, closer to unit BI ratios. Again, the exception is the pier shear forces parameter, to which the difference in choosing one or other reference node is imperceptible. Generally, performance tends to get better as the intensity level increases, mainly for pier shear forces and slightly for the rest of the engineering demand parameters.

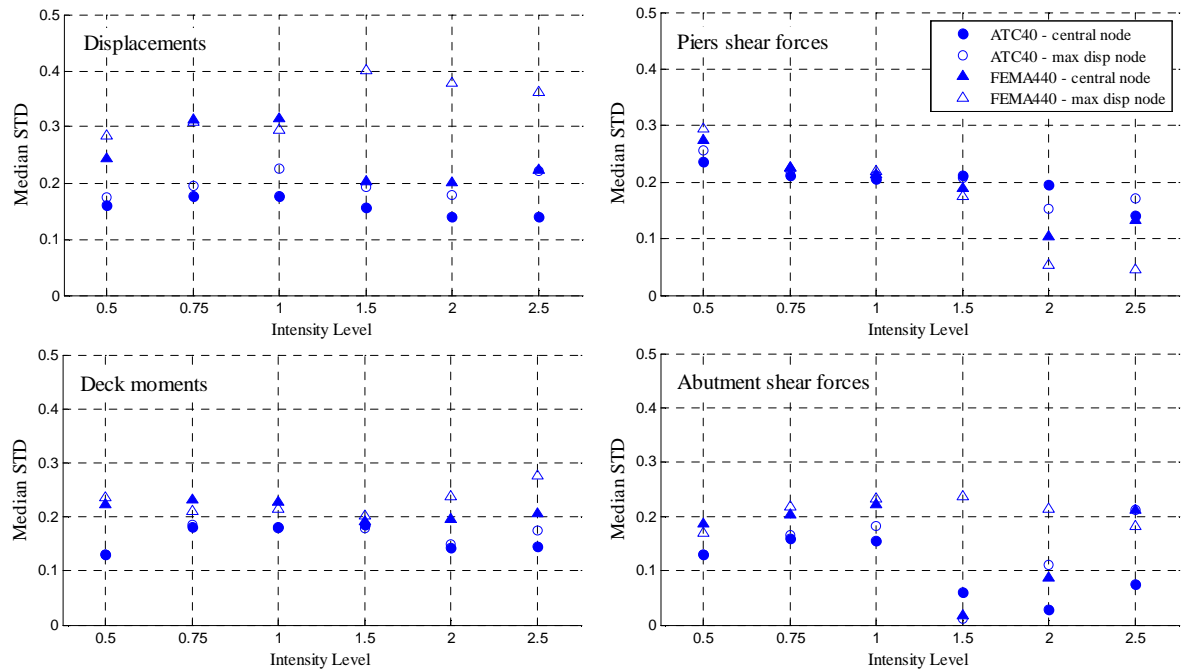


Figure 5.10 – CSM median Standard Deviation (STD) per intensity level.

Looking at the method's behaviour from the dispersion point of view, a tendency for better predictions to be associated to higher scatter levels can be noticed. The FEMA-440 approach presents larger standard deviation with respect to the median BI, normally oscillating between 0.2 and 0.3, or reaching levels of 0.4, if deck displacements are considered. The classical approach barely exceeds 0.2 for all the parameters. Shear force estimates present slightly lower dispersion, barely exceeding 0.2, showing no clear difference between classical or FEMA-440 approaches, for the case of the piers. The version that uses the maximum displacement node as reference can be seen as usually more scattered, which may be due to the fact that its physical location is not constant as the centre of mass of the deck is. Regarding the dispersion behaviour with increasing intensity, it is generally either constant or even decreasing, which may be justified with the larger estimates for strong ground motion intensity being less sensitive to fluctuation of results coming from distinct locations or configurations.

The influence of structural geometry in the results may be scrutinized by plotting the Bridge Indexes according to the structural configuration. Such representation is presented in Figure 5.11 considering the median BI over all the intensity levels.

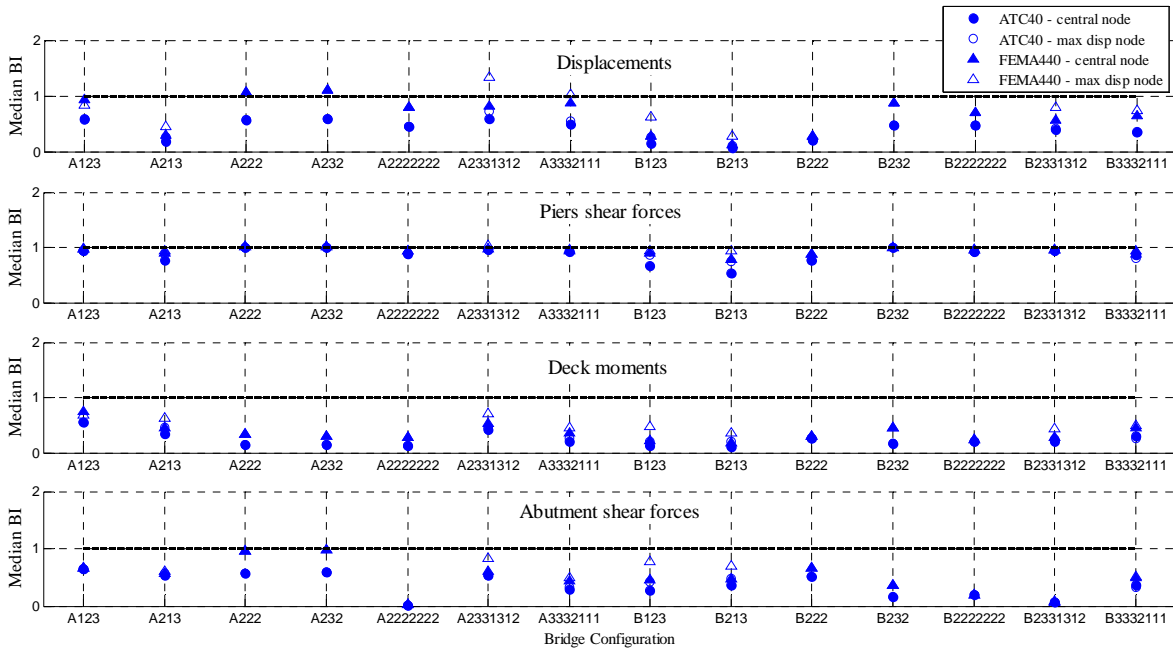


Figure 5.11 – CSM median Bridge Index (BI) per bridge configuration.

The main observations, made according to the plot of results with varying intensity, seem to stand, putting the FEMA-440 version as the most accurate one even if the improvement coming from the use of the deck’s centre of mass node as a reference does not appear so general, being more eloquent for the case of long, irregular configurations. Curiously, lower discrepancy between different versions for the method seems to also occur for irregular configurations, which denotes the effective improvement carried in by the FEMA-440 guidelines, given that, for regular configurations, other variables are eliminated. Regarding shear estimates, the underestimation is higher for irregular configurations. Having in mind that the method is particularly recommended for regular, simple structures, vibrating predominantly in the 1<sup>st</sup> mode, such scenario seems to indicate that the method is not that unstable for non regular structures.

According to what has been exposed, in subsequent applications, the CSM will be employed considering its FEMA-440 version (notwithstanding the slender increase in dispersion), together with the maximum displacement node as reference.

#### 5.4.2.2 N2 Method

Figure 5.12 shows the different performance points, given by displacement targets in the N2 procedure, for the same chosen A213 configuration for example, two intensity levels,



low and high, at the end of the EC8-proposed iterative procedure. The plot is in the  $D^*$ - $V^*$  format (equivalent SDOF system displacement and base shear) and the four distinct pushover curves correspond to the crossed possibilities of load pattern and reference node.

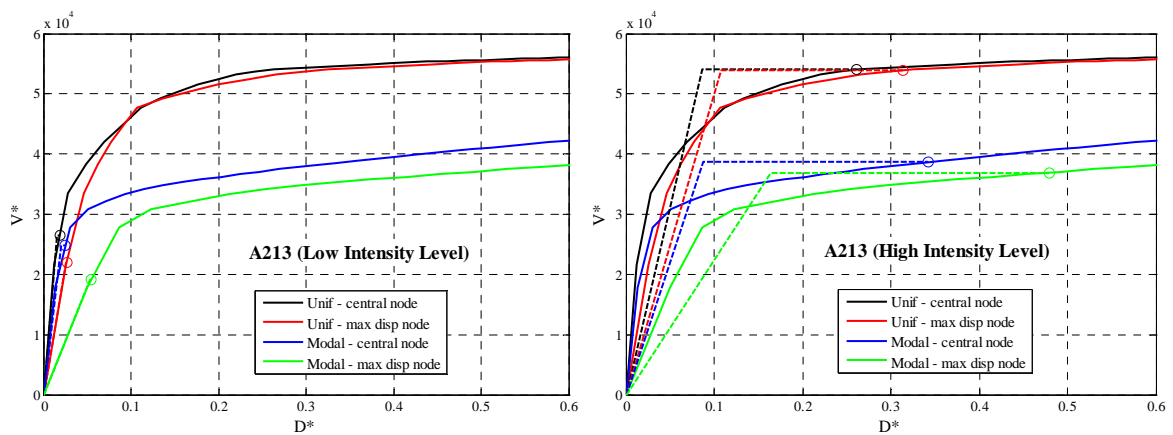


Figure 5.12 – N2 performance points for bridge A213: low and high intensity levels.

The SDOF system bilinear elasto-plastic curves are plotted in order to highlight the differences coming from the possible versions and, for both intensity levels, the divergence is evident, especially for what concerns the modal pattern. The significance of the reference node seems, in turn, to be lower, something that will surely be more visible in the index results that are presented next.

Figure 5.13 and Figure 5.14 show values of Bridge Index and Standard Deviation, for each intensity level, considering the entire set of bridges.

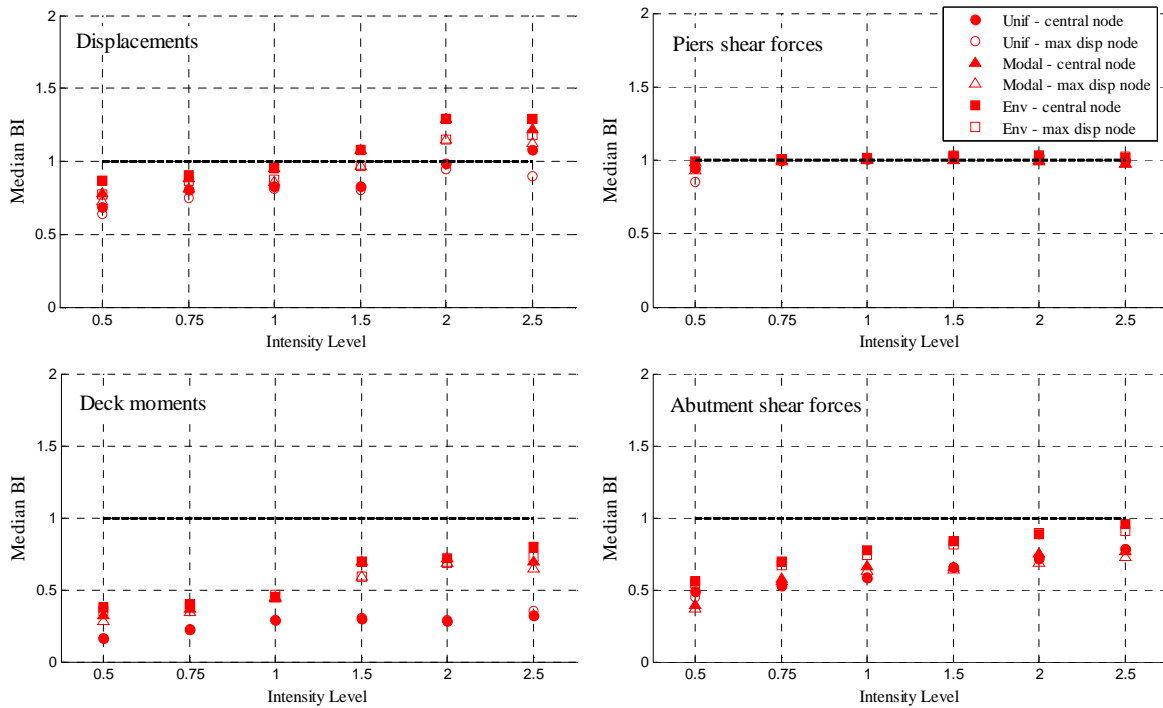


Figure 5.13 – N2 median Bridge Index (BI) per intensity level.

From the evaluation of vertical distances in BI plots, the observation that immediately stands out is that dispersion among different variants of the method is not particularly high, except for the deck bending moments. Indeed, whereas in the estimation of shear forces the differences between the employment of uniform or first mode proportional load distribution does not influence the results much, when deck displacements or moments are considered instead the influence of pushover load shape is noticeable (and not always in the same direction, which somehow explains why EC8 does not recommend the use of one loading shape over the other). The use of the maximum modal displacement node as reference yields, in general, worse results than the central node ones. The envelope shape, on the other hand, seems to somehow “contain” the positive aspects of the two EC8-recommended distributions, leading to better BI results throughout all response parameters.

There is a generalized heavy underestimating trend for deck moments and abutments shears, regardless the considered variant, for all the intensity levels, and for deck displacements for lower nonlinearity. Deck displacements and piers shear forces estimates are, therefore, considerably more reliable. Regarding behaviour of predictions with the increase in intensity level, highly nonlinear stages seem to improve the accuracy of deck

moments and abutment shear results (even if not sufficiently) and lead to slight overestimation of deck displacements.

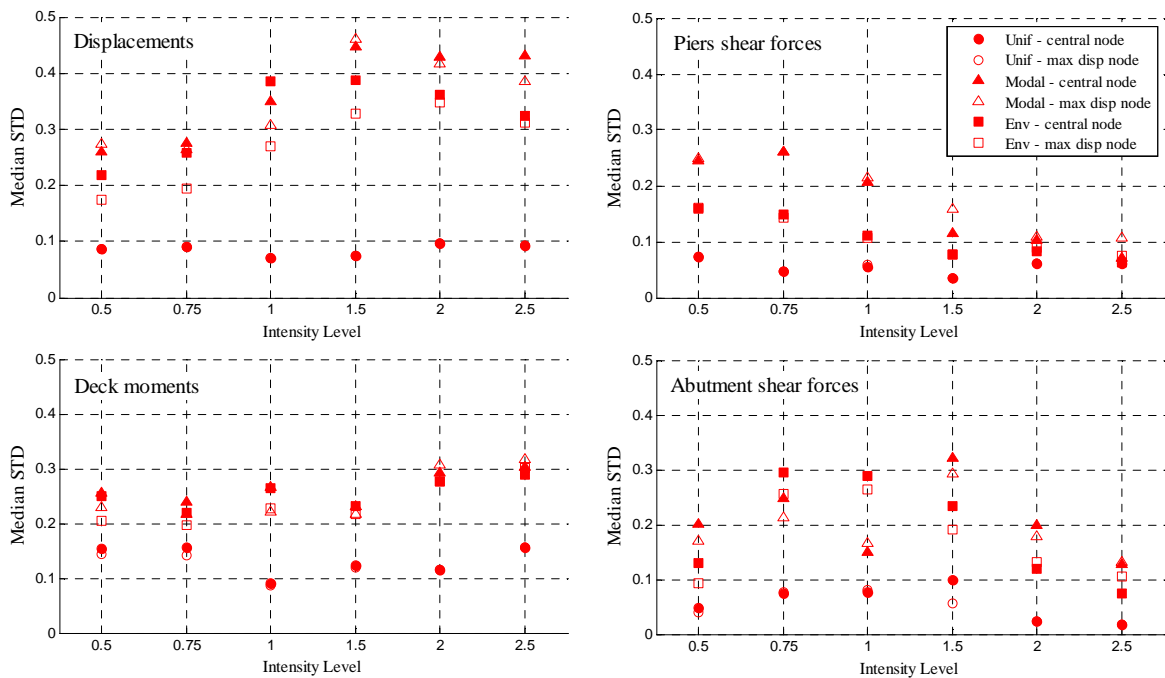


Figure 5.14 – N2 median Standard Deviation (STD) per intensity level.

Together with the scatter within variants of the procedure, the dispersion with respect to the median BI results may be evaluated making use of STD plots. Figure 5.14 shows that dispersion levels are higher for deck displacements, with respect to the other parameters, reaching maximum values of 0.4, substantiating the trend of better BI estimates associated to higher scatter. On the other hand, shear forces at the abutments and deck bending moments usually do not go beyond standard deviations of 0.3 and pier shears of 0.25. With respect to the different variants, the use of the 1<sup>st</sup> mode proportional load pattern results in higher scatter while the opposite trend is precisely found for the uniform load shape. The envelope technique is expectedly in between the two of them, presenting intermediate STD quantities. The difference between the two reference node possibilities is not so obvious, although a tendency for lower dispersion to be associated to the maximum modal displacement node might be found. Again the connection between good BIs and higher STDs seems to stand. No great influence of the seismic intensity on the dispersion occurs, despite a soft increase for displacements and bending moments and the reverse in shear forces.

Figure 5.15 presents BI results in line with bridge configuration, which allows a better understanding of the origin the dispersion.

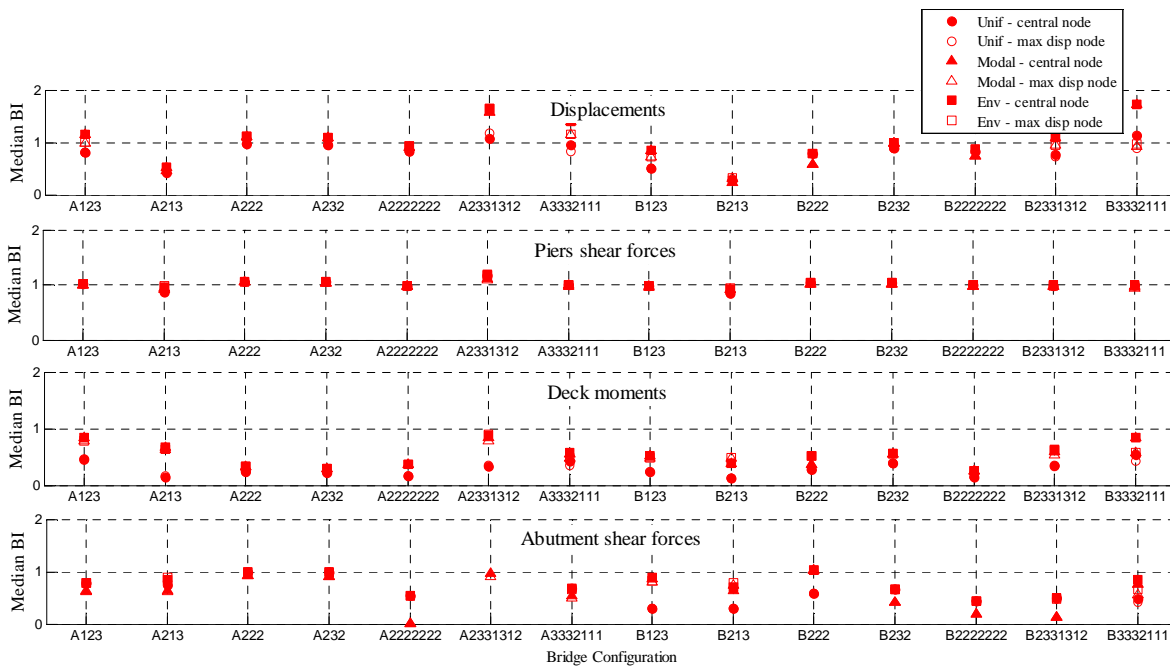


Figure 5.15 – N2 median Bridge Index (BI) per bridge configuration.

In fact, the N2 method may be considered as typically expected behaving NSP, in the sense that estimates are substantially better for the case of regular configurations, 222, 232 and 2222222, throughout all the parameters but particularly for displacements. Within each structural type, even if more visible for regular ones, the difference between the approaches is not so relevant, a pertinent fact denoting that the scatter comes more from the different configurations rather than the different versions of the procedure. Nevertheless, estimates for irregular configurations, whether in underestimating or overestimating fashion, are not completely unacceptable. No significant difference is found between long or short bridges, apart from slightly less underestimation in the latter.

In agreement with the main conclusions herein drawn, the use of the deck’s central node as reference point leads to better predictions hence this will be adopted on subsequent applications, together with the envelope pushover loading shape.

### 5.4.2.3 Modal Pushover Analysis

Figure 5.16 shows the different performance points, yielded by the MPA, for the chosen A213 configuration, two intensity levels, low and high, at the end of each of the modal analysis. For the selected bridge, the first and second modes only have been considered relevant. In the end, the quantities will be SRSS combined. The plots are in the Displacement-Force format (equivalent SDOF system displacement and base shear) and the two distinct pushover curves correspond to the two reference node location possibilities.

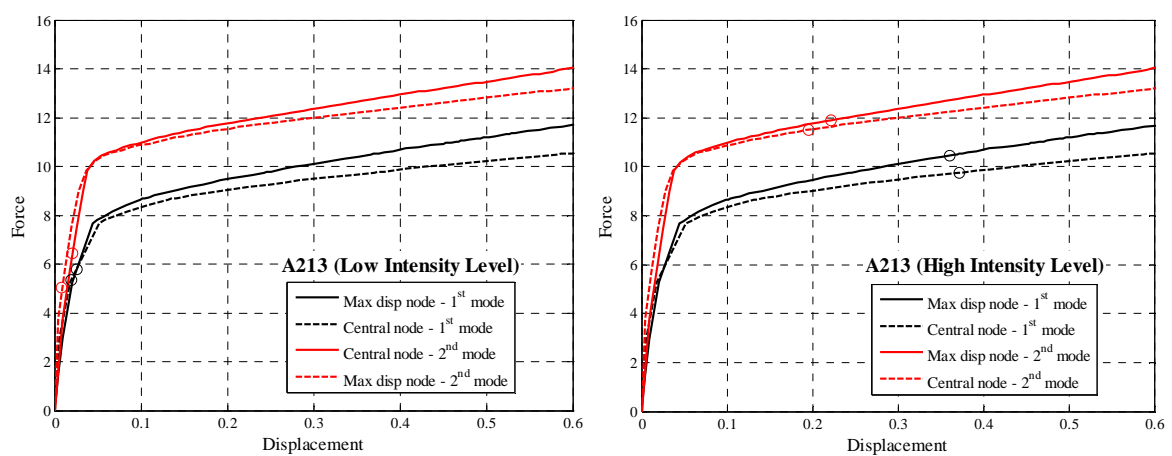


Figure 5.16 – MPA performance points for bridge A213: low and high intensity levels.

Modal Pushover Analysis has been taken as dependent on the reference node location only and the main observation that can be made is that the influence is slight. For both intensity levels the difference in the performance points is minimal, especially for the first mode, even though the pushover curves corresponding to different reference nodes are equally distant for both vibration modes.

Figure 5.17 and Figure 5.18 show values of median Bridge Index and Standard Deviation for each intensity level, concerning the entire set of bridges.

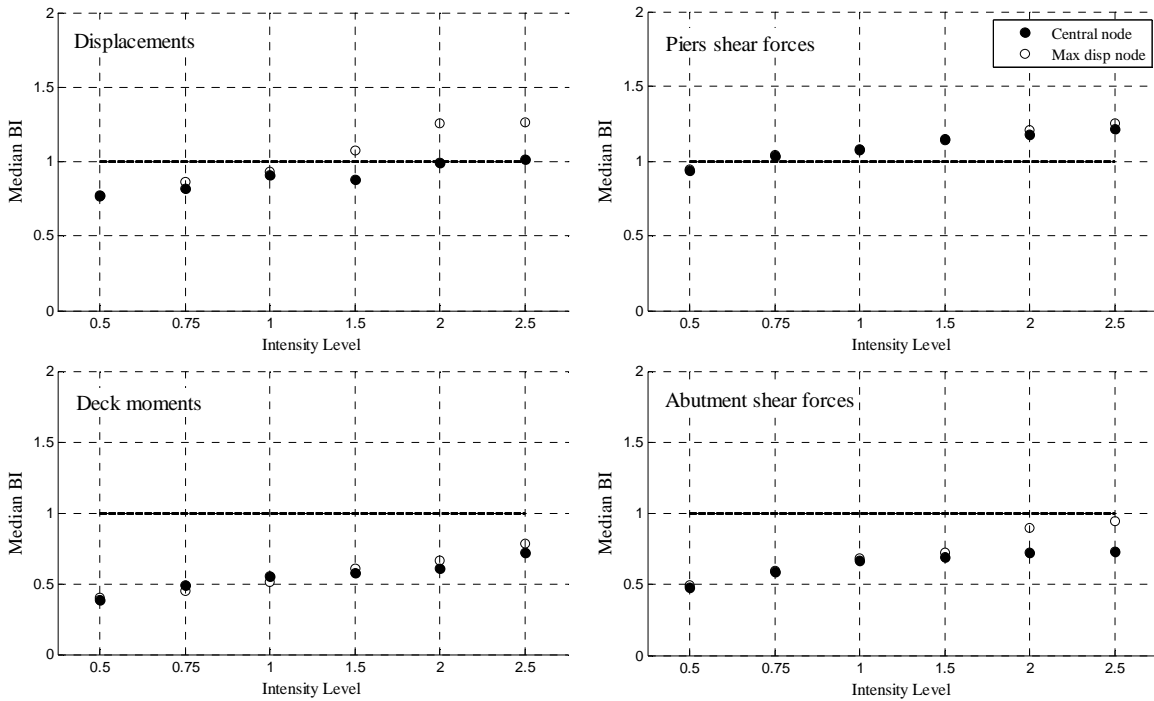


Figure 5.17 – MPA median Bridge Index (BI) per intensity level.

The global picture for the results of this method is not much different from what has been seen in the other procedures: deck displacements and shear forces at the piers are better captured, leading to BIs closer to unit with respect to deck bending moments and shear forces in the abutments, which are underestimated for all the intensity levels, heavily for the lower ones. For the two mentioned better estimated parameters, the centre of mass of the deck as reference seems to work better, given that the use of the maximum displacement node as reference typically overestimates NDA results. The general tendency is that one, indeed, to have increasing predictions as seismic input intensity increases. In fact, contrarily to what has been observed in other procedures, overestimation of shear forces at the piers occurs for higher intensity, which may indicate an exaggerated effect of the modal combination that is carried out. Furthermore, the estimates of deck bending moments and shear at the abutments are poor, independently from the reference node location of seismic intensity.

Looking at scatter of results in terms of dispersion relatively to the median BI, again, lower STDs are encountered for generalized shear predictions (modest 0.1 or less), whereas the deck displacements and bending moments predictions are associated to standard deviations of 0.2 or 0.25. The distinction in terms of reference node type is not immediately visible,

although the use of maximum displacement node as reference is affected by larger scatter. Such output is constant and no surprises arise when the structures step in nonlinear behaviour. No significant pattern is identified with the changes in nonlinearity. Higher intensity levels do not necessarily yield higher dispersion.

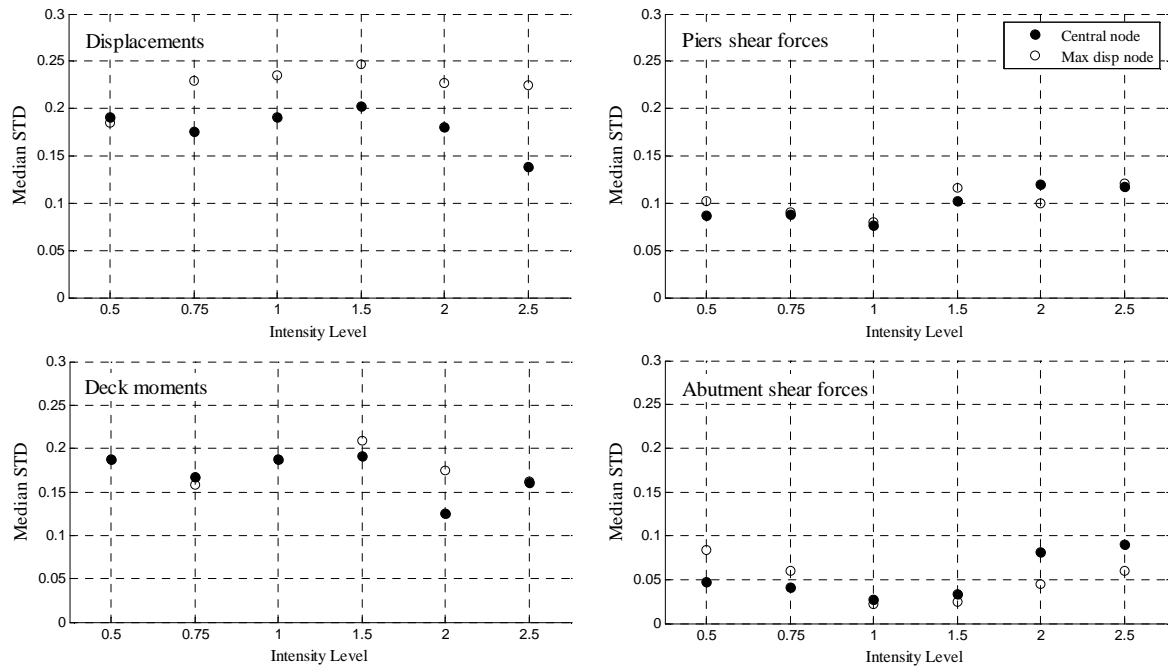


Figure 5.18 – MPA median Standard Deviation (STD) per intensity level.

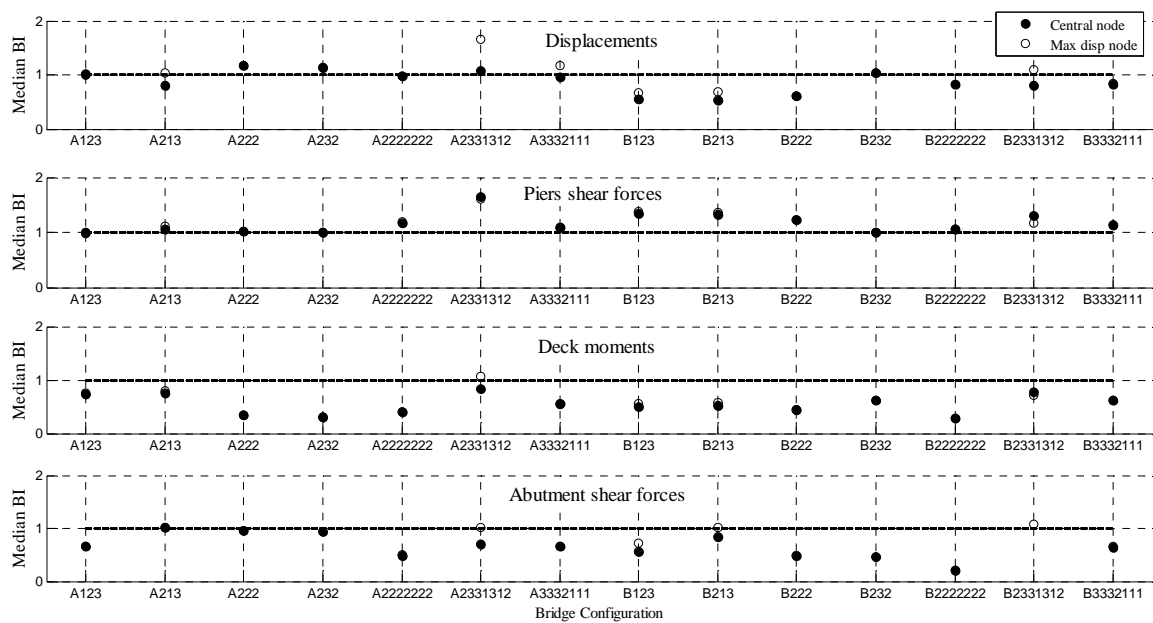


Figure 5.19 – MPA median Bridge Index (BI) per bridge configuration.

MPA results in terms of bridge configuration are not straightforward to interpret, given their apparent irregularity or somewhat absence of rule, as showed by Figure 5.19. The first impression, when looking at displacements, is that the choice for a reference node is not obvious: whilst for the majority of the bridges, the central is preferable, for some others, the maximum modal displacement node stands out. With respect to type of abutments, the performance of type-B abutment bridges seems definitely to be less well captured, especially for the regular ones. The overestimation found for shear forces at the piers comes from the long type-A bridges and the type-B ones. The deck bending moments estimates are generally poor and the same stands for abutments shear, where the procedure behaves quite inferiorly for long configurations.

On subsequent applications of the method, based on the intensity level results, the centre of mass of the deck reference node modality was adopted.

#### 5.4.2.4 Adaptive Capacity Spectrum Method

ACSM exposure of results will exceptionally feature the global representation plots, in order to provide higher clearness, as well as additional useful criteria, to the analysis of the eleven versions. Figure 5.20 shows the graphical results for the performance points corresponding to the different possible spectral reductions, at the end of the iterative procedure for the configuration A213, at low and high intensity levels.

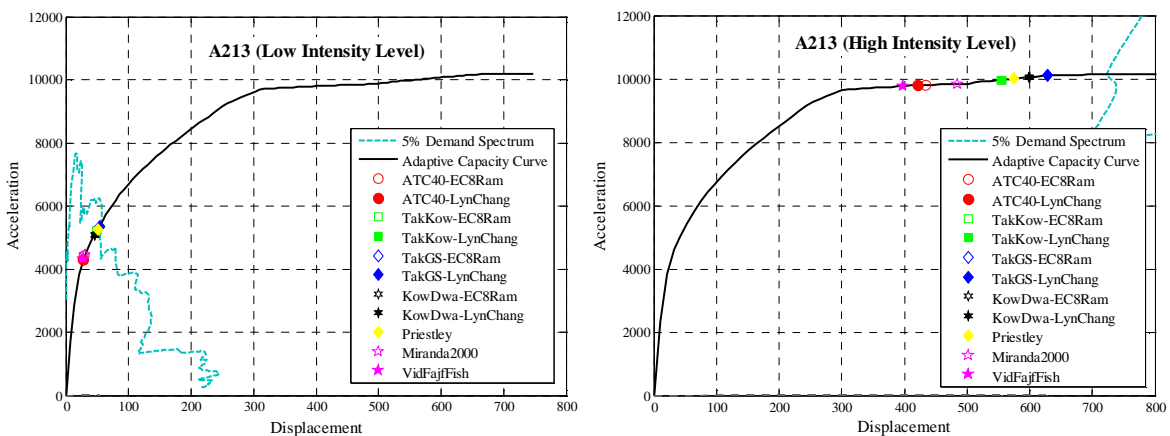


Figure 5.20 – ACSM performance points for bridge A213: low and high intensity levels.

The plots are in the ADRS format (Acceleration Displacement Response Spectrum) and contain one single pushover/capacity curve, the adaptive, the original response/demand



spectrum for 5% damping and eleven performance points, coming from the intersection of each reduced response spectrum, not plotted for the sake of simplicity, with the capacity curve.

For the low intensity level no relevant hysteric damping and energy dissipation are expected, which becomes clear from the concentration of performance points near the intersection with elastic response spectra. Nevertheless, some approaches, ATC-40 and ductility based ones, present already considerable reduction, which corresponds to higher prediction for equivalent viscous damping (elastic plus hysteretic). For higher nonlinearity levels, even if not so obvious, the same distinction is observed.

Figure 5.21 represents graphically the global median BI values and Figure 5.22 the corresponding STDs, both referring to each spectrum scaling modality.

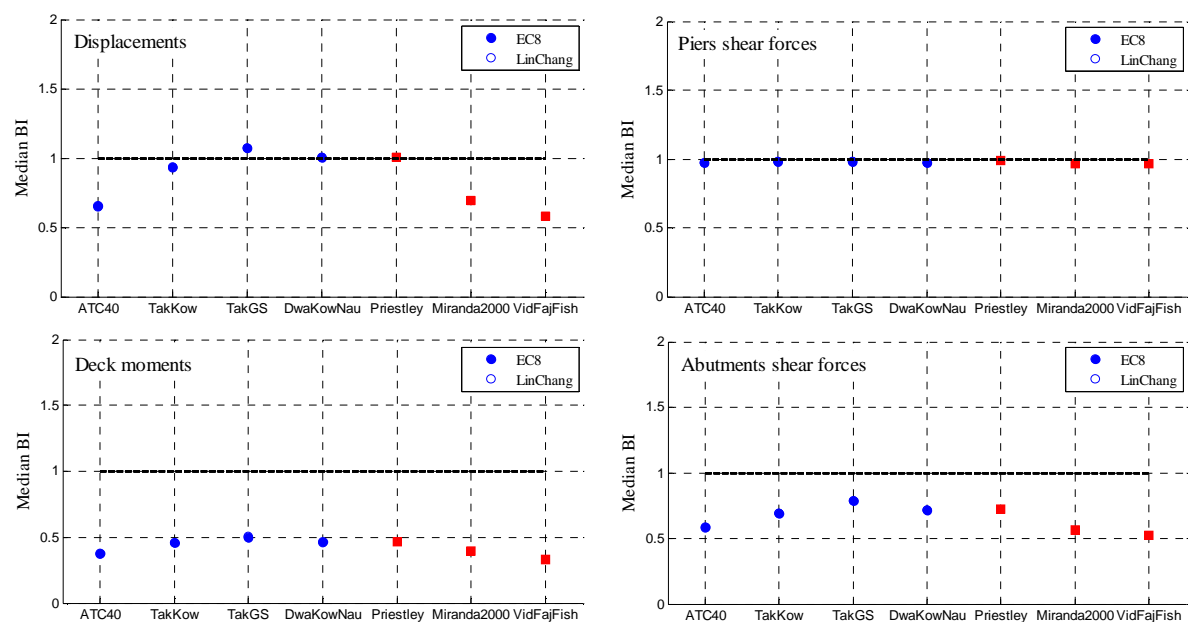


Figure 5.21 – ACSM global median Bridge Index (BI).

Considering the results shown, the first conclusion is that it is the employed damping model, rather than the chosen damping-dependent spectral reduction equation, that conditions the results; there is essentially no visible difference between LinChang and EC8Ram results. Generally, it seems that the approaches TakKow, DwaKowNau and Priestley lead to the best global indexes, especially for what displacements are concerned, where major differences are found, with a global median BI fairly close to one and global median STD, around 0.15, that is not excessive. On the other hand, the two ductility-based

approaches (Mir2000 and VidFajFish) and the damping-based ATC-40 method show the worst results when compared to nonlinear dynamic analyses. This trend seems to contradict opposite results, found in previous studies (Bertero *et al.*, 1991; Bertero, 1995; Reinhorn, 1997; Chopra and Goel, 1999; Fajfar, 1999, 2000), which state that inelastic spectra-based methods yield better results with respect to their elastic highly-damped counterparts. However, such findings come from the use of a different NSP from the Adaptive Capacity Spectrum Method (ACSM), which, within the elastic highly-damped methods, is expected to yield more consistent results in the assessment of the seismic response of bridges (Pinho *et al.*, 2007; Pinho *et al.*, 2009) when compared to other NSPs, and this may explain the difference.

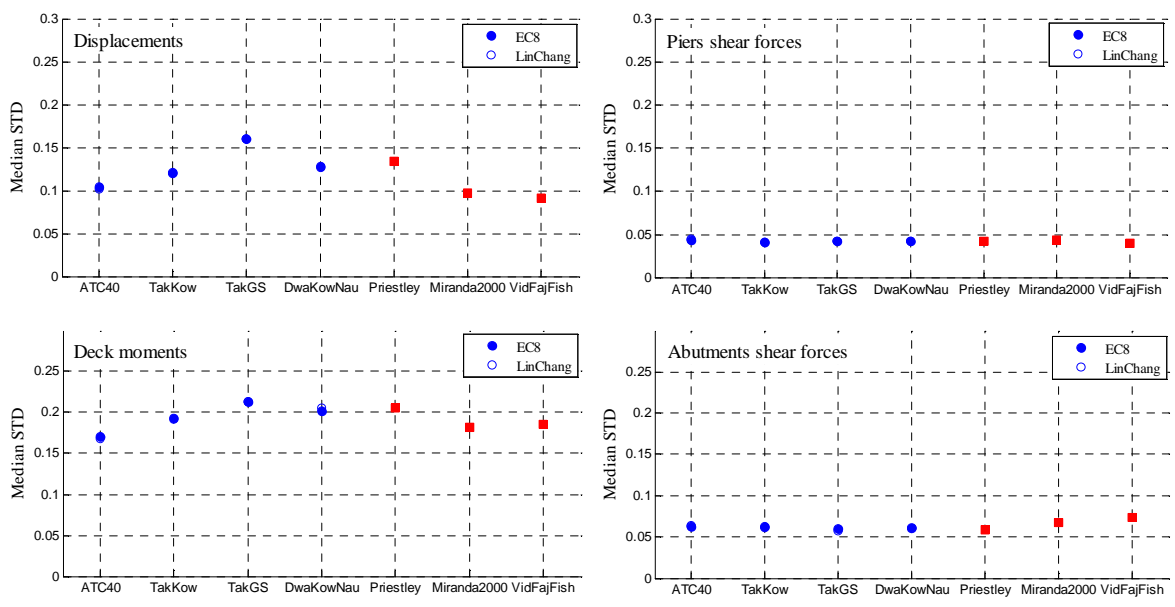


Figure 5.22 – ACSM global median Standard Deviation (STD).

The underpredicting trend of ATC-40 is probably due to the well known overprediction that such approach carries out within the equivalent damping estimation in structures which will not exactly exhibit elastoplastic behaviour.

Similar tendency is found when ductility based reduction factors are used. Mir2000 approach has been primarily developed for elastoplastic behaviour but has also been widely verified for other models such as Takeda or Clough, proving to work well for periods longer than 1.2 seconds, which is not the case of the considered bridge structures with maximum periods of about 0.8 seconds. One would therefore expect overprediction,

as found by Miranda and Ruiz Garcia (2002) for short periods. However, the low ductility levels achieved for the considered bridge (see Figure 5.23) structures have lead to barely unitary displacement modification factors. VidFajFish approach, on the other hand, is known to be highly dependent on period and ductility for the short period region, which may apply to the selected bridge structures; for this region, the R factor increases linearly with increasing period, remaining constant for the rest of the periods, which may cause some excessive reduction, and, hence, underprediction, given that periods tend to be low, as early stated, for this sort of structures.

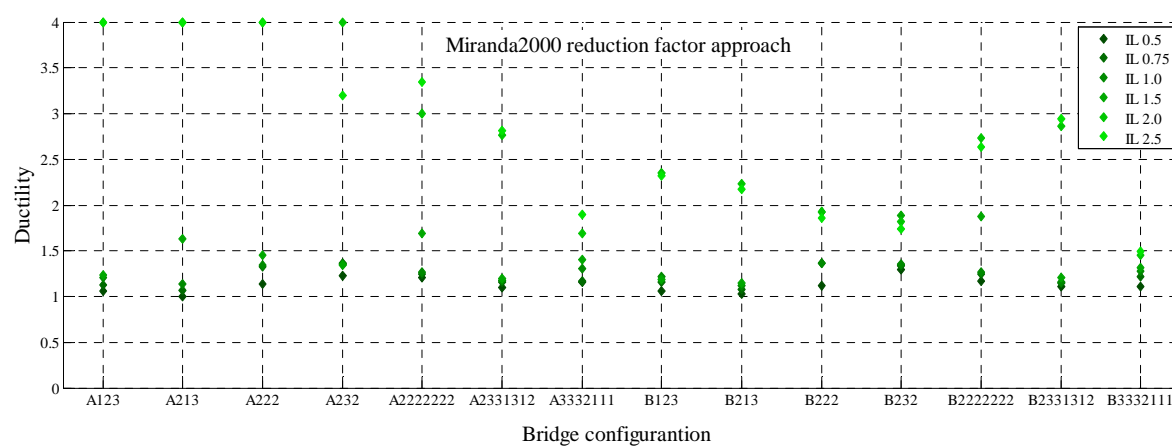


Figure 5.23 – Ductility level achieved using Miranda2000 reduction factor approach.

The Gulkan and Sozen approach, based on the Takeda hysteretic model, is overpredicting displacements. According to Equation (5.5) and Figure 5.3, it is the one with lowest equivalent damping prediction, among all the approaches, for ductility levels not higher than approximately 3. Adding to this the fact that most cases of application correspond to ductility levels equally distributed between 1 and 3, (Figure 5.24 and Figure 5.25) one may explain the overprediction by the underestimation of damping-based energy dissipation.

The superiority found when using TakKow, DwaKowNau or Priestley approaches is firstly, in opposite to the others, due to the intermediate nature on estimating the equivalent viscous damping. Additionally, the latter two, which are the most recent, have been particularly developed and therefore, more suitable, to the structural behaviour where bridges fit in. DwaKowNau's equation, for instance, depends on the effective period which is another advantage, whereas Priestley's expression refers exactly to bridge piers.

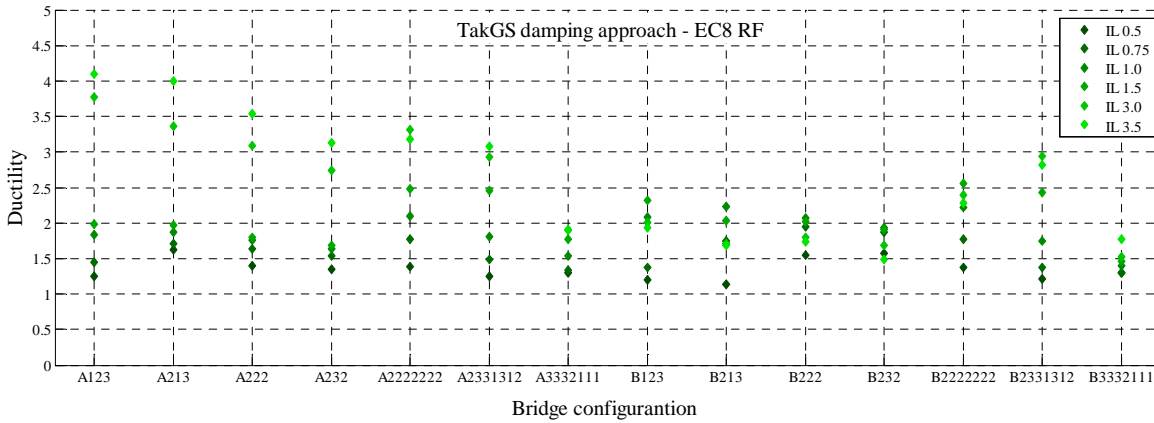


Figure 5.24 – Ductility level achieved using TakGS damping approach and EC8 reduction factor.

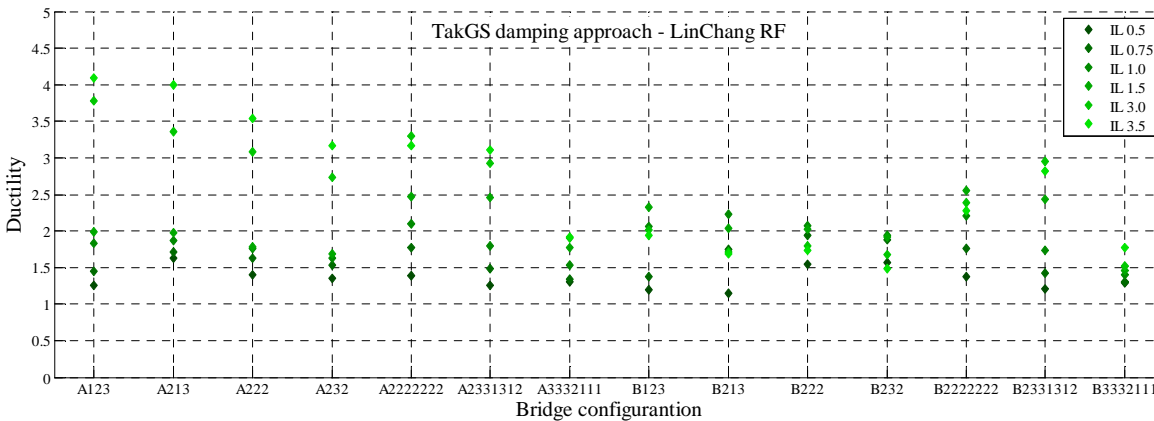


Figure 5.25 – Ductility level achieved using TakGS damping approach and LinChang reduction factor.

As far as the type of parameter is concerned, there is high coherence of results within different variants for shear forces at piers whereas the main differences come from the rest of parameters. A general heavy underestimating trend may be again observed for the deck bending moments and abutments shear. Dispersion levels are rather low for shear predictions (and independent of the reduction factor model) and higher for the deck engineering demand parameters, with maximum STDs of 0.2 or 0.15 for deck bending moments or displacements. Shear force predictions are associated to version-independent low scatter without relevant accuracy loss.

All global observations care for scrutiny and, therefore, Figure 5.26 shows, at each intensity level, the median Bridge Index over the 14 bridge configurations. Given that no relevant difference has been found between EC8 and LinChang spectral reduction factors,

for the subsequent plots, and for the sake of simplicity, only the EC8-employed RF version of each ACSM variant has been represented.

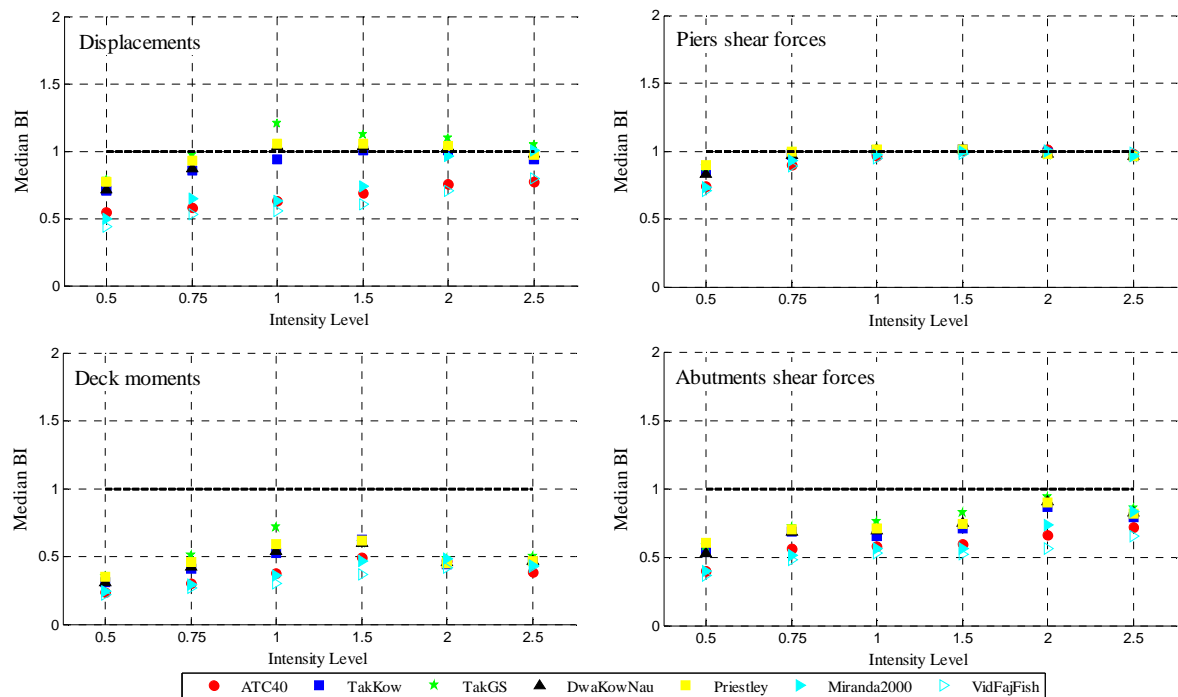


Figure 5.26 – ACSM median Bridge Index (BI) per intensity level.

Observing this new set of results, it turns out apparent that amongst the three approaches previously mentioned to be performing superiorly, the one proposed by Priestley *et al.* (2007) seems to be slightly better, even if only marginally, very closely followed by that of Dwairi *et al.* (2007). Such superiority is more evident for deck displacements, deck bending moments and shear at the abutments. Dwairi *et al.* approach seems then to introduce a not relevant dependency of the coefficient  $C_{ST}$  on the effective period. In addition, it is also noted that there is a general tendency for the displacements and shear forces predictions to improve with increasing intensity level, probably due to the fact that for low levels of nonlinearity, thus dissipation, current damping and RF relationships overestimate the reduction. For the case of piers shear forces dependence on spectral reduction approach is practically inexistent. As expected (see Figure 5.21), ATC-40 damping model seems to overestimate damping, leading to underestimated displacements at each intensity level.

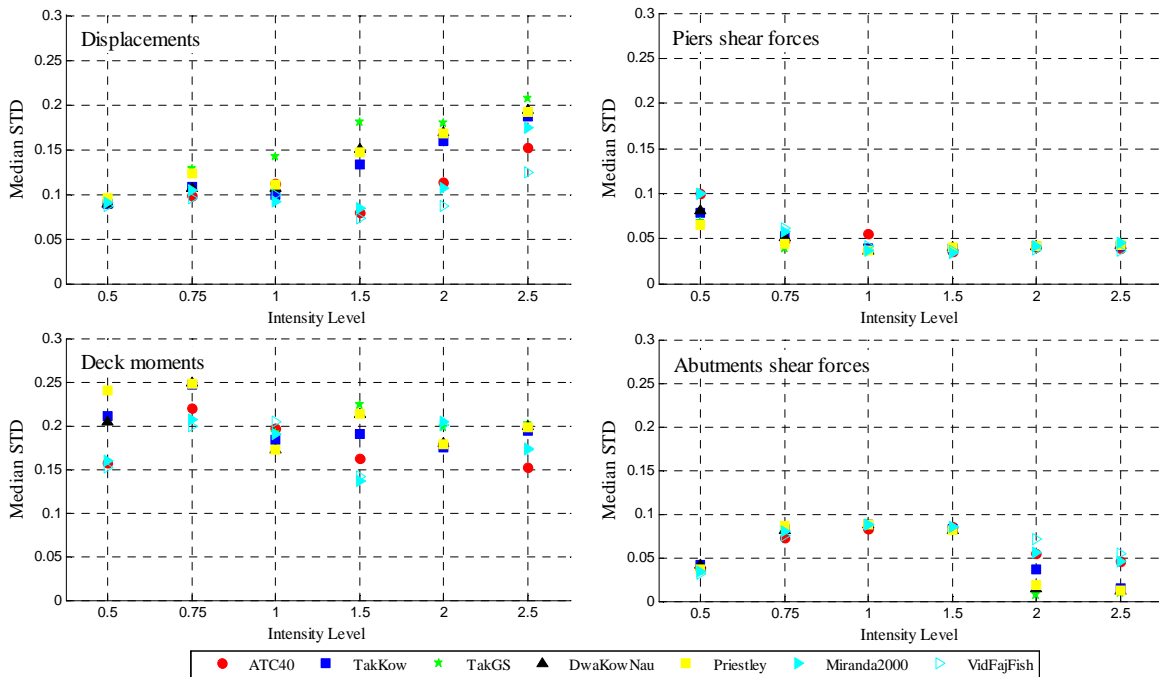


Figure 5.27 – ACSM median Standard Deviation (STD) per intensity level.

As for the standard deviation, Figure 5.27, this did increase with growing intensity, for the case of deck displacements, to nearly twice the initial one. The differences between variants arise for deck displacements and bending moments only and again, generally, the worst modalities predicting Bridge Index, ATC-40 and ductility-based ones, have lower, but not considerably different, dispersion levels. In other words, the higher scatter associated to Priestley’s approach, or even very similar TakKow and DwaKowNau, does not seem to compromise the better median BI estimates. Shear predictions, whether at the piers or abutments level, stand for the lowest scatter levels, barely reaching 0.1.

Figure 5.28 shows the median BI across all intensity levels, for each bridge configuration. The response predictions do not appear to be very bridge-dependent, and the observations/conclusions previously drawn hold for the majority of configurations; e.g., the Priestley approach consistently leads to the closest-to-unity BIs. It is also observed that major variations in the predictions, according to the different variants, occur for irregular, long bridges. Notwithstanding such variation, the displacements and shear forces at the piers are fairly well predicted, whilst deck moments and abutments shear forces estimates are invariantly poor. BI ratios are better in the case of regular bridge configurations and there is smaller dispersion with respect to the spectral reduction approach. An overestimating trend for short bridges and underestimating for longer ones can also be

observed, with the latter cases leading also to larger scatter. These observations generally stand for all the engineering demand parameters herein considered.

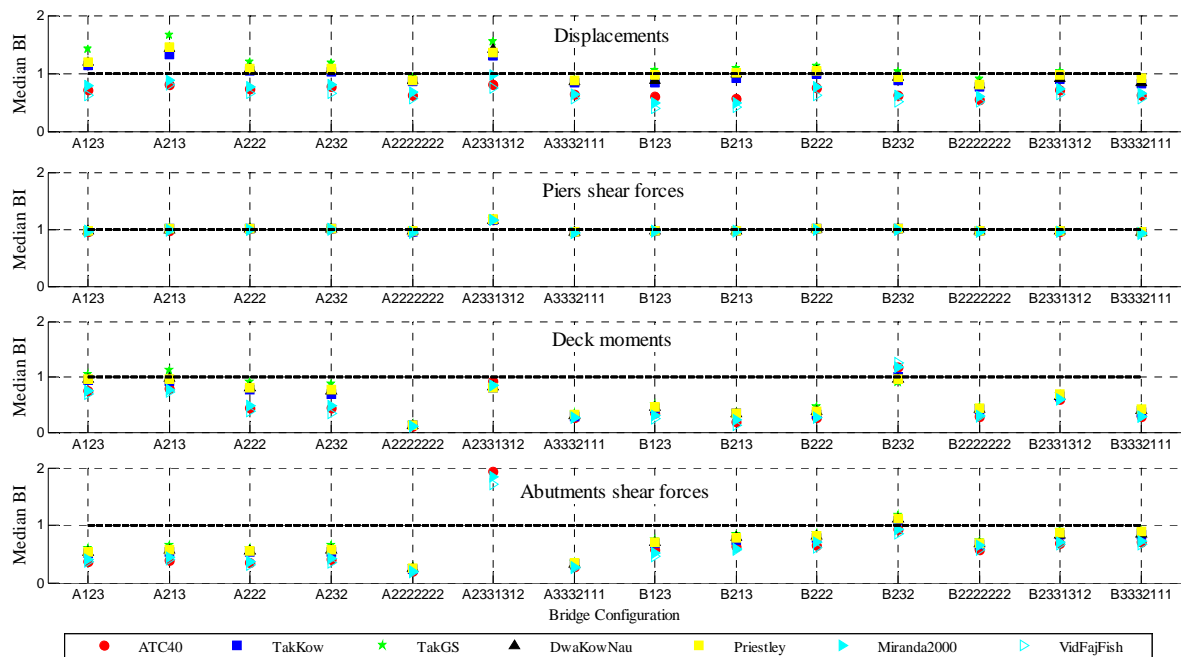


Figure 5.28 – ACSM median Standard Deviation (STD) per intensity level.

### 5.4.3 Comparative study results

Having identified the “optimum configuration” of all NSPs considered here, it is now possible to proceed with the parametric comparison of the four approaches, with the purpose of emphasizing relative advantages and disadvantages and, eventually, coming up with suggestions for possible preferred choices, if any. The study is again carried out on the basis of Bridge Index and Standard Deviation comparison, starting from the somewhat global perspective, where the entire set of results (for all bridges and for all intensity levels) are first considered together, and then sub-structured in terms of seismic input intensity and bridge model.

#### 5.4.3.1 Global results

Recalling Section 5.4.1, a global results overview consists in the computation of the bridge index per NSP over all the 14 bridges and 6 intensity levels and is extremely useful, since it provides a general picture of the results, enabling an easier interpretation if the choice for one of the procedures is intended. This representation of results caters for (i) comparison

with dynamic analyses (it is recalled that BI represents the ratio between NSP and NDA results), (ii) relative comparison of the accuracy of the different NSPs, and (iii) appreciation of the results dispersion (plots include overall median BI for every method, in filled markers, and mean BI  $\pm$  mean STD error bars).

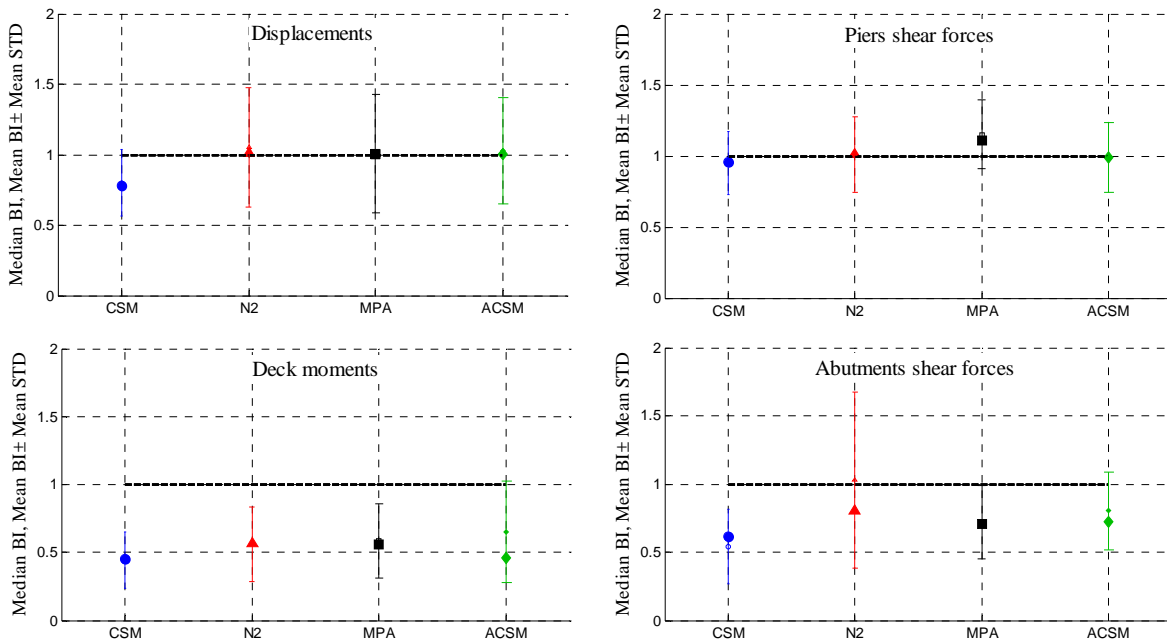


Figure 5.29 – Global Bridge Index and Standard Deviation.

From the observation of Figure 5.29, it is conspicuous that all nonlinear static procedures, with the exception of Capacity Spectrum Method, are able to predict displacement response with effectively good accuracy, evidencing also reasonable dispersion levels. The traditional CSM underpredicts the NDA estimates, whereas N2 and the more recent approaches, MPA and ACSM, yield global median unitary ratios, bearing an increase in the scatter to do so, though. Shear forces at the piers are accurately estimated by all procedures, despite a slight overprediction of MPA, coupled with highly satisfying standard deviation. On the contrary, deck moments, mostly, and shear forces at the abutments are underestimated in relatively heavy fashion by all methods, even if the scatter levels are relatively low. Still, the inferiority of CSM stands. Regarding dispersion levels, the observed tendency is to have low scatter in deck bending moments and shear force predictions (maximum values of 0.5) except for N2, which has approximately the double of that value. Higher STD values are obtained when predicting displacement. N2 may be considered, in most of the situations, the method with the highest dispersion levels, whilst



the opposite part is somewhat assumed by CSM. Another interesting observation is the fact that, if global mean indexes had been computed, there would have been some slight improvement, particularly for ACSM.

#### 5.4.3.2 Intensity level results

At each intensity level, the median Bridge Index over the 14 bridge configurations is computed for each of the four NSPs (see Figure 5.30). The results not only confirm the observations made in the previous section, but also add some insight on how these may be influenced by the intensity of the input motion.

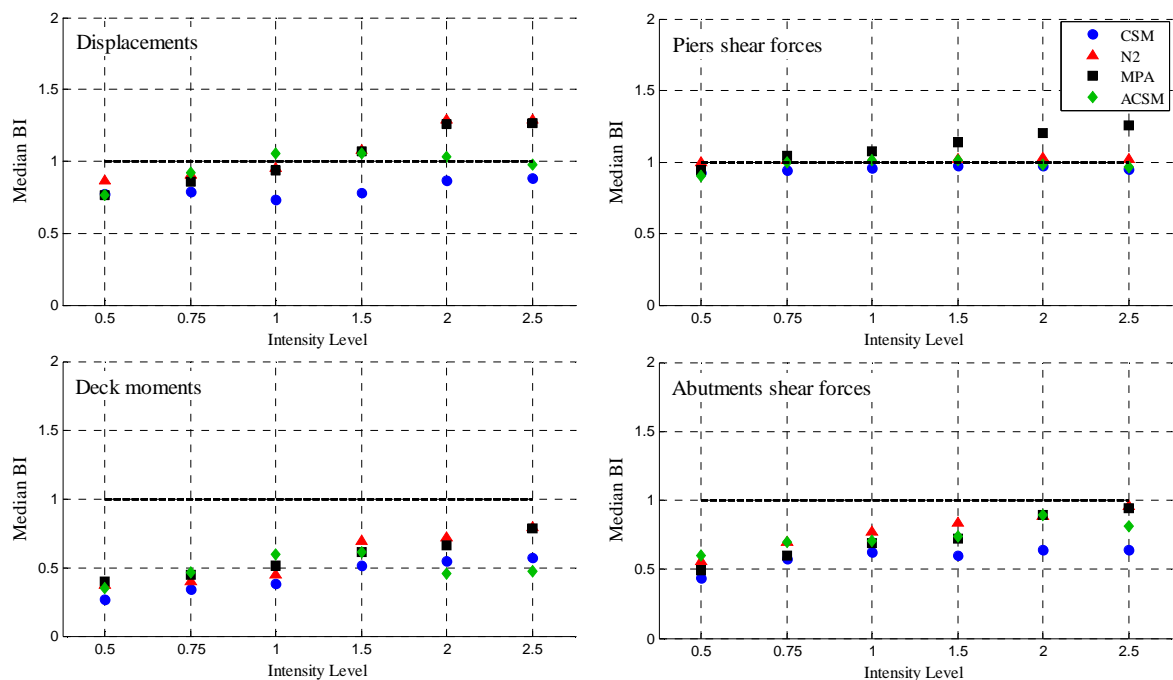


Figure 5.30 – Median Bridge Index per intensity level.

When global indexes showed, in Figure 5.25, a large similarity between the four procedures, an intensity level results' overview will certainly clear out some changes in their behaviour, especially at high nonlinear stages. It is observed that important variations are observed in displacement response estimates, with slight underprediction at lower intensity levels, for all NSPs, evolving to overprediction at high intensity, for MPA and N2, underprediction for CSM, while ACSM manages to keep a steadier closeness to NDA results. These differences between the four methods may be justified with the fact that

major conceptual differences exist between them, such as the reference node choice or the use of an envelope of different displacement shapes for the case of N2.

Regarding shear forces, as the seismic intensity increases, the accuracy in the predictions at the bridge piers is constant, with the exception of MPA, which overestimates NDA results. This will probably have to do with overrated higher mode effects, which in turn become more important as the intensity of the seismic action increases (because the fundamental period elongates, hence its spectral amplification diminishes, increasing the relative importance of higher modes). Apart from a general global underestimating showed by CSM, the rest of the methods behave similarly. Some points of similarity can, however, be found between N2 and MPA or CSM and its adaptive version, given that both share ductility or damping based spectral reduction, respectively.

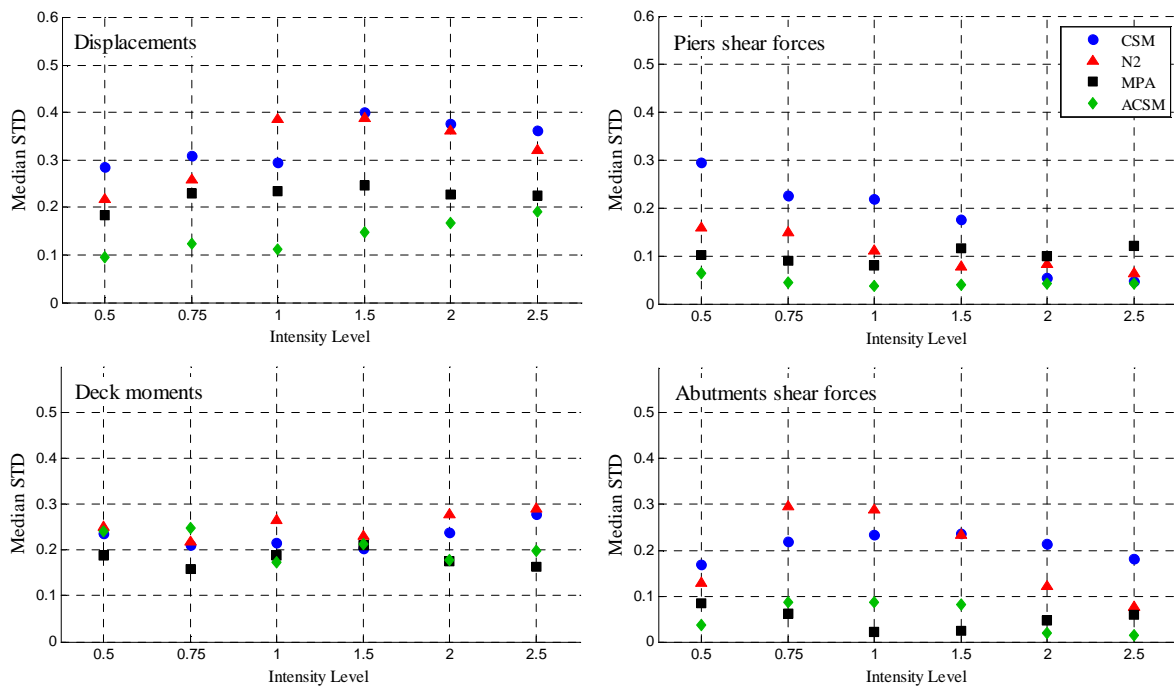


Figure 5.31 – Median Standard Deviation per intensity level.

For what concerns the dispersion of the results, this did not prove to be much dependent on intensity level. Indeed, global conclusions are confirmed by Figure 5.31, where STD levels oscillate in line with the nonlinear static procedure being employed, rather than the seismic intensity variation. Traditional methods, CSM and N2, yield the predictions with largest dispersion, reaching 0.4 for deck displacements and 0.3 for the other parameters, whereas

to MPA and ACSM correspond STDs of 0.2 or 0.1 for deck or shear quantities, respectively.

#### 5.4.3.3 Bridge configuration results

Herein, for each bridge configuration, the median Bridge Index and Standard Deviation across the 6 intensity levels is plotted considering each of the four nonlinear static procedures (see Figure 5.32 and Figure 5.33).

As expected, the response predictions do appear to be very bridge-dependent, even if the observations/conclusions previously drawn still hold for the majority of configurations. The best displacement response estimates (in terms of BIs being close to unity, and STDs being close to zero) are obtained for the regular bridge configurations (e.g., 222, 232 and 2222222), as one would expect, though good displacement estimates are also obtained for semi-regular and irregular bridges, especially if one considers results coming from higher modes considering procedures MPA and ACSM; this certainly constitutes good news for NSPs and their application to assessment of bridge response when the focus is on deformations.

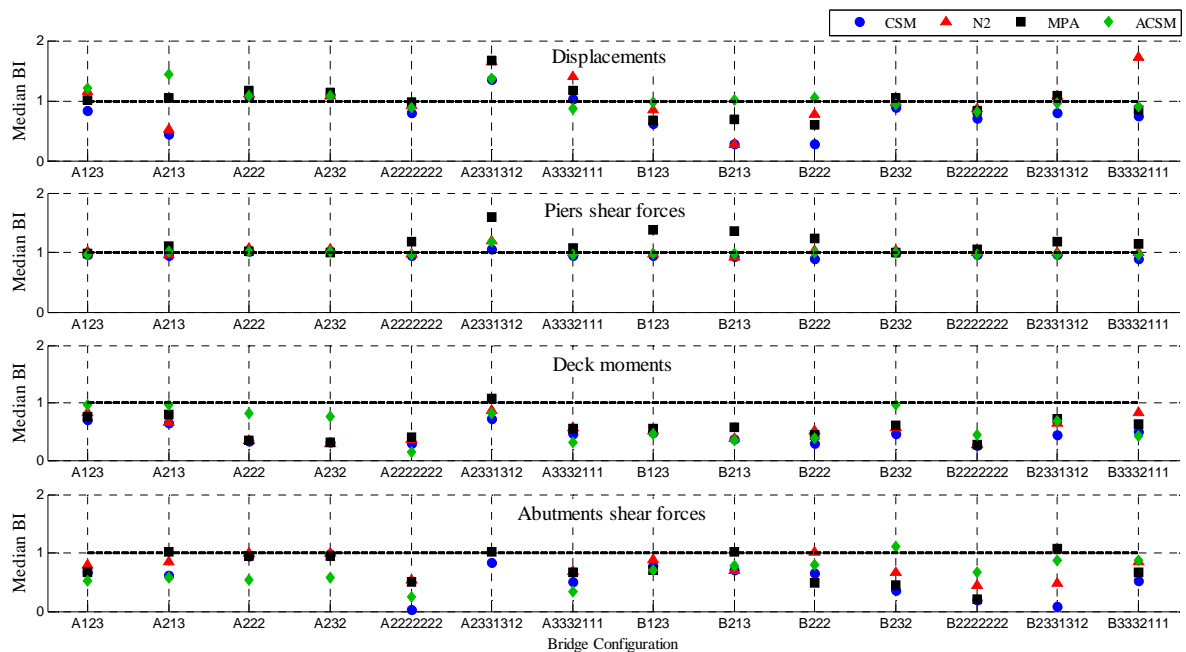


Figure 5.32 – Median Bridge Index per bridge configuration.

CSM and N2 are many times the most underpredicting ones. An overestimating trend for short bridges and an underestimating one for longer ones can also be observed in the results. The same gist, or maybe even more evident, may be encountered for the rest of parameters where, however, general underestimation occurs. The overestimation of MPA for the shear predictions at the piers occurs mostly for irregular and type-B abutments bridges.

The largest scatter is, in general, associated to both long and irregular bridges, an aspect that is extremely noticeable from the observation of Figure 5.33, mainly in displacements and abutments shear forces. As for the bridge sort of abutments, no relevant differences between bridges with abutments of type A (continuous deck-abutment connections) or type B (deck supported on linear pot bearings) is noticeable. Such finding stands for the abutments shear predictions, as well as for the remaining parameters.

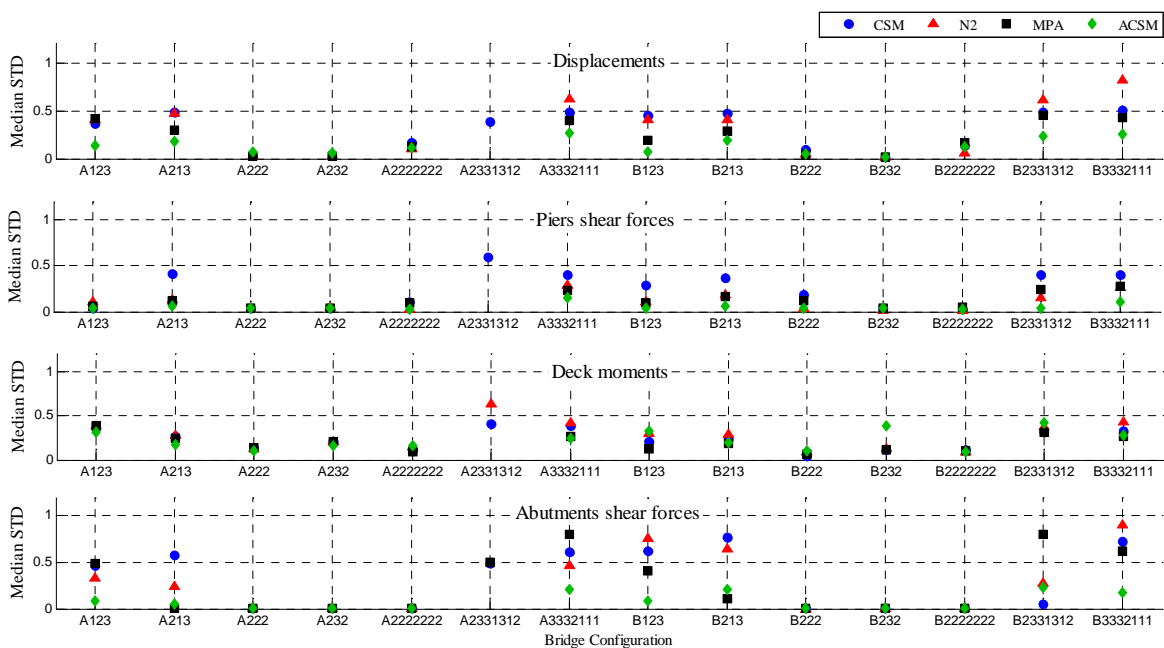


Figure 5.33 – Median Standard Deviation per bridge configuration.

The observation of results at a bridge configuration level enabled the recognition of the considerable variation that such extensive, statistical comparative study features. The use of global indexes is extremely useful to draw general conclusions but it does naturally mask the influence of the different structural characteristics. In order to investigate the extent of such influence, the results have been plotted again, in the global (Figure 5.34) and intensity level (Figure 5.35) fashion, filtering the configurations according to the different

categories: regular (REG), irregular (IRREG), short, long, type-A and type-B abutments. Given that shear forces at the piers have been estimated with high accuracy by all the procedures, across all the intensity levels and bridge configurations and heavily underestimated prediction were obtained for the deck moments and abutments shears, only the displacements predictions were scrutinized.

The individuation of the results in different categories shows, at first glance, that the variables that most affect the global predictions (and corresponding standard deviation) are the length of the bridge and the type of abutments, given that the distinction between regular and irregular configurations does not yield BIs significantly different from the results all together. Long configurations, which are certainly more affected by higher modes, are less well captured by CSM and N2 procedures. Furthermore, even if global median BI is not necessarily much worse, with respect to short configurations, such outcome corresponds to an extremely higher standard deviation. The same happens between regular and irregular configurations: the former feature more accurate predictions and, at the same time, much lower uncertainty, which certainly highlights its higher suitability to be analysed through the use of NSPs.

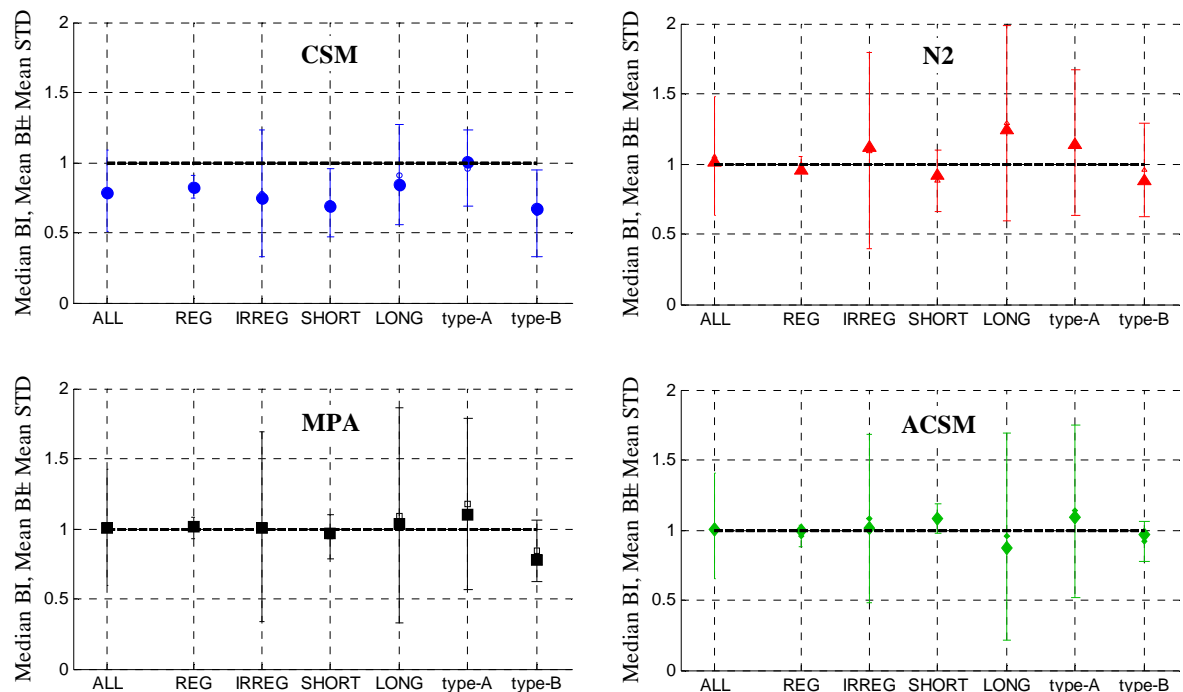


Figure 5.34 – Global Displacements Bridge Index and Standard Deviation according to bridge category.

Regarding the type of abutment, a constant trend throughout all the procedures could not be found although, generally, type-B abutments bridges are underpredicted together with lower corresponding STD.

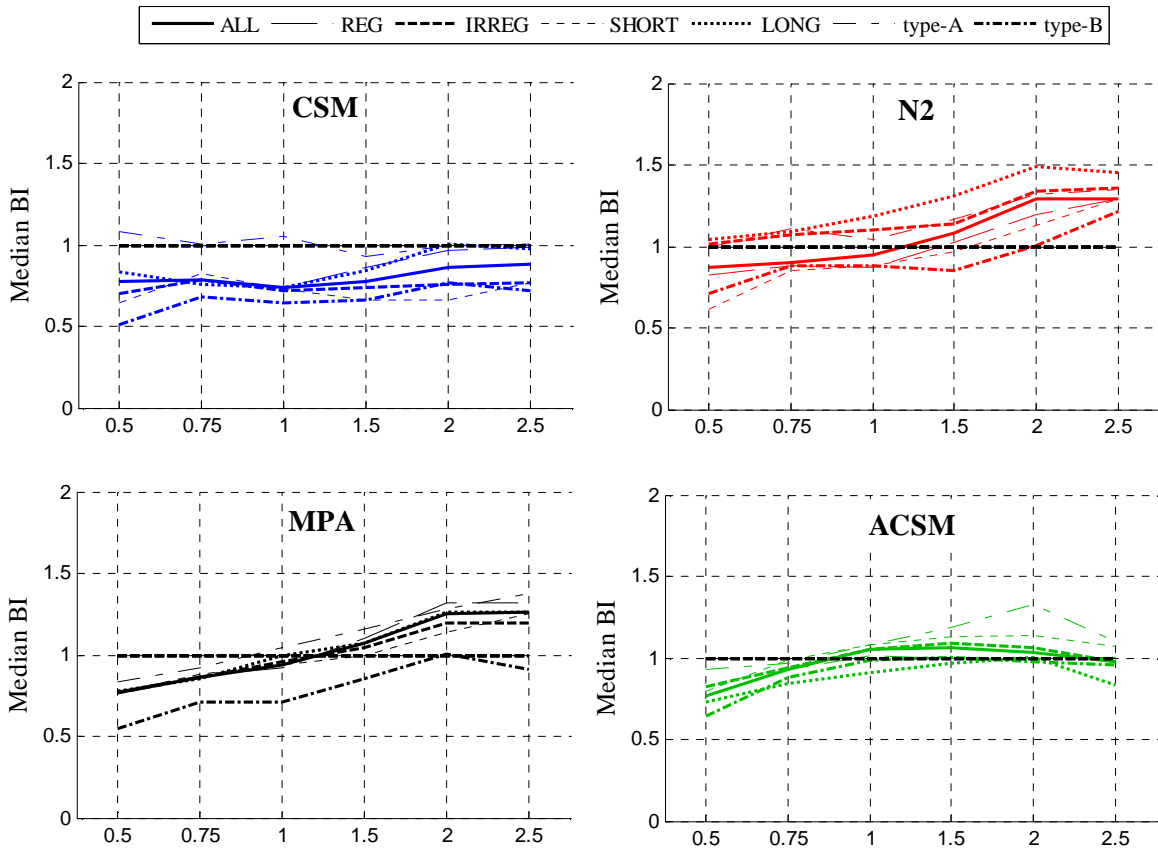


Figure 5.35 – Median Displacement Bridge Index per intensity level according to bridge category.

Another interesting conclusion, which is quite visible from Figure 5.35 as well, is the fact that classical procedures, CSM and N2, feature higher variation across intensity levels and bridge structural characteristics, with respect to recent, improved approaches, such as MPA and ACSM.

A different perspective is provided by Figure 5.36, in which results are compared, by NSP, side by side, in terms of the distinct defined characteristics: regularity, length and abutment type. The relevancy of each of the categories to the relative performance of the nonlinear static procedures becomes even more visible and, clearly, from a median point of view, rather than regularity, length and abutment type are the factors that influence the most the results (extremely higher scatter within results for irregular configurations should, however, be kept in mind). Indeed, depending on the type of bridges being taken into

account, the methods can move from under- to overestimation, which strengthens the importance of looking at the results from a category perspective. Another immediate observation is that it becomes even clearer that higher modes accounting NSPs, MPA and ACSM, perform superiorly than the other two.

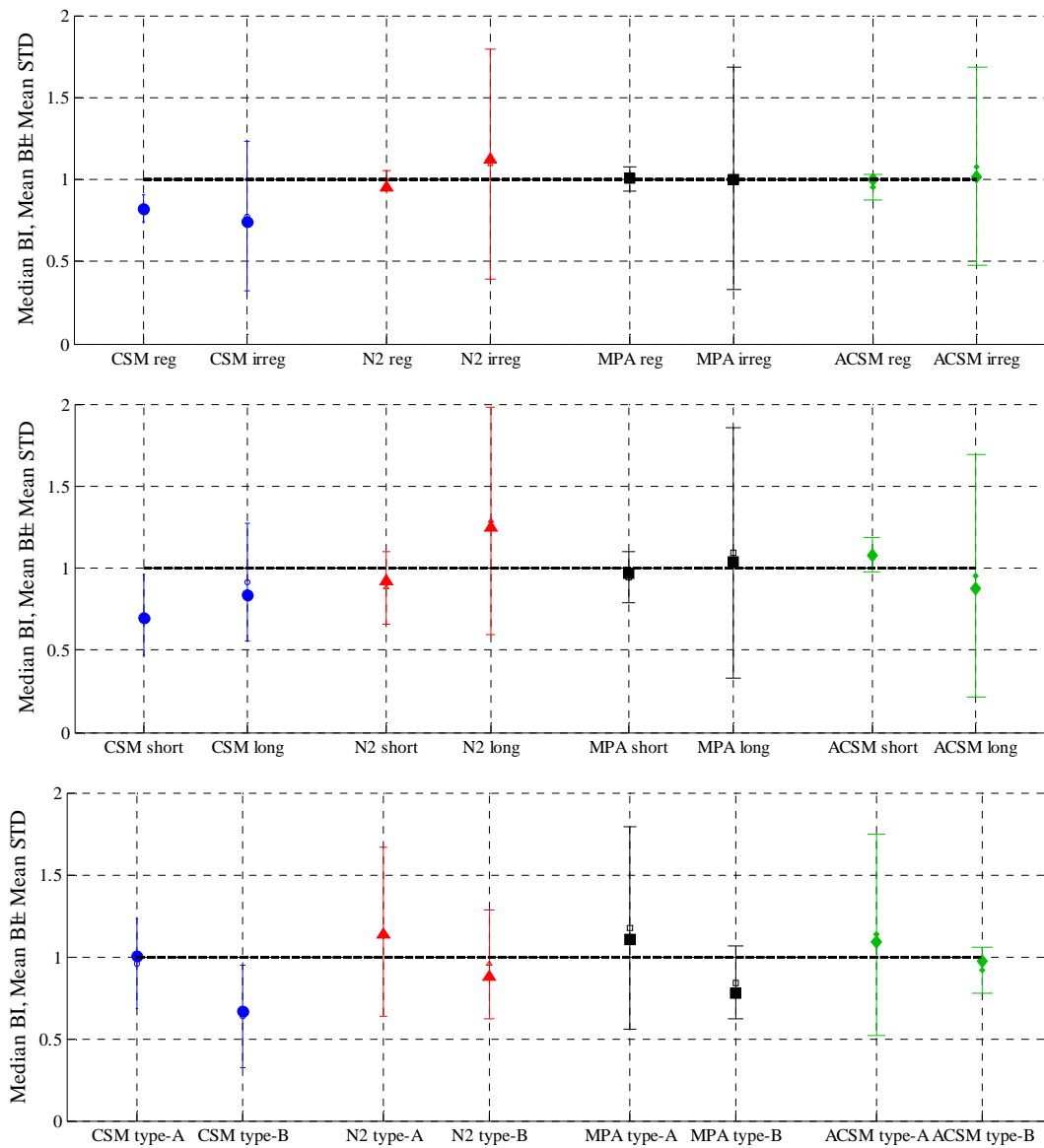


Figure 5.36 – Global Displacements Bridge Index and Standard Deviation according to bridge category.

## **5.5 Conclusions**

This chapter dealt essentially with the application of static methods to estimate the response, or demand, of the structure when subjected to earthquake loading. The motivation for using such procedures has come mostly from two aspects: their undeniable simplicity without expected accuracy loss, constituting a viable alternative to nonlinear dynamic analysis, and their sense of opportunity in the present-day context, for what concerns the seismic assessment and design of structures, given that dynamic analysis seems far from being univocally recommended by codes and guidelines as the main response prediction tool. Additionally, if buildings have consistently been considered and validated in the past as object of successful NSP application, bridges still represent, to some extent, unexplored field, regarding their adequacy to the use of the same NSPs.

The ability of four commonly used Nonlinear Static Procedures in predicting the structural response of bridges subjected to earthquake action has therefore been appraised and compared; two pioneering “classical” methods (CSM and N2) were considered along with two of their more contemporary counterparts (MPA and ACSM). The evaluation was systematically carried out over a relatively large number of structural configurations, considering different response parameters and using several accelerograms scaled to a number of intensity levels. A preliminary study, on the exact same basis, was also carried out with a view to better understand the terms of each of the employed procedures as well as to establish their optimum configuration. The following main observations could be made.

- The Capacity Spectrum Method has clearly benefited from the improvements introduced in the FEMA-440 report, which allowed the attainment of superior predictions, with respect to those obtained using the antecedent ATC-40 formulae. The main modification introduced by the FEMA-440 guidelines concerned the estimation computation of equivalent viscous damping, which was considered in the traditional ATC-40 version as given by the parallelogram hysteresis loops. This way of computing energy dissipation has been recognized as overstating, as well as the Newmark-Hall spectral reduction factors that are used. Seems therefore easily understandable that the new equations, more realistic, have moved CSM indexes closer to unity. Such improvements, however, led to still moderately



underestimated estimates of NDA results for all the considered engineering demand. Having in mind that CSM is a 1<sup>st</sup> mode completely based procedure, parameters such as shear forces or bending moments will probably be more affected by the absence of superior modes contribution to the response. Dispersion levels have proved to be substantial. The recommended choice of the centre of mass of the deck as reference node has proven, globally, to be efficient, even if the maximum modal displacement reference node has shown some marginal upgrading for irregular configurations.

- The N2 method is favoured by the consideration of an envelope pushover load shape that bounds the two alternative load profiles suggested by EC8; first mode proportional and uniform. Such outcome is due to the fact that none of the two possible load patterns led to consistently better predictions. The envelope version, however, does not avoid the need for two pushover analyses, which may be seen as a disadvantage. For regular configurations, one of the load patterns, arbitrarily chosen, is enough given that displacement estimates are fairly good, as well as the shear forces ones, for the piers. On the other hand, for the rest of the parameters, deck moments and shear at the abutments, results tend to be much worse. The median to actually low scatter associated to the method is a positive aspect. The demand, and corresponding spectral reduction, has been based on inelastic smoothed design spectrum, something that has not contributed as decisively as expected, when compared to overdamped spectra, for the accuracy of predictions. It is also recalled that the optional iterative procedure, proposed by EC8 to optimize the equivalent bilinearization process, was employed here and has significantly contributed positively to the performance of the method. The proposal of such feature on a non-compulsory basis seems, at least, arguable. Despite the little difference, the reference node taken as the centre of the deck has worked better.
- Modal Pushover Analysis is quite a strictly defined procedure, in the sense that few windows are left open for improvement or testing. Based on the modal classical theory, involves the repetition of the main steps for each single relevant mode and considers spectral reduction as based on inelastic quantities (response spectrum or displacement empirical ratios) or on Response History Analysis of the SDOF modal systems. The latter was not tested given that it would imply comparable

effort to pure dynamic analysis of the MODF structure. The reference node location was, hence, the only tested variable, and difficulties have been encountered to distinguish the performance of one to the other alternative. The method seems not to be sensitive to this issue. Underprediction for parameters other than deck displacements is still found for deck moments and abutment shear forces. Pier shear forces, on the other hand, come out overpredicted for high intensity levels, which will probably have to do with the consideration of higher modes. Scatter levels are still noticeable but the main drawback that can be pointed out, is the substantial increase in the computational effort of the analysis, brought by the inclusion for an additionally unclear number of relevant nodes. The user would therefore be faced with a necessary evaluation of the compromise between accuracy/relevance of including one more vibration mode, and consequent computation time increase.

- The Adaptive Capacity Spectrum Method enables the consideration of higher modes within a single pushover analysis. Moreover, the reference node choice is unnecessary as well, given that a displacement-based, step-by-step updated, equivalent location is obtained from the actual deformed shape of the structure. The remaining source of debate is the spectral reduction and therefore eleven different possible approaches for considering the energy dissipation capacity, by applying spectral reduction factors, has been carried out. Nine of the spectrum scaling schemes were damping-based whilst the other two were ductility-based. In general, results have indicated that the choice of an appropriate spectral reduction method is an important issue within the ACSM, given that considerable differences have been found when employing different commonly employed approaches, especially for what concerns estimates of deck displacements. In particular, in case of damping-based reduction, the employed damping model proved to be much more relevant than the chosen spectral reduction equation. In general, damping-dependent methods perform better than their ductility-based counterparts. In particular the proposal by Priestley *et al.* (2007) seemed to lead to the best predictions, very closely followed by those of Kowalsky (1994) and Dwairi *et al.* (2007). On the other hand, the ATC-40 damping model tends to overestimate structural dissipation, leading to underestimation of displacement results. Typically, moments and shear forces at the abutments were considerably underestimated, as it has been

observed for all the other NSPs, which seems to indicate that shear amplification coefficients should perhaps be introduced in NSP formulations. On the other hand, with the employment of an appropriate spectral reduction factor, excellent response displacement and pier shear forces estimates may be obtained with such nonlinear static procedure.

Generally, with the exception of CSM, the NSPs proved to be able to predict displacement response with relatively good accuracy for all sorts of bridge configurations (regular, irregular, short, long, etc), something that certainly does lend some reassurance with regards to the employment of such methodologies for assessing response displacements and deformations. Given the actual tendency to move the focus of seismic analysis and design from forces to displacements, such outcome is even more encouraging. As for the rest of the parameters, the prediction of shear forces at the piers was definitely superior, apart from some overestimating trend presented by MPA, leading to consecutive unitary ratios to THA. On the other hand, deck moments and shear at the abutments have been constantly underestimated, in heavy fashion. The assumption of the deck remaining elastic, regardless the intensity level and the typically complex modelling of the abutments may have lead to the poorness of the estimates. Dispersion levels were not negligible, though, regardless the procedure and, thus, the interpretation of global median results should be handled with care. Furthermore it has been observed that good median estimates were typically associated to higher scatter.

Definitely, the endeavour that was carried out was extensive and covered a series of bridge configurations and intensity levels, so, a statistical approach to the results was needed, in order to look at the performance of each NSP at a distance that would ease conclusions. However, at the same time, such reduction of indexes may work against thoroughness, eventually leaving important information behind, which will constitute the main limitation of such study. As a consequence, regular, irregular, short, long, type-A abutments and type-B abutments configurations have been studied in deeper detail. The procedures proved to be quite affected by changes in deck length and type of abutments, in median ratios between nonlinear static and dynamic analysis and corresponding standard deviation, which was much less for short bridges and type-B abutments. The same has been found for the irregular bridges, featuring extremely high dispersion, when compared to the regular

ones. Moreover, it has been concluded that recent approaches (ACSM and MPA) present lower uncertainty levels with respect to their application to bridges in a general fashion.

If a single NSP should be recommended over the rest, such choice would be based on two key aspects. The first is that, undeniably, if a consistent and systematic use of a Nonlinear Static Procedure is intended, at a reasonable level of trust, then one of the procedures that take into account higher modes contribution should be used. This issue assumes additional relevance because bridges are inherently irregular structures. Indeed, the transversal direction is commonly the vulnerable one, which together with the existence of a usually long deck behaving elastically, makes superior modes particularly significant for what seismic analysis is concerned. It is common to find bridges where the second and subsequent modal participation factors are relevant, when compared to the first. CSM and N2, pioneering procedures, relying on the 1<sup>st</sup> mode quantities, presented, on the author's point of view, naturally inferior performance for this particular sort of structural schemes. Between the two more recent proposals, ACSM would probably be the most reliable choice, since results have shown that, closely followed by N2, it presents a good compromise between predictions of shear forces and displacements at the piers, assumed to be the most relevant engineering demand parameters. It has also proved to show lower dispersion among the different bridge categories. To this extent, MPA could be pointed out as well but its overestimating trend in piers shear forces make it not so appealing. The procedure might be compromised by the need for a reliable adaptive pushover analysis, which is still not as spread out as it would be desirable. In any case, it has the fundamental advantage, when compared to MPA, of overcoming the repetition of as many pushover analyses as the considered modes.

Conclusions on the accuracy of different structural response prediction tools enable one to optimize the probabilistic characterization of the seismic demand, to use in the following Chapter 6, together with the contribution from Chapters 3 and 4, with respect to seismic input and nonlinear modelling.

## 6. Safety Assessment

As soon as all the relevant elements of a typical seismic analysis procedure are properly defined, the final step becomes the safety assessment itself. Such endeavour may, similarly to all the safety problem components, feature different approaching scenarios, even though it will fundamentally consist in the comparison of the demand, coming from the effects caused by the seismic ground motion input, with the capacity of the structural elements to accommodate them, which is characterized according to the geometry, material properties, nonlinear behaviour models, among others. Putting it simply, the safety assessment of a single structural system can be carried out through the computation of a safety interval, that is, the deterministic difference between the capacity and the demand, or a failure probability, which will require statistical characterization of the variables that are part of the process.

The deterministic approach is most likely the one that practitioners are most familiarized with, given that it certainly goes along with the traditional designing mode or structural safety verification. For a certain limit state, demand and capacity are computed, using mean or characteristic values for the input variables, and the previously mentioned difference is determined, implying the fulfilment or not of the limit state. The uncertainty coming from the several variables may be globally accounted for using a safety factor, applied to increase the demand and/or reduce the capacity. Such approximate procedure

surely cares for consistency and, therefore, the probabilistic approach tends to gain weight in the actual safety assessment scene. Indeed, the statistical definition of uncertainty can be quite simple, either from the capacity or the structural demand point of view, consisting essentially in replacing a single value by a typical distribution, of known mean and standard deviation, which will represent the variable at stake in a more accurate fashion.

### **6.1 Failure probability computation**

The failure probability of a structural element, within a single failure mode, may be obtained according to Equation (6.1), where  $X$  is a vector containing the basic random variables  $x$ , in which the structural safety is settled;  $g(X)$  is the limit state function associated to the failure mode under consideration and  $f_X(x)$  is the joint probability density function of the vector  $X$ , characterizing the way how the variables define the structural safety problem. This is, according to Borges and Castanheta (1985), a commonly employed procedure, corresponding to the simplest basic problem of structural safety.

$$p_f = \int_{g(X) \leq 0} f_X(x) dx \quad (6.1)$$

Regarding the considered failure mode, failure will occur when  $g(X) < 0$ , safety will be verified if  $g(X) > 0$  and the failure surface, recalling that one is facing a multiple variables problem, will be given by the condition  $g(X) = 0$ . Based on such considerations, the failure probability can be rewritten as Equation (6.2), where  $prob[g(X) \leq 0]$  represents the probability that  $g(X)$  has to be in the failure domain and  $F_g$  is the cumulative distribution function of  $g(X)$ .

$$p_f = prob.[g(X) \leq 0] = F_g(0) \quad (6.2)$$

The solution of Equation (6.1) will involve multidimensional integration with the integral dimension being the same as the number of basic variables in vector  $X$ , the physical variables such as loading, material properties or geometrical data, which incorporate the

uncertainty associated to the regarded failure mode. Depending on the number of variables and on whether the expression of  $g(X)$  is simple or not, the analytical solution for the integral will be less or more demanding, if possible.

In a structural engineering context, the safety problem, represented by the expression  $g(X)$ , will be essentially dependent on two continuous, independent assumed, variables:  $R$ , standing for a measure of resistance, and  $S$ , the structural response. The limit state function is in this case simply given by, in other words, the difference between the capacity and the demand, as shown in Equation (6.3)

$$g(X) = R - S \quad (6.3)$$

The corresponding joint probability density function,  $f_X(x)$ , a surface that can be represented in the plane  $(S,R)$  by lines of equal constant density of probability, is given by Equation (6.4), once that  $R$  and  $S$  are independent. The failure domain,  $F$ , opposite to the condition that  $S$  does not exceed  $R$ , will naturally be as expressed in Equation (6.5).

$$f_{R,S}(r,s) = f_R(r) \cdot f_S(s) \quad (6.4)$$

$$F = R < S = R - S < 0 \quad (6.5)$$

Considering the assumptions in Equations (6.3) to (6.5), the failure probability will be, in the end, given by Equations (6.6) or (6.7), where  $f_S(s)ds$  is the probability of  $S$  within the interval  $[s, s+ds]$  and  $F_R(s)$  is the cumulative distribution function of  $R$ , the probability of  $R$  being less than the value of  $S$  corresponding to  $s$ . In addition, as  $R$  and  $S$  are independent, the probability of both occurring at the same time is given by the product of each of the probabilities of occurring separately, i.e.  $f_S(s) \cdot F_R(s)ds$ .

$$p_f = \text{prob.}(R - S \leq 0) = \iint_F f_{R,S}(r,s) dr ds = \int_{-\infty}^{+\infty} f_S(s) \cdot \int_{-\infty}^S f_R(r) dr ds \quad (6.6)$$

$$p_f = \int_{-\infty}^{+\infty} f_S(s) \cdot F_R(r) dr ds \quad (6.7)$$

As mentioned by (Freudenthal *et al.*, 1966), the sum for all the values of S yields the convolution integral of Equation (6.7), illustrated in Figure 6.1.

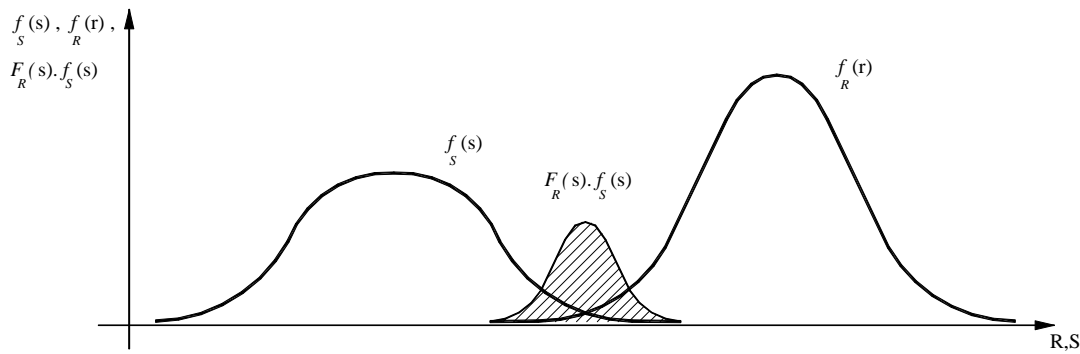


Figure 6.1 – Basic reliability problem

At this point, it is clear that statistical distributions for the resistance, R, and structural effects, S, caused by the seismic action, are needed if the failure probability is the intended outcome of the safety assessment process. As far as resistance is concerned, possible measures for variable R may be simulated experimentally, numerically or even complementing one with the other. Numerical simulation will definitely expedite the computation process, enabling the capacity definition to be incorporated within the global procedure. On the other hand, experimental assessment, even if inherently limited when it comes to obtaining large dimension samples, has undeniably accurate relevance. However, statistical characterization, i.e. distribution fitting for a variable, requires considerable sampling size, which can be impracticable if based on experimental campaigns. Such fact will lead, therefore, for experimental simulation to play a complementary role, mainly useful for calibration or validation scenarios. As a matter of fact, the different parameters that may be used to represent capacity, such as rotational capacity, ultimate curvature



ductility or shear strength, are typically expressed as a function of basic material properties, concrete and steel, which assume their own statistical distributions. Working out the resistance distribution, represented by  $F_R$  function in Equation (6.7), does not turn up, thus, as a difficult task. It will require at most, the use of a simulation algorithm, pure Monte Carlo or improved Latin Hypercube, for the sampling attainment.

The estimate of the distribution of the structural effects, variable  $S$ , is, on the other hand, dependent on a higher number of analysis steps and variables. The first aspect to bear in mind is that the statistical layout of the parameter representing the response measure may not be straightforward to obtain and not necessarily similar to the distribution of the intervening variables. Indeed, different structural systems, subjected to variable intensity, and corresponding nonlinearity levels, will have different distributions for the same response measuring parameter. Moreover, input ground motion will feature variability in intensity and number, that is, several analyses need to be carried out corresponding to a sufficient number of intensity levels, capturing multiple nonlinearity levels, and distinct types of earthquake records.

As a result, if capacity characterization presented itself as intuitive and relatively simple, demand statistical definition, to confront the former with, involves quite a few nonlinear structural analysis as well as different types of uncertainty to be accounted for. To skip the need to define the continuous probability density function of the seismic effects on top of reducing the number of computational demanding analyses, a numerical standardized methodology is established and systematically followed.

### ***6.1.1 Seismic action – intensity level probability density function***

The intensity level probability function represents, at each seismic intensity level, usually expressed in terms of peak ground acceleration, the density of probability at each point in the sample space of that random variable. The probability of the variable falling within a specific set is given by the integral of its density over the set.

To characterize an event such as the occurrence of an earthquake, believed to be highly unusual, it is common to use the extreme value theory, a branch of statistics dealing with the extreme deviations from the median of probability distributions. Within the extreme value theory, the generalized extreme value distribution has been defined, combining three

types of distinct distribution families, also known as type I, II and III extreme value distributions. It is believed that such three types of distributions are enough to model the maximum or minimum of the collection of random observations from the same distribution. Consequently, if the seismic action is to be defined by means of peak ground acceleration, a maxima-related extreme value distribution will definitely fit such endeavour. If a resistance-side variable is to be characterized, a minima extreme value distribution would, instead, be more suitable.

The generalized extreme value distribution is a flexible three-parameter model that combines the aforementioned maximum extreme value distributions and has the probability density function given by Equation (6.8), where  $\mu \in \Re$  is the location parameter,  $\sigma > 0$  the scale parameter and  $\xi \in \Re$  the shape parameter.

$$f(x; \mu, \sigma, \xi) = \begin{cases} \frac{1}{\sigma} \exp \left\{ - \left[ 1 + \xi \left( \frac{x - \mu}{\sigma} \right) \right]^{-1/\xi} \right\} \left[ 1 + \xi \left( \frac{x - \mu}{\sigma} \right)^{-1/\xi} \right] & k \neq 0 \\ \frac{1}{\sigma} \exp \left[ - \left( \frac{x - \mu}{\sigma} \right) - \exp \left( - \frac{x - \mu}{\sigma} \right) \right] & k \rightarrow 0 \end{cases} \quad (6.8)$$

$$1 + \xi \left( \frac{x - \mu}{\sigma} \right) > 0$$

The shape parameter,  $\xi$ , will define the tail behaviour of the distribution and, therefore, its type, each one corresponding to the limiting distribution of block maxima from a different class of underlying distributions. Distributions whose tails decrease exponentially, such as the Normal, lead to type I, with  $\xi$  tending to zero. Distributions whose tails decrease as a polynomial, such as Student's t, lead to type II, with  $\xi$  positive. Distributions whose tails are finite, such as the Beta, lead to type III, with  $\xi$  negative. Types I, II and III are often referred to as the Gumbel, Fréchet and Weibull extreme value distribution families, which can be arguable, in terms of inconsistency. To be exact, the Type I and Type III cases actually correspond to the mirror images of the usual Gumbel and Weibull distributions, respectively. The Type II case is equivalent to taking the reciprocal of values from a standard Weibull distribution. The Type I distribution, Gumbel related to, has early been used in applications of extreme value theory to engineering problems and, as related to the

maxima, is frequently the chosen one to characterize seismic action intensity. Indeed the extreme value theory claims that it is suitable if the distribution of the underlying sample data is of the normal or exponential type. Its probability density function, following the general expression in Equation (6.8), is given by Equation (6.9), which can be written in a more simplified manner, as in Equation (6.10), where  $z=(x - \mu)/\sigma$ .

$$f(x|\mu,\sigma) = \frac{1}{\sigma} \exp\left[-\left(\frac{x-\mu}{\sigma}\right) - \exp\left(-\frac{x-\mu}{\sigma}\right)\right] \tag{6.9}$$

$$f(z,\sigma) = \frac{e^{-z-e^{-z}}}{\sigma} \tag{6.10}$$

The Type I distribution is unbounded, defined for the entire real domain, and admits a minima version. Its general shape remains the same for all parameter values. The location parameter,  $\mu$ , shifts the distribution along the real line and the scale parameter,  $\sigma$ , expands or contracts the distribution. Figure 6.2 plots the probability density function,  $f(x/\mu,\sigma)$ , for different combinations of  $\mu$  and  $\sigma$ , where the variable  $x$  is the peak ground acceleration, used to characterize the seismic intensity level, expressed in  $\text{cm/s}^2$ .

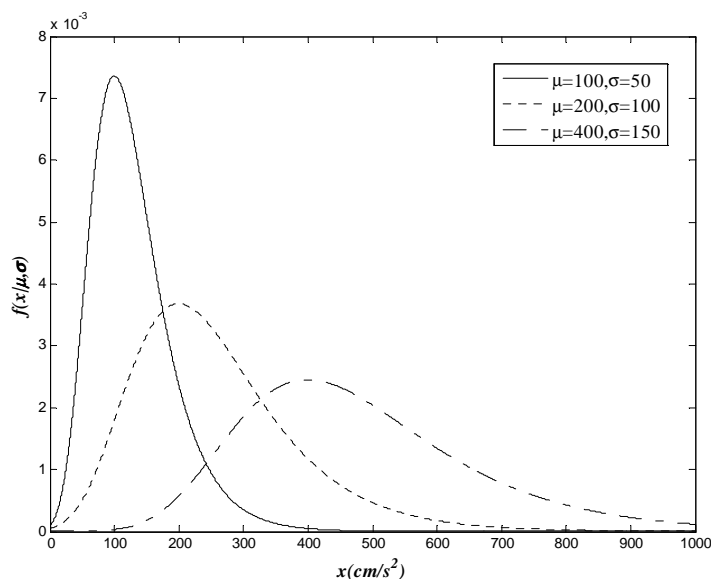


Figure 6.2 – Extreme value Type I (Gumbel associated) distribution probability density functions for different combinations of location and scale parameters.

### **6.1.2 Capacity distribution**

The structural resistance can be analysed considering the structure as a whole, or by scrutinizing its individual elements, studying the resistance of each in separate. When the structure in study is a bridge, the application of the latter case is more intuitive, given that the resisting elements are extremely well defined as well as the failure mechanisms. In other words, considering that the deck will assume elastic behaviour and neglecting possible soil failure at the foundations, the piers will be the crucial elements, behaving nonlinearly and causing the bridge collapse as soon as the first attains rupture. The density of probability will therefore be expressed as a function of the action effects on such elements, as well as the corresponding capacity.

Regardless of the selected procedure to carry out the safety assessment, as long as a probabilistic analysis is intended, the capacity of the piers cross sections needs to be determined and characterized by means of a statistical distribution, quantified in terms of ultimate ductility permitted by the cross section at the bottom of the piers or the corresponding top displacement. This is because the input data of the models are often quite uncertain, requiring them to be considered as random variables. Such capacity definition must certainly be able to incorporate the uncertainty associated to the variables on which the ultimate capacity depends. Apart from the geometrical characteristics, for the case of a cross section made up of reinforced concrete, the resistance will be a function of the material ultimate properties, the yielding and peak tensions, and corresponding strains, which are expected to contribute the most to the variability of the capacity controlling variable.

A proper characterization of the intended distribution will consist on repeated random simulation of the intervening variables, using their distributions and an appropriate algorithm, until a sample is obtained. The appropriateness of the simulation procedure will focus predominantly on the best relation between sample size and associated reliability. The main goal is to make use of a simulation technique able to yield samples as small as possible, and consequently faster, that are still good representatives of the underlying distribution. Among the available solutions the, let us say, traditional approach would be the Monte Carlo sampling scheme, based on pure random simulation. A more recent and innovative technique is the Latin Hypercube (McKay *et al.*, 1979; Iman *et al.*, 1981),

which has been gaining popularity among scientific studies due to the claimed efficient reduction in the necessary sampling size.

### **6.1.3 Latin Hypercube Sampling**

Safety assessment based on reliability calculations will involve repetitive simulation of several properties, which may become, mainly if carried out for complex, finite-element modelled structures, quite time-consuming and demanding in terms of computational effort. In order to overcome such drawback, advanced simulation techniques are required based on relatively simple integrated modifications in the existing general procedures. The Latin Hypercube sampling (LHS) simulation procedure (Olsson and Sandberg, 2002; Olsson *et al.*, 2003) fits that set of techniques and can be seen as a particular case or version of the standard Monte Carlo (SMC) numerical simulation, with the need for a smaller number of runs, tens to hundreds, to achieve a reasonably accurate random distribution. The LHS may in fact be incorporated into an existing Monte Carlo model fairly easily and work with variables following any analytical probability distribution. Such key features are accomplished by means of the stratification of the theoretical probability distribution function of input random variables. The method is not restricted to the estimation of statistical parameters of structural response but offers a quite broad usage domain that goes from sensitivity analysis to Bayesian updating, among other possibilities. It has been found that LHS is very efficient for estimating mean values and standard deviations in stochastic structural analysis (Ayyub and Lai, 1989; Florian and Navratil, 1993; Novák *et al.*, 1997) but only slightly more efficient than the SMC for estimating small probabilities, which can definitely occur when assessing the seismic failure of bridges. Additionally it has been found that, under some particular conditions, LHS is considerably more efficient than the SMC version if the probability of failure is dominated by a single stochastic variable, which again may be verified in the ultimate limit states for reinforced concrete cross sections depending essentially on the ultimate steel strain. It seems thus far relevant the application of LHS on such endeavour, expected to perform from slightly to considerably better than SMC.

The LHS strategy is actually rather straightforward, making use of stratified sampling, within a simple concept: the probability ranges of probability distribution functions for input random variables are divided into  $N$  equivalent intervals,  $N$  being the number of

realizations. Assuming that the structural problem has  $M$  input variables  $X_j$ , with  $j=1:M$ , the range  $[0,1]$  of each cumulative distribution function  $F(X_j)$  is divided into  $N$  different non-overlapping intervals of equal probability  $1/N$ , as illustrated in Figure 6.3. Each of those intervals is then represented by its centroid,  $C_{ij}$ , the abscissa of  $X_j$  for the average value of each  $1/N$  probability interval.

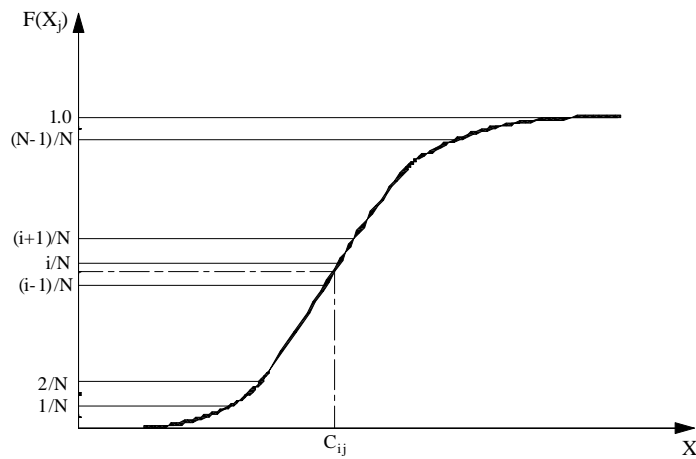


Figure 6.3 – Division of the cumulative distribution function  $F(X_j)$  in  $N$  intervals.

The following step is to use the centroids for the simulation process, this is, the centroids are selected randomly based on random permutations of integers 1 to  $N$  and representative values are obtained via inverse transformation of the cumulative distribution function. It is however mandatory that every interval, or centroid, is used, or simulated, once during the random process. Such condition can be seen as the main advantage of the LHS strategy: the regularity of probability intervals on the probability distribution function and the assurance that all of them are accounted for ensures good quality samples, even for a small number of realizations,  $N$ . The final output will be a matrix of random permutations of the centroids, with dimension  $N \times M$ , where each column corresponds to one of the input variables and each row to a particular simulation.

Looking further into the LHS algorithm, where the sampling space will be  $M$ -dimensional, let  $P$  denote a matrix  $[N \times M]$  containing in each column a random permutation of  $1, \dots, N$  and  $R$  a same size matrix of independent random numbers from the uniform  $(0,1)$  distribution. Using those matrices the basic sampling plan is established and represented by the matrix  $S$ , as follows in Equation (6.11).

$$S = \frac{1}{N}(P - R) \quad (6.11)$$

Each element of  $S$ ,  $s_{ij}$ , is mapped according to the corresponding variable distribution  $F(X_j)$  as in Equation (6.12), where  $F_{X_j}^{-1}$  is the inverse cumulative distribution function for the variable  $X_j$ .

$$x_{ij} = F_{X_j}^{-1}(s_{ij}) \quad (6.12)$$

The vector  $x_i = [x_{i1} \ x_{i2} \ \dots \ x_{im}]$  will correspond to the input data for one deterministic computation.

The condition of each centroid being used only once can be observed in a simple example simulation in Figure 6.4. The sampling space size is  $5 \times 2$ , five realizations of two input variables. Each column and each line are taken once and all the sampling space is used, which might not have happened if the SMC simulation scheme had been used.

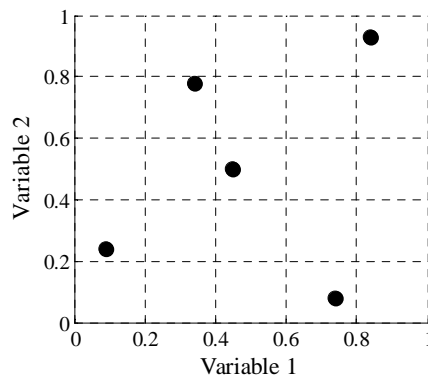


Figure 6.4 – Latin Hypercube example sampling space for two variables and five realizations.

Nevertheless, there is no assurance that spurious correlation does not appear, even if the distribution function of each variable is efficiently employed. Figure 6.5 illustrates how an unwanted spurious correlation in the sample can occur despite the verification of the simulation LHS conditions. It has, however, been easily demonstrated by Iman and Conover (1982) that such scenario can be reduced by modifying the permutation matrix  $P$ , used in Equation (6.11).

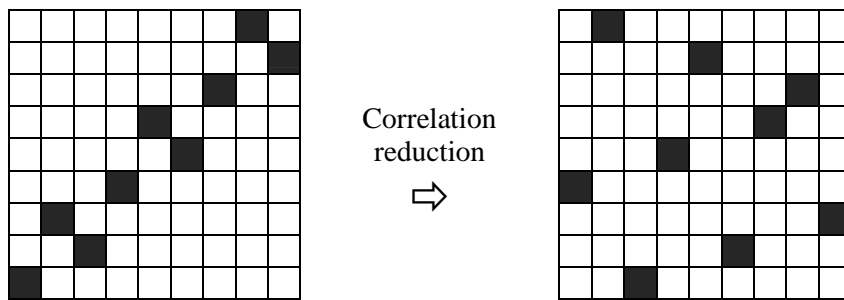


Figure 6.5 – Unwanted (*left*) and reduced (*right*) correlation of sampling plan (Olsson and Sandberg, 2002).

The procedure is quite simple and basically consists in mapping the elements of matrix  $P$ , divided by the number of realizations plus one, on the (0,1) Gaussian distribution. The covariance of this new matrix is computed and then Cholesky decomposed, which, according to proper dealing, will lead to a final alternative matrix,  $P^*$ , high-level spurious correlation free, that substitutes the original  $P$  one. The only limitation of the procedure is the number of realizations to be higher than the basic input variables,  $N > M$ , so as to allow the Cholesky decomposition. Such condition, given the type of structural analysis at stake, will however hardly become restrictive.

#### 6.1.4 Seismic structural effects

Once the resisting structural elements are properly characterized and the seismic action is defined, the structure will be subjected to the latter and the seismic effects quantified and appropriately compared with the capacity. The way such comparison is carried out, which can assume several different versions, will be determined by the type of collapse probability, depending on how the uncertainty associated to the different variables is taken.

The classical approach, following Figure 6.1 and Equation (6.7), is to build the probability density function of the seismic effects, submitting the structure to increasing seismic intensity levels, along the entire domain, and develop the so-called vulnerability function, the element that enables the conversion of seismic action into seismic demand. This is a local variability version, given that uncertainty of the action and the capacity are considered separately, in local, distinct stages.



If one chooses, still within the local variability approach, to limit the seismic action to a specific intensity level, the probability of failure is equally possible to get and possibly full of interest, because directly connected to a particular ground motion level. The seismic effects can be again characterized again through their probability density function recurring to different demanding earthquake records, characterized by the same intensity level, though.

If the goal is to carry out a series of independent realizations, where the uncertainty of each variable is taken simultaneously and accordingly, then the structural effect consists in the seismic demand for each run, which is directly compared to the capacity, determined for the same structural properties.

#### ***6.1.5 Failure probability with local uncertainty***

The traditional approach, which has been originally developed and applied in the work by Costa (1989), presents as essential target the definition of the structural effects probability density function, which will be confronted to the resistance one. In order to do so, it is evident the need for a relationship between the seismic intensity and the response control variable, coming from the nonlinear analysis of the structure, or any other reliable tool, for that specific ground motion level. That relation is usually named vulnerability function and is essentially a mapping function, establishing the connection between the seismic intensity, its probability and the actual effect in the structure, confronted with the capacity to reach the final collapse probability.

The element from where the whole process starts is the seismic action,  $A$ , often characterized in terms of peak ground acceleration (PGA), one of the possible measures of intensity. The probability density function,  $f_{ag}$ , of the maximum annual peak ground acceleration for a specific site is therefore used and comes from corresponding hazard studies. The Hazard scenario for a specific site may be defined as a function of the peak ground acceleration or, according to more recent tendencies, acceleration spectral ordinates for a period that is similar to the fundamental period of the structure. Even if the use of spectral acceleration is claimed by many as more accurate, given that it centres the analysis on the structure's fundamental mode of vibration, the peak ground acceleration seems to still stand as a reliable intensity measure, as observed in the results of the study in

Chapter 3. Nevertheless, to the same peak ground acceleration there might correspond different types of ground motion records, concerning nature (real or artificial), duration, magnitude, epicentral distance, among other characteristics. For that reason a set of distinct accelerograms must be considered, reflecting wide-ranging frequency content. For a predefined, not very large, number of intensity levels, corresponding to different return periods and probabilities of occurrence, the records are scaled to match that specific PGA. Nonlinear dynamic analysis is carried out using each of the scaled accelerograms, yielding a sample of the response measure that accounts for record associated variability. For each ground motion intensity, and corresponding PGA, a statistical value, defined by the mean or median response measure, is computed and a polynomial function is adjusted to those points, putting up the vulnerability function, illustrated in Figure 6.6, the function that turns the seismic action into the demand. The curve will be a 2<sup>nd</sup> degree, or higher, polynomial, due to the nonlinear structural behaviour with increasing intensity.

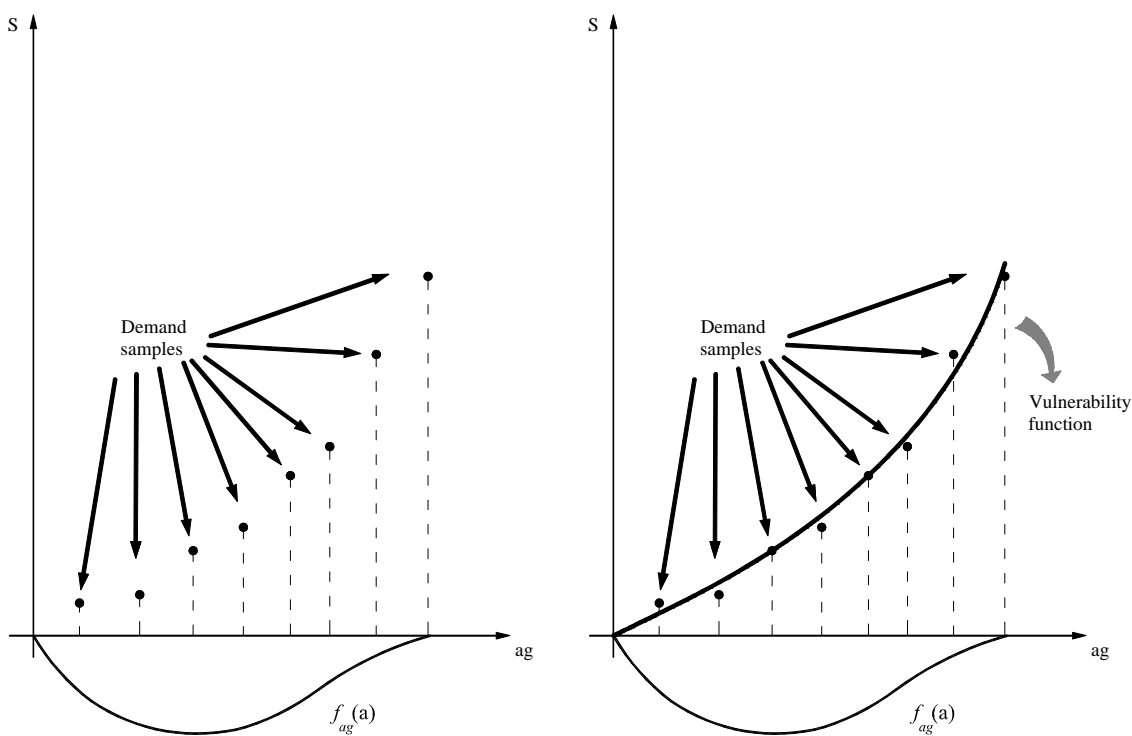


Figure 6.6 – Fitting of the vulnerability function to demand points (LESSLOSS, 2004b).

The material properties used for the structural analyses may be considered on a deterministic basis, through their mean or characteristic values, or making use of their statistical distribution. If the latter is employed, corresponding to the global uncertainty

version of the proposed method, the number of structural analyses will necessarily increase but the statistical meaning of the computed failure probability will be superior. Further details on the use of such global simulation procedure, taking into account the variability of the seismic action and material properties all together are discussed in Section 6.1.7.

The vulnerability function may be estimated recurring to pushover analysis, whose validity in estimating nonlinear response of structure has been recognized in Chapter 5. The advantages in using such nonlinear static approach are immediate given that  $N$  nonlinear dynamic analyses are avoided, greatly simplifying the entire process, as much as higher the number of realizations is. The abscissa for the vulnerability curve will be the peak ground acceleration of the response spectra used in the nonlinear static procedure to locate the performance point in the pushover curve and quantify the control variable. There will be, therefore, two variants for the failure probability computation version herein accounted for, based on the distinct ways to get to the structural effects, compared in Chapter 5: nonlinear static and dynamic analysis.

Once the vulnerability function is properly defined, the statistical distribution of the response measure can be easily obtained through a numerical procedure based on equal areas under the probability density function, i.e. probability of occurrence, along with the changing of the variable from peak ground acceleration to the response measure itself. The domain of the seismic action probability density function,  $f_{ag}(a)$ , is divided into small increments, let us say  $d_{ag}$ . For each increment  $d_{ag}$  the area  $A1$ , see Figure 6.7 (*left*), is determined based on the ordinate of the  $f_{ag}$  function for the centroid of  $d_{ag}$ . The value  $f_{ag}(d_{ag})$  is converted into the value of the structural effects' probability density function  $f_S(s)$  for the centroid of the corresponding  $ds$ , guaranteeing that areas  $A1$  and  $A2$  in Figure 6.7 (*right*) are the same.

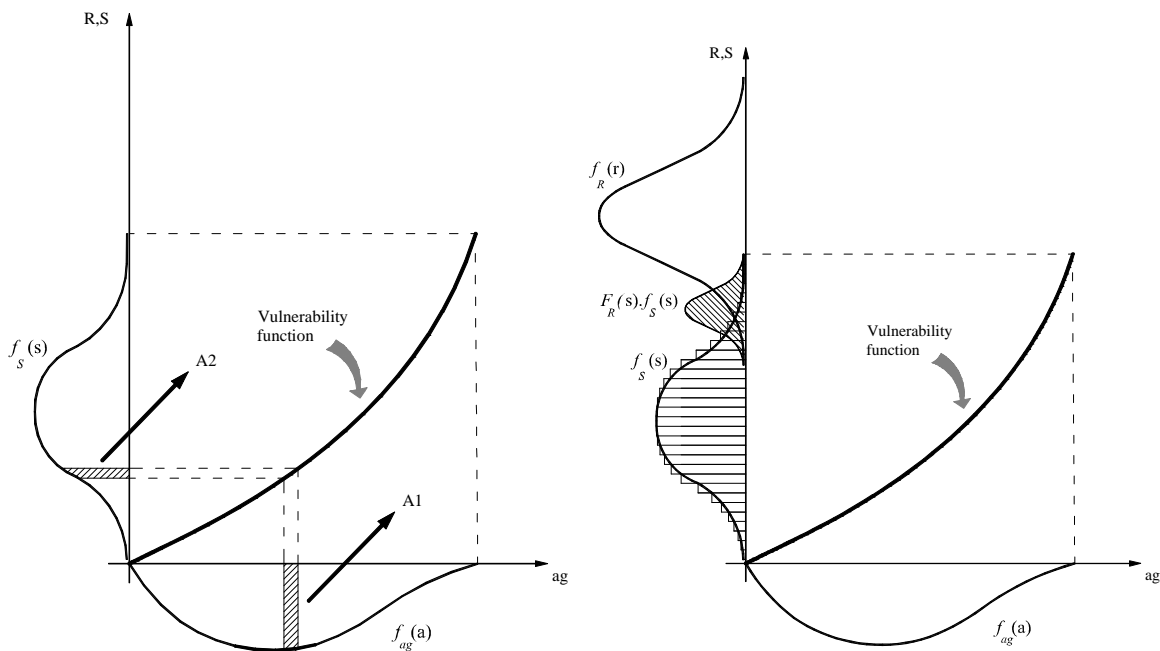


Figure 6.7 – Blockwise definition of the probability density function  $f_s(s)$  (left); Failure probability computation (right) (LESSLOSS, 2004b).

The variable  $s$ , used to measure the seismic effects, as well as the resistance, will refer to the piers, which are the resisting nonlinear behaving structural elements, and is usually taken as the ductility at the base or the top displacement. The final step will be to cross the capacity and the seismic demand distributions, computing the integral in Equation (6.7).

The entire process may be schematically depicted in Figure 6.8, which illustrates the traditional version of the procedure described so far.

The seismic intensity is characterized by its probability density function, the curve 1. Analogously, at each intensity level of the seismic action, for which curve 1 is defined, the effect in the structure is obtained, in terms of a chosen parameter, ductility or displacement, for instance. The so-called vulnerability function, curve 3, is therefore built, representing the structural effects of the seismic action long with increasing intensity. This sort of information is fundamental to cross with the seismic action probability density function and generate the statistical distribution of the structural effects, curve 4. In other words, by putting together the probability density associated to a seismic level and its effect in the structure, one can obtain the probability density of such effect to be verified.

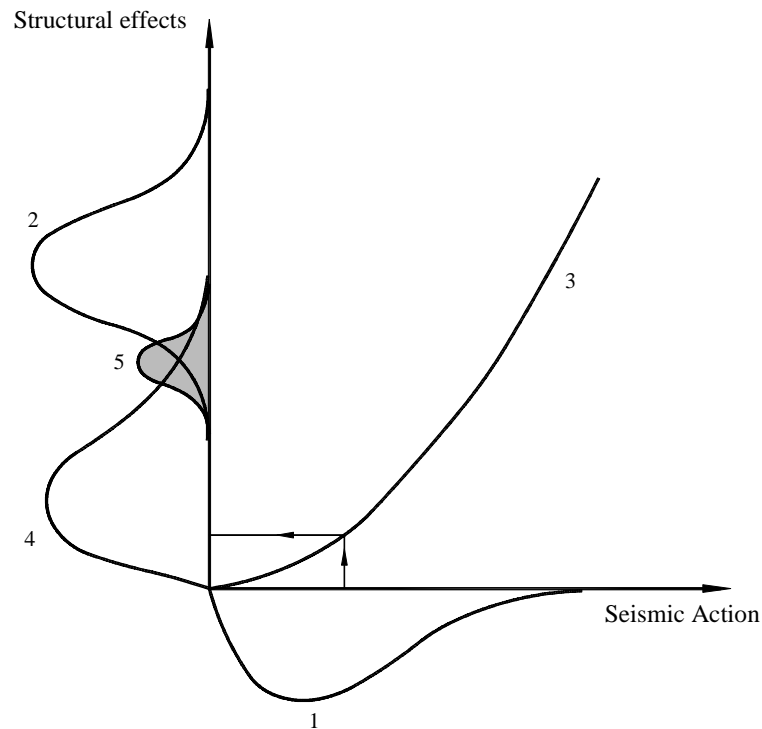


Figure 6.8 – Failure probability computation with local uncertainty – traditional approach

At the same time, the distribution of the structural capacity, curve 2, in terms of the same response parameter used to define curves 3 and 4, ductility or displacement, needs to be set up. This step is typically carried out by means of a simulation procedure, such as Monte Carlo or Latin Hypercube sampling methods, based on the statistical distributions of the variables with relevant uncertainty, usually cross section material properties. Finally, the intersection of capacity with demand, managed by the convolution integral, will yield the intended failure probability.

#### ***6.1.6 Failure probability for a given intensity level***

Additionally, a different meaning can be given to the failure probability coming from the integral in Equation (6.7), depending on the level of restrictions that is considered within the adopted procedure. Indeed, the global collapse probability computation method just described uses the probability density function of the seismic action defined for the entire intensity domain, taking into account the relative probability of occurrence of different intensity levels, within a specific hazard local scenario.

On the other hand, if the ground motion intensity is constricted to a specific level, the computation of the failure probability is still possible, according to Figure 6.9.

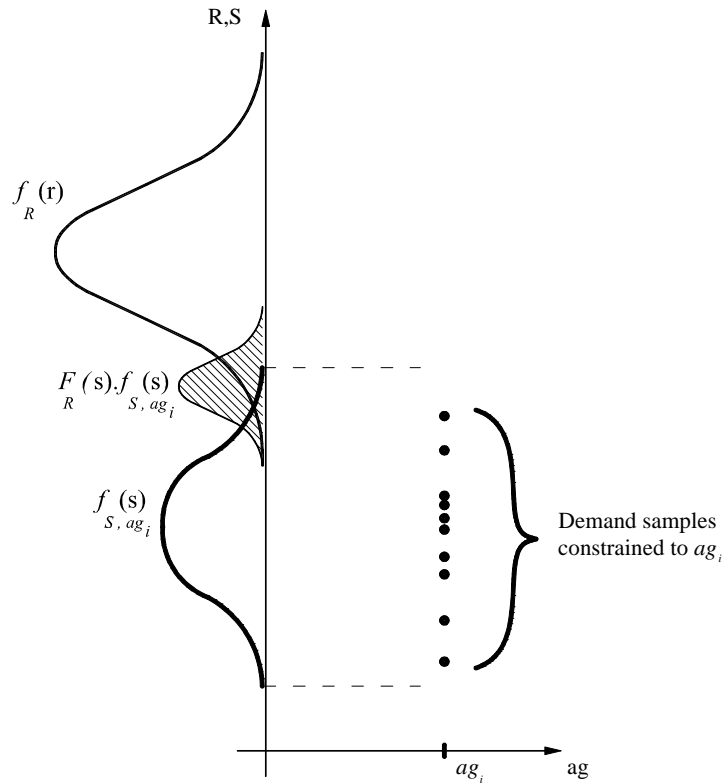


Figure 6.9 – Response measure constrained to the ground acceleration  $a_{gi}$  (LESSLOSS, 2004b).

Such number will be equivalent to a point in the structure’s fragility curve, the probability of occurrence of the limit state under consideration for a specific intensity level of earthquake ground motion. The main difference when following this approach will be the structural effects distribution definition, although the principle remains the same. A set of different ground motion records is used, all of them with a specific peak ground acceleration level  $a_{gi}$ , and the probabilistic distribution of the structural effects,  $f_{S,agi}$ , is defined with the response measure sample coming from that set of accelerograms, whereas, in the global procedure, the mean or median for each intensity was computed. This sort of approach will definitely require less computational effort but will, at the same time, call for a sufficiently large number of records, needed to achieve a reliable distribution of the structural effects. In the end, Equation (6.7) is solved numerically, replacing  $f_S(s)$  by  $f_{S,agi}$ , leading to the failure probability  $p_f(a_{gi})$ , the fragility curve ordinate for that abscissa. If the whole process is repeated, a pointwise definition of the fragility curve of the bridge is acquired, which can be used, if intended, to compute the global failure probability, making use of the Hazard local function within the entire considered  $a_g$  domain.

### 6.1.7 Failure probability with global uncertainty

A sort of alternative approach for the failure probability computation described in 6.1.5 is to consider the uncertainty associated to the different intervening variables in a global fashion, this is, all at the same time, within a global procedure, carried out for each iteration step, from the beginning to the end.

It is recalled that, in the procedures described so far, uncertainty has been taken into account independently; this is, for each eligible variable, a statistical distribution, that is able to define it, is the element that carries the associated uncertainty and is used all at once. Examples are, in Figure 6.8, the conversion of distribution 1 into distribution 4 through curve 3 or the intersection of the entire distributions 2 and 4 to yield the convolution integral.

On the other hand, the approach herein presented uses the statistical distributions of the different variables in a different manner. Firstly, the distributions are defined, characterizing each purely input variable, the seismic action and the resistance. Once that initial step is completed, the assessment procedure is carried out completely, but individually, recurring to those distributions. Within a global statistical simulation process, the already described Latin Hypercube, each variable with known uncertainty, seismic intensity level, type of record and material properties, is randomly simulated, the nonlinear dynamic analysis is carried out using such parameters, the structural effects and the capacity are determined and the difference between those two numbers, usually referring to ductility or displacement, is computed. A statistical distribution will be then adjusted to that difference, which will lead to the computation of the collapse probability in a different mode. Data for each realization is obtained through the application of the LHS technique (see Section 6.1.3 for further detail) in a broader sense, taking as basic input variables the material properties, the seismic intensity level and earthquake record all together.

Figure 6.10 roughly illustrates the process just described. A vector of input variables, consisting of the seismic intensity level,  $a_g$ , type of ground motion record and the relevant material properties, is put up by random simulation, according to predefined distributions, and capacity is computed, expressed in available ductility,  $\mu_R$ . Nonlinear dynamic analysis is carried out on the structural model, built with the simulated properties, for the specified

accelerogram with  $a_g$  level, and the demanded ductility,  $\mu_S$ , a point of the previously mentioned vulnerability function, is obtained.

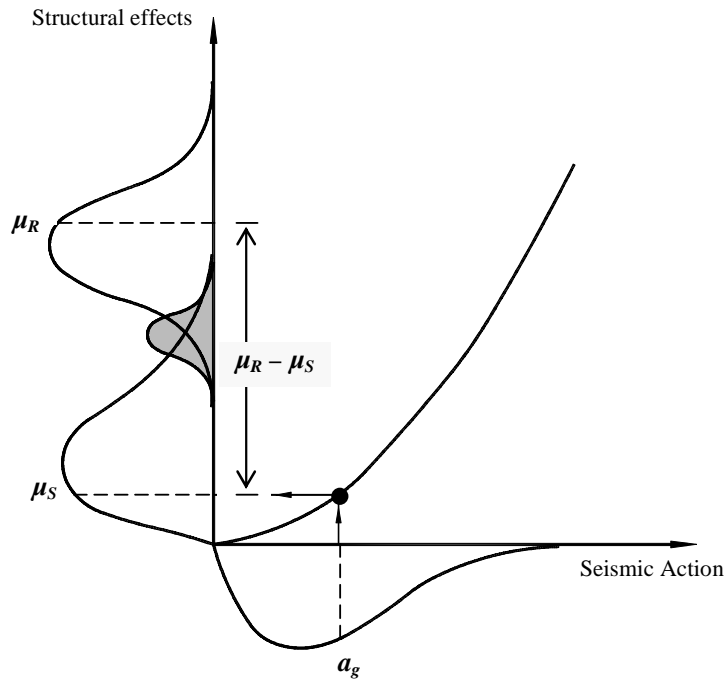


Figure 6.10 – Failure probability computation with global uncertainty – alternative approach

The difference  $\mu_R - \mu_S$ , eventually non-positive, will represent some sort of safety gap. The main concept behind this procedure is that the entire process, until the computation of the available ductility margin, can be repeated N times in order to fit a statistical distribution to that variable. As illustrated in Figure 6.11 the knowledge of such a distribution will enable the computation of the failure probability as the area under the corresponding probability density function,  $f_{R-S}$ , for a value of  $\mu_R - \mu_S$  least than zero.

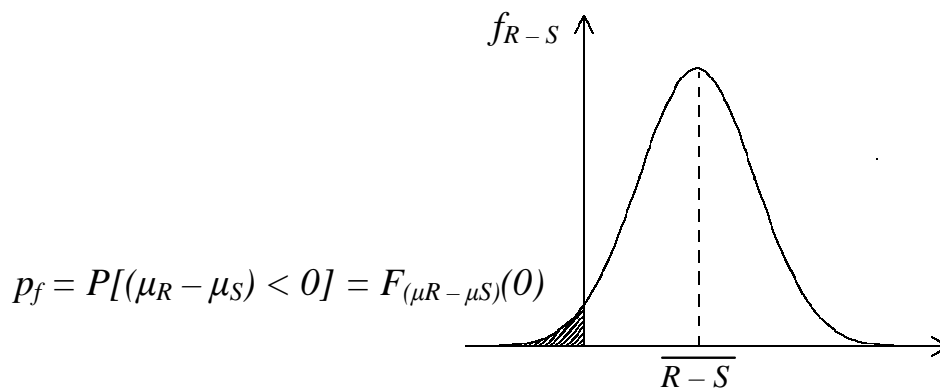


Figure 6.11 – Safety margin distribution and failure probability definition



This way of looking at the safety assessment procedure, within a bridge structures context, will be largely influenced by two important aspects. The first, and the most important one, has to do with the random simulation algorithm, used to build the samples for each variable that cares for statistical characterization. The procedure herein chosen was the Latin Hypercube sampling method, as an alternative to the pure Monte Carlo sampling scheme, and will definitely influence the significance of the results, being important to avoid biased samples, as a warranty of data consistency. The more solid the simulation algorithm is, the more reliable the findings will be, given that widely representative samples, for intensity level, for instance, will be needed to assure that the structure will be pushed to its limits. Additionally, such approach will be extremely sensitive to the type of distribution that is assumed for the variables, mainly the ones on the seismic action definition side, type of record and intensity level. Whereas the first may be characterized through a uniform distribution, the latter is usually described by extreme value distributions, which are known to be susceptible when working on the tails region, essential for the failure probability computation – see Figure 6.11.

### **6.1.8 Reliability index**

As a complement to the safety assessment and to soothe eventual lacks of accurateness, associated to the collapse probability being given by the area under the probability density function, other safety measuring parameters may be taken into account. An example of such indirect safety measures is the reliability index,  $\beta$ , which essentially settles on the distance from the mean R–S to the origin, quantified in standard deviations of the variable R–S, according to Equation (6.13).

$$\beta = \frac{\overline{R-S}}{\sigma_{R-S}} \quad (6.13)$$

Within such definition, which considers the mean safety margin together with its dispersion, the smaller the value of the reliability index the higher the probability of failure will be.

Moreover, the convolution integral computation might not be, for some cases, at least, an easy task, leading to the need for a numerical solution. The use of this indirect evaluation parameter becomes, for that reason, at least, appropriate. Reliability index can also be easily related to central factors of safety.

## **6.2 Application to a set of bridges**

The performance comparison of the several safety assessment methodologies will be, again, carried out using the set of bridge structures and real earthquake records described in Chapter 4, Section 4.3. Three different versions for the failure probability computation will be considered: traditional numerical safety assessment with nonlinear dynamic analysis of structural effects (NSA-NDA), using plastic hinge models of the bridge configurations (faster and validated in Chapter 4); traditional numerical safety assessment with a nonlinear static procedure (chosen from the possible alternatives validated in Chapter 5) to estimate structural effects (NSA–NSP) and safety assessment based on global simulation with Latin Hypercube sampling (LHS).

Prior to the safety assessment itself, a brief calibration study is, however, carried out with the main purpose of defining the parameters for the application of the simulation technique, the Latin Hypercube, which is fundamental. Among others, the number of realizations or the relative importance of the different input basic variables on the capacity computation, are aspects that are worth looking into, so as to optimize the use of the algorithm. Such sensitivity analysis gains special relevance for the particular context of structural nonlinear analysis of bridges (Monteiro *et al.*, 2009).

Random simulation is used twice within the current endeavour. First, and commonly to all the approaches, it is used to build the capacity distribution, based on the repeated computation of the available ductility of the cross section at the base of the piers, based on equal number of realizations of the relevant concrete and steel tensions and strains. Furthermore, sustaining the LHS approach, the variables intensity level and type of record are added to the hypercube and N nonlinear dynamic analyses, equal to the number of realizations, are conducted.

### 6.2.1 Latin Hypercube sampling in capacity definition

The capacity definition, when made up in terms of available ductility in curvature of the piers cross section, settles on the geometric characteristics and material properties, the steel and concrete stress-strain models. For a given cross section, with a certain axial load, the cracking, yielding and ultimate points of the monotonic moment-curvature diagram are determined using well known criteria for the mentioned stages definition, by means of a fibre-type section discretization. The variability in material properties is, however, widely recognized as typically significantly higher than uncertainty surrounding section dimensions (Grant *et al.*, 1978; Frangopol *et al.*, 1996). The parameters that are admitted to assume relevant variability are, therefore, the concrete peak stress,  $f_c$ , steel yielding stress,  $f_y$ , and corresponding ultimate strains,  $\varepsilon_c$  and  $\varepsilon_s$ . A normal distribution is adopted for each of the variables with mean values corresponding to the material class. Different scatter levels are assumed, characterized by increasing coefficients of variation, 5%, 10% and 15%, for all the variables at once, or individually to better scrutinize their relative importance in the ductility computation. At the same time, the number of realizations needed to stabilize the result is sought, for each of the dispersion levels. The parametric study will focus, hence, the significance of the input variable, the corresponding coefficient of variation and the number of realizations.

The plot on the left of Figure 6.12 illustrates the evolution of the mean value of the computed ductility for the section of one of the piers, intermediately axially loaded. Five representatives sampling sizes have been chosen: 20, 50, 100, 200 and 500. Both of the parameters, coefficient of variation and number of realizations, denote a similar tendency for the mean ductility to become completely stable for 200 realizations. The same trend is found when the COV results are looked at. It seems however acceptable the use of 100 realizations as sample size, given that dispersion is not that considerable, neither across input variables COVs nor sample size.

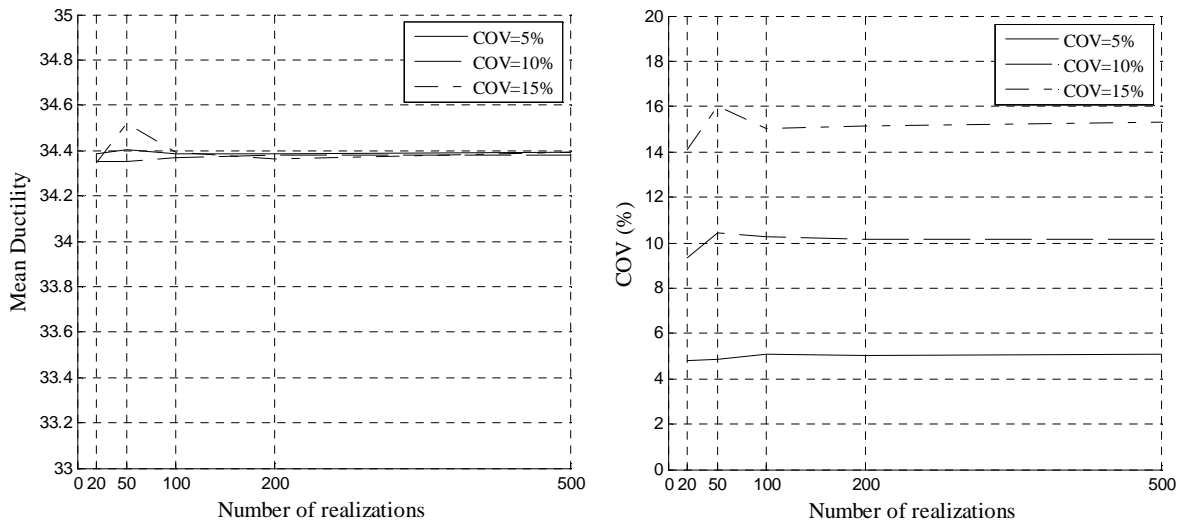


Figure 6.12 – Mean available ductility (*left*) and corresponding COV (*right*) versus number of realizations for different coefficients of variation.

The ability of the method to build reliable samples is defined, on the one hand, in terms of the necessary number of realizations to assure representativity, whereas, on the other hand, one can question the robustness of the method for successive repetitions of the procedure. In other words, there is the concern of wondering if two samples of the same size, independently obtained, will have sufficiently close mean numbers. In order to check on whether such aspect is pertinent or not, the procedure originating the results in Figure 6.12 *left* has been repeated ten times, recording the history of mean values for ultimate ductility along with sampling size. The results for the different considered COVs are plotted in Figure 6.13.

It is evident from the observation of the plots that, especially for the lower COVs, 5% and 10%, 100 realizations, or even 50, will be enough for the variation of the mean ductility across repetitions of the simulation algorithm to lose significance. The worst scenario is definitely for the case of only 20 realizations, for a COV of the input variables of 15%, for which variation is, anyhow, less than 1%. The main conclusion is thus that, for what concerns the trustworthiness of the procedure, oscillation of mean values between repetitions is not relevant. This sort of variability will be further investigated when using the LHS procedure for direct obtainment of the failure probability through the safety margin.

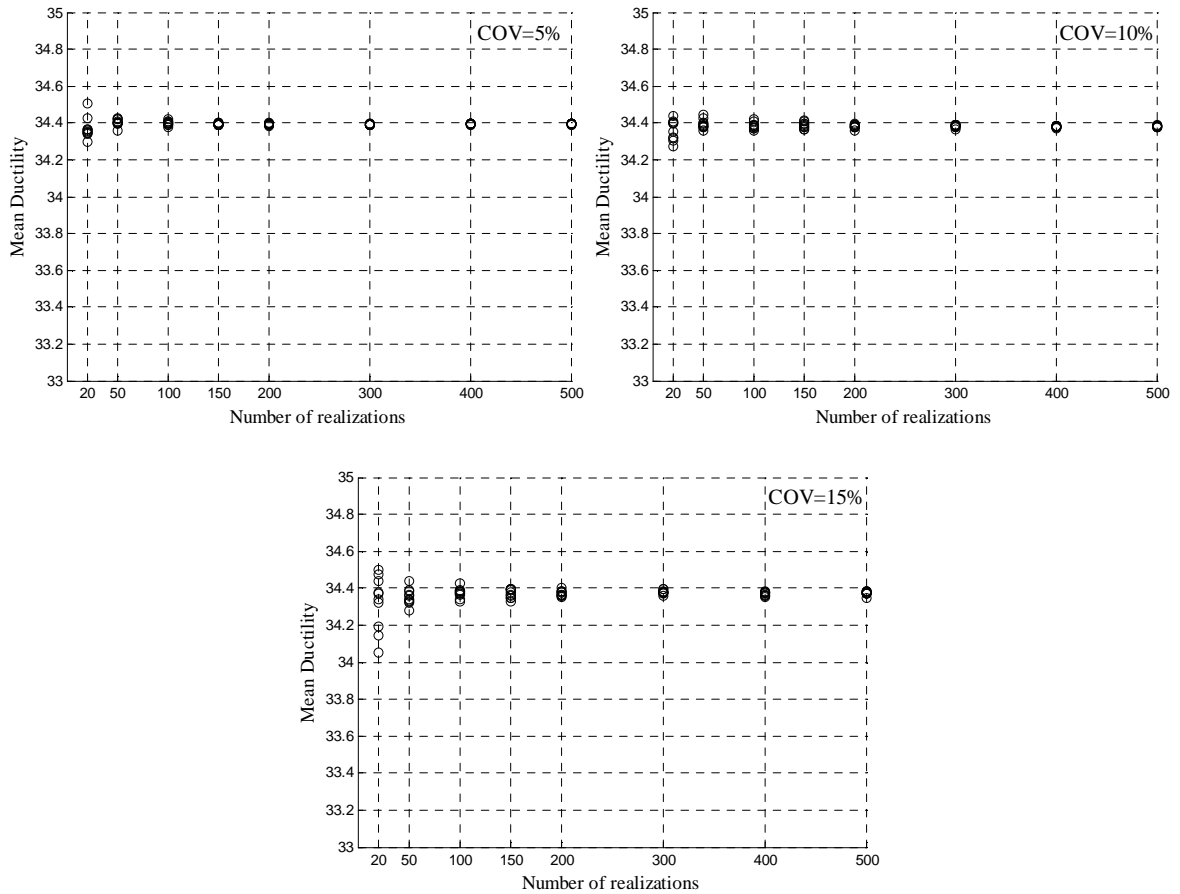


Figure 6.13 – Mean available ductility versus number of realizations for several sampling repetitions and different input variables COVs.

If each variable is considered to be the only one with known standard deviation, while the remaining are kept constant with the mean value, its relative influence in the final result, the ductility, in this case, can be studied, as in Figure 6.14.

From the observation of the results, the ultimate curvature of the piers cross sections comes out as fundamentally dependant on the steel ultimate strain. Not only the coefficient of variation reaches a peak value, but also the scatter among different numbers of realizations is higher, when just the scatter in  $\epsilon_y$  is considered. Such trend is not found for any of the other variables, but only when all are considered to have the same dispersion, which denotes that failure of the section is being caused by the reinforcement.

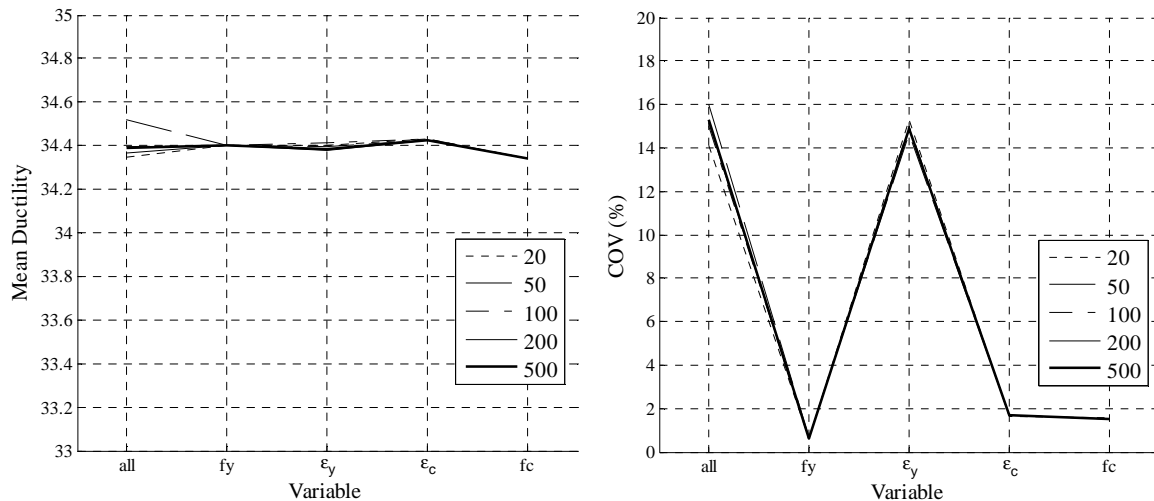


Figure 6.14 – Mean available ductility (*left*) and corresponding COV (*right*) for different numbers of realizations according to the dispersion of input variables.

A limitation of such preliminary plots is the fact that equal standard deviation, or COV, has been assumed for all the four basic input variables, tensions and strains, when it is well known that concrete related variables present larger uncertainty when compared to the steel ones. Some studies have been carried out in the past with the purpose of quantifying uncertainty in nonlinear behaviour of reinforced concrete members. One of those studies, (Kappos *et al.*, 1999), focused, partially, at least, the quantification of variability in input parameters, namely, the material properties. The model uncertainty in commonly used confinement models was quantified and introduced in probabilistic modelling of members' ductility, through fibre model analysis. Such work goes along with the approach followed herein that uses the available curvature ductility of the cross sections to assess the failure probability.

For what concrete related variables are concerned, the ultimate concrete strain deserved particular scrutiny, given that it has been considered by the authors as often the governing parameter influencing failure, when it comes to ductility. Such strain, predicted by a confinement model, is assumed as the one corresponding to  $0.85f_c$ . The approach that was followed to estimate variability in such parameter consisted in comparing analytical values of  $\epsilon_{cu}$  given by currently adopted models (Park *et al.*, 1982; Scott *et al.*, 1982; Sheikh and Uzumeri, 1982; Kappos, 1991) with results from experimental tests (Vallenas *et al.* (1977), Sheikh and Uzumeri (1980), Scott *et al.* (1982) and Moehle and Cavanagh (1985)) and get the uncertainty from there. The amount of scatter that has been encountered in comparison

ratios is considerable, with COVs ranging from 32 to 36%, even if mean values are very close to unity, confirming  $\varepsilon_{cu}$  as highly uncertain. As for the concrete compressive strength,  $f_c$ , referring to cylinder measures, a study of Barlett and McGregor (1996), specifically on this matter, has come up with COVs around 18%. For both of these concrete-related variables, as typically occurs, a normal distribution has been assigned. Analogously, the same characterization needs to be done regarding steel parameters, knowing in advance that scatter will be certainly lower. The work carried out by the Joint Committee for Structural Safety (JCSS, 1995) and by Pipa and Carvalho (1994) on variability for tempecore steel in various European countries indicate a value of 6% for the yielding and ultimate steel strengths,  $f_y$  and  $f_u$ , COV and 9% for the ultimate strain,  $\varepsilon_{su}$ , one. A normal distribution is again currently admitted for the parameters.

Table 6.1 indicates the assumed coefficients of variation for the intervening material properties, which have been defined according to what is proposed in (Kappos *et al.*, 1999), except for the concrete ultimate strain, that has been reviewed into a slightly lower amount.

Table 6.1 – Admitted coefficients of variation (COV) of material properties.

Parameter	COV (%)
Concrete ultimate strain ( $\varepsilon_{cu}$ )	30%
Concrete compressive strength ( $f_c$ )	18%
Steel ultimate strain ( $\varepsilon_{su}$ )	6%
Steel yield strength ( $f_y$ )	9%

If the parametric calibration is now conducted considering the dispersion levels just presented, new plots for the behaviour of the mean ductility numbers for different sample sizes can be obtained. Even if the admitted dispersion is considerably different, the plots in Figure 6.15 denote results that are rather smooth. The tendency previously found, that 200 realizations is the needed number of realization for the mean to stabilize, still stands. Analogously, and even surprisingly, the resulting COV for the available cross section ductility is extremely steady around 10%. Nevertheless, such findings may be understood by recalling that, according to results in Figure 6.14, the variable with higher influence is the steel ultimate, which assumes a significantly low coefficient of variation whereas the variables with higher uncertainty, the concrete ones, in turn are not so relevant for the

ductility estimation of the hollow sections in consideration. It seems therefore logical that the results are little or not worsened at all by the changes.

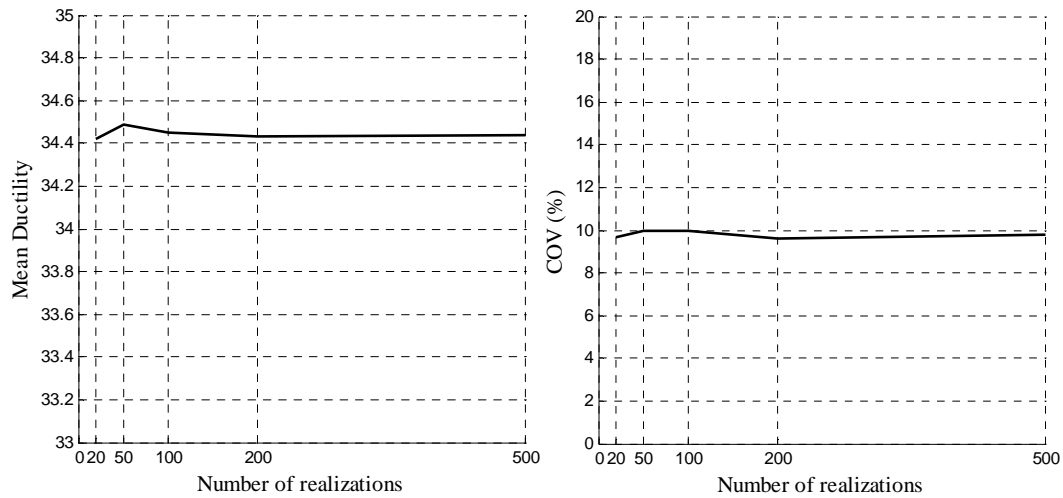


Figure 6.15 – Mean available ductility (left) and corresponding COV (right) versus number of realizations.

Regarding the variability of the sampling method within several repetitions, illustrated in the plot of Figure 6.16, the main previous observations can still be made, reinforcing the conclusion that from 200 realizations on, expect for one or another punctual occurrence, the steadiness of results is noticeable, in both senses of the variability.

According to the brief parametric study, within the subsequent applications, the capacity of the piers cross sections has been characterized using samples of 200 occurrences.

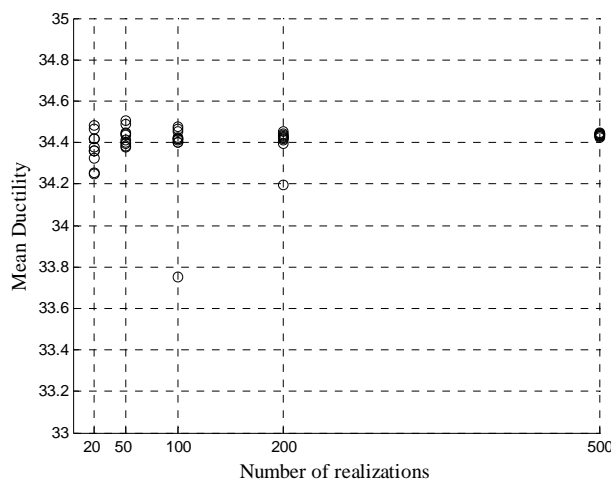


Figure 6.16 – Mean available ductility versus number of realizations for several sampling repetitions.



### 6.2.2 Seismic action probability density function

The seismic intensity level has been set in terms of peak ground acceleration (PGA), which, according to the major observations made in Chapter 3, together with spectral acceleration intensity measure, leads to the less scattered mean estimates when using real records. Nevertheless it does indubitably disregard specific information on the earthquake record, which will surely introduce limitations on following calculations. In line with this approach, a seismic scenario in terms of probability density of peak ground accelerations for a specific region needed to be chosen. The seismic action probability density used in this framework is based on the studies of Duarte and Costa (Duarte and Costa, 1991; Costa, 1993), where seismic conditions for the Portuguese regions were idealized by means of a source-zones model with non-radial attenuation functions. Two types of earthquake scenarios are considered, according to what is expected for Portuguese seismicity, corresponding to nearby moderate magnitude (type 1) and long distance large magnitude (type 2) earthquakes (Costa, 1993). A hazard model for a period of 50 years was adopted, calibrating parameters  $\mu$  and  $\sigma$  for the type I Gumbel distribution, as detailed in Section 6.1.1, from numerical results obtained from source-zones models:  $\mu = 87.36\text{cm/s}^2$  and  $\sigma = 1/0.00225$  for type 1 and  $\mu = 60.5\text{cm/s}^2$  and  $\sigma = 1/0.0031$  for type 2. Figure 6.17 plots the assigned distributions.

It is important to bear in mind that the probability density function is defined with respect to the probability of exceedance of the PGA parameter, which enables that any set of earthquake records are used, as long as referenced to their PGA. Such approach will almost certainly be seen as limited, relying on the strength of the defining parameter. The selected records will be therefore scaled to match the peak ground acceleration level given by the extreme value distribution.

It seems evident, however that the seismic scenario representing the Portuguese hazard is not particularly demanding, which will possibly not take the bridges response into high nonlinear stages. The probability density function has therefore been adapted in order to allow the structural response to be clearly nonlinear, so as to fully understand the performance of the different assessment techniques. Moreover, the nature of the parametric study that is herein conducted is essentially comparative, in terms of distinct procedures and different bridge configurations, rendering the probability density function somewhat

irrelevant, as long as the intended comparison purpose is fulfilled. The final adopted distribution for the seismic intensity is plotted in Figure 6.18, in comparison with the Portuguese ones, and was calibrated with the intent of higher probability density peak at higher peak ground acceleration, higher  $\mu$ , together with lower dispersion, lower  $\sigma$ .

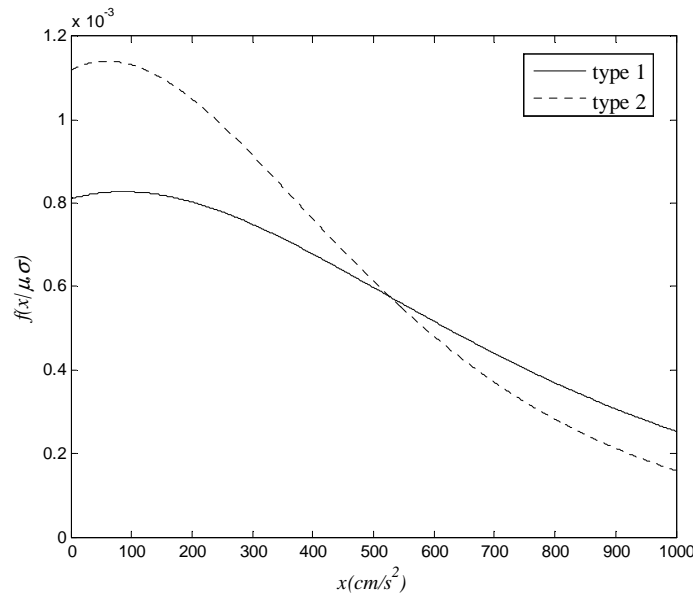


Figure 6.17 – Probability density function (extreme value Type I, Gumbel associated) for two expected Portuguese earthquake scenarios.

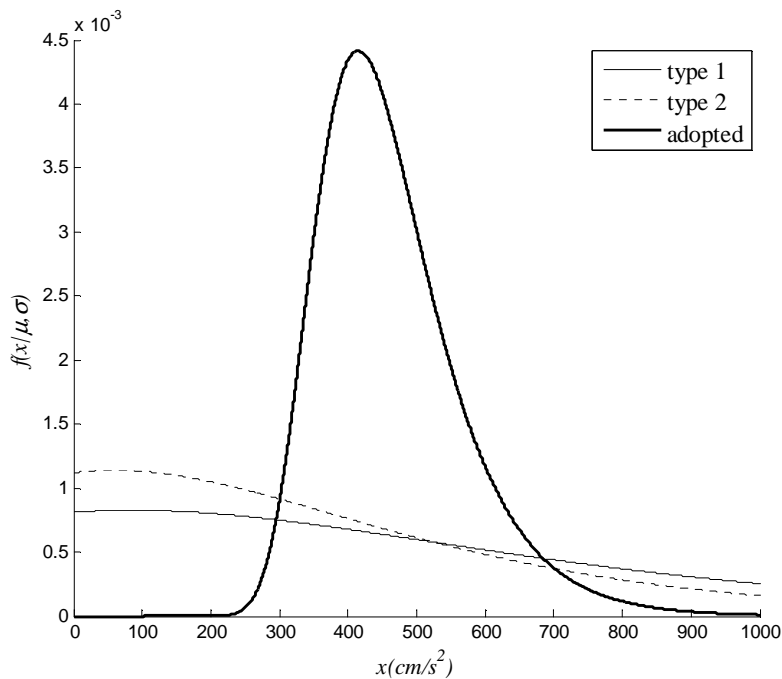


Figure 6.18 – Adopted probability density function (extreme value Type I, Gumbel associated,  $\mu = 415cm/s^2$  and  $\sigma = 0.012$ ).

### **6.2.3 Failure probability with traditional NSA approach**

Within this approach, the vulnerability function will be the main needed element, given that the failure probability is computed considering the uncertainty locally, characterizing the structural response for the entire domain of the intensity level distribution (see Section 6.1.5) in terms of measured curvature ductility,  $\mu$ , at the base of the piers. According to Section 6.1.4, the vulnerability function may be built up from nonlinear dynamic analysis or from pushover analysis, within a nonlinear static approach. Results from the application of both possibilities come in what follows.

#### **6.2.3.1 Vulnerability function from nonlinear dynamic analysis**

The domain of the probability density function has been taken as from 0 to 1000cm/s<sup>2</sup> and discretized in steps of 100cm/s<sup>2</sup>. At each step, that is, each intensity level, each of the ten real earthquake records (SAC, 1997), identified in Section 4.3, was scaled so that its individual PGA would match that specific level. Nonlinear dynamic analysis using those records was run, and the ductility in curvatures was measured at the base of each pier (the piers in short configurations will be named from P1 to P3 and in long configuration from P1 to P7). Due to the main drawback in using dynamic analysis with real ground motion records, which is the scatter associated, for a given intensity level, different response measures will be obtained from the accelerograms of the selected ensemble and the dispersion is indeed usually high. The procedure that has been adopted was to take the mean of the ductility observations and adjust the polynomial vulnerability function to those quantities. The fitting is carried out to a 2<sup>nd</sup> degree polynomial by means of the least squares method. In order to comply with the boundary conditions of the real problem, the curve will cross the origin of the (PGA, $\mu$ ) coordinates system, given that nonzero ductility makes no sense for zero intensity. This condition will surely affect the curve fitting but the quality of the adjustment is, however, in general, rather good, something that can be seen in Figure 6.19 and Figure 6.20.

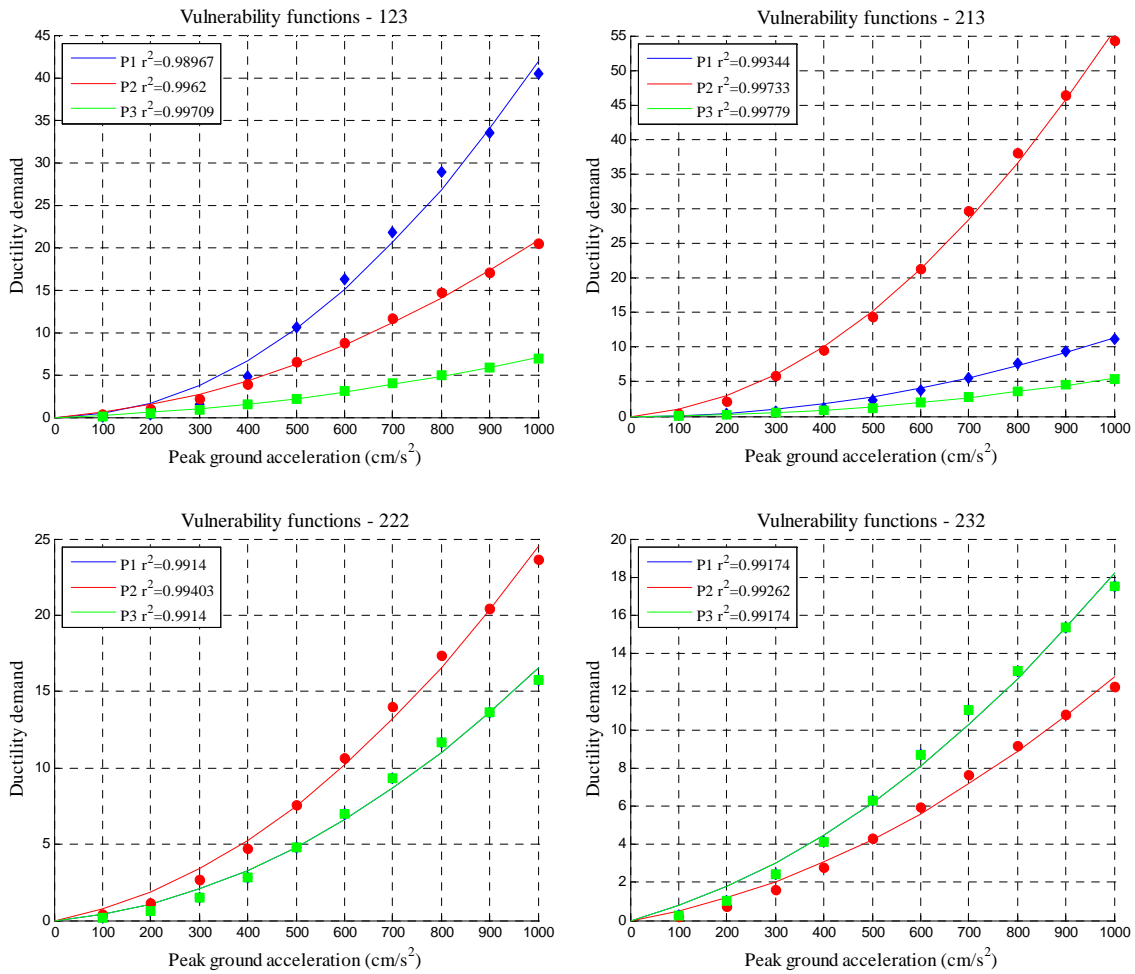


Figure 6.19 – Pier vulnerability functions for short configurations.

The observation of such plots lead to the immediate conclusion that the adjustment is fairly accurate, which sometimes is even more relevant for higher intensity levels. Indeed, regardless the type of configuration, in terms of length or regularity, or the height, position or stress level of the pier that is being considered, the correlation coefficient,  $r^2$ , is always extremely close to one.

As for the information on the seismic, transmitted by the vulnerability functions, piers in short bridges tend to absorb higher ductility levels, which is expected, in the sense that a shorter deck will probably indicate a stiffer bridge. Within the same configuration, the central piers or the 7m ones, the lower, repeatedly correspond to the upper curves, the ones corresponding to higher ductility demand. On the other hand, irregular configurations are

generally more affected by the seismic action, given that the demand is approximately the double, or even more, that the regular ones’.

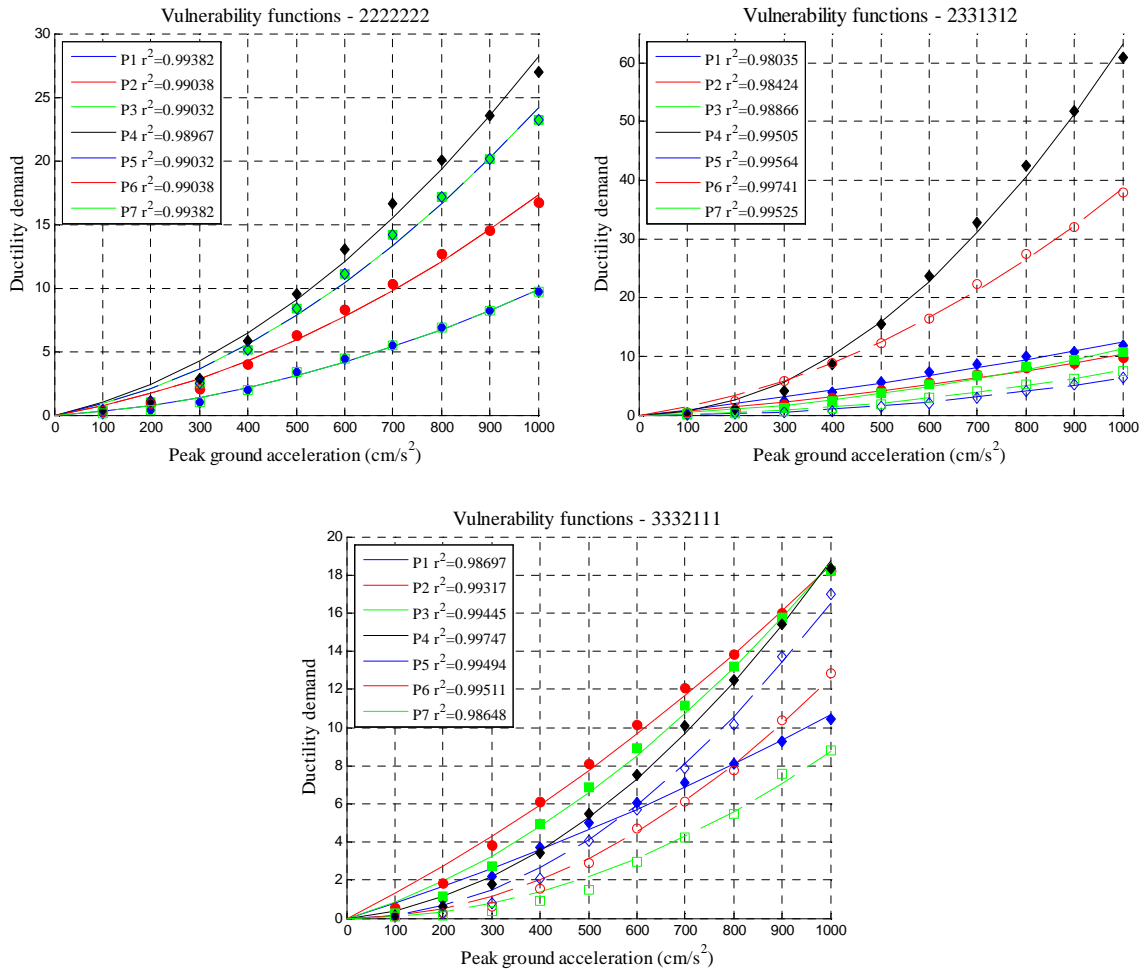


Figure 6.20 – Pier vulnerability functions for long configurations.

In one of the long configurations, the 3332111 one, an inversion of the relative placement between the vulnerability functions occurs. The ductility demand for piers P4, P5 and P6 increases significantly, becoming higher than the P1 one, which was superior for low intensity. Such apparently minor finding may become actually quite important, depending on the position of the seismic action probability density function. A pier with higher ductility demand for the highest intensity levels may be safer than the rest in a seismic scenario where low peak ground accelerations are more likely to occur.

At this point, it should be recalled that the vulnerability functions are given by polynomials fit to the mean of the ductility demands, coming from the dynamic analyses with the ten

real accelerograms. It has been, as a matter of fact, encountered high dispersion in such predictions, of different earthquake records, even if their peak ground accelerations have been standardized to the same amount. Figure 6.21 and Figure 6.22 plot the ductility demand, at each configuration, for the pier at highest load, when subjected to each of the ground motion records.

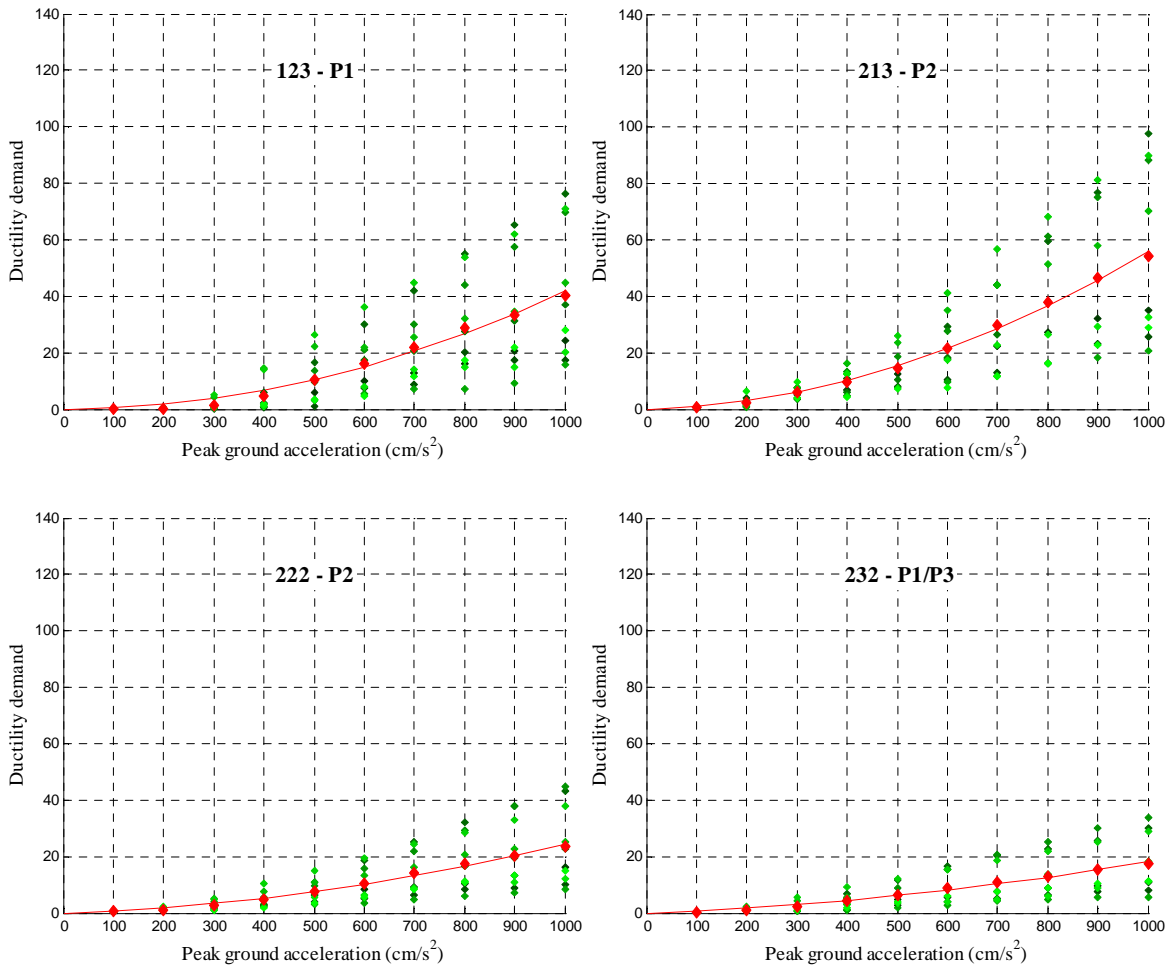


Figure 6.21 – Ductility demand for short configurations.

The scatter is rather visible, and seems more noticeable for irregular bridges, where the ductility demand is higher, which seems expectable. Dispersion increases significantly with intensity, given that the higher the nonlinearity level, the more diverse the different earthquake records response predictions will be. The different coloured dots, corresponding to the different accelerograms, show, additionally, that the records invert positions for different intensity levels. There is, unequivocally, great variability

intrinsically associated to the seismic action. This internal uncertainty, referring to record-to-record or scaling technique variability, is much more significant than the one associated to the intensity level one. The main analysis outcome, the failure probability, will certainly be largely influenced by such parameter.

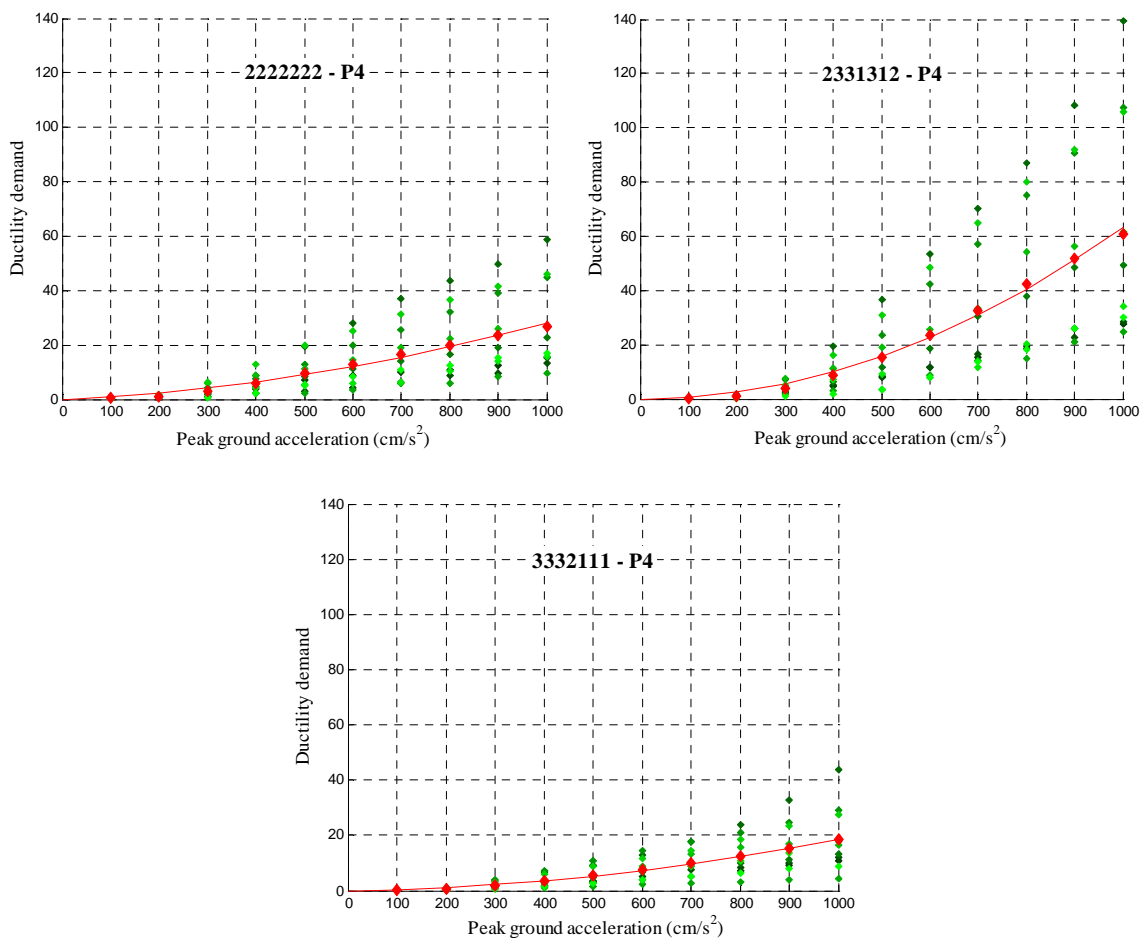


Figure 6.22 – Ductility demand for long configurations.

Another possible glimpse at the seismic action related variability is the plot of the vulnerability functions that correspond to seismic demand coming from the real accelerograms. Figure 6.23 and Figure 6.24 illustrate those functions, again for the piers with highest demand per configuration. The observations previously made still stand, with the dispersion being highly visible for the irregular and short configurations. In such cases, the predictions for the ductility demand may exhibit fluctuation between 100% under and above the mean values, at the maximum considered peak ground acceleration of 1g, approximately. The mentioned inversion of relative placement between the vulnerability

functions positions is additionally found when moving from one accelerogram to another. The global picture is the reinforcement of the awareness of the variability related to the seismic effects.

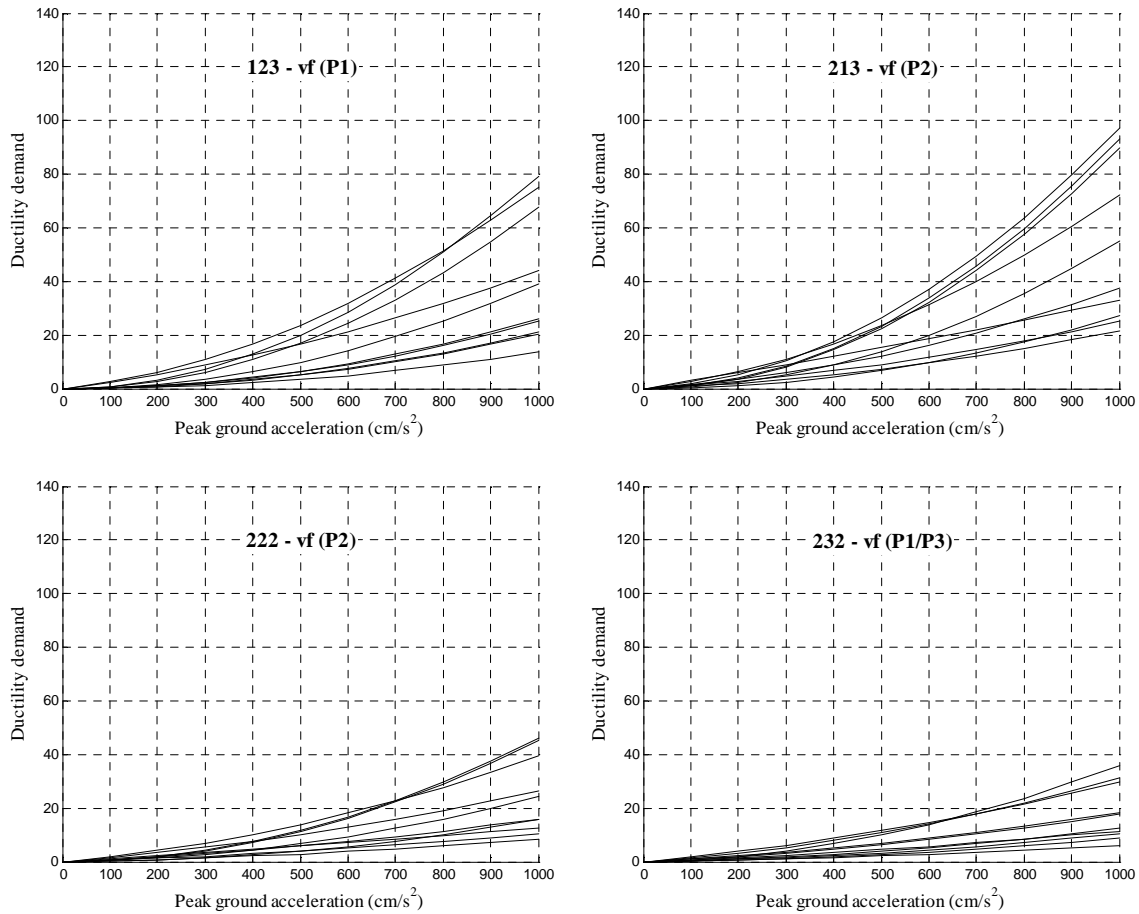


Figure 6.23 – Vulnerability functions for short configurations using different ground motion records.



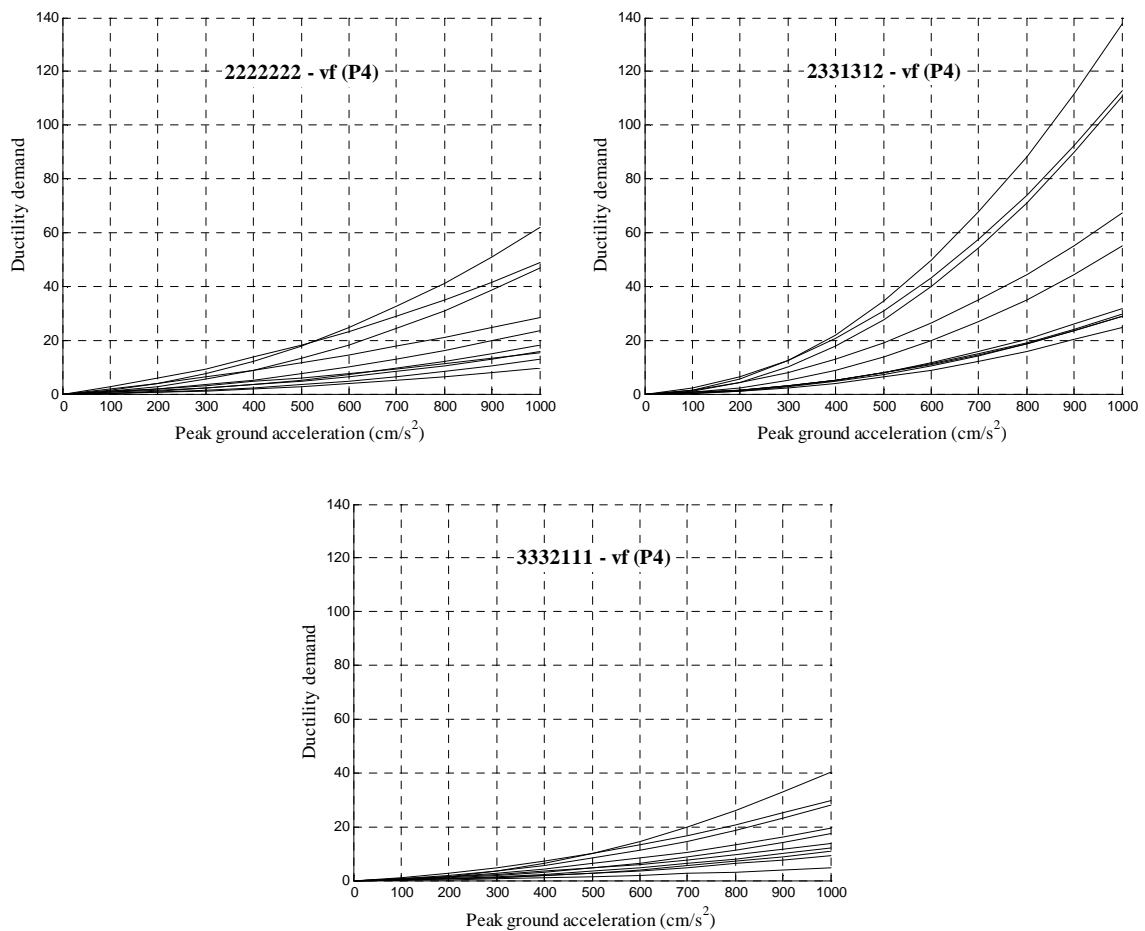


Figure 6.24 – Vulnerability functions for long configurations using different ground motion records.

### 6.2.3.2 Vulnerability function from nonlinear static analysis

As an alternative to the long dynamic analysis traditionally used to predict the seismic structural effect and, consequently, define the vulnerability function, pushover analysis may be used instead. Within a predefined nonlinear static procedure, for each intensity level, herein expressed in peak ground acceleration, the structure is pushed until a level corresponding to the considered PGA, the performance point is found and the ductility in curvatures is obtained.

As for this matter two sensitive issues arise, possibly compromising the vulnerability functions estimate. The first has to do with the use and validity of nonlinear static analysis itself, a topic that has already been largely discussed, whereas the other refers to the need of associating peak ground acceleration to a specific pushing level. Such task may be

accomplished by means of the response spectrum that is used within the nonlinear static procedure (NSP), which is the way of representation of the seismic action in such sort of methodology. For each intensity level, the response spectrum will therefore be scaled so that its zero ordinate, the peak ground acceleration, matches the intensity at stake. The validity of such approach is logical, but arguable, and shall be taken into account when analysing differences in vulnerability function predictions. Recalling the observations drawn in Chapter 5, any Nonlinear Static Procedure has proved itself as acceptably able to predict the response of structural systems, when subjected to earthquake loading. Consequently, one of the traditional methods, implemented in the European code (CEN, 2005b), the N2 method, has been chosen to obtain pushover-based vulnerability curves. The pushover analysis may be conventional or adaptive (see Chapter 5 for further details) and both possibilities have been used. According to the recommendations on the application of the N2 method, two loading distributions, uniform and 1<sup>st</sup> mode proportional (*mod* and *uni*), shall be tested. Additionally, two reference nodes have been considered: centre of mass of the deck and maximum modal displacement (*centr* and *max*), leading to a total of four variants using conventional pushover and one corresponding to the adaptive pushover, which skips the need for a reference node or load pattern.

The comparison between the vulnerability functions, coming from the different types of static analyses, is represented, together with the dynamic analysis one (NDA), for each of the tested configurations, from Figure 6.25 to Figure 6.31.

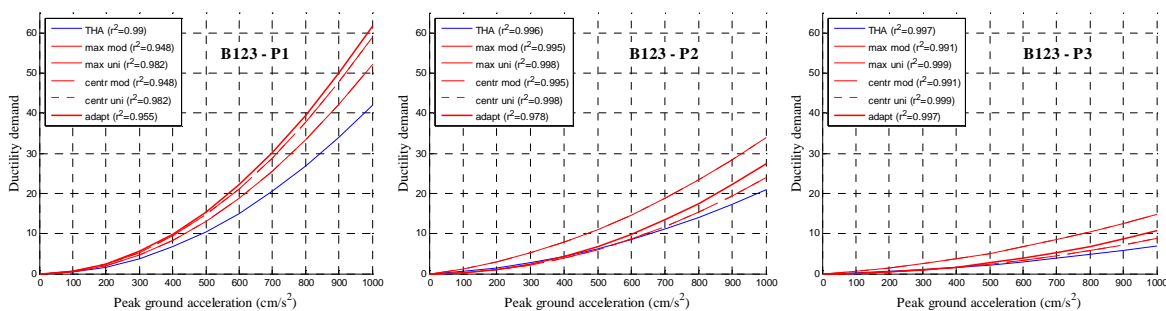


Figure 6.25 – Vulnerability functions according to different approaches – configuration 123.

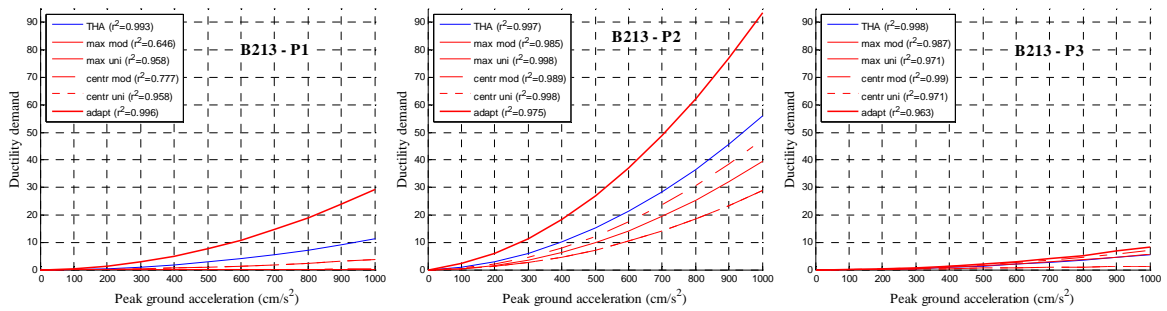


Figure 6.26 – Vulnerability functions according to different approaches – configuration 213.

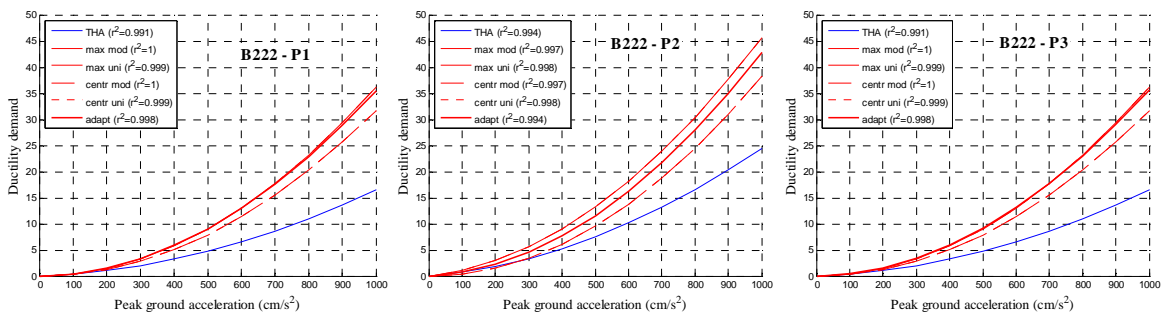


Figure 6.27 – Vulnerability functions according to different approaches – configuration 222.

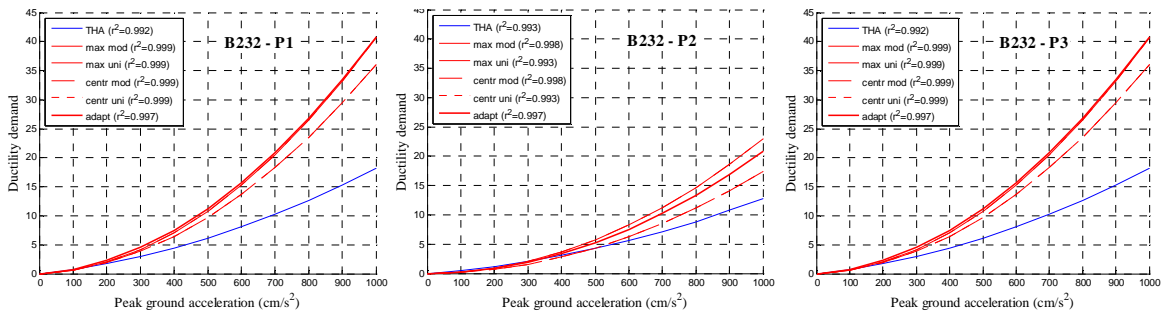


Figure 6.28 – Vulnerability functions according to different approaches – configuration 232.

The observation of the plots referring to the short configurations denotes the particular finding that pushover-based vulnerability functions are, generally, conservative, overpredicting the dynamic analysis ones, regardless the location of the pier that is being observed or the ductility level. This tendency is, nevertheless, more evident for regular configurations where, curiously, the nonlinear static predictions and the nonlinear dynamic ones are less in agreement. Within each configuration, the agreement between different

curves seems to be worse for the pier with higher ductility demand, especially visible for the configuration 123, 213 and 232, where the differences among piers are higher.

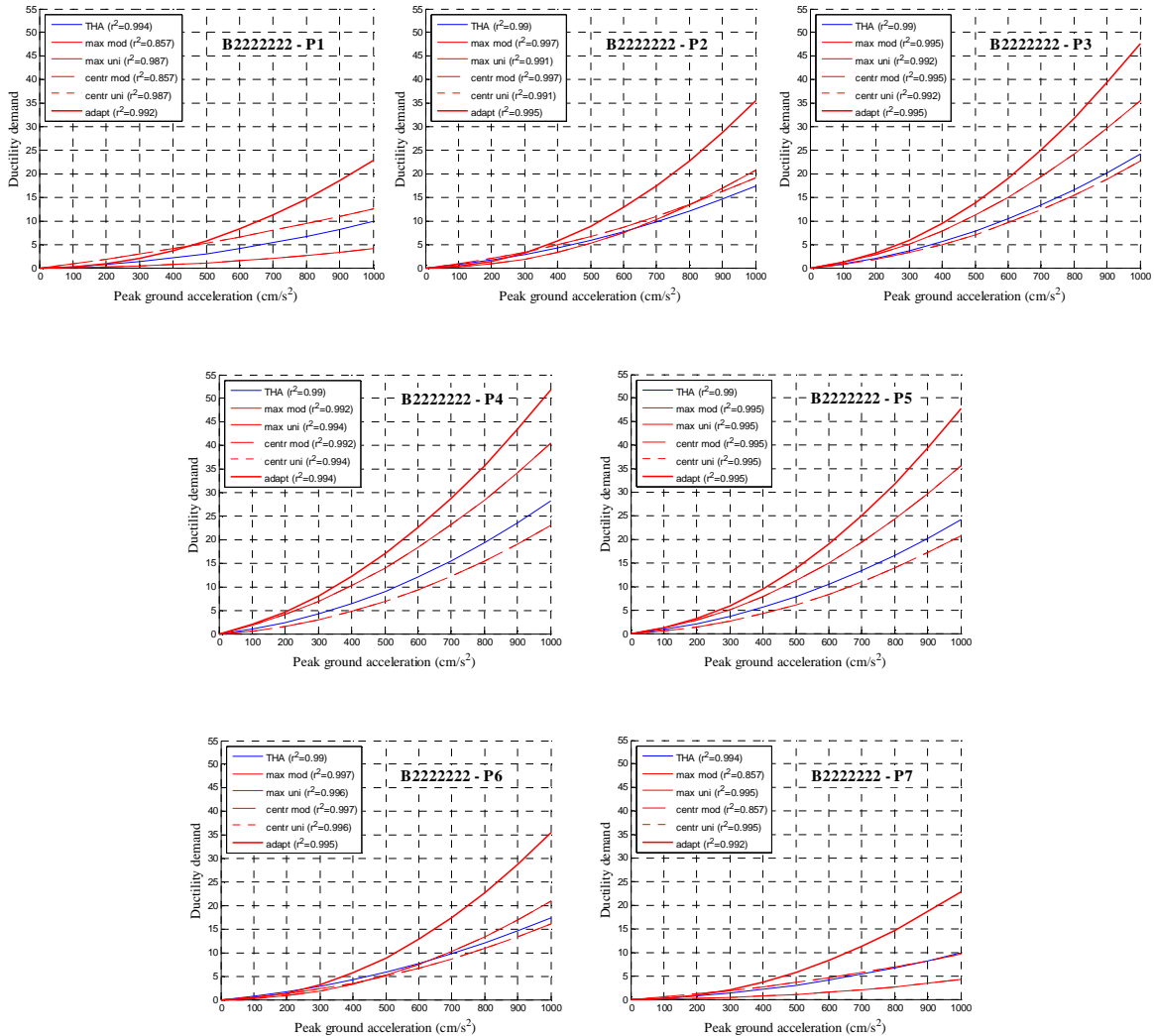


Figure 6.29 – Vulnerability functions according to different approaches – configuration 2222222.

As for the differences between the several pushover approaches, the adaptive analysis is recurrently the most conservative, being actually the only that always overestimates THA, an effect that is even more pronounced for the piers with higher ductility demand. Regarding conventional pushover variants, not much relevant pattern can be found, given that the different versions are not that far from each other, except for the fact that modal loading shape seems to yield more overpredicting results, closer to the adaptive pushover curves. For what concerns long, regular configurations, herein represented by bridge 2222222, the results are not so different from what has been observed for short ones, which

seems, at a certain level, logical, given that the “disruption” introduced by higher deck length is somewhat balanced by the regularity in the piers. The results are, however, steadier from pier to pier, with the previous main observations still standing, regardless of the demand level. Adaptive pushover analysis is again overpredicting, sometimes largely, whereas the different versions of conventional pushover do not diverge considerably, with a tendency for the uniform load shape, together with the centre of mass of the deck as reference node, to work better.

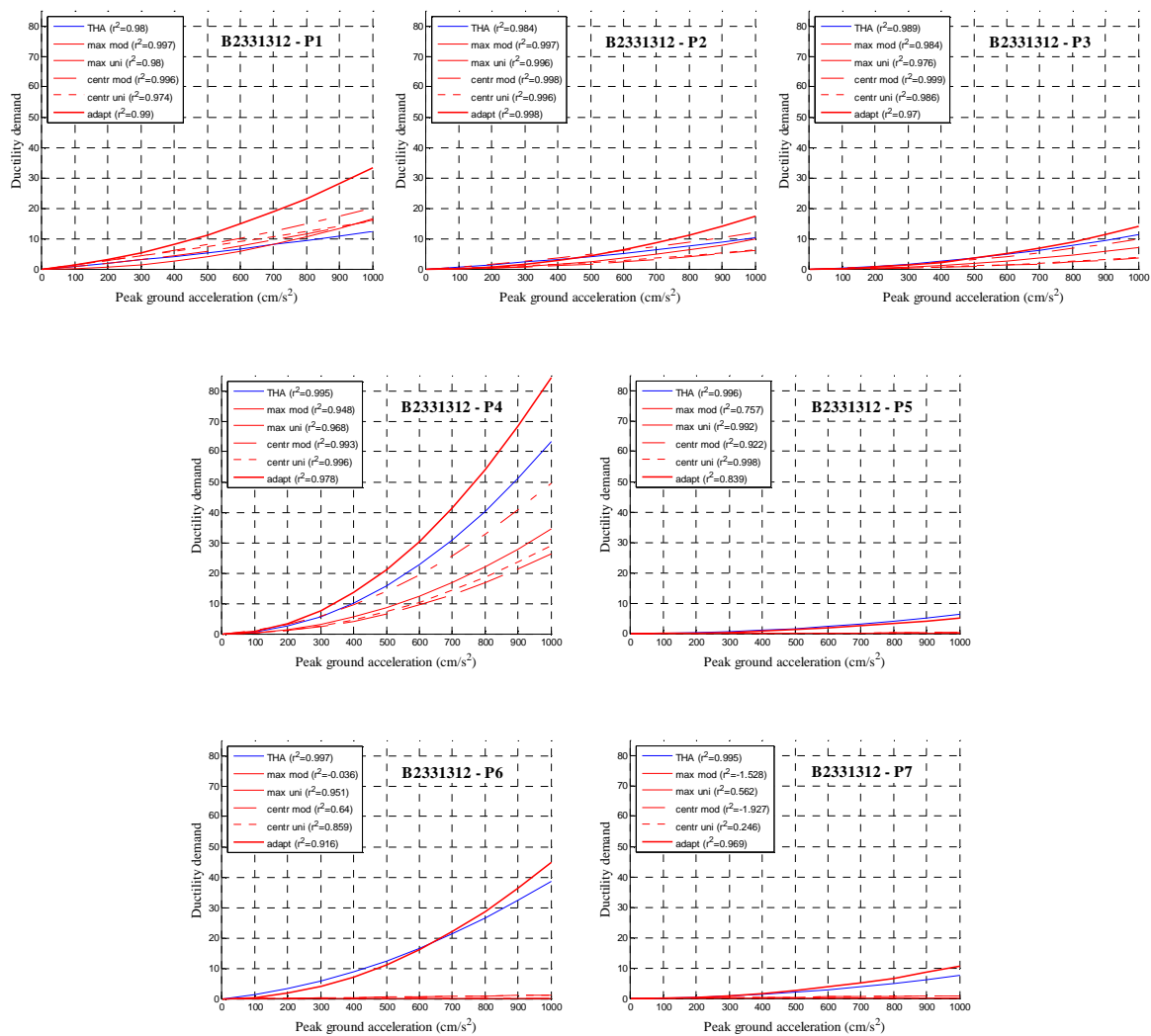


Figure 6.30 – Vulnerability functions according to different approaches – configuration 2331312.

If irregularity is introduced when looking into long configurations, some changes are found in results output, mainly because the differences in the behaviour of the several piers get more pronounced. Even if the adaptive pushover remains overestimating is many

situations, for some piers, such as short ones, near to the abutments, it is actually the only able way to represent the ductility demand using pushover analysis, as in P5, P6 and P7 in 2331312 configuration. For the majority of the remaining piers, the 1st mode proportional load shape version, using deck central node, is the most reliable. It is additionally noteworthy that the critical pier, corresponding to the higher ductility demand, has nonlinear dynamic analysis predictions bounded by those two variants, something that has been verified for all the configurations.

The second long irregular configuration, 3332111, confirms the tendency that has been encountered for the rest of the analysed bridges. The piers P6 and P7, short and close to the abutments are expected to present difficulties in predictions and so it is. For the latter, again, adaptive pushover analysis is the one managing to capture the ductility effects, whereas, for the P6 pier, no pushover analysis works. This is, nevertheless, the only pushover complete inability situation that has been found. Two important aspects shall be taken into consideration herein: overprediction coming from adaptive pushover is not so notorious, a part that is, for the configuration at stake, taken by the conventional modal pushover analysis. It is, however, possible, for a large number of cases, to enclose NDA vulnerability functions by the predictions of the two most promising pushover techniques. For this specific configuration, worst results correspond, in any case, to the piers where the demand is lower.

According to the representation of the several vulnerability functions, considering all sorts of configurations, there is definitely room for the use of pushover analysis for the estimation of ductility demand in the piers. Except for a couple or so of exceptional situations, where adaptive pushover has been the only able to provide acceptable estimations, generally, the simplest approach, that makes use of conventional pushover, is enough to obtain highly satisfactory results, namely for the critical pier.

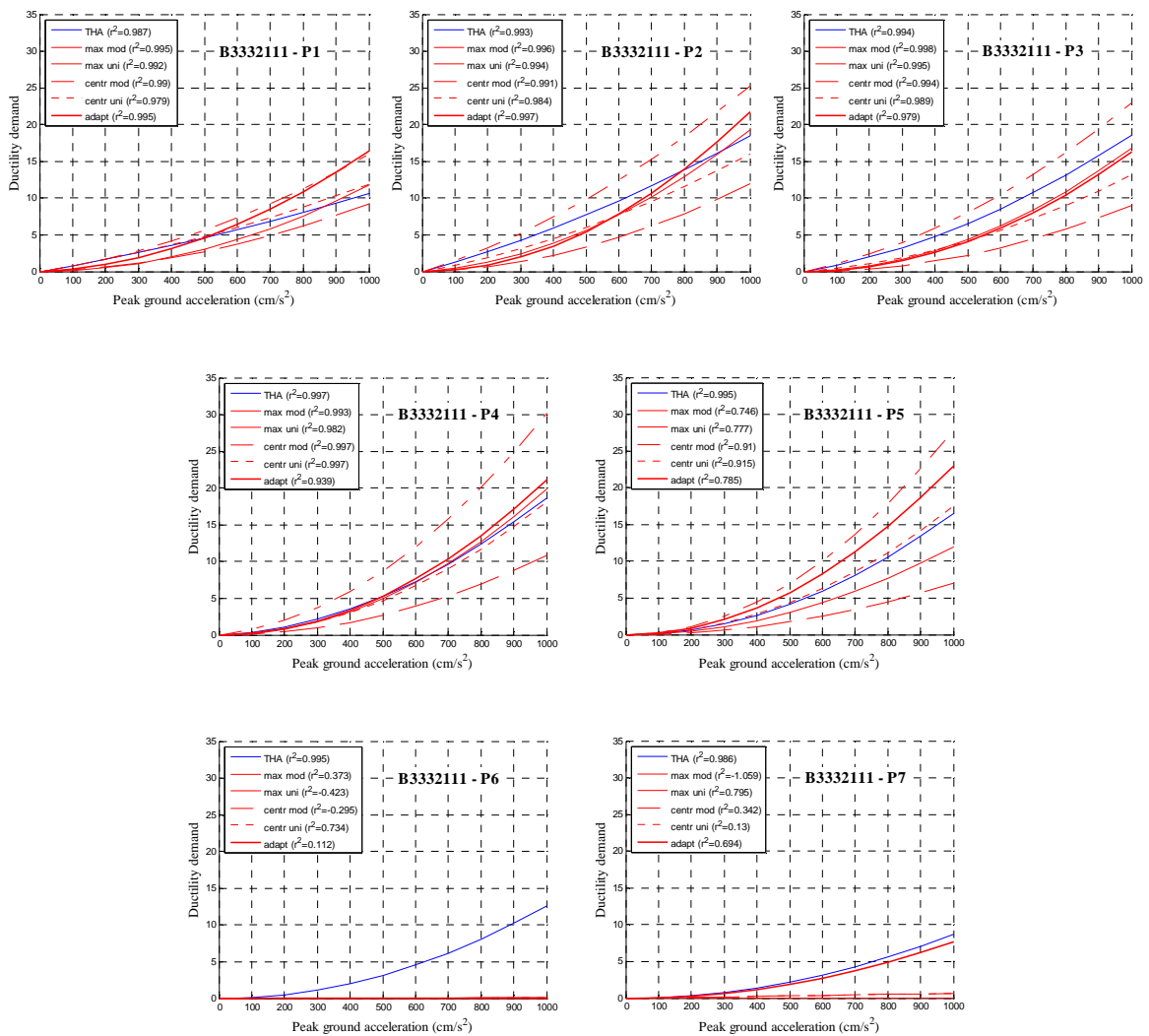


Figure 6.31 – Vulnerability functions according to different approaches – configuration 3332111.

In order to clarify, and to some extent quantify the quality of the different pushover approaches, the results may be presented differently, through the computation of an index able to represent, even if in a median fashion, the accuracy in the predictions for each pier of each configuration. A measure that is easy to compute and actually quite effective, especially when it comes to comparison of different versions, is the root mean square deviation (RMSD). In statistics, the root mean square deviation is frequently used to measure the differences between values predicted by a model or an estimator and the values actually observed, being a good measure of precision. RMSD is given by the square root of the mean squared error, which is given, in turn, by the differences, also called residuals, between observed data and corresponding model prediction. A small MRSD indicates a tight fit of the model to the data. Additionally, in some areas of study, the

RMSD may be used to compare differences between two vectors representing different predictions for the same variable, measuring the distance between oblong objects, expressed by vectors, as in Equation (6.14).

$$RMSD = \sqrt{\frac{\sum_{i=1}^n (\mu_{PUSH} - \mu_{NDA})^2}{n}} \quad (6.14)$$

Herein, the vectors to compare will be seen as the NDA ductility demand values,  $\mu_{NDA}$ , and the several pushover based approaches,  $\mu_{PUSH}$ . This sort of statistical measure will allow the direct numerical comparison of proximity between pushover-based vulnerability functions and NDA ones. Figure 6.32 and Figure 6.33 plot the root mean square deviation based on the predictions for each pier, of every configuration.

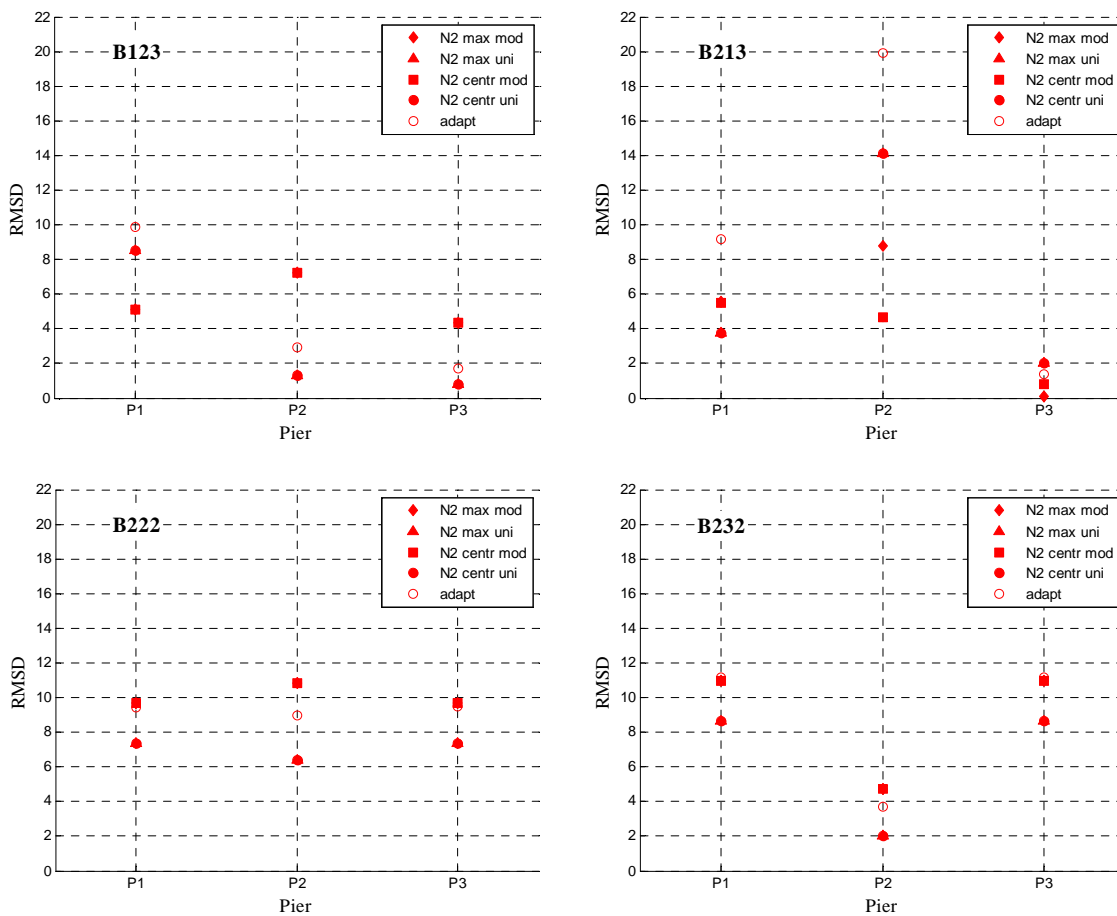


Figure 6.32 – Root mean square deviation for short configurations.



When looking at different versions results for short configurations it is clear to notice that adaptive pushover analysis does not introduce any relevant improvement with respect to the conventional approaches, given that is never the approach with lowest RMSD, independently from the pier that is being considered. Within conventional pushover based approaches, the results from versions that make use of the same load shape come out typically close, which denotes the greater importance of such parameter with respect to the reference node choice. In line with that output, the uniform load pattern generally yields lower residuals, this is, differences between pushover and NDA-predicted ductility demand. However, for irregular short configurations, major discrepancy occurs and, for the critical piers, modal load shape does actually work better, as verified in P1 and P2 in 123 and 213 configurations, respectively, due to their small height together with determinant location. For regular short configurations, the differences between variants are quite less noticeable.

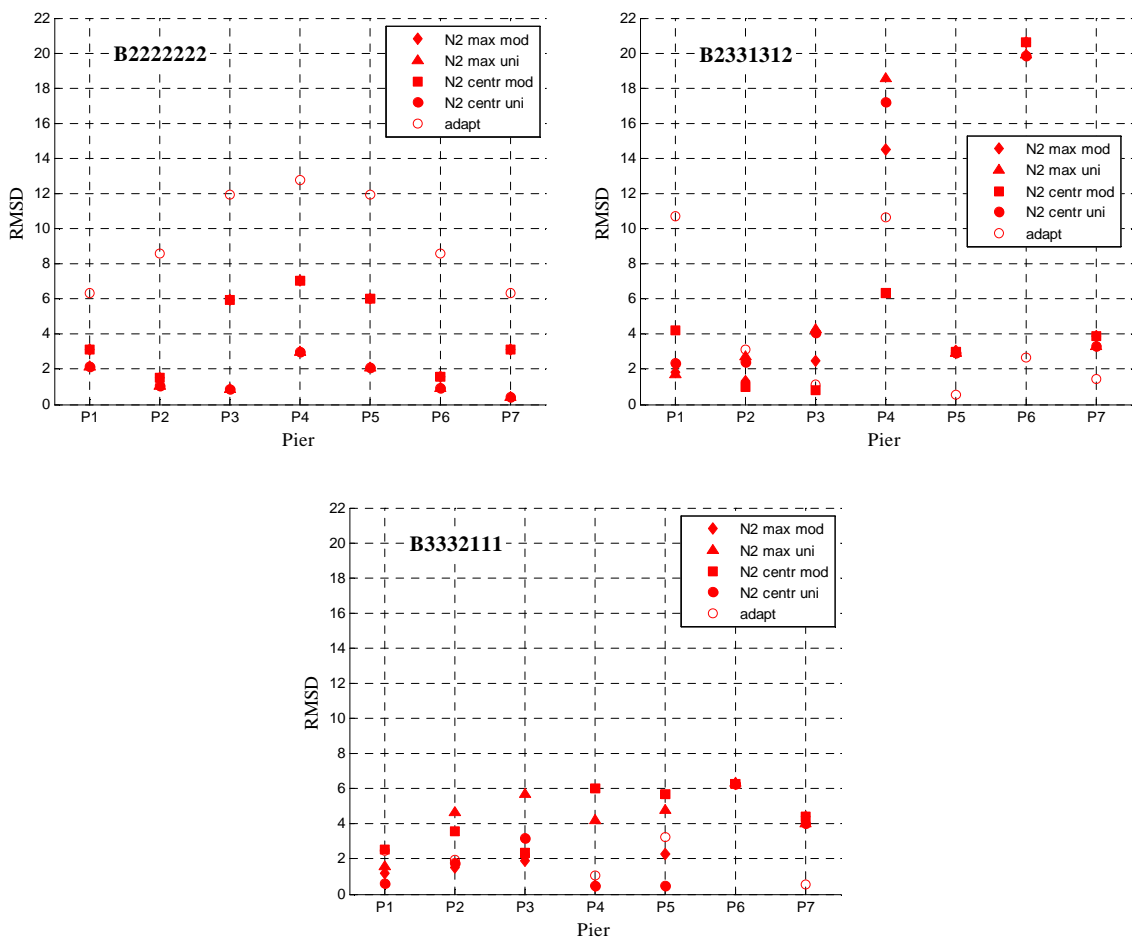


Figure 6.33 – Root mean square deviation for long configurations.

For the case of the long configurations, especially for the two irregular ones, containing short piers, the adaptive pushover usefulness in estimating vulnerability functions is more visible, contrarily to the regular 2222222, where it is always the poorest approach. The best versions correspond frequently, in long configurations, to lower RSMDs, which seems to denote that pushover enables a better to NDA in this sort of bridges. Regarding the rest of the observations that have been made for short configurations, the main conclusions stand. Conventional pushover with uniform load shape is recurrently the best option, with reduced RMSD, whereas the reference node is not a decisive aspect, even if the centre of mass of the deck tends to be a more reliable choice.

The use of pushover analysis in the estimation of vulnerability functions proves itself practical and useful, at least for a quick estimate of the sort of ductility demand level that should be expected for a certain configuration. The use of conventional pushover with 1st mode proportional loading pattern or the consideration of the maximum modal displacement as reference node do not represent, however, worthy alternatives. Adaptive pushover may be used in large configurations, in short, abutment-near piers, so as to complement or even replace unreliable vulnerability functions obtained with conventional pushover analysis.

### ***6.2.3.3 Structural effects and failure probability***

With the definition of the vulnerability function the probability density curve of the structural effects becomes easily obtainable by means of equivalence of areas, as detailed in 6.1.5. The statistical distribution of the seismic effects,  $S$ , used in the computation of the collapse probability of Equation (6.7), becomes therefore defined and able to be used in the numerical process. The cumulative distribution function of the capacity is the crossed with the probability density of the seismic effects, through the computation of the convolution integral.

The capacity has been defined as drift-limited or not, which can result in important changes on the available ductility and consequent safety evaluation. Table 6.2 presents the failure probability, in numbers, using nonlinear dynamic analysis to compute the seismic effects, with or without limiting the drift capacity of the piers.

Table 6.2 – Failure probability using traditional NSA-NDA procedure (local uncertainty).

	<b>Failure Probability</b>	<b>Pier 1</b>	<b>Pier 2</b>	<b>Pier 3</b>	<b>Pier 4</b>	<b>Pier 5</b>	<b>Pier 6</b>	<b>Pier 7</b>
<b>123</b>	w/o drift control	<b>2.75E-02</b>	3.85E-03	1.71E-09	-	-	-	-
	w/ drift control	<b>2.75E-02</b>	3.96E-03	3.82E-03	-	-	-	-
<b>213</b>	w/o drift control	5.02E-05	<b>1.34E-02</b>	1.58E-11	-	-	-	-
	w/ drift control	6.17E-05	<b>1.34E-02</b>	4.09E-04	-	-	-	-
<b>222</b>	w/o drift control	5.36E-04	<b>2.48E-03</b>	5.37E-04	-	-	-	-
	w/ drift control	6.15E-04	<b>2.55E-03</b>	6.16E-04	-	-	-	-
<b>232</b>	w/o drift control	<b>6.53E-04</b>	4.99E-05	<b>6.54E-04</b>	-	-	-	-
	w/ drift control	7.50E-04	<b>5.41E-03</b>	7.51E-04	-	-	-	-
<b>2222222</b>	w/o drift control	1.13E-06	2.86E-04	1.34E-03	<b>2.32E-03</b>	1.34E-03	2.87E-04	1.14E-06
	w/ drift control	4.68E-07	2.97E-04	1.41E-03	<b>2.43E-03</b>	1.42E-03	2.98E-04	4.70E-07
<b>2331312</b>	w/o drift control	5.39E-07	2.64E-08	6.49E-06	<b>1.25E-02</b>	1.81E-10	5.58E-03	1.18E-08
	w/ drift control	1.16E-07	1.01E-03	2.44E-03	<b>1.25E-02</b>	1.98E-04	5.58E-03	3.54E-10
<b>3332111</b>	w/o drift control	1.50E-08	1.65E-04	2.74E-04	<b>3.59E-04</b>	2.26E-04	4.96E-05	4.24E-07
	w/ drift control	2.93E-03	<b>1.38E-02</b>	1.27E-02	3.76E-04	2.26E-04	4.96E-05	4.24E-07

The highlighted fields correspond to the pier with highest failure probability, which is assumed as the bridge failure probability. The critical pier is generally the shortest one, type 1, 7 meters height, (as in configurations 123, 213 or 2331312) or the central one, when there are no significant differences in height (as in regular configurations 222, 232, 2222222). Furthermore, for most cases, the behaviour-commanding pier stands, whether the drift limitation is considered or not. The exception occurs for configurations 232 and 3332111, where the critical pier changes with the drift restriction, herein established at a maximum of 5%. This shifting takes place especially in type 3 piers, taller, 21 meters height, given that a relatively small curvature at the base of the pier will correspond, due to its significant height, to a relatively large displacement at the top, leading the drift to rapidly reach the imposed limit. Within 232 configuration, the central pier becomes therefore the decisive one, as opposed to the shorter, next to the abutments, type 2 piers, which ruled the bridge behaviour when no drift limitation was imposed. In 3332111 configuration, in turn, the critical pier went from the central pier P4, 14 meters height, to a taller one, closer to the abutments, again a type 3 one. Curious is the fact that a lower mean ductility capacity, induced by the drift limitation, does not necessarily lead to a lower failure probability. In fact, looking at the extreme piers P1 and P7, both type 2 ones, in 2222222 and 2331312 configurations, the described situation can be observed, where carrying out a 5% drift limitation for the piers capacity, the collapse probability

diminishes, in one or two orders of magnitude. The interpretation is quite straightforward and has to do with two aspects. Firstly, recurring to Table 6.3, it can be noticed that, for the particular case of such piers, the available ductility becomes little inferior when drift-limited, with a reduction of less than 4%.

Table 6.3 – Ductility capacity (mean and standard deviation) considering, or not, drift limitation.

		<b>Ductility Capacity</b>		<b>Pier 1</b>	<b>Pier 2</b>	<b>Pier 3</b>	<b>Pier 4</b>	<b>Pier 5</b>	<b>Pier 6</b>	<b>Pier 7</b>
<b>123</b>	w/o drift control	Mean		34.27	34.49	34.00	-	-	-	-
		STD		3.28	3.29	3.30	-	-	-	-
	w/ drift control	Mean		34.27	34.03	14.20	-	-	-	-
		STD		3.28	2.73	1.50	-	-	-	-
<b>213</b>	w/o drift control	Mean		34.15	34.63	34.00	-	-	-	-
		STD		3.28	3.29	3.30	-	-	-	-
	w/ drift control	Mean		32.91	34.63	14.22	-	-	-	-
		STD		2.32	3.29	1.50	-	-	-	-
<b>222</b>	w/o drift control	Mean		34.14	34.49	34.14	-	-	-	-
		STD		3.28	3.29	3.28	-	-	-	-
	w/ drift control	Mean		32.90	34.03	32.90	-	-	-	-
		STD		2.31	2.73	2.31	-	-	-	-
<b>232</b>	w/o drift control	Mean		34.14	34.35	34.14	-	-	-	-
		STD		3.28	3.28	3.28	-	-	-	-
	w/ drift control	Mean		32.89	17.30	32.89	-	-	-	-
		STD		2.31	1.63	2.31	-	-	-	-
<b>2222222</b>	w/o drift control	Mean		<b>34.16</b>	34.43	34.35	34.38	34.35	34.43	<b>34.16</b>
		STD		<b>3.28</b>	3.29	3.28	3.28	3.28	3.29	<b>3.28</b>
	w/ drift control	Mean		<b>32.95</b>	33.88	33.66	33.73	33.66	33.88	<b>32.95</b>
		STD		<b>2.34</b>	2.66	2.56	2.60	2.56	2.66	<b>2.34</b>
<b>2331312</b>	w/o drift control	Mean		<b>34.16</b>	34.29	34.22	34.51	34.23	34.57	<b>34.16</b>
		STD		<b>3.28</b>	3.28	3.28	3.29	3.28	3.29	<b>3.28</b>
	w/ drift control	Mean		<b>32.95</b>	16.77	16.12	34.51	16.14	34.57	<b>32.96</b>
		STD		<b>2.34</b>	1.59	1.57	3.29	1.57	3.29	<b>2.33</b>
<b>3332111</b>	w/o drift control	Mean		34.02	34.29	34.22	34.38	34.49	34.57	34.29
		STD		3.29	3.28	3.28	3.28	3.29	3.29	3.28
	w/ drift control	Mean		14.32	16.77	16.10	33.73	34.49	34.57	34.29
		STD		1.50	1.59	1.57	2.60	3.29	3.29	3.28

On the other hand, corresponding standard deviation is nearly one third lower, which alters significantly the shape of the assumed normal distribution, contracting it, an effect that becomes more significant than the shifting caused by the reduction in the mean value. Better understanding is enabled by Figure 6.34, which plots the distributions at stake.

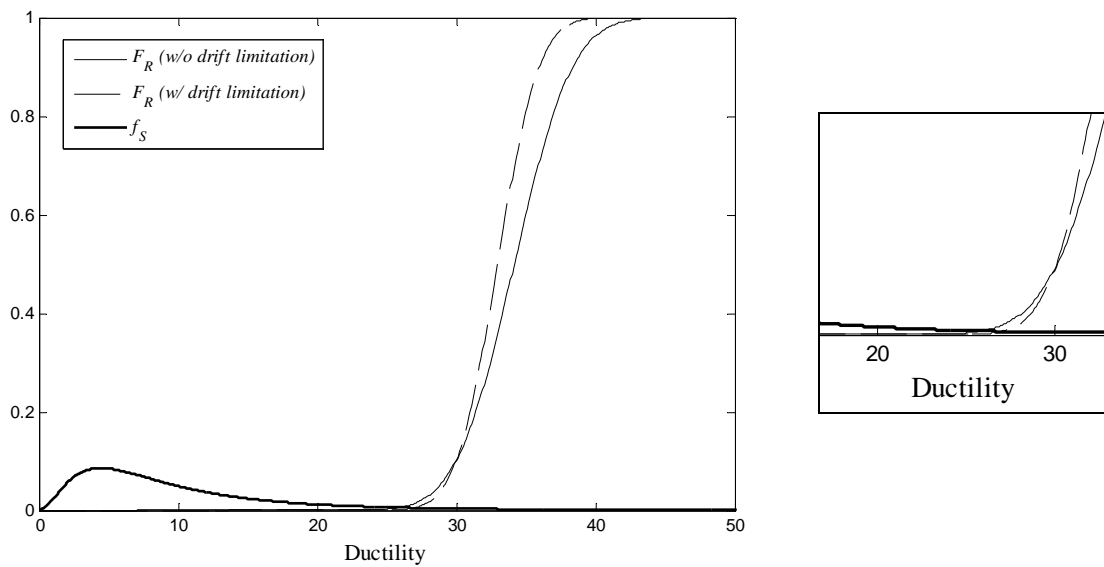


Figure 6.34 – Drift control influence in pier P1, configuration 2222222, behaviour.

It is possible to observe that the important region for the failure probability computation, according to Equation (6.7), is the interval where the functions cross each other, given that for the rest of the ductility domain the ordinates of  $F_R$  or  $f_S$  are residual. Within that zone, the cumulative distribution function corresponding to the drift limited capacity is under the non-restrained one, notwithstanding the lower higher mean value. For that reason, the failure probability, on the latter case, turns out higher, even if mean ductility capacity is equally superior. Additionally, such detected inversion in the expected behaviour occurs for the piers with extremely low failure probability, confirmed by the probability density function of the seismic effects,  $f_S$ , in Figure 6.34, corresponding to small orders of magnitude from  $10^{-6}$  to  $10^{-10}$ , something that definitely calls out some unpredictability on the numerical computation.

Collapse probability for the several bridges is presented in Figure 6.35, allowing in particular the relative comparison of the different configurations performance. Results have been sorted in crescent order of failure probability with drift limitation.

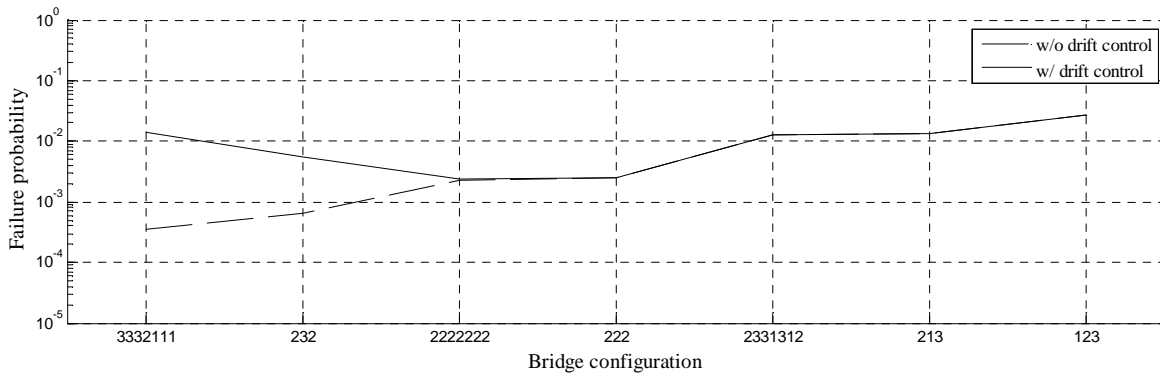


Figure 6.35 – Failure probability, according to bridge configuration – traditional NSA-NDA approach.

Globally, there is agreement between considering the top deformation of the piers limitation or not, given that the trend of results is similar. The exception occurs when a type 3 pier becomes the most vulnerable one, such as in configurations 232 and 3332111, previously mentioned. Together with the numbers, the plot suggests, therefore, that capacity of piers of 21 meters height, the tallest ones, was overestimated. It can be said, in addition, that the maximum drift constraint somehow smoothes the results, turning them more uniform according to more realistic conditions. Moreover, the distinction between regular and irregular configurations is immediate from Figure 6.35, the latter being more vulnerable, all in the right side of the plot. A final observation goes to the fact that high orders of magnitude have been found:  $10^{-2}$  in irregular bridges and  $10^{-4}$  to  $10^{-3}$  for regular ones, which is, to some extent, significant.

Once more the seismic action will have a preponderant part, and the failure probability that, traditionally, is computed using mean ductility demand, will vary considerably from one earthquake record to another. The effects caused by such variability will be, however, of distinct magnitude, depending on the bridge configuration or the pier characteristics. Figure 6.36 illustrates, for short configurations, at each pier, the failure probability computed individually, employing a single vulnerability function, coming from each of the ten used ground motion records, or computed through the mean vulnerability function. The same output, for long configurations, is presented in Figure 6.37. Nonlinear dynamic analysis was used.

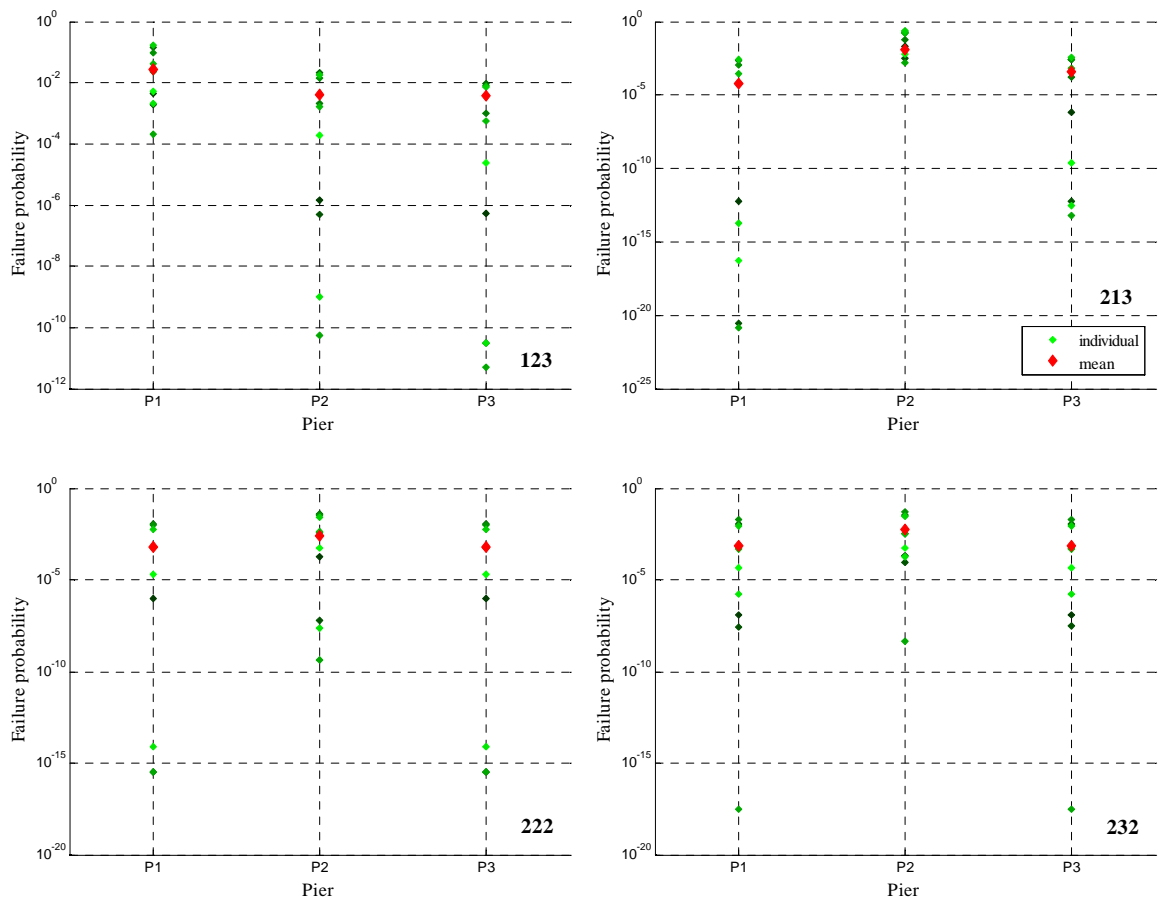


Figure 6.36 – Failure probability for short configurations.

From the observation of the plots, for both types of configuration, the finding that the dispersion within the seismic response prediction has spread up itself to the final collapse probability computation is notorious. Equally confirmed is the perception that larger variability is found for the critical piers, the ones with higher demand and, consequently, higher failure probability. This will certainly constitute the essential issue, concerning the relevance of the dispersion introduced by the seismic action, when the safety assessment is carried out by means of nonlinear dynamic analysis. Indeed, especially for the case of critical piers, the question that arises has essentially to do with the validity of using the mean demand obtained with a certain number of accelerograms instead of the maximum measured response. EC8 (CEN, 2005b) indicates that the average response effects may be assumed if at least seven independent records are used. If less than that number of input motions, with a minimum of three, is used, then the maximum response of the ensemble shall be assumed.

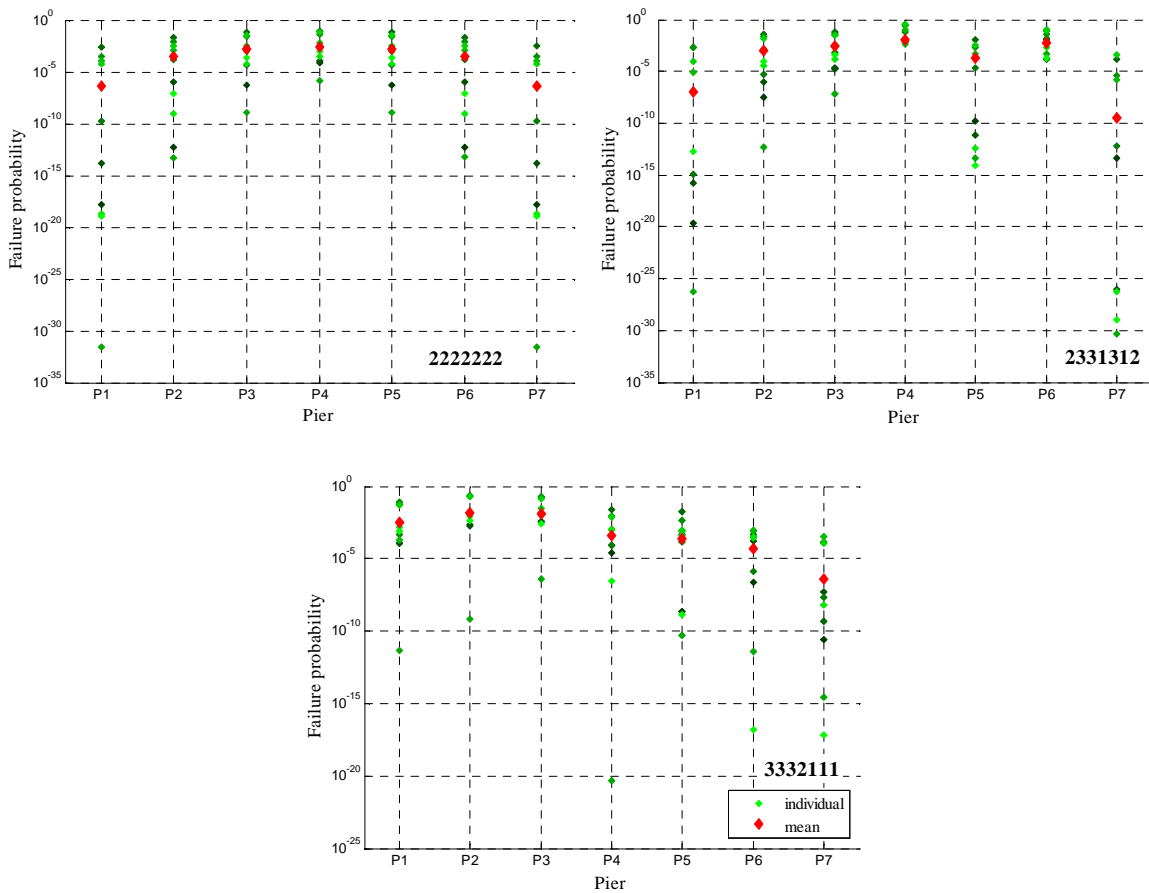


Figure 6.37 – Failure probability for long configurations.

Herein, the failure probability computed from the application of a single ground motion record can be substantially higher than the 10-records average demand one as the just presented plots indicate, with differences up to ten times more being encountered. Such findings are, nevertheless, associated to a standardizing criterion, applied to the accelerograms, based on peak ground acceleration, which definitely represents a part in the results that can not be neglected. In any case, average results when carrying out dynamic analysis with real earthquake records, must be used with care.

Furthermore, it can be stated, at least to some extent, that, considering the general behaviour of the bridges across the several piers, variability in collapse probability is larger for regular configurations than for irregular ones. In the latter, there is typically a pier, or a couple of them, considerably more affected, where large discrepancies in predictions are found, whereas, among the rest, there is general consensus in failure probability estimates.



The failure probability calculation has been carried out as well as a function of the sort of vulnerability function origin: nonlinear static analysis or nonlinear dynamic analysis. The differences that have been found between such vulnerability curves may assume higher or lower importance, depending on the shape of the seism action probability density function. With the purpose of continuing to draw attention to those several demand prediction possibilities, given the major importance of such variable within the traditional methodology, collapse probability for each pier, using each variant, has been computed. The failure probability, at the different piers, according to different approaches to estimate the vulnerability function, is plotted, for short configurations, in Figure 6.38 and, for long ones, in Figure 6.39.

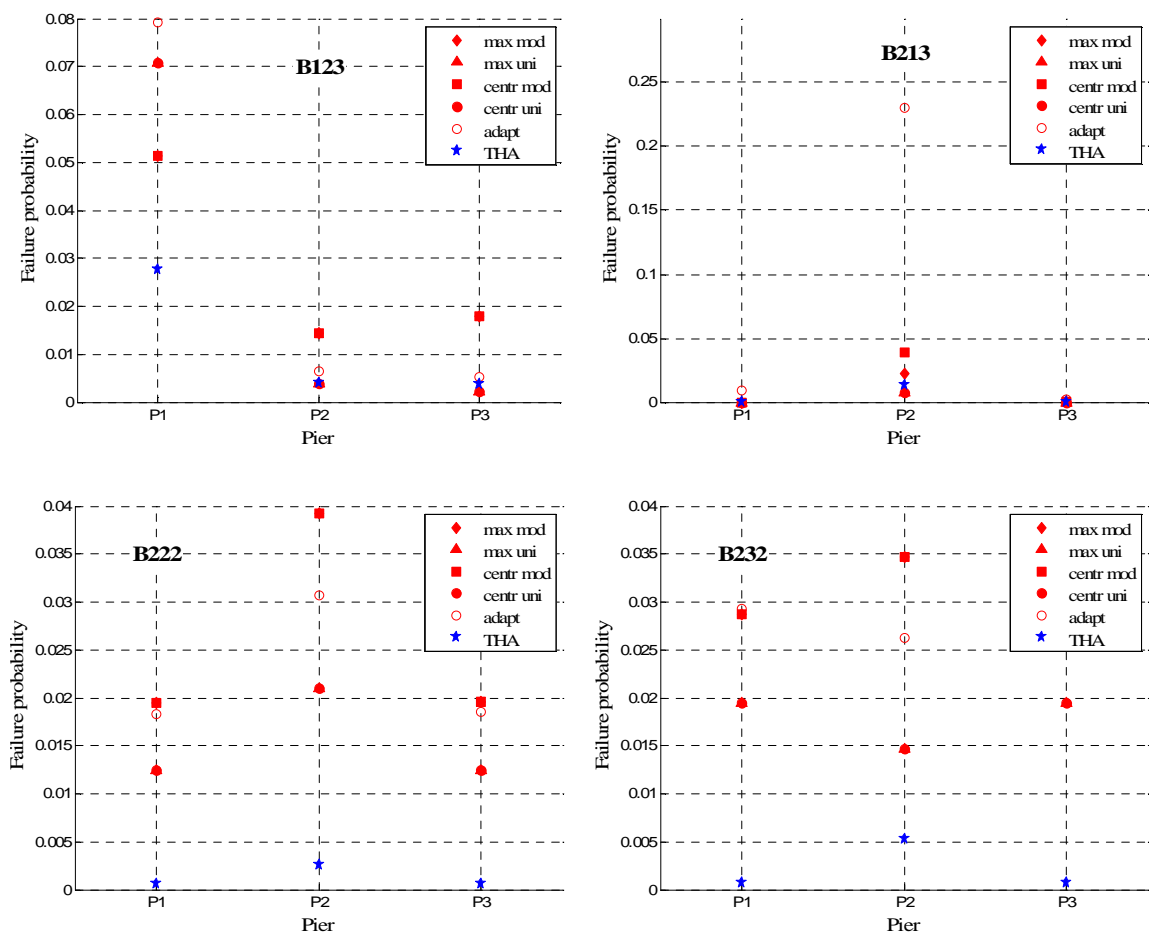


Figure 6.38 – Failure probability, for short configurations, using different vulnerability functions.

The first immediate remark induced by the plots is the intense underestimation given by nonlinear dynamic analysis, more prominent for regular, short configurations. On the other

hand adaptive pushover and conventional pushover based procedures, with 1st mode proportional load shape, regardless the reference node, yield the highest and most overpredicting failure probabilities, with respect to NDA numbers. Larger differences are expectedly found for the case of the critical piers.

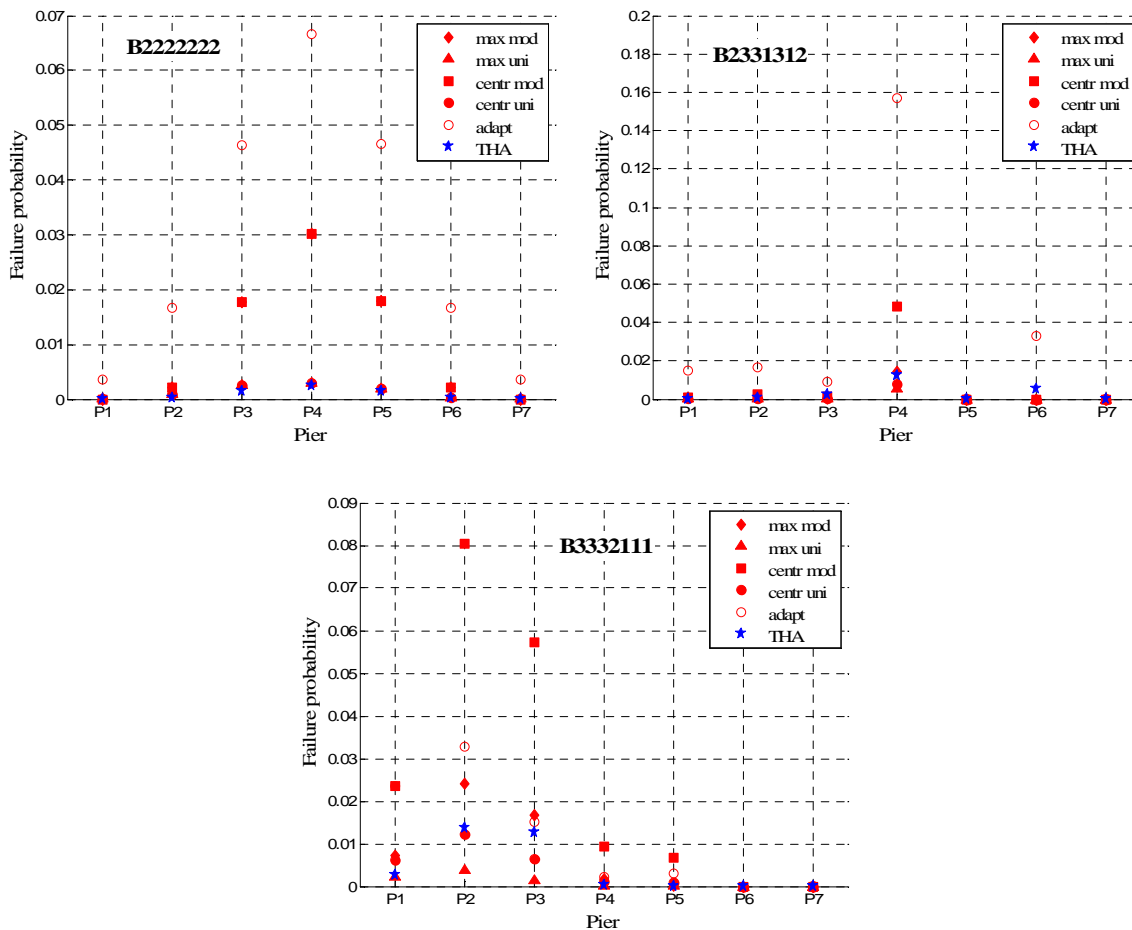


Figure 6.39 – Failure probability, for long configurations, using different vulnerability functions.

With respect to long configurations, results tend to be more uniform, with the main discrepancies occurring at the piers submitted to higher demand. Even though nonlinear dynamic analysis is not as overestimated as for short configurations, adaptive pushover continues to be the methodology yielding higher collapse probability. The tendency for the pushover based techniques to play largely in a conservative mode is therefore confirmed. This surely constitutes a motivating feature, given that simplified procedures are certainly expected to behave cautiously.

In agreement with the typical definition of the failure probability of a bridge, assumed as the highest among the piers' individual collapse probabilities, Figure 6.40 sums the results for all the bridges in the same plot. Given that the relevance of the reference node in the final results is minor, such comparison for the entire set of bridges will differentiate conventional pushover in terms of load pattern only.

A first conclusion that can be reinforced, in agreement with what has already been seen, when looking at the comparison for the whole set of bridges, is that regular configurations have the lowest collapse probabilities, even though larger variability has been found from different approaches predictions in those bridges. Regarding the sort of pushover to use, if a simple static analysis is intended, modal load pattern does not introduce any significant advantage when compared to the uniform one, which is in addition even simpler to apply. Adaptive pushover approach, in general the most overpredicting of all, does not seem gainful as well. No important differences are found concerning the length of the configuration: short bridges are slightly less safe than the long ones together with a little less dispersion within different variants.

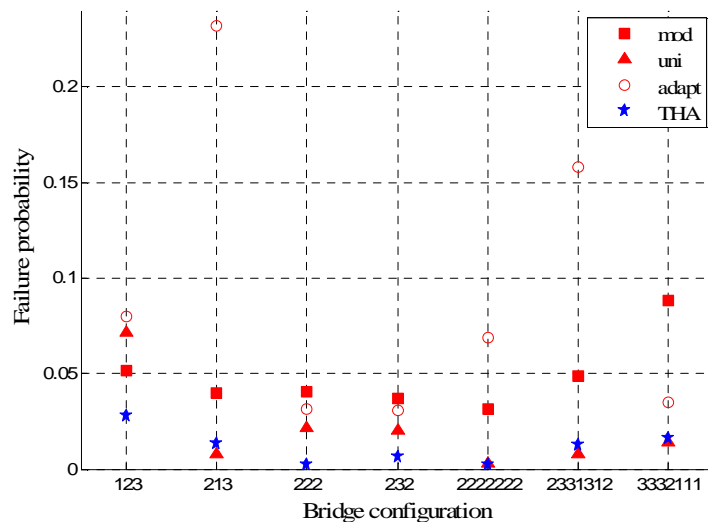


Figure 6.40 – Failure probability, according to bridge configuration.

The results that have been summarized indicate a tendency for the static analysis approach to be conservative, useful, even in its simpler form, the conventional uniform loading shape version, with respect to the dynamic analysis. Within a methodology where the structural effects need to be estimated through a large number of nonlinear analyses, this

feature constitutes an important advantage, at least for a preliminary analysis. The used procedure, considering local uncertainty consideration, has proved itself quite influenced by the extreme variability that characterizes the seismic action. Additionally, the capacity definition, in terms of practical limitations or statistical characterization plays a rather important part, easily conditioning the most vulnerable pier. Moreover, the method has the clear advantage of not needing to recur to distribution fitting of the nonlinear seismic effects, using an equivalent area under probability density functions based numerical procedure instead.

#### ***6.2.4 Failure probability with global uncertainty LHS approach***

Within the alternative that considers the uncertainty of all the variables simultaneously, in a global fashion, at each repetition of the entire procedure the demanded ductility,  $\mu_S$ , is obtained at the base of the pier and compared to the respective available one,  $\mu_R$ . The difference between these two quantities is computed and, therefore, a sample of  $N$  realizations for such variable is obtained, which will enable achieving the collapse probability as the zero-ordinate of the corresponding cumulative distribution ( $\mu_R - \mu_S$ ) function.

##### ***6.2.4.1 Simulation process calibration***

Contrarily to the continuous transformation of the seismic probability density function into the corresponding structural effects one, from a global simulation procedure perspective herein used, the effects are characterized in terms of a sample, of a specific predetermined size, of ductility demand numbers. Such discrete data will follow a statistical distribution, requiring characterization. Goodness of fit tests constitute the best tool for that purpose and may be carried out for the relevant distributions. Ductility demand is basically a function of the structural and material properties, which typically follow a normal distribution, and the seismic intensity, characterized by an extreme value distribution. Consequently, the structural effects will likely follow one of those distributions, with the goodness of fit tests focusing on such possibility.

The first parameter to test in this sort of procedure is the size of the sample that will enhance superior results, in the stability sense, without compromising computational effort. Similar endeavour focused capacity definition and, according to results that have been

presented in Section 6.2.1, a minimum of one hundred realizations were necessary to reach consistency in predictions. For the present case, 10, 20, 50, 100, 200 and 500 repetitions of the procedures have been carried out, fitting an extreme value distribution to the difference between the computed capacity and the structural demand, assuring that both variables were computed using the same  $n$ th randomly simulated material properties, seismic intensity and earthquake record.

Figure 6.41 illustrates the evolution of the distribution fitting to structural effects data for the short, regular configuration 222. Plotting the results for all the configurations and piers would be extremely exhaustive, hence, a simple regular pier has been chosen to test the method. Histograms for the different sampling sizes are plotted for the central P2 pier, the one with highest demand, as well as the corresponding probability density function of the extreme value distribution that best fits the data.

The influence of the sampling size is rather evident from the observation of the plots, with the histograms corresponding to 10, 20, 50 and 100 realizations being typically less adjustable to the expected extreme value distribution, notwithstanding the fact that corresponding hypotheses of the data following such distribution were not rejected by Kolmogorov-Smirnov tests in such cases. Logically, 10 and 20 realizations samples will hardly have statistical meaning and even 50 as sample size is extremely arguable. In any case, such numbers have been included in the parametric study not only to confirm such evidence but to test the method's toughness and to help finding out its optimum application mode as well. The turning point is, nevertheless, fairly marked and corresponds to 200 realizations, with no conspicuous advantage in moving on to 500 realizations. It seems reasonable that, within a failure probability computation process, a superior size of the samples ought to be needed, in comparison with the hundred stabilizing number found for the capacity characterization. In addition, the plots refer to the central pier of a regular configuration, which will expectedly reduce instability levels within the results coming from nonlinear analysis.

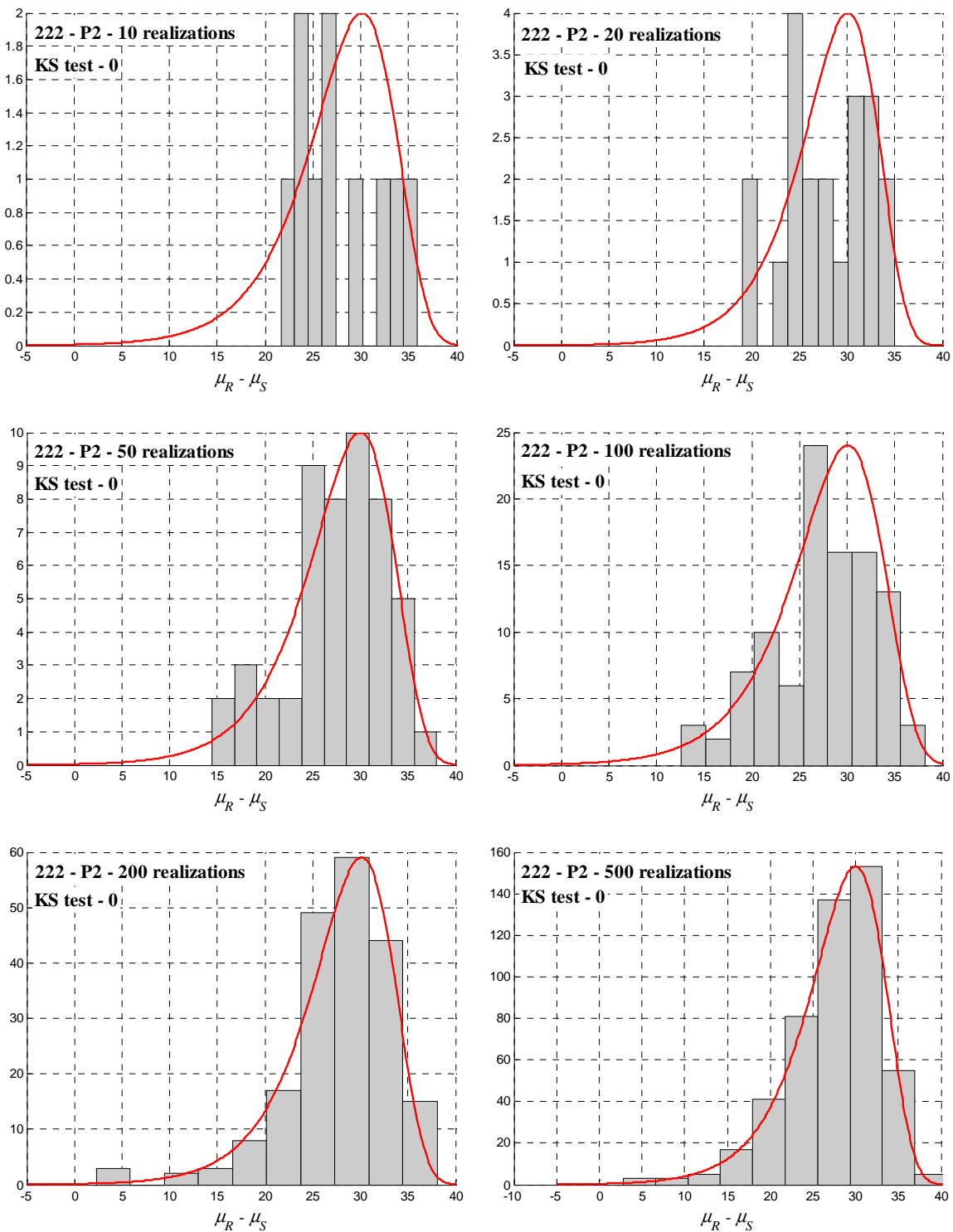


Figure 6.41 –  $(\mu_R - \mu_S)$  histogram and adjusted extreme value distribution probability density function for pier P2 in configuration 222, for different numbers of realizations.

The possibility of other configurations, likely to behave in a trickier fashion, requiring more than 200 realizations is real and must be examined. The variability introduced by the

heterogeneous seismic action has been herein widely recognized and, therefore, the study of such effect, together with the needed number of realizations, for all the configurations, is of high interest. The complete procedure has been carried out including the accelerogram as an input variable or using each earthquake record independently to compute the collapse probability. Figure 6.42 illustrates the failure probability obtained for each configuration, in green, using a single independent ground motion record, or, in red, randomly selecting it, as a variable. The failure probability is taken from the pier subjected to highest demand.

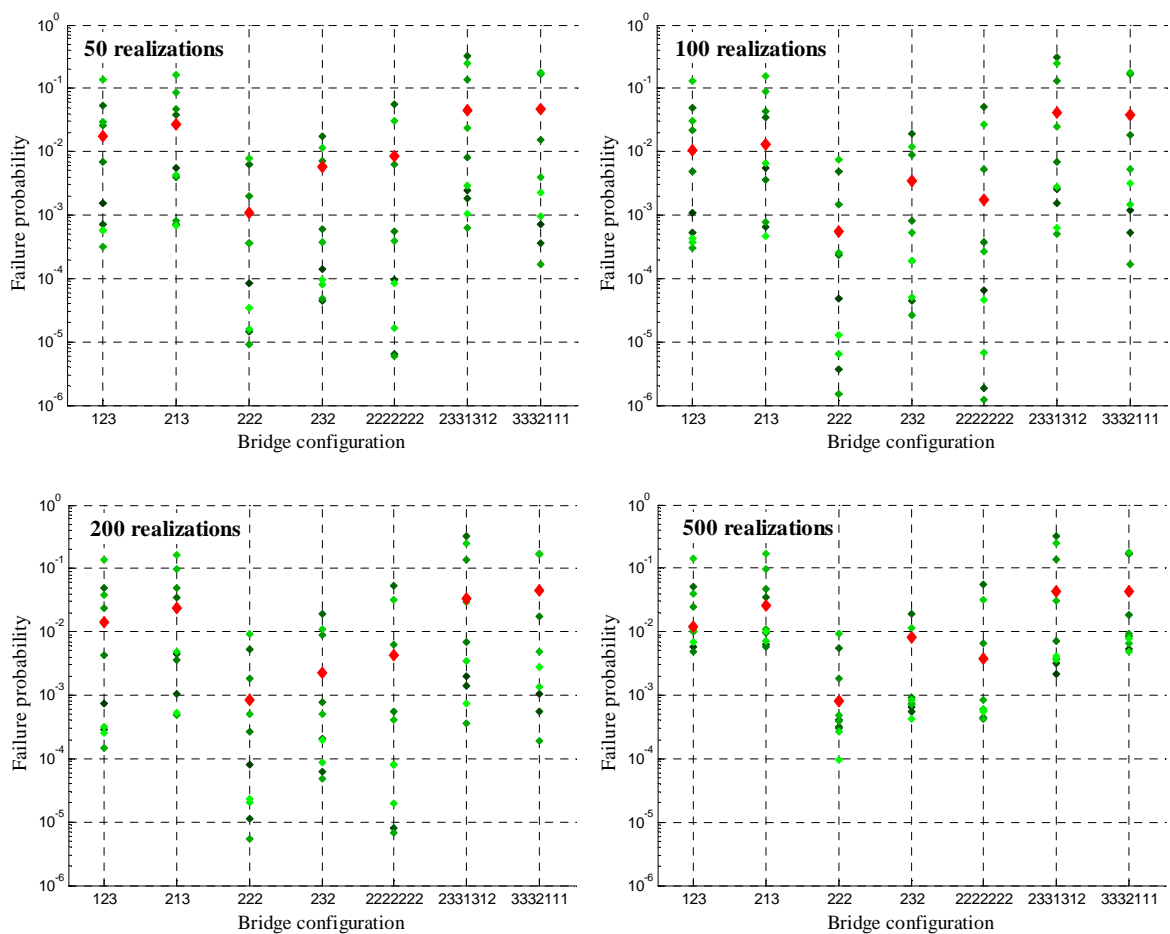


Figure 6.42 – Failure probability, using each record in separate or considering the record as an input variable, for different numbers of realizations.

There are two important aspects to retain from the observation of the plots. The first is the confirmation of the considerable dispersion that this sort of procedures involve, as a consequence of the disperse nature of the seismic action. The use of ten different records makes the collapse probability to range from order of magnitude  $10^{-6}$  to  $10^0$ , for the lower

sampling sizes. The other finding is that, from 200 realizations on, but especially visible when using samples of 500 realizations, the scatter reduces approximately one third, with no failure probabilities under  $10^{-4}$ . It is significant to recognize, at the same time, that the reduction has occurred upwards, that is, the reduction in the variability has been made by eliminating the lowest values, which denotes that a higher refinement level of the global simulation procedure enables a safer assessment of the seismic vulnerability.

When analysing the evolution of results with the number of realizations, a sort of internal variability of the method, using global Latin Hypercube simulation, is being observed. The external variation of the results can be seen when carrying out again the whole procedure more than once, repeating all the simulation process. Three repetitions of the method have been performed and the changes in the obtained failure probability have been plotted against each other. Again, the plots for the different series of repetitions are plotted, in Figure 6.43, for the central pier of the regular, short 222 configuration.

The observation of the plots corresponding to the use of the different ground motion records individually, indicates that, for all the accelerograms, as expected, there is considerable variability when using 10 or 20 realizations, whether within the method, across the number of realizations, or from one repetition to the other. If 50 or 100 realizations are carried out, the scatter reduces to median levels and stability is definitely reached when samples of 200 or 500 realizations are used. The discrepancy of the results that has been found between different records is certainly due to their particular characteristics, given that they are real ones. Similar studies have been conducted in the recent past (Carvalho, 2009), leading to equally encouraging results regarding the use of Latin Hypercube sampling in a global safety assessment procedure, where the dispersion in both *directions* was similarly lower. Nevertheless, such work was carried out taking coefficients of variation for the material properties as constant and lower, especially for the concrete, which will several times govern the structural behaviour, near the rupture. Herein, a much realistic approach has been adopted for the material properties statistical models, which enhances even more the Latin Hypercube algorithm performance.



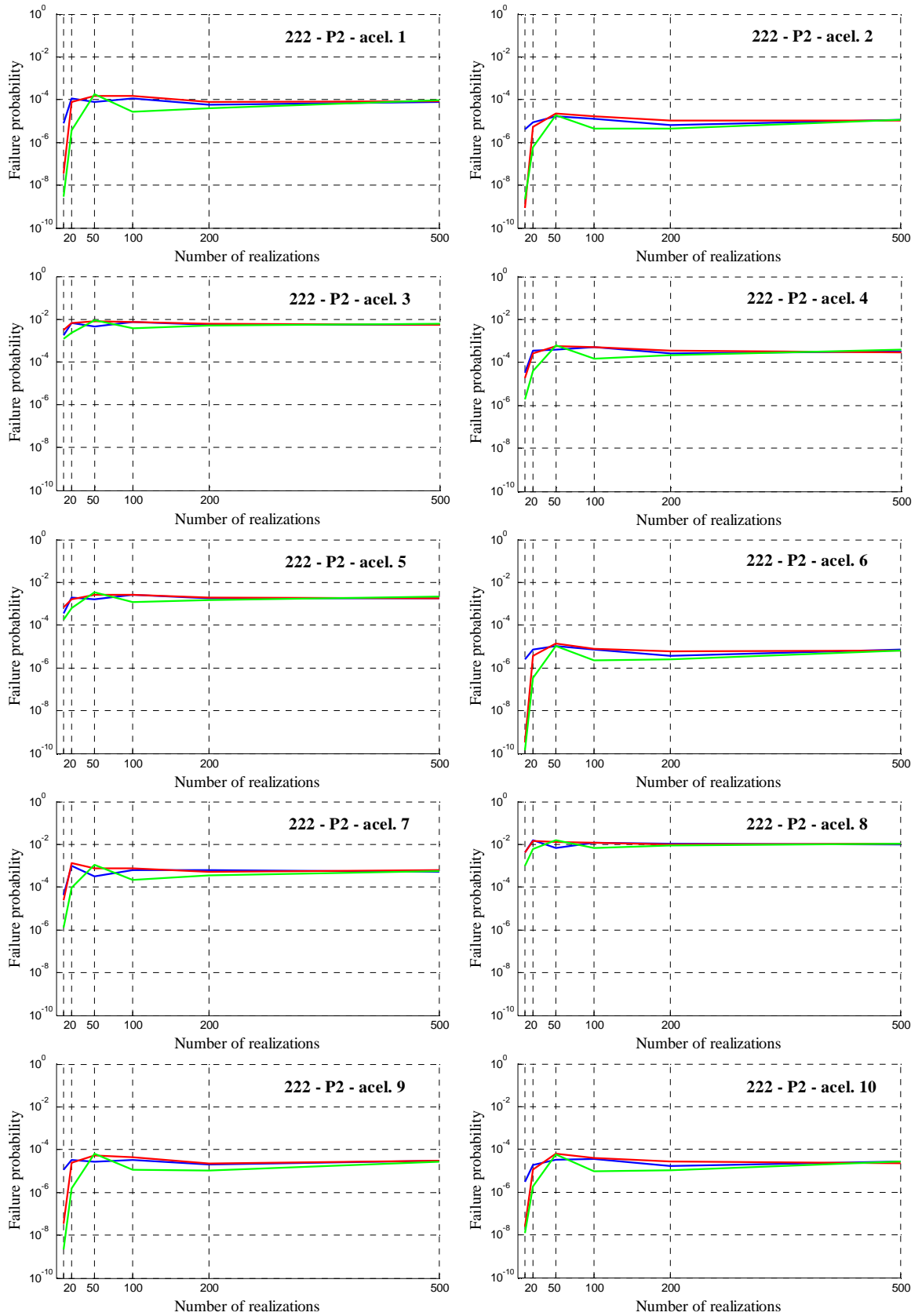


Figure 6.43 – Failure probability for pier P2 in configuration 222, for different numbers of realizations, using each of the earthquake records.

Applying the procedure as originally thought, this is, taking the type of record as an input variable, which follows a uniform distribution, the same plots can be drawn, repeating again the whole analysis for three independent times. The sampling size has equally been tested by means of the number of realizations. The behaviour of the failure probability with the number of realizations, computed for the most vulnerable pier at each configuration for different series, is hence illustrated in Figure 6.44.

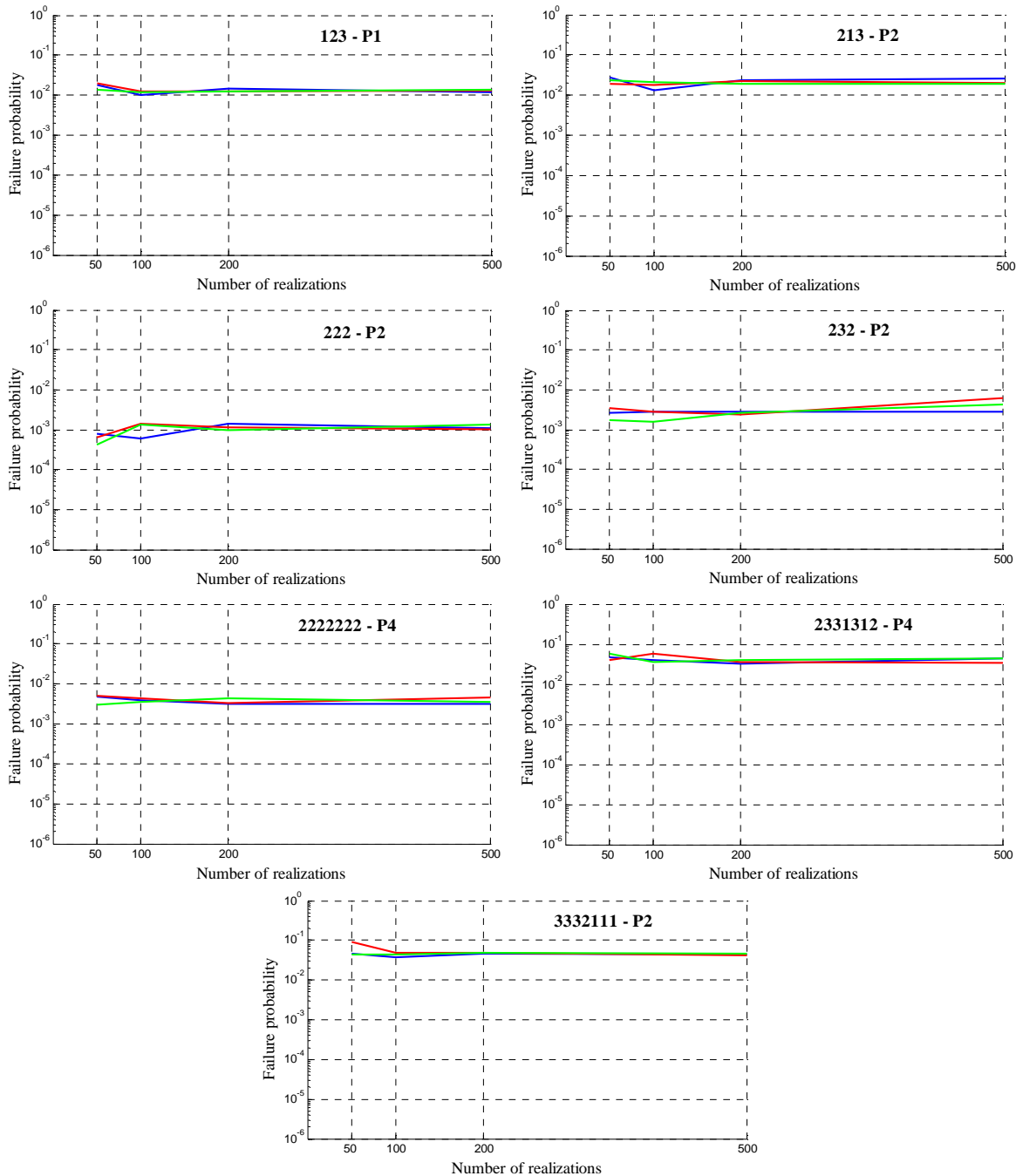


Figure 6.44 – Failure probability of the critical pier, according to different numbers of realizations, considering earthquake record as input variable.

Given that higher scatter has been encountered when using 10 and 20 realizations and for the sake of computational demand reduction, the extension of such parametric analysis to the rest of the configurations has been carried out disregarding such sampling sizes.

The immediate perception is that, if the accelerogram is considered as an additional input variable for the global simulation procedure, the scatter of the method is still barely noticeable. The methodology proves itself to be resistant to the introduction of a new variable of high variability, such as the seismic action is, in intensity and type of record. The difference from one repetition to another is indeed minimal, except for the 2222222 configuration. In terms of sample size, collapse probability stabilizes after 200 realizations.

#### 6.2.4.2 Structural effects and failure probability

Based on the considerations taken from the parametric study carried out on the number of realizations, the computation of the failure probability has been considered to be taken from the application of the Latin Hypercube sampling using samples with 200 realizations. Again, the calculations have taken into account the drift capacity limitation of the piers. The resulting numbers for the collapse probability, carrying out drift control or not, are presented in Table 6.4, where the highlighted values correspond to the critical pier.

Table 6.4 – Failure probability using the global simulation LHS approach.

	Failure Probability	Pier 1	Pier 2	Pier 3	Pier 4	Pier 5	Pier 6	Pier 7
<b>123</b>	w/o drift control	<b>1.37E-02</b>	1.37E-03	1.59E-04	-	-	-	-
	w/ drift control	<b>1.37E-02</b>	6.63E-04	5.41E-03	-	-	-	-
<b>213</b>	w/o drift control	1.48E-04	<b>2.06E-02</b>	7.60E-05	-	-	-	-
	w/ drift control	7.89E-06	<b>2.06E-02</b>	1.63E-03	-	-	-	-
<b>222</b>	w/o drift control	7.92E-04	<b>2.51E-03</b>	7.92E-04	-	-	-	-
	w/ drift control	1.21E-04	<b>1.43E-03</b>	1.21E-04	-	-	-	-
<b>232</b>	w/o drift control	<b>1.44E-03</b>	3.99E-04	<b>1.44E-03</b>	-	-	-	-
	w/ drift control	5.77E-04	<b>5.19E-03</b>	5.77E-04	-	-	-	-
<b>2222222</b>	w/o drift control	2.16E-04	9.05E-04	3.12E-03	<b>5.54E-03</b>	3.12E-03	9.05E-04	2.16E-04
	w/ drift control	7.53E-06	2.55E-04	1.52E-03	<b>3.47E-03</b>	1.52E-03	2.55E-04	7.53E-06
<b>2331312</b>	w/o drift control	1.55E-03	6.31E-04	4.88E-04	<b>3.86E-02</b>	9.18E-05	7.78E-03	1.25E-04
	w/ drift control	3.74E-04	5.44E-03	5.24E-03	<b>3.86E-02</b>	4.33E-04	7.78E-03	7.23E-06
<b>3332111</b>	w/o drift control	3.45E-04	<b>1.97E-03</b>	1.04E-03	4.05E-04	2.29E-04	1.20E-04	8.59E-05
	w/ drift control	1.51E-02	<b>4.83E-02</b>	3.19E-02	1.93E-04	2.29E-04	1.20E-04	8.59E-05

The reduction of the capacity of the piers, when applicable, through the consideration of a drift limit does not necessarily turn out into a higher failure probability. This is actually a tendency that had already been found in the traditional methodology results, related to the probabilistic nature of the procedures, which involve distribution fitting and convolution integrals in the sensitive corresponding tails regions. Nevertheless, and again not a novelty, such situation occurs mainly for medium height piers, usually near to the abutments. Such piers, as verified previously with Table 6.3, are little affected by the drift control, in terms of mean capacity, whereas the coefficient of variation is quite reduced. This will contribute to the changing in the shape of the probability density function, altering the expected failure probability. The effect caused by the drift limitation in the  $(\mu_R - \mu_S)$  distribution is illustrated in Figure 6.45 for the case of piers P1 and P3 in 222 configuration.

When the drift control is activated, the mean ductility capacity is slightly inferior, as it can be seen from the maximum of the probability density functions. On the other hand, due to the reduction in the dispersion, the shape of the probability density function for the case of drift capacity reduction gets more contracted and becomes superior to the non limited capacity one for a margin between demand and capacity,  $\mu_R - \mu_S$ , around 20.

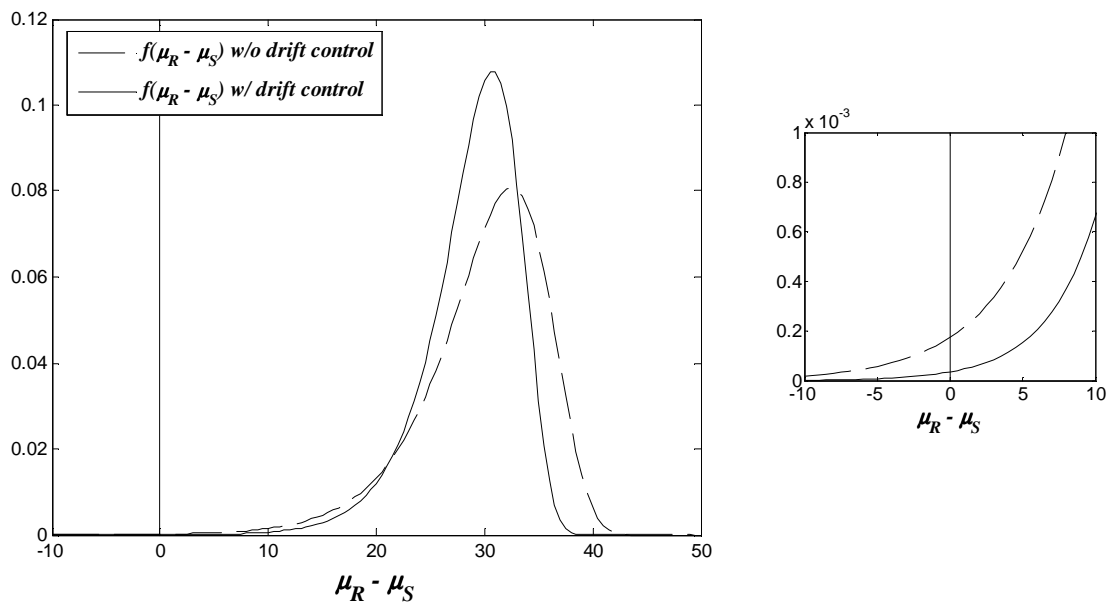


Figure 6.45 – Drift control influence in piers P1/P3, configuration 222, behaviour.

Given that failure probability is computed through the area under the probability density function for safety margins under zero, in the end, drift limitation will hence correspond to lower vulnerability, as illustrated by the detail of the relevant region on the right.

The effect of considering or not drift limitation when it comes to the accurateness of the distribution fitting to the variable corresponding to the difference ( $\mu_R - \mu_S$ ), is not much visible. Indeed, not all the configurations had their failure probability commanded by drift limited capacity, as confirmed through Table 6.4, remaining the graphical verification that distribution fitting is not worsened by the inclusion of such criteria. The configurations where such is actually relevant are the ones with critical piers of type 2 or type 3: 222, 232, 2222222 and 3332111. Figure 6.46 illustrates the difference in the histograms and corresponding probability density functions of the adjusted distribution, for the critical pier of those configurations.

The observation of the plots indicates that the drift limitation of the ductility capacity,  $\mu_S$ , does not induce quality loss, to what concerns the distribution fitting to the variable  $\mu_R - \mu_S$ . when the shifting occurs, typically for the type 3 piers, as already detailed before, the probability density function can become even better adjusted, which seems to happen for configuration 232 and 3332111, the latter with the same fitting quality, at least. When the critical pier is of type 2, the effect of the drift is not so pronounced, no significant shifting in  $\mu_R - \mu_S$  axis occurs and, even though the adjustment is not compromised, the shape of the best-fitting extreme value distribution becomes visibly more tightened, reducing the failure probability, which is in agreement to what had been discussed and confirmed in Figure 6.45.

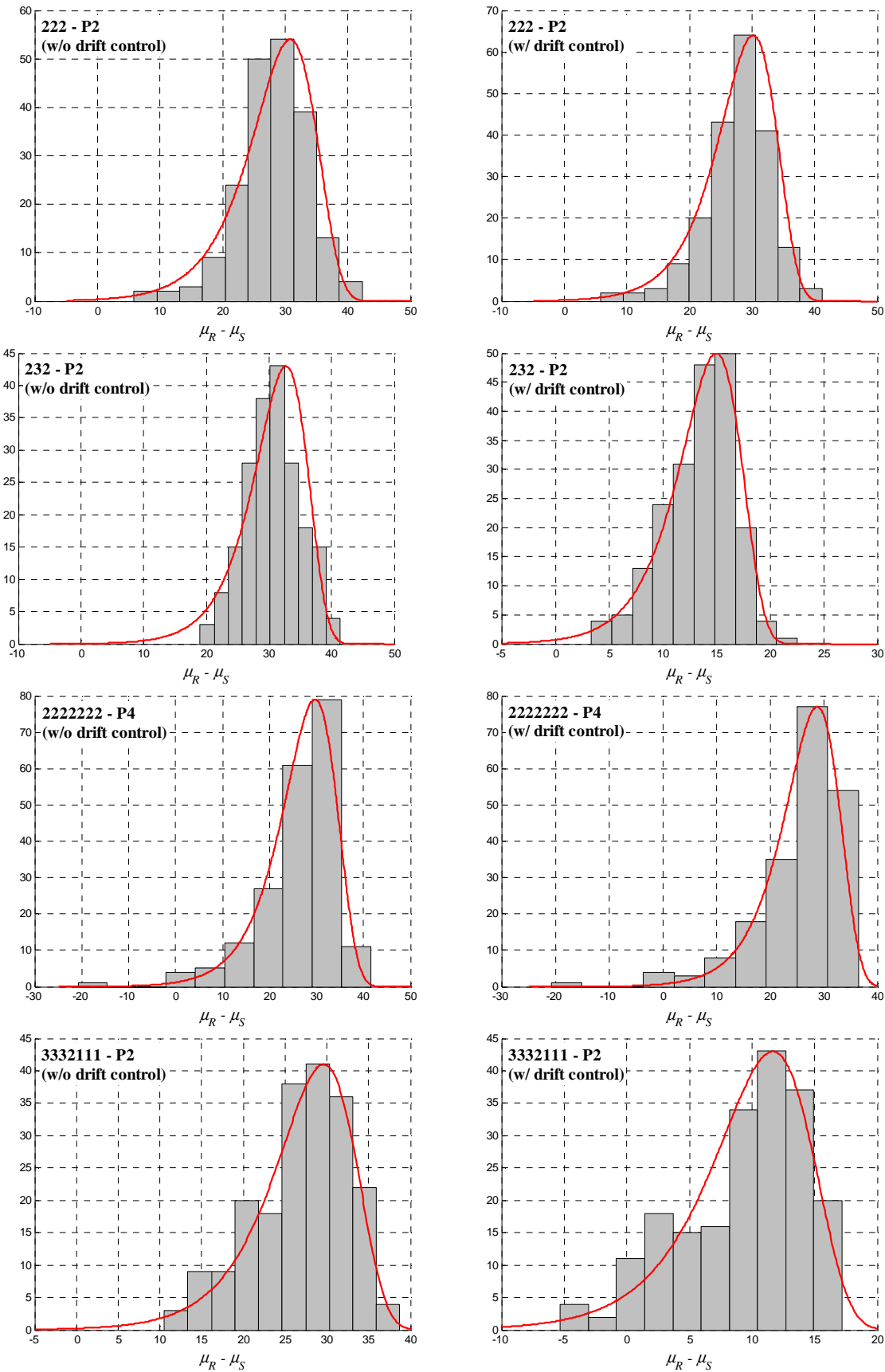


Figure 6.46 –  $(\mu_R - \mu_S)$  histogram and adjusted extreme value distribution probability density function, for configurations affected by capacity drift control.

Failure probability for the different configurations is summarized in Figure 6.47, sorted in crescent order of results considering drift limitation.

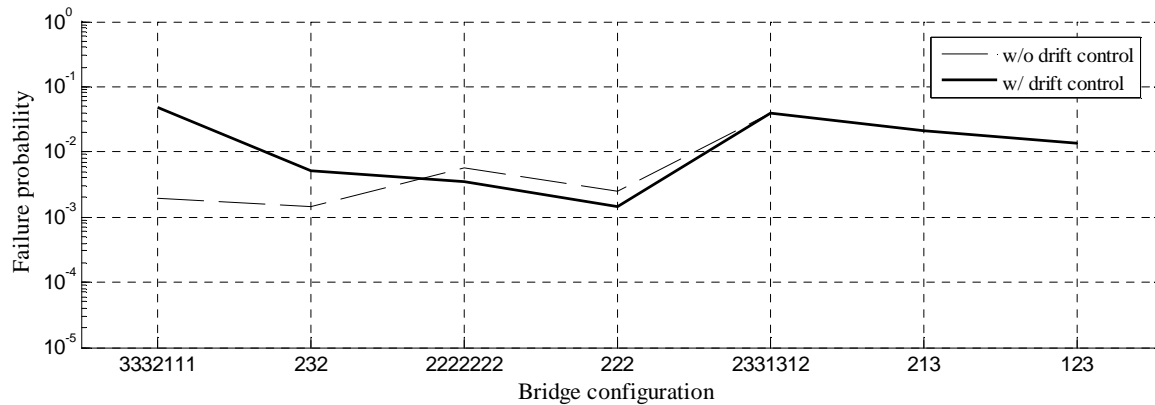


Figure 6.47 – Failure probability, according to bridge configuration – global simulation LHS approach.

Similarly to the traditional safety assessment procedure, which considers the variability of each component separately, there is a fairly consensual evolution of the collapse probability across the different configurations, whether drift limitation is carried out or not. Major differences occur for the configurations where the critical pier is a type 3 one, 21 meters high, the one that is most affected by the capacity reduction. Again the distinction between regular and irregular bridges is extremely pronounced, the primer being safer, together with a tendency for the short configurations to be less vulnerable as well. The aforementioned inversion in the expected behaviour of type 2 piers is visible for the configurations 222 and 2222222, where the critical pier fits such profile.

### 6.2.5 Comparison of methodologies

The final focus of this section will be the comparison of the failure probability results obtained with the different methodologies, which differ essentially on how the uncertainty of the variables is accounted for: local or globally. The distinction in terms of drift limiting the results or not is carried out as well, so as to evaluate to what extent such parameter influences the agreement of the procedures. The collapse probability obtained for each of the procedures, drift limiting or not the capacity, is plotted in Figure 6.48.

Major differences for the different possibilities of computing the failure probability occur for the configurations 3332111 and 232, although such discrepancy has more to do with the consideration or not of drift limitation criteria, rather than the methodology itself. It has even been verified that the commanding pier changes for configuration 232, when drift limitation is carried out, in the global simulation mode (LHS) approach. Within these configurations, there are type 3 piers, 21 meters tall, in a vulnerable position, which, together with being highly affected by top displacement limitation, leads to differences in safety that are more pronounced. There is a general tendency for the global Latin Hypercube simulation procedure to yield higher failure probabilities, whether the drift is limited or not, which has certainly to do with the inclusion of more variables, characterized with high uncertainty, in the global simulation process.

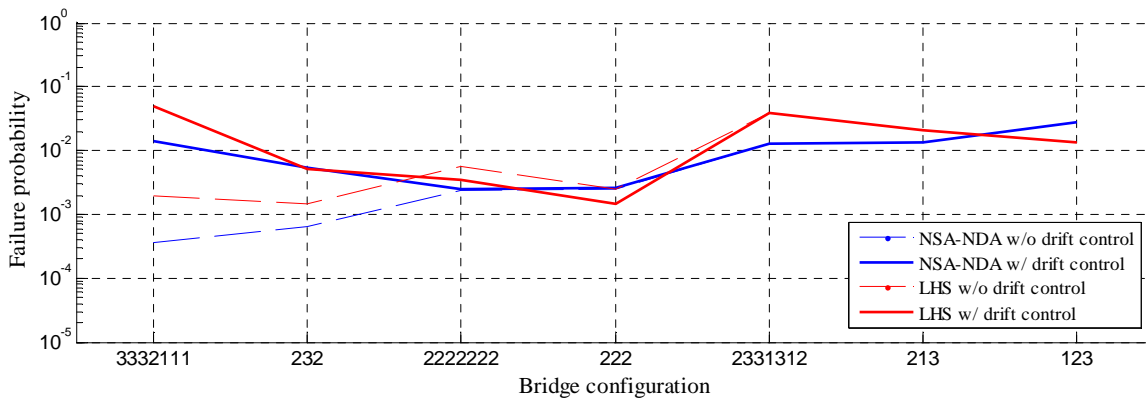


Figure 6.48 – Failure probability, according to bridge configuration, for all the NDA-based versions.

Nevertheless, it is quite appealing to realize that, except for the two aforementioned configurations, and despite eventual inversions in the relative position, the four collapse probabilities, corresponding to the four variants, are of the same order of magnitude. Regarding the configuration type, irregular configurations are, in general, on the right, which means, higher vulnerability, whereas there seems to be no connection of the failure probability with the length of the bridge.



Filtering the results in Figure 6.48, comparison of the two methodologies is presented in Figure 6.49, without drift control, and in Figure 6.50, with drift control of the piers capacity.

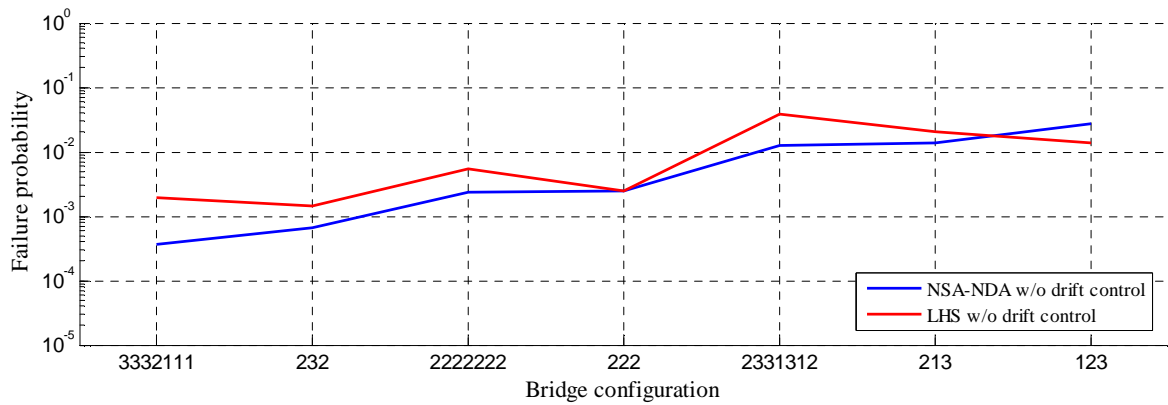


Figure 6.49 – Failure probability, without drift limitation, according to bridge configuration.

As previously forecasted, the differences are now much smoother. The failure probability trends along with the configuration type are notoriously in agreement. Moreover, the tendency for the LHS procedure to be on the safer side is confirmed, with the exception of configuration 123.

When drift control is included in the capacity computation, the methodologies get even closer, which seems understandable, given that such limiting criteria will definitely, at least to some extent, envelope the capacity. Higher failure probability is still generally obtained with LHS procedure, despite the reduction already observed and explained in configuration 222. The increase in the collapse probability of configurations 3332111 and 232, for both methodologies, is clearly observable, as a result of the vulnerable type 3 pier, which is highly drift-limited.

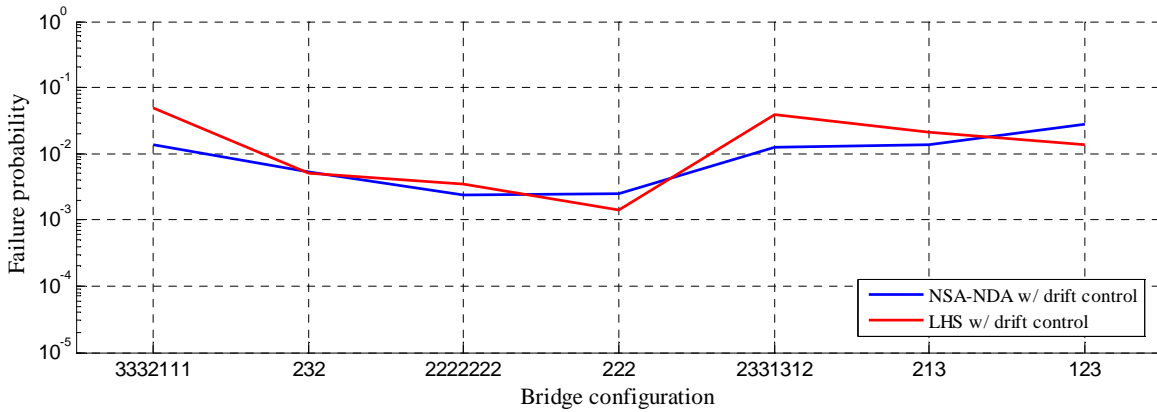


Figure 6.50 – Failure probability, with drift limitation, according to bridge configuration.

In Figure 6.51 pushover-based methodologies are plotted together with the already presented nonlinear dynamic analysis based ones. For the sake of simplicity, only conventional pushover, with uniform load pattern and central reference node, and adaptive pushover versions are presented.

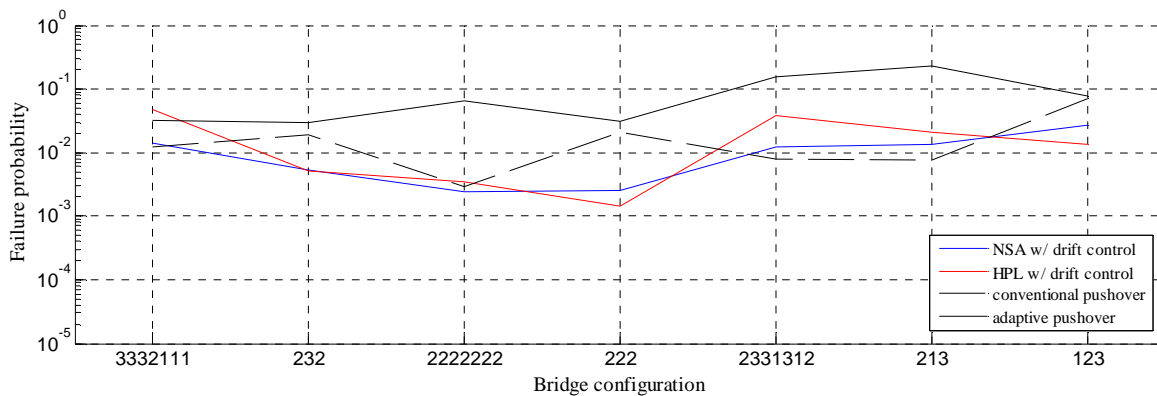


Figure 6.51 – Failure probability, with drift control, according to bridge configuration, for NDA and pushover-based versions.

The general picture is that pushover-based estimation of structural effects leads, in most of the cases, to higher failure probability, especially for the adaptive type, which is frequently associated to a failure probability one order of magnitude above. Such finding had already been visible from Figure 6.40. Similarity between the two types of pushover is not noticeable neither between pushover and NDA variants. These results reinforce the belief that pushover analysis is more likely to play a supporting part in the probabilistic methods, when compared to dynamic analysis.

### **6.3 Conclusions**

The analysis of different ways of looking into the safety assessment issue constituted the main objective of this chapter. Alternative procedures have been proposed, corresponding to different possible modes of incorporating the variability of the numerous intervening variables: material properties, type of record and intensity level. An innovative statistical sampling method has been used to characterize capacity as well as to compute failure probability within a global simulation procedure. Moreover, failure probability was computed recurring to two possible demand prediction techniques: nonlinear dynamic or static analysis. The parametric study of all the necessary elements for the safety evaluation, the observation of the performance of the alternative methodologies and the final comparison of results can be summarized by the conclusions that follow.

- The Latin Hypercube Sampling method revealed itself as a relying technique, when used to obtain capacity or demand distribution samples of lower size than the traditional Monte Carlo or FORM ones. For the capacity characterization of the piers cross sections, in terms of available ductility, which is a relatively simple calculation, 50 to 100 realizations proved to be able to provide stable mean results, without excessive dispersion. In addition, the method proved to be quite effective and stable within several independent repetitions. The variables that were considered for the capacity definition consisted of the material properties, only, with the ultimate steel strain being the most influent one. The sampling algorithm was equally efficient when the variables were taken with higher, but more realistic as well, coefficients of variation, which reached 30%, for some cases.
- The traditional methodology to compute the collapse probability required the definition of vulnerability functions, corresponding to 2<sup>nd</sup> degree polynomials adjusted to the mean ductility demand for increasing seismic intensity, obtained with nonlinear dynamic analysis. The curve fitting was extremely easy, together with high correlation coefficients, denoting the quality of the least squares method adjustment, for every configuration, every pier and every nonlinearity level.
- The use of nonlinear static analysis for the seismic demand prediction has been confirmed as a valid approach, even if generally overpredicting with respect to nonlinear dynamic analysis. Curve fitting to demand obtained through such means

was in the same way well succeeded. despite the fact that an adaptive pushover analysis is a more suitable choice for the prediction of the behaviour of irregular configurations, a conventional pushover, with a uniform load pattern, has lead to rather acceptable estimates for regular configurations. This is an important conclusion, if one keeps in mind the need for convincing methodologies and definitely less complex and time consuming than nonlinear dynamic analysis to be incorporated in actual seismic design and/or assessment of structures by practitioners.

- The traditional approach can be quite sensitive in terms of statistical characterization and a slight change in the dispersion might affect much more the failure probability than the median available ductility, as has been observed. The fact that probabilistic methods work over the tails of the distributions, convoluting number of very low orders of magnitude explains such behaviour and indicates that distribution fitting must be handled with care.
- With the seismic action being introduced as a variable for the global uncertainty procedure, the needed sampling size increased to 200 realizations, in order to reach consistent failure probabilities, for all sorts of bridge configurations as well as for different repetitions. Such increase was expected and is easily understandable, given that the procedure involves nonlinear dynamic analysis of a sometimes considerably irregular geometrical configuration. Furthermore, taking the seismic action as a variable induces a great additional amount of dispersion. The recommendations on the use of the LHS scheme in bridges safety assessment point to perform at least 200 realizations, which is, in any case, quite feasible computationally.
- The distribution fitting has been carried out with success and has, in agreement, been markedly superior, in quality, from 100 or 200 realizations on, with no advantage in carrying out 500 realizations. The goodness of fit has been evaluated with Kolmogorov-Smirnov test. However, some distribution samples of size 50 have passed the same test, so, to the author's belief, further probing, recurring to other available tests, needs to be carried out. This aspect is underlined by the fact that the global LHS methodology is quite easily affected as well by slight changes

in the probabilistic parameters characterizing the fitted distributions, again, for the same reason of working on the tails.

- In both of the methodologies, whether the uncertainty is considered locally or globally, the seismic action variables, earthquake record and intensity level, influenced the results outstandingly, especially the accelerogram that was being considered. The debate on realizing if the seismic action variability does not excessively outshine the variability of the rest of the variables is therefore settled. This aspect is certainly increased by the fact that real ground motion records have been used. It has been, however, interesting to notice that, despite the extreme variability, the global LHS methodology behaved quite soundly, enabling reliable results to be reached. The simulation technique seems hence to be able to incorporate highly different sorts of variables, with different distribution types and, mainly, distinct levels of uncertainty. Additionally, this conclusion strengthens the awareness of the need for a proper handling of the seismic action in terms of earthquake records, in gender and number.
- For what concerns the sort of bridge configuration, the trend that has been found is for irregular configurations to be less safe, whereas, regarding the deck length, no relevant correlation has been detected. Moreover, regular configurations seem to put the different procedures closer to each other, whilst, for irregular ones, the dispersion is slightly superior.
- The central piers, or at least the ones that are not close to the abutments, are typically submitted to higher demand, hence, the most vulnerable ones. Such conclusion can be easily taken from the 222 or 2222222 configurations, with all piers of the same height, where the critical piers are the central ones, notwithstanding the flexibility that has been considered within the modelling of the abutments. With respect to the remaining configurations, the definition of the decisive pier will depend on their type: 1, 2 or 3, and how far the drift limitation criterion affects them. Type 1 piers, 7 meters high, are typically very restrictive, even when not centrally located, something that is easily explainable by their naturally higher stiffness, standing for superior action effects, bearing lower ductility at the base cross section of their piers. As a consequence, the drift control will not be relevant, once the displacements at the top are already inherently

limited. This sort of pier has been found to condition configurations 123, 213 and 2331312 configurations. On the other hand, type 3 piers have been extremely influenced by the top transverse deformation restriction, with their capacity being strongly reduced, becoming the critical piers for configurations 232 and 3332111. As for the 14 meters high piers, type 2, due to their medium height, no significant changes in the ductility permitted by the material and cross section properties are introduced by the drift controlling.

- The two key alternative procedures to compute the collapse probability ended up being very concordant for the majority of the configurations. The methodology that considers the uncertainty of all the variables, including the seismic action, in a global fashion, using the LHS algorithm, yielded, however, more severe results. Such expected higher failure probabilities have definitely to do with the inclusion of a larger number of variables and corresponding uncertainty. The acknowledgment of this feature leads to the recognition as well of the major importance that the seismic action variability has in worsening the vulnerability of the bridges. The exception goes for the traditional approach, when implemented with the use of pushover analysis to estimate the demand, which yielded considerably less safe scenarios, constituting an upper envelope, on the conservative side.
- The distance between the two methodologies gets even lower if the drift deformation control of the piers is carried out, denoting that such limitation contributes to standardization of results. Such effect is particularly visible in the reduction of the dispersion that had been initially found in Figure 6.48 for configurations 232 and 3332111.

# 7. Conclusions

## 7.1 Concluding remarks

The present work targeted the probabilistic seismic safety assessment of single reinforced concrete existing bridges. To accomplish so, different methodologies, corresponding to the use of different methods for structural response prediction, combined with different ways of incorporating the uncertainty associated to the different variables of the safety verification problem, have been proposed, calibrated and compared. The computation of the structural failure probability made use of advanced statistical treatment, featuring distribution fitting of the relevant variables and numerical random sampling of variables using the Latin Hypercube sampling technique.

In addition to the distinct approaching methodologies for reaching a collapse probability that have been considered, independent calibration studies have been conducted, covering the different aspects around the assessment process, namely, the seismic action input characterization, the nonlinear structural modelling and the structural response estimation. Such studies were carried out with the purpose of better understanding the influence of each issue in the seismic behaviour of bridges, providing useful information and recommendations for analysis accuracy and optimization.

All the comparison/calibration studies have been carried out on a rather wide set of structural bridge configurations, featuring different locations: regular, semi-regular and irregular, in terms of pier heights and relative position, short and long, with different types of abutments. In addition, the selected seismic input case study was equally wide ranging, so as to include relevant seismic dispersion in the analyses. Different intensity levels were considered, looking into the bridges behaviour in elastic field as well as pushing them into high nonlinear stages. In order to appropriately organize all the information coming from all the configurations, earthquake records and intensity levels, results were treated, when possible, throughout the computation of statistical measures, with the intent of identifying patterns and drawing as much generalist as possible conclusions.

The study of the seismic action characterization constituted the first logical step and went over different topics, well known in the literature. The following observations were made.

- Focusing the use of accelerograms as the most complete seismic input element type, the first question remained on the choice between using real or artificial ground motion records. Looking at the first option, a case study of 20 different earthquake records was considered within a European integrated project framework. Different ground motion scaling parameters were tested for the standardization of accelerograms for use in nonlinear dynamic analysis. The parameters were all based on quantities taken/computed from the accelerograms themselves or from the corresponding response spectra. Identification of optimum scaling techniques, through evaluation of resulting dispersion, has shown that typically used peak ground acceleration or spectral acceleration for the first vibration period of the structure being analysed performed better. Such findings have then been employed in the probabilistic framework developed in Chapter 5, which made use of peak ground acceleration probability density functions, to characterize the seismic Hazard.
- The issue of the selection of real records for analysis was afterwards addressed, a task of renowned importance, given the heterogeneity which characterizes the available real accelerograms databases. Typically carried out following criteria based on seismological parameters, such as magnitude or epicentral distance, the work herein undertaken tried to adopt a different perspective, looking at the effects



of the earthquakes on the structure, in terms of displacement ductility demand. The same set of records was used to run nonlinear dynamic analysis on a long, irregular existing bridge, the Lordo viaduct, used within the mentioned research project. Selection of the records causing very discrepant results, differing substantially from the general trend, was carried out by means of clustering analysis, which is based on likeliness measures, used to aggregate similar individuals. The application of the clustering procedures allowed the obtaining of a much more homogeneous set of records, with considerable reduction in the associated scatter. Such a technique may be easily/efficiently used in reducing dispersion, provided that a proper statistical software package is available, when selecting real accelerograms to carry out safety assessment studies, which are largely influenced by the scatter around the records.

- A brief incursion to alternative intensity measure approaches, more elaborated, not simply obtained from the accelerogram quantities or corresponding response spectra, was carried out. Particularly, an intensity measure based on pushover analysis and displacement based theory simplified parameters has been proposed and its potential has been demonstrated for a wide set of bridge cases. The inclusion of such intensity measure in the study carried out in Chapter 6, as an additional approach to the estimation of structural demand, as mentioned in Section 7.2, can now be explored.
- Artificial accelerograms have been considered as well, generated to be compatible with the spectrum corresponding to the mean of the real records. Final comparison with real records scaled according to the two most advantageous techniques has been carried out. Artificial accelerograms proved to be a valid alternative for the seismic analysis of the studied bridge, featuring considerable less dispersion as well as being less conservative than the real records, especially when scaled by means of spectral acceleration parameter. Their consideration in bridges safety assessment procedures is, hence, expected to lead to similar results with much less computational demand.

Modelling of the structural system for seismic analysis has been afterwards looked at, in terms of the issues of main interest and pertinence, focusing mainly on material nonlinearity, given that geometrical nonlinearity is usually seen as less relevant. The study

on material nonlinearity consideration, addressed in Chapter 4, lead to the following findings.

- The main distinction in terms of approaching ways has been made between the use of distributed or concentrated plasticity models or, in other words, fibre models or plastic hinge models. Both the modelling alternatives have been tested with the use of beam-column bar elements 3D models, using two well-known structural analysis programs: SeismoStruct for spread plasticity and SAP2000 for lumped plasticity. To the employment of fibre models, the input of the concrete and steel constitutive laws was enough, whereas, for the concentrated plasticity ones, a characterization of the plastic hinge constitutive law, based on the same material models, was required. Consequently, a summary of several available material models has been presented and the description of the used ones has been carried out, with the selection being based mainly on past experience on such matter.
- Within the use of the plastic hinge based modelling, different important issues have been addressed. Calibration of elements with plastic hinges development at the extremities of the piers was done in terms of plastic hinge length, location as moment-curve defining curve. Both length and location of the plastic hinge proved to be not greatly relevant; three different approaches for the parameters were tested in hollow and full reinforced concrete sections (from the piers of the main case study bridges) and results did not present significant variation. The moment-curvature constitutive law of the plastic hinges was approximated by a trilinear curve, which enables optimization, in terms of time and computational effort, of the concentrated plasticity approach. Furthermore, the fibre model corresponding moment-curvature was brought in for comparison, with both the curves matching quite well.
- The main comparison between the two modelling schemes was extended to the comparison of the structural response prediction of the different bridge configuration of the selected case study. Nonlinear static procedures (NSP) were the chosen tool for the bridges analysis, using, for this case, the N2 Method, recommended by the EC8 and confirmed as suitable to the analysis of bridges in Chapter 5. Moreover, the NSP was applied using capacity curves obtained with

different load patterns and reference nodes. The comparison of the capacity curves, the immediate output of the pushover analyses, obtained for the different configurations, denoted a fairly good agreement between the two modelling alternatives, regardless of the employed load pattern or reference node. Slight differences that were punctually found correspond to slightly higher base shear prediction for the case of plastic hinges models. Furthermore, comparison on the structural response of the bridges at their performance point was evaluated through the computation of ratios of the different models' response for different response parameters, across increasing intensity levels. Again, fairly good matching of results has been encountered, despite minor differences that have, nevertheless, been found.

- The global conclusion pointed out that both modelling solutions provided agreeing outputs, whether fibre or plastic hinge based. Such agreement was sustained within the computation of capacity curves as well as structural response estimated by means of nonlinear static analysis. Such outcome surely brings some reassurance in the recognition of the validity of more simplified plastic hinge models, as long as duly calibrated in its parameters, for use in seismic analysis of bridges, when compared to the certainly more precise fibre models. This outcome also sustained the use of plastic hinge models in the extensive probabilistic framework carried out in Chapter 6, accounting for considerable time and computational savings.

The prediction of the structural response of bridges, the scope of Chapter 5, was evaluated recurring to different nonlinear analysis schemes, namely, nonlinear static analysis and nonlinear dynamic analysis. For what concerns the use of nonlinear static procedures, the existing high variability on the possible alternatives lead to an extensive parametric study, selecting four commonly employed methods for comparison: Capacity Spectrum Method, N2 Method, Modal Pushover Analysis and Adaptive Capacity Spectrum Method. Preliminarily, each of the procedures was calibrated with a view to find its optimum configuration, which was then selected for the final comparison. For the sake of generality and consistence the comparative evaluation of the different methods was carried out for the described case study and seismic input and throughout the same response parameters. The following conclusions are worth underlying:

- Regarding the individual calibration of the methods, different variants for each of them were tested, mainly in terms of loading pattern for the pushover analysis (N2), pushover curve reference node (CSM, N2 and MPA), spectral reduction, based on equivalent viscous damping or ductility (CSM and ACSM). Significant differences have been found in the NSPs performance, when applied in such different variants. More than the reference node choice or the loading shape, the spectral reduction factors issue, together with the variability in the estimation of equivalent viscous damping, particularly affected the methods, which denoted the need for the preliminary calibration.
- Generally, the nonlinear static procedures provided evidence on their ability to accurately predict the structural response of bridges, in terms of displacements, except for the Capacity Spectrum Method, and pier shear forces, for all sorts of bridge configurations (regular, irregular, short, long, etc), when compared to nonlinear dynamic analysis results, which is commonly seen as the most reliable tool for structural performance estimation. Regarding the remaining parameters, an underestimating pattern has been found for all the methods, in deck moments and abutment shear forces. Globally, the Adaptive Capacity Spectrum Method behaved more consistently, followed closely by N2 and Modal Pushover Analysis. For the case of heavily underestimated deck moments and shear at the abutments, the Capacity Spectrum Method stood as the poorest one, despite the unsatisfactory behaviour of all the procedures. With filtering the results according to different structural categories (in terms of regularity, deck length and type of abutments) less scattered estimates were obtained using MPA and ACSM. It seems, therefore, that such methods, including higher modes effects, are definitely more adequate to accurately estimate the nonlinear performance of structures, as an alternative to complex nonlinear dynamic analysis. Such conclusion seems understandable, especially for bridge structures, to which superior vibration modes with important modal participation factors are typically associated. Moreover, such conclusions have validated the use of nonlinear static analysis techniques in other topics, such as the modelling calibration issues in Chapter 4, or probabilistic safety assessment in Chapter 6.

- If one method should be chosen over the others, such choice should mostly be based on two aspects: the demonstrated condition that the method includes higher modes contribution and the ability to keep a steady accurate level of response prediction for the set of different deformation/force tested parameters. Under such circumstances, the Adaptive Capacity Spectrum Method could be the choice, followed by the N2 Method and Modal Pushover Analysis.

Finally, the evaluation of the actual methodologies for the seismic safety assessment was carried out in Chapter 6, making use of the observations made in Chapters 3, 4 and 5, regarding Seismic Input, Nonlinear Modelling and Seismic Demand, respectively.

Two distinct methodologies have been proposed for the safety assessment leading to the computation of the failure probability of the structure, which differ essentially on the way of incorporating the uncertainty associated to the several variables of the whole process, represented by their statistical distributions, which have been whether assumed or determined. The uncertainty has been considered locally or globally, with a higher number of variables corresponding to the latter. Moreover, different variants to those methodologies were tested, including different ways of estimating the structural response, enhanced by the conclusions in Chapter 5. The following summarizing observations can be made.

- The use of the Latin Hypercube Sampling method in characterizing the structural capacity has been found efficient and simple, requiring a significantly lower number of random realizations than other comparables methods. The number of realizations needed for the sampling results to stabilize was expectedly lower for the case of capacity characterization rather than for global probabilistic computation. The estimation of the distribution of the available ductility in curvatures of the piers cross sections required samples sized of a maximum of 50 realizations, with input variables being restricted to the material properties. No uncertainty was considered in the geometrical properties.
- All the nonlinear dynamic analyses, needed for both the methodologies, were carried out using plastic hinges models, easier to incorporate within an automatic

global computation/simulation procedure. Such feature was supported by the conclusions drawn in Chapter 4.

- The traditional methodology, corresponding to the local uncertainty consideration, has made use of vulnerability functions obtained either through nonlinear dynamic analysis or nonlinear static analysis, as enabled by the prescriptions in Chapter 5, on Seismic Demand. The vulnerability functions were obtained by 2<sup>nd</sup> degree polynomial curve fitting to the individual ductility demands corresponding to different intensity levels. Such process was successful and straightforward with high quality of the adjustment being noted. The use of nonlinear static vulnerability functions has proven to be valid, even if sometimes too much conservative.
- If the seismic action, input record and intensity level, is included as a variable, then the aforementioned global simulation procedure is being followed, which features the computation of the collapse probability by adjusting a distribution to the variable given by the difference between the capacity and the demand. For that case, the sampling size, within the Latin Hypercube sampling scheme, increased to 200, which continues to be, in any case, computationally low demanding. The goodness-of-fit of the distributions adjusted to the safety interval variable (distance going from ductility capacity to ductility demand) was verified by means of the Kolmogorov-Smirnov test, which provided positive results for almost all the cases.
- Irregular bridges have been found to be less safe to the considered seismic action and resulted in higher agreement between the different methodologies. On the other hand, no noticeable trend has been found with respect to the deck length. The central or the shortest piers were systematically the critical ones, sometimes with huge differences in its failure probabilities, when compared to the more slender ones. An additional criterion to the probability computation, in terms of maximum allowable drift for the piers, was added, resulting in quite interesting results, changing sometimes the critical pier.
- The two key alternative procedures to compute the collapse probability have proven to be quite in agreement for the majority of the configurations. The added consideration of the uncertainty of the seismic action yielded, however, more

severe results, which has to do with the inclusion of a larger number of variables and corresponding uncertainty. The two methodologies get even closer if the drift deformation control of the piers is carried out, denoting that such limitation actually contributes to the results.

Seismic assessment of bridges, within a probabilistic context, is a highly dense and controversial topic, as has been demonstrated, not only due to the statistical approach to the safety problem itself but also to all the uncertainty that surrounds its different components. The work herein carried out over the Seismic Input, Nonlinear Modelling and Seismic Demand issues, following a natural path that would lead to the optimization of the safety assessment process, has highlighted several obstacles (and variability) that the engineering community is still facing nowadays. Hopefully, a contribution to that same community, on those specific topics, has been provided. Moreover, notwithstanding the difficulties in standardizing procedures and approaching tactics, it has been observed that conceptually different probabilistic seismic Safety Assessment methodologies are not as random and uncertain as many times feared. This surely reaffirms the soundness and the need for probabilistic seismic assessment (and design) methodologies to become a reality in bridge engineering practice.

## **7.2 Future developments**

The presented work aimed to contribute with a general overview of all the steps that more or less generally need to be taken when carrying out the probabilistic seismic safety assessment of existing reinforced concrete bridges.

Regarding the seismic action characterization, the clustering techniques may be further probed by extending the case study to a larger number of records and, mostly, to different structural configurations. The use of artificial accelerograms has not been thoroughly developed. The use of different types of synthetic records, such as wavelet enriched ones, can be investigated. Moreover, the effect of artificial records should be tested inside the probabilistic assessment study as a less demanding alternative to the real records in dynamic analysis. Several improvements, regarding the proposed preliminary displacement-based intensity measure, can be carried out as well, characterizing more thoroughly the advantageous effects of such standardizing technique in nonlinear seismic

analysis. Furthermore, the simple underlying premises certainly enable its consideration within a probabilistic assessment study, of a single structure or a whole region network.

Concerning the nonlinear modelling field, the damping consideration can be an aspect that greatly influences the structural behaviour. Within this work, no parametric calibration study on the elastic damping was presented, given that typically such portion is considered to be very low when dealing with bridge structures, where there are few physical phenomena that may call for such modelling. It is, however, believed that with the consideration of higher elastic damping values, numerical instability may arise, requiring additional studies to better understand such phenomenon in reinforced concrete bridges.

Within the structural response topic, different alternative simplified procedures, including additional variables in the parametric study, can be tested, and further improving of the prediction of shear forces should be looked for. Additionally, Nonlinear Static Procedures may possibly start to be employed in the near future by practitioners as the first genuine nonlinear analysis methods introduced in common design office practice. Consequently, preparation of such methods to be easily applied, eventually involving some generalization degree, can be initiated.

Finally, and focusing on the main goal of this work, the probabilistic safety assessment of bridges, there is still a long way to go before such probabilistic methods can become widespread. On that matter, the contribution herein given is limited and can be improved in some aspects. The probability computation of the proposed methodologies is achieved at the tails of the distributions, which are known to be problematic. Statistical refinement of the methods can be a possible improving path, in order to bring more confidence to the vulnerability estimates. In addition, more goodness-of-fit tests can be carried out, discarding improper distributions, or even different distributions, similar to the extreme value type ones, herein considered, can be tested, with a view to warrant the attainment of more solid failure probability predictions.



# References

## A

- Aktan, A. E., Pecknold, D. A. and Sozen, M. A. (1974) R/C Column Earthquake Response in Two Dimensions. *Journal of the Structural Division*, 100(10), pp. 1999-2015
- Aktan, A. E. and Ersoy, U. (1979) Analytical Study of R/C Material Hysteresis. *Proceedings of the AICAP-CEB Symposium on Structural Concrete Under Seismic Actions*, CEB Bulletin d'Information no. 132, pp. 97-104
- Alavi, B. and Krawinkler, H. (2004) Behavior of moment-resisting frame structures subjected to near-fault ground motions. *Earthquake Engineering & Structural Dynamics*, 33(6), pp. 687-706
- Alfawakhiri, F. and Bruneau, M. (2000) Flexibility of superstructures and supports in the seismic analysis of simple bridges. *Earthquake Engineering & Structural Dynamics*, 29(5), pp. 711-729
- Alvarez, J. C. (2004) Displacement-based design of continuous concrete bridges under transverse seismic excitation. M.Sc. Thesis, ROSE School, European School for Advanced Studies in Reduction of Seismic Risk, Pavia, Italy
- Ambraseys, N., Smit, P., Sigbjornsson, R., Suhadolc, P. and Margaris, B. (2002) *Internet-Site for European Strong-Motion Data*. European Commission, Research-Directorate General, Environment and Climate Programme
- Antoniou, S., Rovithakis, A. and Pinho, R. (2002) Development and verification of a fully adaptive pushover procedure. *Proceedings of the 12th European Conference on Earthquake Engineering*, September 9-13, London, UK
- Antoniou, S. and Pinho, R. (2004) Development and verification of a displacement-based adaptive pushover procedure. *Journal of Earthquake Engineering*, 8(5), pp. 643-661
- Arède, A. and Pinto, A. V. (1996) *Reinforced concrete global section modelling: definition of skeleton curves*. Special Publication No.I.96.36, Institute for Systems, Informatics and Safety, Joint Research Center, Ispra, Italy
- ASCE (2005) *Minimum Design Loads for Buildings and Other Structures (7-05)*. American Society of Civil Engineers, Reston, VA
- ATC (1996) *Seismic Evaluation and Retrofit of Concrete Buildings, Volumes 1 and 2*. Report No. ATC-40, Applied Technology Council, Redwood City, CA
- ATC (1997) *NEHRP Guidelines for the Seismic Rehabilitation of Buildings*. Report No. FEMA-273, Federal Emergency Management Agency, Washington, DC
- ATC (2005) *Improvement of Nonlinear Static Seismic Analysis Procedures*. Report No. FEMA-440, Federal Emergency Management Agency, Washington, DC

Aydan, Ö, Kumsar, H., Toprak, S. and Barla, G. (2009) Characteristics of 2009 L'Aquila earthquake with an emphasis on earthquake prediction and geotechnical damage. *Journal of The School of Marine Science and Technology*, 7(3), pp. 23-51

Ayyub, B. M. and Lai, K. L. (1989) Structural reliability assessment using latin hypercube sampling. *Proceedings of the ICOSSAR'89*, August 8-11, San Francisco, USA

## B

Baker, J. W. and Cornell, C. A. (2006) Spectral shape, epsilon and record selection. *Earthquake Engineering & Structural Dynamics*, 35(9), pp. 1077-1095

Bal, I. E., Crowley, H. and Pinho, R. (2008) Displacement-Based Earthquake Loss Assessment for an Earthquake Scenario in Istanbul. *Journal of Earthquake Engineering*, 12(S2), pp. 12-22

Banon, H., Irvine, H. M. and Biggs, J. M. (1981) Seismic damage in reinforced concrete frames. *Journal of the Structural Division*, 107(9), pp. 1713-1729

Barbat, A. H. and Canet, J. M. (1994) *Estructuras sometidas a acciones sísmicas: Cálculo por ordenador*. Centro Internacional de Métodos Numéricos en Ingeniería, Barcelona (in Spanish)

Bartlett, F. M. and MacGregor, J. G. (1996) Statistical analysis of the compressive strength of concrete in structures. *ACI Materials Journal*, 93(2), pp. 158-168

Basoz, N. and Kiremidjian, A. (1998) *Evaluation of Bridge Damage Data from the Loma Prieta and Northridge, California Earthquakes*. Technical Report MCEER-98-0004, Stanford University, Stanford, California

Bazoant, Z. P. and Bhat, P. D. (1977) Prediction of Hysteresis of Reinforced Concrete Members. *Journal of the Structural Division*, 103(1), pp. 153-167

Bazzurro, P. (1998) Probabilistic Seismic Demand Analysis. Ph.D. Thesis, Stanford University - Department of Civil and Environmental Engineering, Stanford, CA, USA

Bazzurro, P. and Luco, N. (2006) Do Scaled and Spectrum-matched Near-Source Records Produce Biased Nonlinear Structural Responses? *Proceedings of 8th U.S. National Conference on Earthquake Engineering*, April 18-22, San Francisco, CA, USA

Bertero, V. V. and Popov, E. P. (1976) *Experimental and Analytical Studies on Hysteretic Behaviour of Reinforced Concrete Rectangular and T-Beams*. Technical Report 02/76, Earthquake Engineering Research Center, University of California, Berkeley, CA

Bertero, V. V., Aktan, A. E., Charney, F. and Sause, R. (1984) Earthquake Simulator Tests and Associated Experimental, Analytical, and Correlation Studies of One-Fifth Scale Model. *Special Publication, Earthquake Effects on Reinforced Concrete Structures*, American Concrete Institute, SP84(13), pp. 375-424

Bertero, V. V., Anderson, J. C., Krawinkler, H. and Miranda, E. (1991) *Design Guidelines for Ductility and Drift Limits*. Report No. UCB/EERC-91/15, Earthquake Engineering Research Center, Berkeley, CA

Bertero, V. V. (1995) *Tri-services manual methods*. Vision 2000 Performance Based Seismic Engineering of Buildings, Vol. 1, Part 2, Appendix J, J1-J8, Structural Engineer Association of California, Sacramento, CA

- Bommer, J. J. and Martínez-Pereira, A. (1999) The effective duration of earthquake strong motion. *Journal of Earthquake Engineering*, 3(2), pp. 127-172
- Bommer, J. J. and Acevedo, A. B. (2004) The Use of Real Earthquake Accelerograms as Input to Dynamic Analysis. *Journal of Earthquake Engineering*, 8(S1), pp. 43-91
- Borges, J. F. and Castanheta, M. (1985) *Structural Safety, Curso 101*. LNEC, Lisboa (in Portuguese)
- Bozorgzadeh, A., Megally, S., Restrepo, J. I. and Ashford, S. A. (2006) Capacity Evaluation of Exterior Sacrificial Shear Keys of Bridge Abutments. *Journal of Bridge Engineering*, 11(5), pp. 555-565
- Bracci, J. M., Kunnath, S. K. and Reinhorn, A. M. (1997) Seismic Performance and Retrofit Evaluation of Reinforced Concrete Structures. *Journal of Structural Engineering*, 123(1), pp. 3-10
- Bradley, B. A. (2011) Design Seismic Demands from Seismic Response Analyses: A Probability-Based Approach. *Earthquake Spectra*, 27(1), pp. 213-224
- Brancaleoni, F., Ciampi, V. and Di Antonio, R. (1983) Rate-Type Models for Non Linear Hysteretic Structural Behavior. *Proceedings of the EUROMECH Colloquium*, October 10-14, Palermo, Italy
- C**
- Calabrese, A., Almeida, J. P. and Pinho, R. (2010) Numerical Issues in Distributed Inelasticity Modeling of RC Frame Elements for Seismic Analysis. *Journal of Earthquake Engineering*, 14(S1), pp. 38-68
- Calvi, G. M. (1994) *PREC8 - Bridge Models For PSD Testing*. Design Documents, Department of Structural Mechanics, University of Pavia, Pavia, Italy
- Calvi, G. M. and Pinto, P. E. (1995) Irregular bridges designed according to Eurocode 8: numerical and experimental verifications. *Proceedings of the 1st Japan-Italy Workshop on Seismic Design of Bridges*, Public Works Research Institute, Tsukuba, Japan
- Calvi, G. M. (2004) Recent experience and innovative approaches in design and assessment of bridges. *Proceedings of the 13th World Conference on Earthquake Engineering*, August 1-6, Vancouver, Canada
- Carvalho, A. (2009) Avaliação da Segurança Sísmica de Pontes. M.Sc. Thesis, University of Porto, Porto, Portugal (in Portuguese)
- Casarotti, C., Pinho, R. and Calvi, G. M. (2005) *Adaptive pushover-based methods for seismic assessment and design of bridge structures*. ROSE Research Report No. 2005/06, IUSS Press, Pavia, Italy
- Casarotti, C. and Pinho, R. (2006) Seismic response of continuous span bridges through fiber-based finite element analysis. *Earthquake Engineering and Engineering Vibration*, 5(1), pp. 119-131
- Casarotti, C. and Pinho, R. (2007) An adaptive capacity spectrum method for assessment of bridges subjected to earthquake action. *Bulletin of Earthquake Engineering*, 5(3), pp. 377-390

Casarotti, C., Monteiro, R. and Pinho, R. (2009) Verification of spectral reduction factors for seismic assessment of bridges. *Bulletin of the New Zealand Society for Earthquake Engineering*, 42(2), pp. 111-121

CBSC (2007) *California Building Code*. California Building Standards Commission, Sacramento, CA

CEB (1983) *Response of R.C. Critical Regions under Large Amplitude Reversed Actions*. Bulletin d'Information No. 161, pp. 255-284, Comité Euro-International du Béton, Lausanne

CEN (2005a) *Eurocode 8: Design of Structures for Earthquake Resistance - Part 1: General rules, seismic actions and rules for buildings*. EN 1998-2, Comité Européen de Normalisation, Brussels, Belgium

CEN (2005b) *Eurocode 8: Design of Structures for Earthquake Resistance - Part 2: Bridges*. EN 1998-2, Comité Européen de Normalisation, Brussels, Belgium

Chang, G. and Mander, J. B. (1994) *Seismic Energy Based Fatigue Damage Analysis of Bridge Columns: Part II - Evaluation of Seismic Demand*. Technical Report NCEER-94-0013, Multidisciplinary Center for Earthquake Engineering Research (Former NCEER), Buffalo, NY

Charney, F. A. and Bertero, V. V. (1982) *An evaluation of the design and analytical seismic response of a seven-story reinforced concrete frame-wall structure*. EERC Report 82/08, Earthquake Engineering Research Center, University of California, Berkeley, CA

Chopra, A. K. (1995) *Dynamics of Structures: Theory and Applications to Earthquake Engineering*. Prentice-Hall, Englewood Cliffs, NJ

Chopra, A. K. and Goel, R. K. (1999) Capacity-Demand-Diagram Methods Based on Inelastic Design Spectrum. *Earthquake Spectra*, 15(4), pp. 637-656

Chopra, A. K. and Goel, R. K. (2001) *A modal pushover analysis procedure to estimating seismic demands for buildings: Theory and preliminary evaluation*. PERR Report 2001/03, Pacific Earthquake Engineering Research Center, University of California, Berkeley, CA

Chopra, A. K. and Goel, R. K. (2002) A modal pushover analysis procedure for estimating seismic demands for buildings. *Earthquake Engineering & Structural Dynamics*, 31(3), pp. 561-582

Chopra, A. K. and Chintanapakdee, C. (2004) Evaluation of Modal and FEMA Pushover Analyses: Vertically "Regular" and Irregular Generic Frames. *Earthquake Spectra*, 20(1), pp. 255-271

Chopra, A. K. and Goel, R. K. (2004) A modal pushover analysis procedure to estimate seismic demands for unsymmetric-plan buildings. *Earthquake Engineering & Structural Dynamics*, 33(8), pp. 903-927

Chopra, A. K. (2005) Estimating seismic demands for performance-based engineering of buildings. *Congreso Chileno de Sismología e Ingeniería Antisísmica, IX Jornadas*, November 16-19, Concepción, Chile

Clough, R. W. and Johnston, S. B. (1966) Effect of stiffness degradation on earthquake ductility requirements. *Proceedings of the Japan Earthquake Engineering Symposium*, Tokyo, Japan

Clough, R. W. and Benuska, L. (1967) Nonlinear earthquake behavior of tall buildings. *Journal of Mechanical Engineering*, 93(3), pp. 129-146

- Clough, R. W. and Penzien, J. (1993) *Dynamics of Structures*. McGrawHill, New York
- Cofie, N. G. (1984) *Cyclic Stress-Strain and Moment-Curvature Relationships for Steel Beams and Columns*. Report No. 1983-06, Stanford University, Stanford
- Computers&Structures (2006) *SAP2000 - Integrated Finite Element Analysis and Design of Structures*. Computers and Structures, Inc., Berkeley, California
- Cooper, J. D., Friedland, I. M., Buckle, I. G., Nimis, R. B. and Bobb, N. M. M. (1994) The Northridge earthquake: progress made, lessons learned in seismic-resistant bridge design. *Public Roads*, 58(1), pp. 26-36
- Correia, A. A. and Virtuoso, F. B. E. (2006) Nonlinear Analysis of Space Frames. *Proceedings of the III European Conference on Computational Mechanics*, June 5-8, Lisbon, Portugal
- Costa, A. C. (1993) A Acção dos Sismos e o Comportamento das Estruturas. Ph.D. Thesis, University of Porto, Porto, Portugal (in Portuguese)
- Costa, A. G. and Costa, A. C. (1987) *Modelo Histerético das Forças-Deslocamentos Adequado à Análise Sísmica de Estruturas*. Relatório Técnico, Núcleo de Dinâmica Aplicada, National Laboratory of Civil Engineering, Lisbon (in Portuguese)
- Costa, A. G. (1989) Análise sísmica de estruturas irregulares. Ph.D. Thesis, University of Porto, Porto, Portugal (in Portuguese)
- Crisfield, M. A. (1990) A consistent co-rotational formulation for non-linear, three-dimensional, beam-elements. *Computer Methods in Applied Mechanics and Engineering*, 81(2), pp. 131-150
- D**
- Delgado, P. (2000) Vulnerabilidade Sísmica de Pontes. M.Sc. Thesis, University of Porto, Porto, Portugal (in Portuguese)
- Delgado, P. (2009) Avaliação da Segurança Sísmica de Pontes. Ph.D. Thesis, University of Porto, Porto, Portugal (in Portuguese)
- Delgado, R., Marques, M., Monteiro, R., Delgado, P., Romão, X. and Costa, A. (2006) Setting Up Real or Artificial Accelerograms for Dynamic Analysis. *Proceedings of the 1st European Conference on Earthquake Engineering and Seismology*, September 3-8, Geneva, Switzerland
- Duarte, R. T. and Costa, A. C. (1991) Identification of Design Seismic Actions Considering the Nonlinear Behaviour of Structures. *Proceedings of the International Workshop on Seismology and Earthquake Engineering*, April 22-26, Centro Nacional de Prevención de Desastres (CENAPRED), Mexico City
- Dwairi, H. and Kowalsky, M. (2006) Implementation of Inelastic Displacement Patterns in Direct Displacement-Based Design of Continuous Bridge Structures. *Earthquake Spectra*, 22(3), pp. 631-662
- Dwairi, H. M., Kowalsky, M. J. and Nau, J. M. (2007) Equivalent Damping in Support of Direct Displacement-Based Design. *Journal of Earthquake Engineering*, 11(4), pp. 512-530

## E

Eberhard, M. O., Baldrige, S. , Marshall, J., Mooney, W. and Rix, G. J. (2010) *The MW 7.0 Haiti earthquake of January 12, 2010; USGS/EERI Advance Reconnaissance Team Report*. U.S. Geological Survey Open-File Report 2010–1048, USGS, California

Elnashai, A. S. (2001) Advanced inelastic static (pushover) analysis for earthquake applications. *Structural Engineering and Mechanics*, 12(1), pp. 51-69

Elnashai, A. S. (2002) Do we really need inelastic dynamic analysis? *Journal of Earthquake Engineering*, 6(S1), pp. 123-130

Everitt, B. S., Landau, S. , Leese, M. and Stah, D. (2001) *Cluster Analysis*. John Wiley & Sons Inc., New York

## F

Fajfar, P. and Fischinger, M. (1988) N2 - A method for non-linear seismic analysis of regular buildings *Proceedings of the 9th World Conference in Earthquake Engineering*, August 2-9, Tokyo-Kyoto, Japan

Fajfar, P. (1999) Capacity spectrum method based on inelastic demand spectra. *Earthquake Engineering & Structural Dynamics*, 28(9), pp. 979-993

Fajfar, P. (2000) A Nonlinear Analysis Method for Performance Based Seismic Design. *Earthquake Spectra*, 16(3), pp. 573-592

Felippa, C. A. and Park, K. C. (2002) The construction of free-free flexibility matrices for multilevel structural analysis. *Computer Methods in Applied Mechanics and Engineering*, 191(19-20), pp. 2111-2140

Filippou, F. C., Popov, E. P. and Bertero, V. V. (1983a) Modeling of R/ C Joints under Cyclic Excitations. *Journal of Structural Engineering*, 109(11), pp. 2666-2684

Filippou, F. C., Popov, E. P. and Bertero, V. V. (1983b) *Effects of bond deterioration on hysteretic behavior of reinforced concrete joints*. Report No. UCB/EERC-83/19, Earthquake Engineering Research Center, University of California, Berkeley, CA

Fischinger, M., Beg, D., Isakovic, T., Tomazevic, M. and Zarnic, R. (2004) Performance based assessment - from general methodologies to specific implementations. *Proceedings of the International Workshop on Performance-based Seismic Design: Concepts and Implementation*, June 28 - July 1, Bled, Slovenia

Florian, A. and Navratil, J. (1993) Reliability Analysis of the Cable Stayed Bridge in Construction and Service Stages. *Proceedings of the ICOSSAR'93*, August 9-13, Innsbruck, Austria

Frangopol, D. M., Ide, Y., Spacone, E. and Iwaki, I. (1996) A new look at reliability of reinforced concrete columns. *Structural Safety*, 18(2-3), pp. 123-150

Freeman, S. A., Nicoletti, J. P. and Tyrell, J. V. (1975) Evaluation of Existing Buildings for seismic risk - A case study of Puget Sound Naval Shipyard, Bremerton, Washington. *Proceedings of the 1st U.S. National Conference on Earthquake Engineering*, Berkley, USA

Freeman, S. A. (1998) Development and use of capacity spectrum method. *Proceedings of the 6th U.S. National Conference on Earthquake Engineering*, June 1-5, Seattle, USA

Freudenthal, A. M., Garrelts, J. M. and Shinozuka, M. (1966) The Analysis of Structural Safety. *Journal of the Structural Division*, 92(ST1), pp. 267-325

Fujii, M., Kobayashi, K., Miyagawa, T., Inoue, S. and Matsumoto, T. (1988) A study on the application of a stress-strain relation of confined concrete. *Proc., JCA Cement and Concrete*, 42(1988), pp. 311-314

## G

Gasparini, D. A. and Vanmarcke, E. (1976) *SIMQKE: Generation of artificial time histories compatible with a specified target spectrum*. Report No. R76-4, Massachusetts Institute of Technology, Cambridge, MA

Giberson, M. F. (1967) The response of nonlinear multi-story structures subjected to earthquake excitation. Ph.D. Thesis, California Institute of Technology, Pasadena, USA

Goel, R. K. and Chopra, A. K. (1997) Evaluation of Bridge Abutment Capacity and Stiffness during Earthquakes. *Earthquake Spectra*, 13(1), pp. 1-23

Goel, R. K. and Chopra, A. K. (2004) Evaluation of Modal and FEMA Pushover Analyses: SAC Buildings. *Earthquake Spectra*, 20(1), pp. 225-254

Goel, R. K. (2005) Evaluation of Modal and FEMA Pushover Procedures Using Strong-Motion Records of Buildings. *Earthquake Spectra*, 21(3), pp. 653-684

Goel, R. K. and Chopra, A. K. (2005a) Extension of Modal Pushover Analysis to Compute Member Forces. *Earthquake Spectra*, 21(1), pp. 125-139

Goel, R. K. and Chopra, A. K. (2005b) Role of Higher-“Mode” Pushover Analyses in Seismic Analysis of Buildings. *Earthquake Spectra*, 21(4), pp. 1027-1041

Grant, L. H., Mirza, S. A. and Macgregor, J. G. (1978) Monte-Carlo Study of Strength of Concrete Columns. *ACI Journal Proceedings*, 75(8), pp. 348-358

Grimaz, S. and Maiolo, A. (2010) The impact of the 6th April 2009 L’Aquila earthquake (Italy) on the industrial facilities and life lines. Considerations in terms of NaTech risk. *Proceedings of the 4th International Conference on Safety & Environment in Process Industry*, March 14-17, Florence, Italy

Guedes, J. P. M. (1997) Seismic behaviour of reinforced concrete bridges - Modelling, numerical analysis and experimental assessment. Ph.D. Thesis, University of Porto, Porto, Portugal

Gulkan, P. and Sozen, M. A. (1974) Inelastic Responses of Reinforced Concrete Structure to Earthquake Motions. *ACI Journal Proceedings*, 71(12), pp. 604-610

Gupta, B. and Kunnath, S. K. (2000) Adaptive Spectra-Based Pushover Procedure for Seismic Evaluation of Structures. *Earthquake Spectra*, 16(2), pp. 367-392

## H

Hall, J. F. (1995) Northridge earthquake of January 17, 1994: reconnaissance report. *Earthquake Spectra*, 11Supplement C, 521p

Hall, J. F. (2006) Problems encountered from the use (or misuse) of Rayleigh damping. *Earthquake Engineering & Structural Dynamics*, 35(5), pp. 525-545

Hellesland, J. and Scordelis, A. (1981) Analysis of RC bridge columns under imposed deformations. *Proceedings of the IABSE Colloquium*, June 2-5, Delft, The Netherlands

Hoshikuma, J. and Nagaya, K. (1997) Stress-Strain Model for Confined Reinforced Concrete in Bridge Piers. *Journal of Structural Engineering*, 123(5), pp. 624-633

## I

ICC (2006) *International Building Code 2006*. International Code Council, Washington, DC

Iman, R. L., Helson, J. C. and Campbell, J. E. (1981) An Approach to Sensitivity Analysis of Computer Models: Part I - Introduction, Input Variable Selection and Preliminary Variable Assessment. *Journal of Quality Technology*, 13(3), pp. 174-183

Iman, R. L. and Conover, W. J. (1982) A distribution-free approach to inducing rank correlation among input variables. *Communications in Statistics - Simulation and Computation*, 11(3), pp. 311-334

Isakovic, T. and Fischinger, M. (2006) Higher modes in simplified inelastic seismic analysis of single column bent viaducts. *Earthquake Engineering & Structural Dynamics*, 35(1), pp. 95-114

Iwan, W. D. (1980) Estimating inelastic response spectra from elastic spectra. *Earthquake Engineering & Structural Dynamics*, 8(4), pp. 375-388

Izzuddin, B. A. (2001) Conceptual issues in geometrically nonlinear analysis of 3D framed structures. *Computer Methods in Applied Mechanics and Engineering*, 191(8-10), pp. 1029-1053

## J

JCSS (1995) *Probabilistic model code - Part 3: Resistance models*. Joint Committee for Structural Safety, Working document JCSS-RACK-08-01-95

## K

Kaba, S. A. and Mahin, S. A. (1984) *Refined Modeling of Reinforced Concrete Columns for Seismic Analysis*. Report No. UCB/EERC-84/03, Earthquake Engineering Research Center, University of California, Berkeley, CA

Kalkan, E. and Kunnath, S. K. (2006) Adaptive Modal Combination Procedure for Nonlinear Static Analysis of Building Structures. *Journal of Structural Engineering*, 132(11), pp. 1721-1731

Kalkan, E. and Chopra, A. K. (2010) *Practical Guidelines to Select and Scale Earthquake Records for Nonlinear Response History Analysis of Structures*. U.S. Geological Survey Open-File Report 2010, USGS, California



- Kam, W. Y. (2011) *Preliminary Report from the Christchurch 22 Feb 2011 6.3Mw Earthquake: Pre-1970s RC and RCM Buildings, and Precast Staircase Damage*. University of Canterbury, Christchurch
- Kappos, A. J. (1991) Analytical Prediction of the Collapse Earthquake for R/C Buildings - Suggested Methodology. *Earthquake Engineering & Structural Dynamics*, 20(2), pp. 167-176
- Kappos, A. J., Chryssanthopoulos, M. K. and Dymiotis, C. (1999) Uncertainty analysis of strength and ductility of confined reinforced concrete members. *Engineering Structures*, 21(3), pp. 195-208
- Kappos, A. J. and Kyriakakis, P. (2000) A re-evaluation of scaling techniques for natural records. *Soil Dynamics and Earthquake Engineering*, 20(1-4), pp. 111-123
- Karsan, I. D. and Jirsa, J. D. (1969) Behavior of concrete under compressive loadings. *Journal of the Structural Division*, 95(ST12), pp. 2543-2563
- Kawashima, K. (2000) Seismic design and retrofit of bridges. *Bulletin of the New Zealand National Society for Earthquake Engineering*, 33(3), pp. 265-285
- Kawashima, K. (2007) *Seismic Design of Urban Infrastructures*. Lecture Notes, Kawashima Laboratory, Department of Civil Engineering, Tokyo Institute of Technology, Tokyo
- Kent, D. C. and Park, R. (1971) Flexural Members with Confined Concrete. *Journal of the Structural Division*, 97(7), pp. 1969-1990
- Kowalsky, M. J. (1994) Displacement-based design - a methodology for seismic design applied to RC bridge columns. M.Sc. Thesis, University of California, San Diego, La Jolla, CA
- Kowalsky, M. J., Priestley, M. J. N. and MacRae, G. A. (1994) *Displacement-based design, a methodology for seismic design applied to SDOF reinforced concrete structures*. Report No. SSRP-94/16, University of California, San Diego, La Jolla
- Kowalsky, M. J., Priestley, M. J. N. and MacRae, G. A. (1995) Displacement-based design of RC bridge columns in seismic regions. *Earthquake Engineering & Structural Dynamics*, 24(12), pp. 1623-1643
- Kowalsky, M. J. (2002) A displacement-based approach for the seismic design of continuous concrete bridges. *Earthquake Engineering & Structural Dynamics*, 31(3), pp. 719-747
- Krawinkler, H. and Seneviratna, G. (1998) Pros and cons of a pushover analysis of seismic performance evaluation. *Engineering Structures*, 20(4-6), pp. 452-464
- Kunnath, S. K., Reinhorn, A. M. and Lobo, R. F. (1992) *IDARC Version 3.0: A program for the inelastic damage analysis of reinforced concrete structures*. Technical Report NCEER-92-0022, Multidisciplinary Center for Earthquake Engineering Research (former NCEES), Buffalo, NY
- Kurama, Y. C. and Farrow, K. T. (2003) Ground motion scaling methods for different site conditions and structure characteristics. *Earthquake Engineering & Structural Dynamics*, 32(15), pp. 2425-2450

## L

Lawson, R. S., Vance, V. and Krawinkler, H. (1994) Nonlinear static pushover analysis - why, when, and how? *Proceedings of the 5th U.S. Conference in Earthquake Engineering*, July 10-14, Chicago, USA

LESSLOSS (2004a) *European Integrated Project on Risk Mitigation for Earthquakes and Landslides*. <http://www.lessloss.org/>

LESSLOSS (2004b) *European Integrated Project on Risk Mitigation for Earthquakes and Landslides, State of the Art - FEUP Contribution for Topic 2.3b*. <http://www.lessloss.org/>

Lin, Y. Y. and Chang, K. C. (2003) Study on Damping Reduction Factor for Buildings under Earthquake Ground Motions. *Journal of Structural Engineering*, 129(2), pp. 206-214

Luco, N. and Cornell, C. A. (2007) Structure-Specific Scalar Intensity Measures for Near-Source and Ordinary Earthquake Ground Motions. *Earthquake Spectra*, 23(2), pp. 357-392

Lupoi, A., Franchin, P. and Pinto, P.E. (2007) Further probing of the suitability of PUSH-OVER analysis for the seismic assessment of bridge structures. *Proceedings of the 1st US-Italy Seismic Bridge Workshop*, April 19-20, Pavia, Italy

## M

Mackie, K. and Stojadinovic, B. (2004) Fragility curves for reinforced concrete highway overpass bridges. *Proceedings of the 13th World Conference on Earthquake Engineering*, August 1-6, Vancouver, Canada

Mahasuverachai, M. and Powell, G. H. (1982) *Inelastic analysis of piping and tubular structures*. Report No. EERC 82/27, Earthquake Engineering Research Center, University of California, Berkeley, CA

Mander, J. B., Priestley, M. J. N. and Fellow, R. P. (1988a) Observed Stress Strain Behavior of Confined Concrete. *Journal of Structural Engineering*, 114(8), pp. 1827-1849

Mander, J. B., Priestley, M. J. N. and Park, R. (1988b) Theoretical Stress-Strain Model for Confined Concrete. *Journal of Structural Engineering*, 114(8), pp. 1804-1826

Mari, A. R. and Scordelis, A. C. (1984) *Nonlinear geometric, material and time dependent analysis of three dimensional reinforced and prestressed concrete frames*. UC-SESM Report No. 84-12, University of California, Berkeley, CA

Martínez-Rueda, J. E. and Elnashai, A. S. (1997) Confined concrete model under cyclic load. *Materials and Structures*, 30(3), pp. 139-147

McKay, M. D., Beckman, R. J. and Conover, W. J. (1979) A Comparison of Three Methods for Selecting Values of Input Variables in the Analysis of Output from a Computer Code. *Technometrics*, 21(2), pp. 239-245

McKenna, F. (1997) Object oriented finite element analysis: frameworks for analysis algorithms and parallel computing. Ph. D. Thesis, Department of Civil Engineering, University of California, Berkeley,

- 
- McKenna, F. and Fenves, G. L. (2006) *OpenSees - The Open System for Earthquake Engineering Simulation OpenSees*. Pacific Earthquake Engineering Research Center, Berkeley, California
- Megally, S. H., Seible, F., Bozorgzadeh, A., Restrepo, J. and Silva, P. F. (2003) Response of Sacrificial Shear Keys in Bridge Abutments to Seismic Loading. *Proceedings of the FIB Symposium on Concrete Structures in Seismic Regions*, May 6-8, Athens, Greece
- Mehanny, S. S. and Deierlein, G. G. (2000) *Modeling of assessment of seismic performance of composite frames with reinforced concrete columns and steel beams*. Report No. 135, John A. Blume Earthquake Engineering Research Center, Stanford
- Menegotto, M. and Pinto, P. E. (1973) Method of Analysis for Cyclically Loaded RC Plane Frames, Including Changes in Geometry and Non-Elastic Behavior of Elements Under Combined Normal Force and Bending. *Proceedings of the IABSE Symposium on Resistance and Ultimate Deformability of Structures Acted on by Well Defined Repeated Loads*, Lisbon, Portugal
- MIDAS (2006) *MIDAS Civil - Integrated Solution System for Bridge and Civil Engineering* Midas Information Technology Co., Ltd., Seoul, Korea
- Miranda, E. (1993) Evaluation of Site Dependent Inelastic Seismic Design Spectra. *Journal of Structural Engineering*, 119(5), pp. 1319-1338
- Miranda, E. (2000) Inelastic Displacement Ratios for Structures on Firm Sites. *Journal of Structural Engineering*, 126(10), pp. 1150-1159
- Miranda, E. and Ruiz García, J. (2002) Evaluation of approximate methods to estimate maximum inelastic displacement demands. *Earthquake Engineering & Structural Dynamics*, 31(3), pp. 539-560
- Miyamoto, K., Yanev, P. and Salvaterra, I. (2009) *M6.3 L'Aquila, Italy*. Earthquake Field Investigation Report, Global Risk Miyamoto and Miyamoto International
- Moehle, J. P. and Cavanagh, T. (1985) Confinement Effectiveness of Crossties in RC. *Journal of Structural Engineering*, 111(10), pp. 2105-2120
- Moehle, J. P. (1999) *Preliminary Observations on the Performance of Concrete Freeway Structures*. National Information Service for Earthquake Engineering, University of California, Berkeley
- Moehle, J. P. and Eberhard, M. (1999) *Earthquake Damage to Bridges*. Bridge Engineering Handbook, CRC Press, USA
- Moghadam, A. S. and Tso, W. K. (2002) A pushover procedure for tall buildings. *Proceedings of the 12th European Conference in Earthquake Engineering*, September 9-13, London, UK
- Monteiro, R., Casarotti, C. and Pinho, R. (2008a) Using Nonlinear Static Procedures for seismic assessment of irregular viaducts. *Proceedings of the 5th European Workshop on the seismic behaviour of Irregular and Complex Structures*, September 16-17, Catania, Italy
- Monteiro, R., Ribeiro, R., Marques, M., Delgado, R. and Costa, A. G. (2008b) Pushover Analysis of RC Bridges Using Fibre Models or Plastic Hinges. *Proceedings of the 14th World Conference on Earthquake Engineering*, October 12-17, Beijing, China

Monteiro, R., Delgado, R., Crowley, H. and Pinho, R. (2009) Avaliação da segurança sísmica de pontes segundo diferentes metodologias. *1º Congresso Nacional de Segurança e Conservação de Pontes*, 1-3 Julho, Lisboa, Portugal (in Portuguese)

Monti, G. and Nuti, C. (1992) Nonlinear Cyclic Behavior of Reinforcing Bars Including Buckling. *Journal of Structural Engineering*, 118(12), pp. 3268-3284

Monti, G., Nuti, C. and Santini, S. (1996) *CYRUS: CYclic Response of Upgraded Sections. A program for the analysis of retrofitted or repaired sections under biaxial cyclic loading including buckling of rebars*. Report DSSAR No. 2/96, Universit degli Studi G. D'Annunzio, Chieti, Italy

Muguruma, H., Watanabe, S., Tanaka, S., Sakurai, K. and Nakaruma, E. (1978) A study on the improvement of bending ultimate strain of concrete. *Journal of Structural Engineering*, 24(Tokyo, Japan), pp. 109–116

## N

Nau, M. and Hall, W. J. (1984) Scaling methods for earthquake response spectra. *Journal of Structural Engineering*, 110(7), pp. 1533-1548

Neuenhofer, A. and Filippou, F. C. (1998) Geometrically Nonlinear Flexibility-Based Frame Finite Element. *Journal of Structural Engineering*, 124(6), pp. 704-711

Newmark, N. M. and Hall, W. J. (1982) *Earthquake Spectra and Design*. Earthquake Engineering Research Institute, Berkeley, CA,

Nielson, B. G. and DesRoches, R. (2007) Seismic fragility methodology for highway bridges using a component level approach. *Earthquake Engineering & Structural Dynamics*, 36(6), pp. 823-839

Novák, D., Teplý, B. and Keršner, Z. (1997) The Role of Latin Hypercube Sampling Method in Reliability Engineering. *Proceedings of the ICOSSAR 97*, November 24-28, Kyoto, Japan

## O

Olsson, A. and Sandberg, G. (2002) Latin Hypercube Sampling for Stochastic Finite Element Analysis. *Journal of Engineering Mechanics*, 128(1), pp. 121-125

Olsson, A., Sandberg, G. and Dahlblom, O. (2003) On Latin hypercube sampling for structural reliability analysis. *Structural Safety*, 25(1), pp. 47-68

Otani, S. (1974) Inelastic analysis of R/C frame structures. *Journal of the Structural Division*, 100(7), pp. 1433-1449

## P

Padgett, J.E., Nielson, B.G. and DesRoches, R. (2008) Selection of optimal intensity measures in probabilistic seismic demand models of highway bridge portfolios. *Earthquake Engineering & Structural Dynamics*, 37(5), pp. 711-725

Panagiotou, M. and Restrepo, J. I. (2007) *Design and computational model for the UCSD 7-story structural wall building slice*. SSRP 07-09 Report, University of California, San Diego, CA

- 
- Papageorgiou, A., Halldorson, B. and Dong, G. (2001) *TARSCTHS, a computer program for Target Acceleration Spectra Compatible Time Histories*. State University of New York, Buffalo, NY
- Papaoannou, I., Fragiadakis, M. and Papadrakakis, M. (2005) Inelastic Analysis of Framed Structures using the Fiber Approach. *Proceedings of the 5th International Congress on Computational Mechanics (GRACM 05)*, June 29 - July 1, Limassol, Cyprus
- Paraskeva, T. S., Kappos, A. J. and Sextos, A. G. (2006) Extension of modal pushover analysis to seismic assessment of bridges. *Earthquake Engineering & Structural Dynamics*, 35(10), pp. 1269-1293
- Paret, T. F., Sasaki, K. K., Eilbeck, D. H. and Freeman, S. A. (1996) Approximate inelastic procedures to identify failure mechanisms from higher mode effects. *Proceedings of the 11th World Conference on Earthquake Engineering*, June 23-28, Acapulco, Mexico
- Park, R., Kent, D. C. and Sampson, R. A. (1972) Reinforced Concrete Members with Cyclic Loading. *Journal of the Structural Division*, 98(7), pp. 1341-1360
- Park, R. and Paulay, T. (1975) *Reinforced concrete structures*. John Wiley & Sons, Inc., New York
- Park, R., Priestley, M. J. N. and Gill, W. D. (1982) Ductility of Square-Confined Concrete Columns. *Journal of the Structural Division*, 108(4), pp. 929-950
- Paulay, T. and Priestley, M. J. N. (1992) *Seismic design of reinforced concrete and masonry buildings*. John Wiley & Sons, Inc., New York
- Pinho, R. and Antoniou, S. (2005) A displacement-based adaptive pushover algorithm for assessment of vertically irregular frames. *Proceedings of the 4th European Workshop on the Seismic Behaviour of Irregular and Complex Structures*, August 26-27, Thessaloniki, Greece
- Pinho, R., Casarotti, C. and Monteiro, R. (2007) An Adaptive Capacity Spectrum Method and other Nonlinear Static Procedures Applied to the Seismic Assessment of Bridges. *Proceedings of the 1st US-Italy Seismic Bridge Workshop*, April 19-20, Pavia, Italy
- Pinho, R., Monteiro, R., Casarotti, C. and Delgado, R. (2009) Assessment of Continuous Span Bridges through Nonlinear Static Procedures. *Earthquake Spectra*, 25(1), pp. 143-159
- Pinho, R. (2011) *Seismic Assessment and Retrofitting of Existing Structures*. Lecture Notes, ROSE School, Centre for Post-Graduate Training and Research in Earthquake Engineering and Engineering Seismology, Pavia, Italy
- Pinto, A. V., Verzeletti, G., Pegon, P., Magonette, G., Negro, P. and Guedes, J. P. M. (1996) *Pseudo-Dynamic Testing of Large-Scale R/C Bridges*. Report EUR 16378 EN, Joint Research Centre, Ispra, Italy
- Pinto, P. E. and Giuffrè, A. (1970) Il Comportamento Del Cemento Armato Per Sollecitazioni Cicliche di Forte Intensità. *Giornale del Genio Civile*, 5 (in Italian)
- Pinto, P. E. (2001) Reliability methods in earthquake engineering. *Progress in Structural Engineering and Materials*, 3(1), pp. 76-85

Pinto, P. E., Fajfar, P., Chryssanthopoulos, M., Franchin, P., Dolšek, M. and Kazantzi, A. (2007) *Probabilistic Methods for Seismic Assessment of Existing Structures*. LESSLOSS Report No. 2007/06, IUSS Press, Pavia, Italy

Pipa, M. and Carvalho, E. C. (1994) Reinforcing Steel Characteristics for Earthquake Resistant Structures. *Proceedings of the 10th European Conference on Earthquake Engineering*, August 28 - September 2, Vienna, Austria

Priestley, M. J. N. and Park, R. (1984) *Strength and ductility of bridge substructures*. Research Report no. 84-20, University of Canterbury, Christchurch, New Zealand

Priestley, M. J. N. (1993) Myths and Fallacies in Earthquake Engineering - Conflicts Between Design and Reality. *Proceedings of the Thomas Paulay Symposium: Recent Developments in Lateral Force Transfer in Buildings*, SP-157, ACI Special Publication, UC San Diego, La Jolla, USA

Priestley, M. J. N., Seible, F. and Calvi, G. M. (1996) *Seismic design and retrofit of bridges*. Wiley-Interscience, New York

Priestley, M. J. N. (2003) Myths and fallacies in earthquake engineering, revisited. *The 9th Mallet-Milne Lecture, 2003*, IUSS Press, Pavia, Italy

Priestley, M. J. N. and Calvi, G. M. (2003a) Direct Displacement-Based Seismic Design of Bridges. *Proceedings of the ACI Special Seminar on Seismic Design of Bridges*, San Diego, USA

Priestley, M. J. N. and Calvi, G. M. (2003b) Direct displacement-based seismic design of concrete bridges. *Proceedings of the 5th ACI International Conference of Seismic Bridge Design and Retrofit for Earthquake Resistance*, December 8-9, La Jolla, USA

Priestley, M. J. N. and Grant, D. N. (2005) Viscous damping in seismic design and analysis. *Journal of Earthquake Engineering*, 9(2), pp. 229-255

Priestley, M. J. N., Calvi, G. M. and Kowalsky, M. J. (2007) *Displacement-based Seismic Design of Structures*. IUSS Press, Pavia, Italy

## R

Ramberg, W. and Osgood, W. R. (1943) *Description of Stress-Strain Curves by Three Parameters*. Technical Note No. 902, National Advisory Committee for Aeronautics, Washington

Ramirez, O. M., Constantinou, M. C., Whittaker, A. S., Kircher, C. A. and Chrysostomou, C. Z. (2002) Elastic and Inelastic Seismic Response of Buildings with Damping Systems. *Earthquake Spectra*, 18(3), pp. 531-547

Reinhorn, A. (1997) Inelastic analysis techniques in seismic evaluations. *Seismic Design Methodologies for the Next Generation of Codes: Proceedings of the International Workshop*, June 24-27, Bled, Slovenia

Rosenblueth, E. and Herrera, I. (1964) On a kind of hysteretic damping. *Journal of Engineering Mechanics*, 90(4), pp. 37-48

---

**S**

- Saatcioglu, M. and Razvi, S. R. (1992) Strength and Ductility of Confined Concrete. *Journal of Structural Engineering*, 118(6), pp. 1590-1607
- SAC (1997) *Develop Suites of Time Histories*. Project Task 5.4.1 Draft Report, SAC Joint Venture, Sacramento, CA
- Saiidi, M. and Sozen, M. A. (1981) Simple Nonlinear Seismic Analysis of R/C Structures. *Journal of the Structural Division*, 107(5), pp. 937-953
- Sandhu, J. S., Stevens, K. A. and Davies, G. A. O. (1990) A 3-D, co-rotational, curved and twisted beam element. *Computers & Structures*, 35(1), pp. 69-79
- Scott, B. D., Park, R. and Priestley, M. J. N. (1982) Stress-Strain Behavior of Concrete Confined by Overlapping Hoops at Low and High Strain Rates. *ACI Journal Proceedings*, 79(1), pp. 13-27
- Scott, M. H. and Filippou, F. C. (2007) Response Gradients for Nonlinear Beam-Column Elements under Large Displacements. *Journal of Structural Engineering*, 133(2), pp. 155-165
- SeismoSoft (2008) *SeismoStruct - A computer program for static and dynamic nonlinear analysis of framed structures*, available online from <http://www.seismosoft.com>. SeismoSoft Ltd, Pavia, Italy
- Sextos, A. G., Pitilakis, K. D. and Kappos, A. J. (2003) Inelastic dynamic analysis of RC bridges accounting for spatial variability of ground motion, site effects and soil-structure interaction phenomena. Part 1: Methodology and analytical tools. *Earthquake Engineering & Structural Dynamics*, 32(4), pp. 607-627
- Sheikh, S. A. and Uzumeri, S. M. (1979) Properties of Concrete Confined by Rectangular Ties. *Proceedings of the AICAP-CEB Symposium on Structural Concrete Under Seismic Actions*, CEB Bulletin d'Information no. 132, pp. 53-60
- Sheikh, S. A. and Uzumeri, S. M. (1980) Strength and Ductility of Tied Concrete Columns. *Journal of the Structural Division*, 106(5), pp. 1079-1102
- Sheikh, S. A. and Uzumeri, S. M. (1982) Analytical Model for Concrete Confinement in Tied Columns. *Journal of the Structural Division*, 108(12), pp. 2703-2722
- Shibata, A. and Sozen, M. A. (1976) Substitute-Structure Method for Seismic Design in R/C. *Journal of the Structural Division*, 102(1), pp. 1-18
- Shinozuka, M., Feng, M. Q., Lee, J. and Naganuma, T. (2000) Statistical Analysis of Fragility Curves. *Journal of Engineering Mechanics*, 126(12), pp. 1224-1231
- Shome, N. and Cornell, C. A. (1998) Normalization and scaling accelerograms for nonlinear structural analysis. *Proceedings of the 6th US National Conference on Earthquake Engineering*, May 31 - June 4, Seattle, USA
- Shome, N., Cornell, C., Bazzurro, P. and Carballo, J. E. (1998) Earthquakes, Records, and Nonlinear Responses. *Earthquake Spectra*, 14(3), pp. 469-500
- Shome, N. and Cornell, C. A. (1999) *Probabilistic seismic demand analysis of nonlinear structures*. Report No. RMS-35 (Ph.D. Thesis), Stanford University, Stanford, CA

Sinha, B. P., Gerstle, K. H. and Tulin, L. G. (1964) Stress-Strain Relations for Concrete under Cyclic Loading. *ACI Journal Proceedings*, 61(2), pp. 197-211

Spacone, E. (2001) *A Module for Analysis and Design of Segmental Prestressed Concrete Bridges (CASI-TR-01-04)*. Final Report of a CASI FY00 Technology Transfer Grant, Colorado Advanced Software Institute, Fort Collins, CO

Spacone, E., Camata, G. and Faggella, M. (2008) *Nonlinear models and nonlinear procedures for seismic analysis of reinforced concrete frame structures*. Computational Structural Dynamics and Earthquake Engineering, Taylor & Francis,

Stanton, J. F. and McNiven, H. D. (1979) *The development of a mathematical model to predict the flexural response of reinforced concrete beams to cyclic loads, using system identification*. EERC Report No. 79/02, Earthquake Engineering Research Center, University of California, Berkeley, CA

## T

Takeda, T., Sozen, M. and Nielsen, N. (1970) Reinforced Concrete Response to Simulated Earthquakes. *Journal of the Structural Division*, 96(12), pp. 2557-2573

Takizawa, H. (1976) *Notes on some basic problems in inelastic analysis of planar RC structures*. No. 240, Transactions of the Architectural Institute of Japan, Tokyo

Tothong, P. and Luco, N. (2007) Probabilistic seismic demand analysis using advanced ground motion intensity measures. *Earthquake Engineering & Structural Dynamics*, 36(13), pp. 1837-1860

Tothong, P. and Cornell, C. A. (2008) Structural performance assessment under near-source pulse-like ground motions using advanced ground motion intensity measures. *Earthquake Engineering & Structural Dynamics*, 37(7), pp. 1013-1037

## V

Vallenas, J., Bertero, V. V. and Popov, E. P. (1977) *Concrete confined by rectangular hoops and subjected to axial loads*. Report No. UCB/EERC 77/13, Earthquake Engineering Research Center, University of California, Berkeley, CA

Varum, H. S. A. (1996) *Modelo Numérico para a Análise Sísmica de Pórticos Planos de Betão Armado*. M.Sc. Thesis, University of Porto, Porto, Portugal (in Portuguese)

Vaz, C. (1992) *Comportamento Sísmico de Pontes com Pilares de Betão Armado - Verificação da segurança*. Ph.D. Thesis, University of Porto, Porto, Portugal (in Portuguese)

Vidic, T., Fajfar, P. and Fischinger, M. (1994) Consistent inelastic design spectra: Strength and displacement. *Earthquake Engineering & Structural Dynamics*, 23(5), pp. 507-521

## W

Wakabayashi, M. (1986) *Design of earthquake-resistant buildings*. McGraw Hill, New York

Wilson, E. L. (2002) *Three-Dimensional Static and Dynamic Analysis of Structures, A Physical Approach With Emphasis on Earthquake Engineering*. CSI - Computers and Structures Inc., Berkeley, CA



## **Y**

Yashinsky, M. (1998a) Cypress Street Viaduct. US Geological Survey Professional Paper No. 1552-8, pp. 19-26

Yashinsky, M. (1998b) Performance of Bridge Seismic Retrofits during Northridge Earthquake. *Journal of Bridge Engineering*, 3(1), pp. 1-14

Yassin, M. H. M. (1994) Nonlinear analysis of prestressed concrete structures under monotonic and cyclic loads. Ph.D. Thesis, University of California, Berkeley, USA

Yeh, Y. K., Mo, Y. L. and Yang, C. Y. (2002) Seismic Performance of Rectangular Hollow Bridge Columns. *Journal of Structural Engineering*, 128(1), pp. 60-68

## **Z**

Zeris, C. A. and Mahin, S. A. (1988) Analysis of reinforced concrete beam-columns under uniaxial excitation. *Journal of Structural Engineering*, 114(4), pp. 804-820

Zeris, C. A. and Mahin, S. A. (1991) Behavior of reinforced concrete structures subjected to biaxial excitation. *Journal of Structural Engineering*, 117(9), pp. 2657-2673